Precision QCD

Radja Boughezal

Argonne National Laboratory

MITP Summer School 2018: Towards the Next Quantum Field Theory of Nature

Mainz, July 15 - August 3, 2018

Why is QCD relevant?

- Predictions in QCD make possible the wondrous agreement between theory and data observed at the LHC.

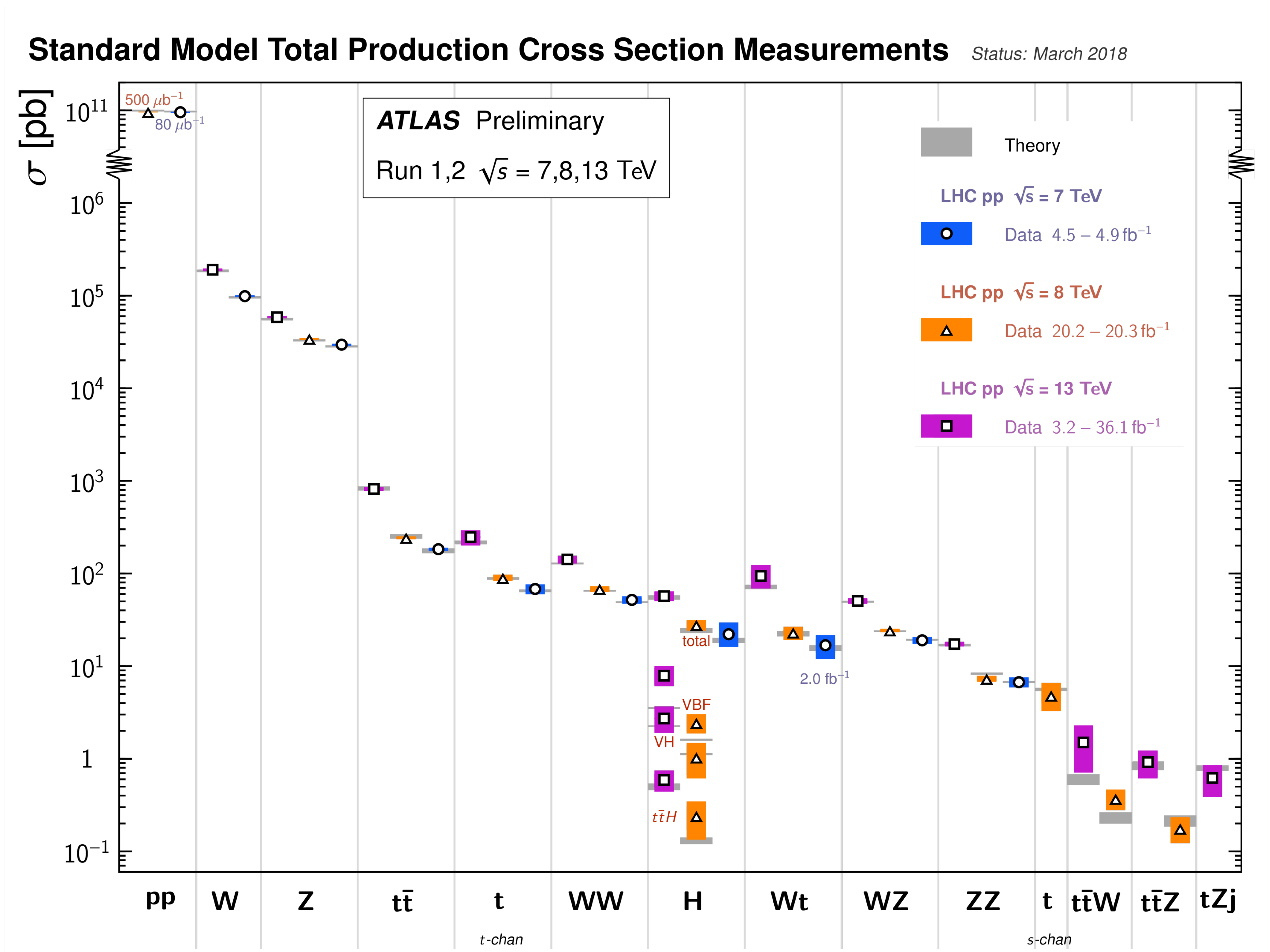

Why is QCD relevant?

- QCD is used at the LHC to enable discovery, as in the case of the Higgs boson.

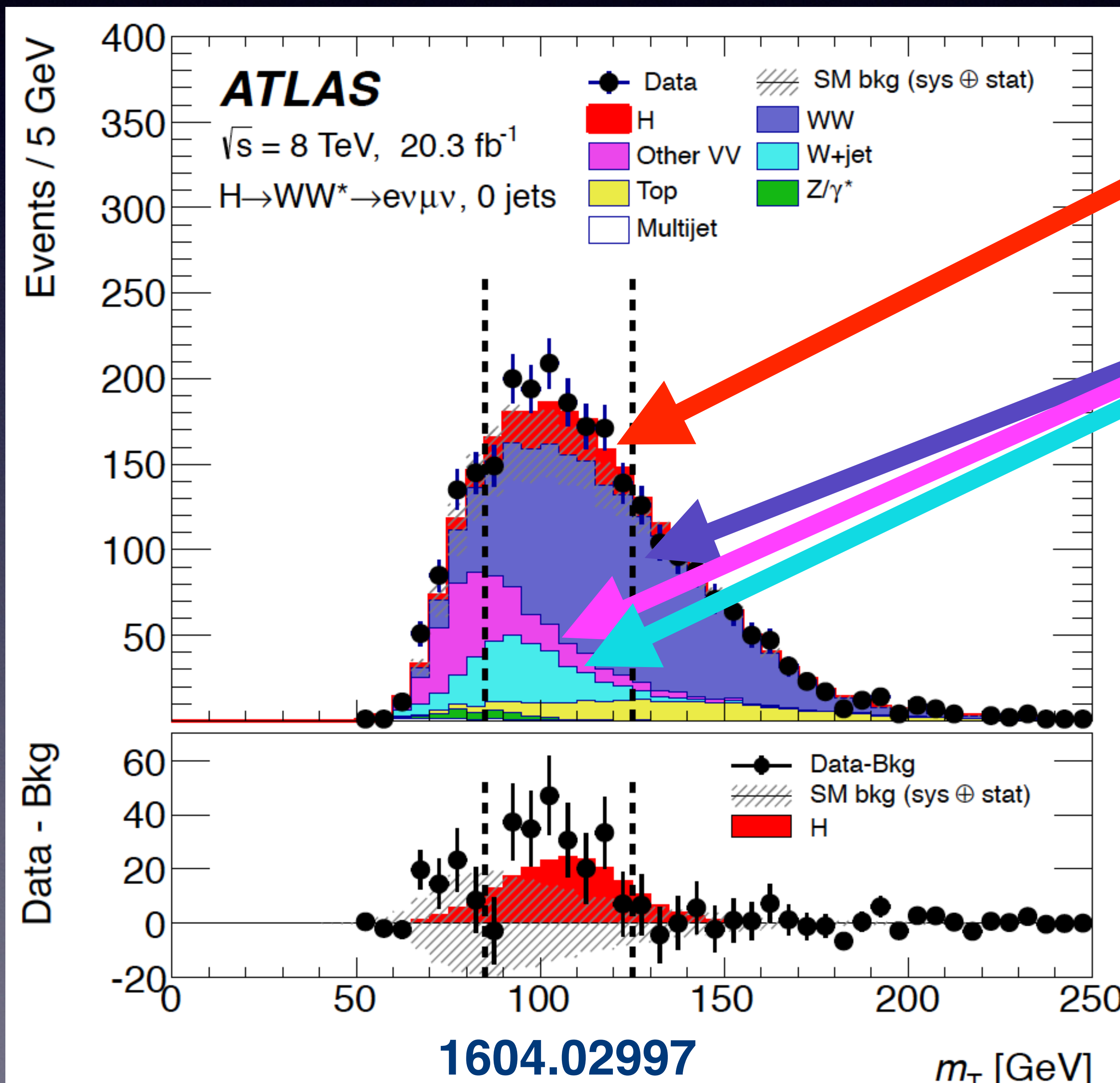

QCD is needed to accurately model both the Higgs signal and its backgrounds

Why is QCD relevant?

QCD is needed to understand the properties of newly discovered particles, such as the Higgs couplings to other particles. This requires theoretical predictions for cross sections as a function of the property to be measured.

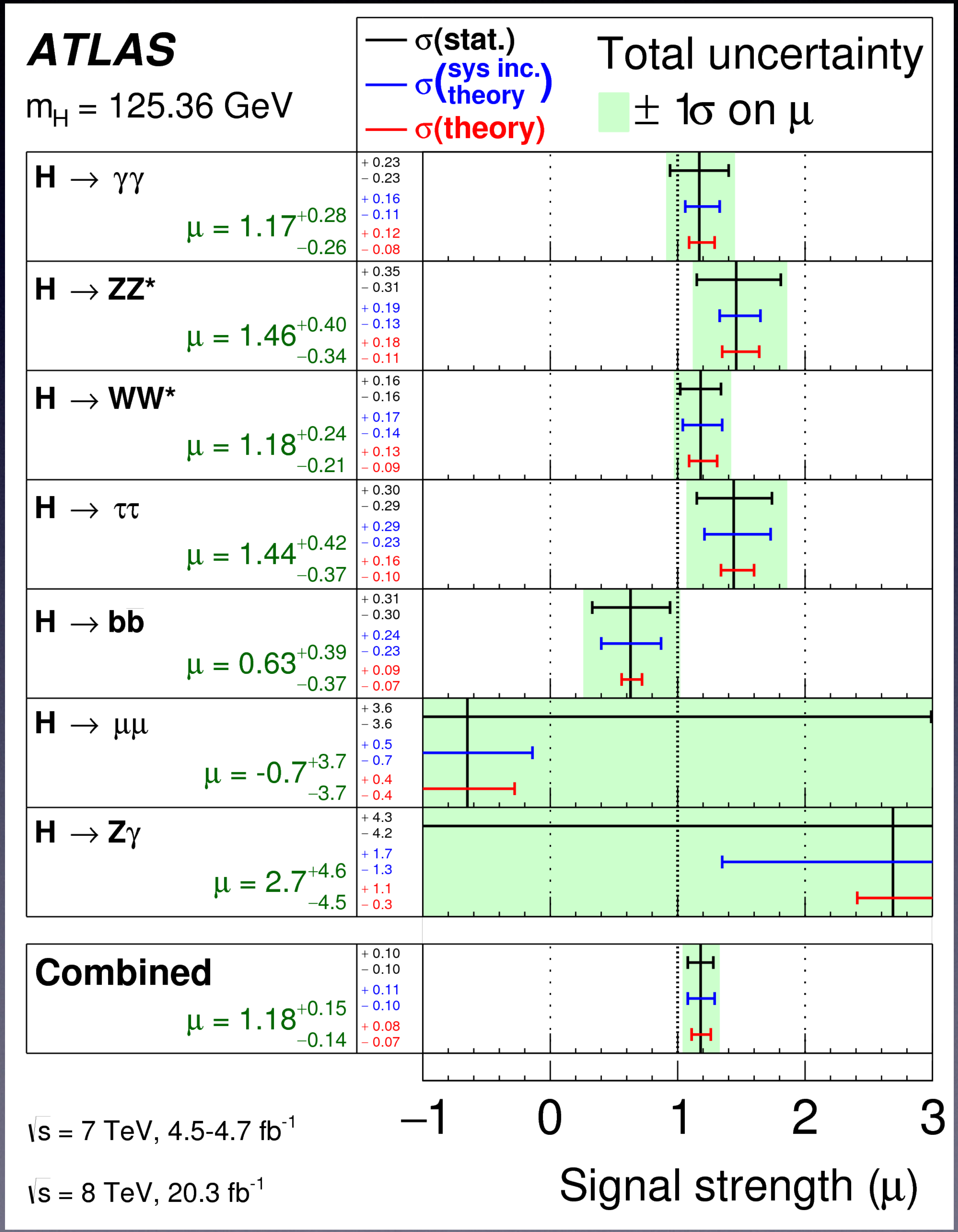

Why is QCD relevant?

- QCD is needed to predict backgrounds to new physics searches (physics beyond the Standard Model). This becomes particularly important for searches with overwhelming backgrounds.

Search for invisible Higgs

dominant background

1610.09218

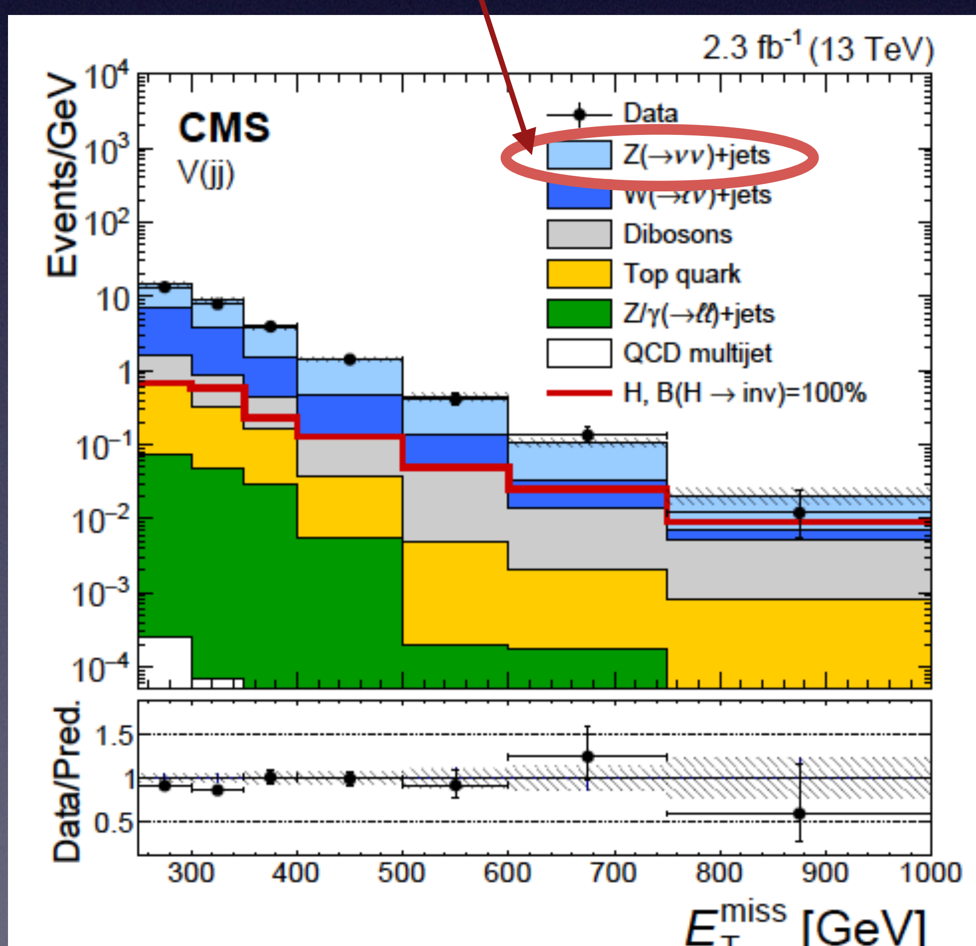

Systematic uncertainty	Impact
Common	
γ+jets/Z($\nu\nu$)+jets ratio theory	32%
W($l\nu$)+jets/Z($\nu\nu$)+jets ratio theory	21%
Jet energy scale+resolution	12%
V-tagging efficiency	12%
Lepton veto efficiency	13%
Electron efficiency	13%
Muon efficiency	8.6%
b jet tag efficiency	5.7%
Photon efficiency	3.1%
E_T^{miss} scale	4.6%
Top quark background normalisation	6.0%
Diboson background normalisation	$< 1\%$
Luminosity	$< 1\%$
Signal specific	
ggH p_T-spectrum	12%
QCD scale + PDF (ggH)	3.0%
QCD scale + PDF (VH)	1.4%
Total statistical only	$-46/+50\%$
Total uncertainty	$-69/+74\%$

Theory ratios of γ+jets/Z(νν)+jets and W(lν)+jets/Z(νν)+jets together with measurements of γ+jets and W(lν)+jets are needed to predict the background

Aim of these lectures

- Give you some basic understanding of QCD, focusing on its perturbative aspects.
- Demonstrate important concepts through calculations of key scattering processes.
- Discuss the physics implications of QCD on relevant LHC processes, demonstrating the importance of the interplay between theory and experiment.
- We will have four lectures, some will be on the blackboard and others on the slides.

What is QCD?

- QCD is the theory that describes strong interactions between quarks and gluons. It is a non-abelian gauge theory with the symmetry gauge group SU(3).

- There are 3 basic ingredients for QCD: quarks, gluons and the strong coupling constant $\boldsymbol{\alpha}_s$.

    - quarks (and their anti-quarks): come in 3 colors in addition to their electric charge. The color makes them different from leptons in QED.

    - gluons: analogous to photons in QED, except they are color charged and there are 8 of them. Unlike photons, they interact with each other.

    - $\boldsymbol{\alpha}_s$: a running coupling constant. It is small at high collider energies and large at small energies. It is larger than the QED coupling constant.

The QCD Lagrangian

$$\mathcal{L}_{\rm QCD} = -\frac{1}{4} F_a^{\mu\nu} F^a_{\mu\nu} + \sum_f \bar{\psi}_i^{(f)} \left(i \not{D}_{ij} - m_f \delta_{ij} \right) \psi_j^{(f)}$$

$$D^\mu_{ij} \equiv \partial^\mu \delta_{ij} + i g_s t^a_{ij} A^\mu_a \,, \qquad F^a_{\mu\nu} \equiv \partial_\mu A^a_\nu - \partial_\nu A^a_\mu - g_s f_{abc} A^b_\mu A^c_\nu$$

⇒ covariant derivative ⇒ field strength

- The terms proportional to g_s in the field strength are responsible for the gluon self-interaction. This is what makes the difference w.r.t. QED.
- t^a_{ij} are color matrices, they are the generators of SU(3).
- QCD interactions do not depend on quark flavor (differences only due to EW)
- We will next split the Lagrangian into its quark and gluon parts and study its details.

Lagrangian: the quark part

- Quarks come in 3 colors: $\psi_i = \begin{pmatrix} \psi_1 \\ \psi_2 \\ \psi_3 \end{pmatrix}$

- The part of the Lagrangian describing quarks and their interactions :

$$\boxed{\mathcal{L}_q = \Sigma_q \overline{\psi}_i^{(q)} \left(i\gamma^\mu \partial_\mu \delta_{ij} - g_s t^a_{ij} \gamma^\mu A_{\mu,a} - m_q \delta_{ij} \right) \psi_j^{(q)}}$$

- The fundamental representation of SU(3) has $(3^2-1)=8$ generators $t^1_{ij} \ldots t^8_{ij}$ corresponding to 8 gluons $A_{1\mu} \ldots A_{8\mu}$, while i and j are color indices = 1,3.

- An explicit representation for these generators is through the Gell-Mann matrices λ^A with $t^A = \lambda^A/2$

$$\lambda^1 = \begin{pmatrix} 0 & 1 & 0 \\ 1 & 0 & 0 \\ 0 & 0 & 0 \end{pmatrix}, \lambda^2 = \begin{pmatrix} 0 & -i & 0 \\ i & 0 & 0 \\ 0 & 0 & 0 \end{pmatrix}, \lambda^3 = \begin{pmatrix} 1 & 0 & 0 \\ 0 & -1 & 0 \\ 0 & 0 & 0 \end{pmatrix}, \lambda^4 = \begin{pmatrix} 0 & 0 & 1 \\ 0 & 0 & 0 \\ 1 & 0 & 0 \end{pmatrix},$$

$$\lambda^5 = \begin{pmatrix} 0 & 0 & -i \\ 0 & 0 & 0 \\ i & 0 & 0 \end{pmatrix}, \lambda^6 = \begin{pmatrix} 0 & 0 & 0 \\ 0 & 0 & 1 \\ 0 & 1 & 0 \end{pmatrix}, \lambda^7 = \begin{pmatrix} 0 & 0 & 0 \\ 0 & 0 & -i \\ 0 & i & 0 \end{pmatrix}, \lambda^8 = \begin{pmatrix} \frac{1}{\sqrt{3}} & 0 & 0 \\ 0 & \frac{1}{\sqrt{3}} & 0 \\ 0 & 0 & \frac{-2}{\sqrt{3}} \end{pmatrix},$$

Lagrangian: the gluonic part

- The gluon Lagrangian is simple: $\boxed{\mathcal{L}_G = -\frac{1}{4} F_a^{\mu\nu} F^a_{\mu\nu}}$

The field strength $F^{\mu\nu}_a$ defined earlier contains the SU(3) structure constants f_{abc}. They are anti-symmetric in all indices and satisfy:

$$\boxed{[t^a, t^b] = i f_{abc} t^c}$$

Some useful identities based on color algebra

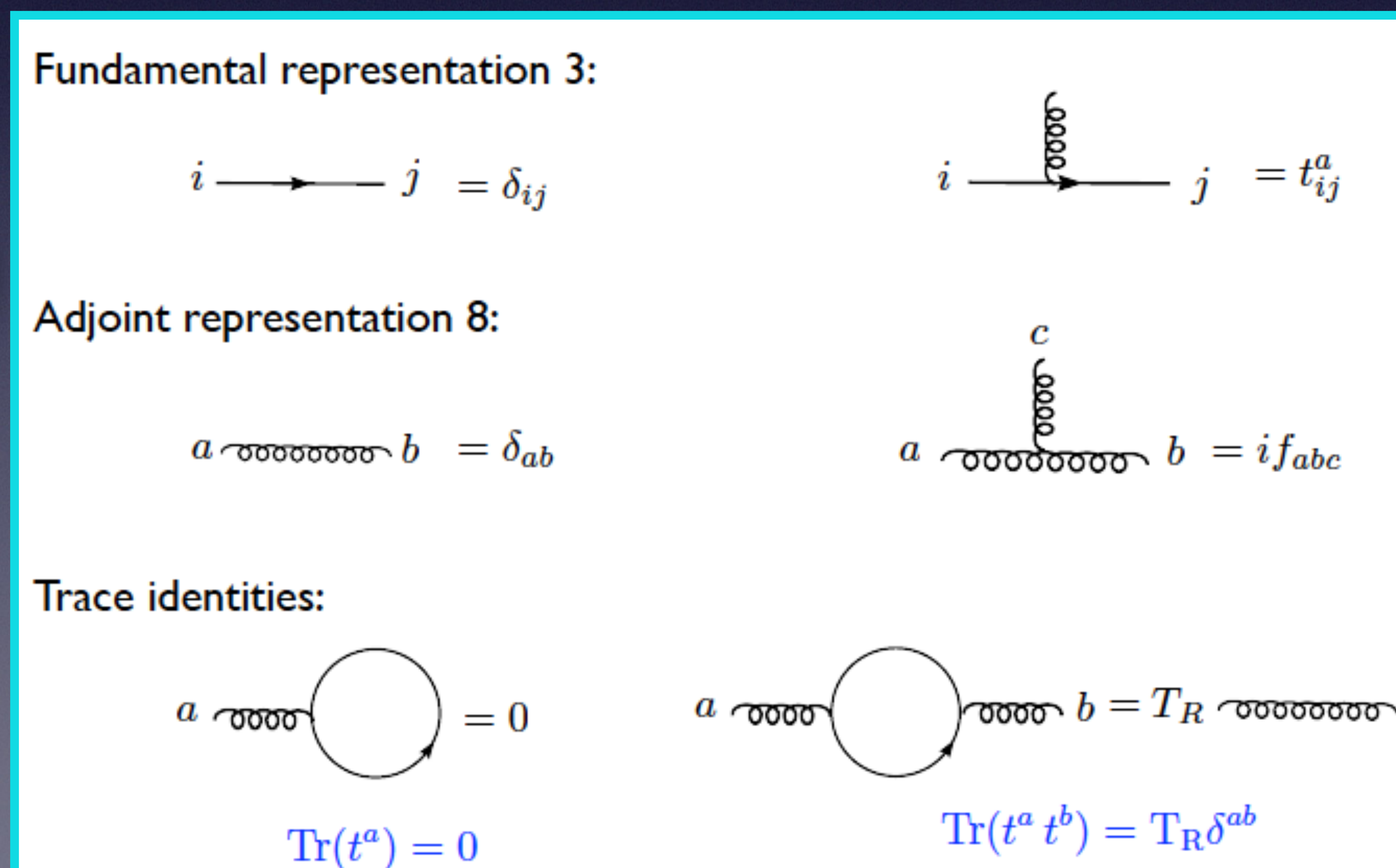

Standard normalization:

$$Tr(t^a t^b) = T_R \delta^{ab}$$

T_R=1/2

Useful relations

$$\sum_A t^A_{ab} t^A_{bc} = C_F \delta_{ac}\,, \quad C_F = \frac{N_c^2 - 1}{2N_c} = \frac{4}{3}$$

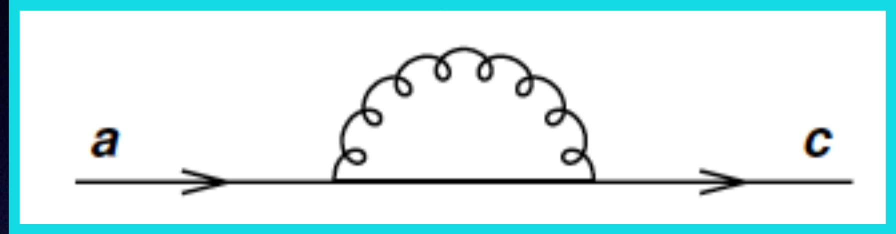

$$\sum_{C,D} f^{ACD} f^{BCD} = C_A \delta^{AB}\,, \quad C_A = N_c = 3$$

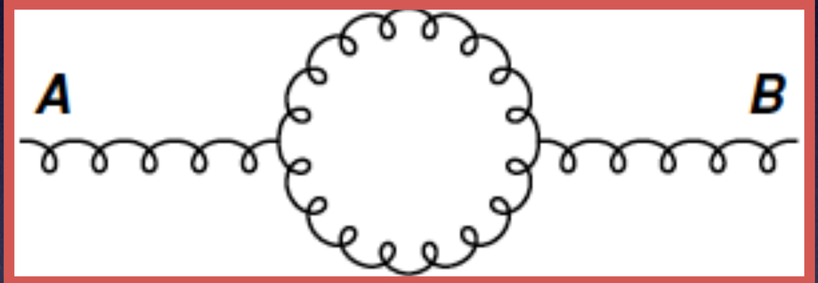

$$t^A_{ab} t^A_{cd} = \frac{1}{2}\delta_{bc}\delta_{ad} - \frac{1}{2N_c}\delta_{ab}\delta_{cd} \quad \text{(Fierz)}$$

Nc = number of colors = 3

Gauge Invariance

- The QCD Lagrangian is invariant under local gauge transformations. This means that redefining the quark and gluon fields at any point in space and time does not change the physical content of the theory.
- The quark and gluon fields as well as the covariant derivative have the following gauge transformations that leave the QCD Lagrangian unchanged:

$$\boxed{\psi \rightarrow \psi' = U(x)\psi} \qquad \boxed{D_\mu \psi \rightarrow D'_\mu \psi' = U(x) D_\mu \psi}$$

$$\boxed{t^a A_a \rightarrow t^a A'_a = U(x) t^a A_a U^{-1}(x) + \frac{i}{g_s} \left(\partial U(x)\right) U^{-1}(x)}$$

U(x) is a unitary 3x3 matrix

Gauge Invariance

- Based on the previous relations, as well as:

$$\bar{\psi} \to \bar{\psi}' = \bar{\psi} U^\dagger(x)$$

$$t^a F^a_{\mu\nu} \to t^a F^{a\prime}_{\mu\nu} = U(x) t^a F^a_{\mu\nu} U^{-1}(x)$$

It is easy to check that the QCD Lagrangian is indeed gauge invariant:

$$-\frac{1}{4} F'^{\mu\nu}_a F'^a_{\mu\nu} = -\frac{1}{4} F^{\mu\nu}_a F^a_{\mu\nu}$$

$$\sum_f \bar{\psi}'^{(f)}_i \left(i\not{D}'_{ij} - m_f \delta_{ij} \right) \psi'^{(f)}_j = \sum_f \bar{\psi}^{(f)}_i \left(i\not{D}_{ij} - m_f \delta_{ij} \right) \psi^{(f)}_j$$

- It is important to note that the field strength alone is not gauge invariant in QCD, unlike QED. This is due to the self interacting gluons.
- A mass term for the gluons would violate gauge invariance and is therefore forbidden, unlike quarks which can have a gauge invariant mass term.

Gauge fixing

- Like in QED, we can't invert the quadratic part of the gluon Lagrangian to obtain its propagator. Need to add a gauge fixing term that depends on an arbitrary parameter ξ. In covariant gauges we have:

$$\boxed{\mathcal{L}_{gauge\ fixing} = -\frac{1}{\xi}(\partial^\mu A_\mu^A)^2}$$

ξ=1: Feynman gauge
ξ=0: Landau gauge

Gluon propagator becomes:

$$\frac{-i}{k^2}\left(g_{\mu\nu} - (1-\xi)\frac{k_\mu k_\nu}{k^2}\right)\delta^{ab} =$$

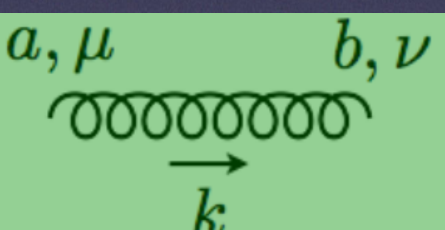

- The gauge fixing term breaks gauge invariance. Physical results are in the end gauge independent. This provides an important check on higher order calculations that should be free from ξ.

Gauge fixing and Ghosts

- In covariant gauges, the gauge fixing term must be supplemented with a ghost term to cancel the unphysical longitudinal degrees of freedom:

$$\boxed{\mathcal{L}_{ghost} = \partial_\mu \eta^{a\dagger} D^\mu_{ab} \eta^b}$$

η: complex scalar field

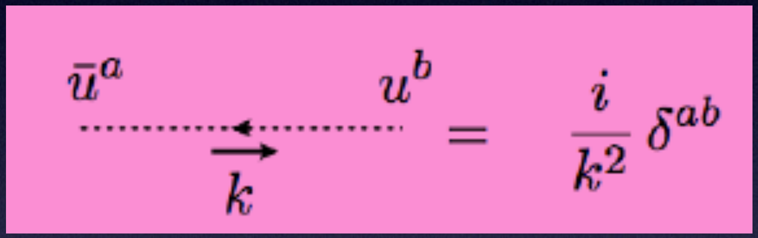

- Certain ``physical'' gauges (axial, light-like) remove the ghosts. We will use Feynman gauge, ξ=1, for our calculations.

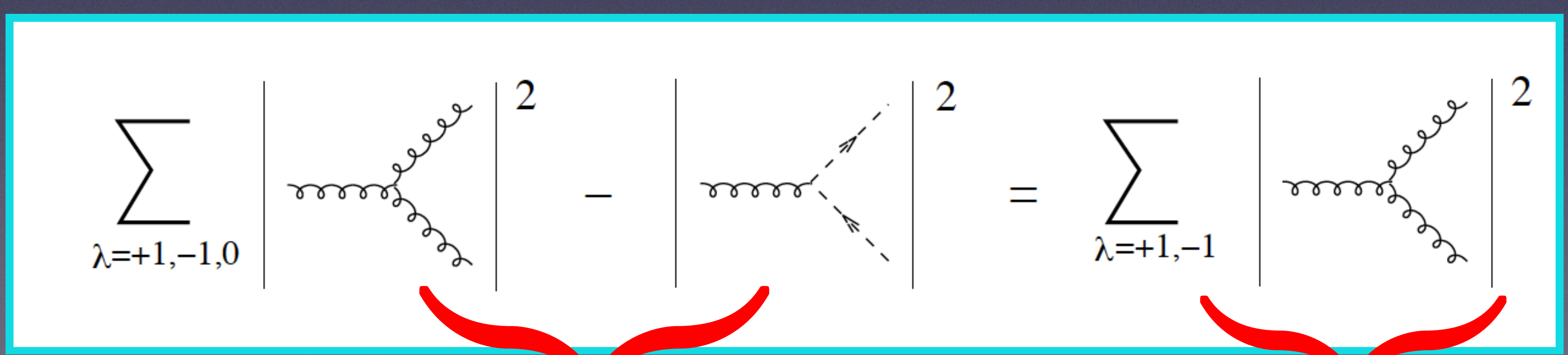

structure of calculation in covariant gauges

structure of calculation in physical gauges

λ: polarizations of gluons

Axial gauges

- We can choose an axial gauge by introducing an arbitrary direction n:

$$\boxed{\mathcal{L}_{axial\ gauge} = -\frac{1}{\xi}(n^\mu A_\mu^A)^2}$$

- The gluon propagator in this gauge becomes:

$$\boxed{d_{\mu\nu} = \frac{i}{k^2}\left(-g_{\mu\nu} + \frac{n_\mu k_\nu + n_\nu k_\mu}{n \cdot k} + \frac{(n^2 + \xi k^2) k_\mu k_\nu}{(n \cdot k)^2}\right)\delta_{ab}}$$

Light cone gauge: $n^2 = 0$, $\xi = 0$

- Only two degrees of freedom for the gluons propagate in this gauge (hence the term physical gauge). We can check that this is the case by using these two constraints:

$$\boxed{d^{\mu\nu} k_\nu = 0 = d^{\mu\nu} n_\nu}$$

k^2=0 for an on-shell gluon

Feynman rules:

Useful reference: Ellis, Stirling, Webber, *QCD and Collider Physics*

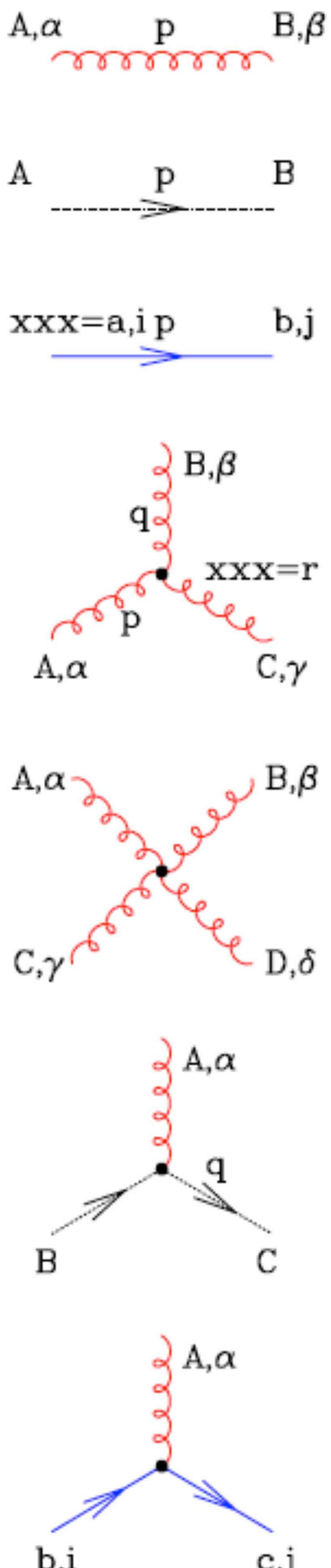

$$\delta^{AB}\left[-g^{\alpha\beta}+(1-\lambda)\frac{p^{\alpha}p^{\beta}}{p^{2}+i\epsilon}\right]\frac{i}{p^{2}+i\epsilon}$$

$$\delta^{AB}\frac{i}{(p^{2}+i\epsilon)}$$

$$\delta^{ab}\frac{i}{(\not{p}-m+i\epsilon)_{ji}}$$

$$-g\ f^{ABC}\left[(p-q)^{\gamma}g^{\alpha\beta}+(q-r)^{\alpha}g^{\beta\gamma}+(r-p)^{\beta}g^{\gamma\alpha}\right]$$

(all momenta incoming)

$$-ig^{2}\ f^{XAC}f^{XBD}\ [g^{\alpha\beta}g^{\gamma\delta}-g^{\alpha\delta}g^{\beta\gamma}]$$
$$-ig^{2}\ f^{XAD}f^{XBC}\ [g^{\alpha\beta}g^{\gamma\delta}-g^{\alpha\gamma}g^{\beta\delta}]$$
$$-ig^{2}\ f^{XAB}f^{XCD}\ [g^{\alpha\gamma}g^{\beta\delta}-g^{\alpha\delta}g^{\beta\gamma}]$$

$$g\ f^{ABC}q^{\alpha}$$

$$-ig\ (t^{A})_{cb}\ (\gamma^{\alpha})_{ji}$$

The running coupling

- All couplings run (QED, QCD, EW), this means they depend on the momentum scale Q^2 of the studied process. Gluon self-couplings lead to a profound difference between QED and QCD running of the coupling.

- Consider the **QED beta function** (just the electron contribution). The QED evolution equation of the coupling constant **α**(Q^2):

$$Q^2 \frac{d\alpha}{dQ^2} = \beta_{QED}(\alpha), \quad \beta_{QED} = \frac{\alpha^2}{3\pi} + \mathcal{O}(\alpha^3)$$

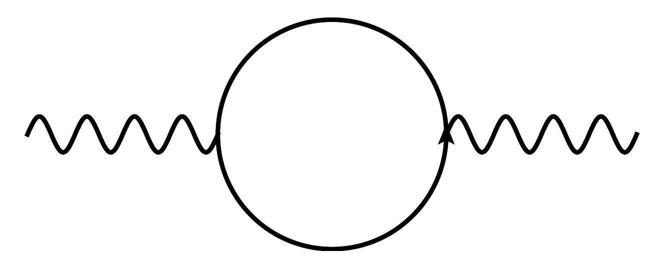

$$\alpha(Q^2) = \frac{\alpha_0}{1 - \frac{\alpha_0}{3\pi} \ln\left(\frac{Q^2}{m_e^2}\right)}$$

$\alpha_0 \approx 1/137$

Coupling constant grows with energy; hits a *Landau pole* when denominator vanishes. QED becomes strongly-coupled at high energies.

The running coupling

- Consider now the **QCD beta function**. Gluon self-couplings reverse the sign of the beta function:

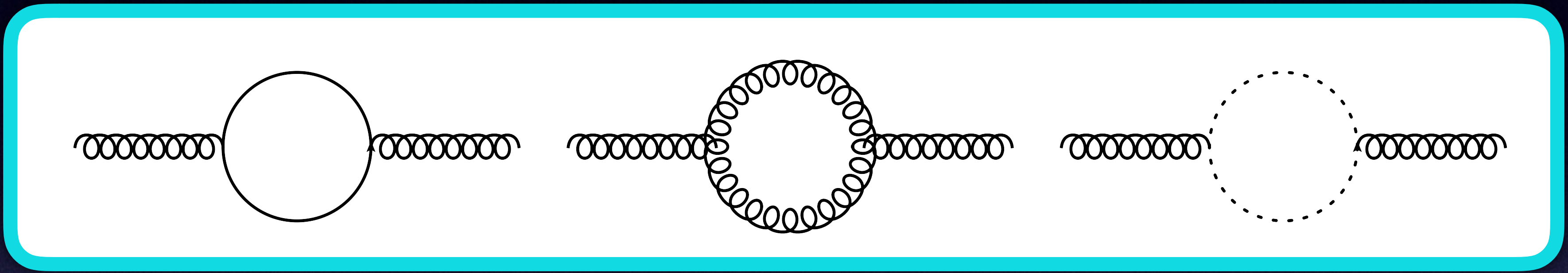

$$Q^2 \frac{\partial \alpha_s}{\partial Q^2} = \beta(\alpha_s), \quad \beta(\alpha_s) = -\alpha_s^2(b_0 + b_1\alpha_s + b_2\alpha_s^2 + \dots),$$

$$b_0 = \frac{11C_A - 2n_f}{12\pi}, b_1 = \frac{17C_A^2 - 5C_A n_f - 3C_F n_f}{24\pi^2}$$

- Lets solve the QCD evolution equation for **α**s assuming $\beta(\alpha_s) = -\alpha_s^2 b_0$

$$\boxed{\alpha_s(Q^2) = \frac{\alpha_s(Q_0^2)}{1 + b_0\alpha_s(Q_0^2)\ln\frac{Q^2}{Q_0^2}} = \frac{1}{b_0 \ln\frac{Q^2}{\Lambda^2}}}$$

The running coupling

Asymptotic freedom:

$$\alpha_s(Q^2) = \frac{\alpha_s(Q_0^2)}{1 + b_0 \alpha_s(Q_0^2) \ln \frac{Q^2}{Q_0^2}} = \frac{1}{b_0 \ln \frac{Q^2}{\Lambda^2}}$$

note the sign change compared to QED

- αs(Q) becomes small at high scales Q, the perturbative expansion improves. Quarks and gluons are almost free.
- αs(Q) becomes large at small scales Q, perturbative expansion fails. Quarks and gluons interact strongly and confine into hadrons.

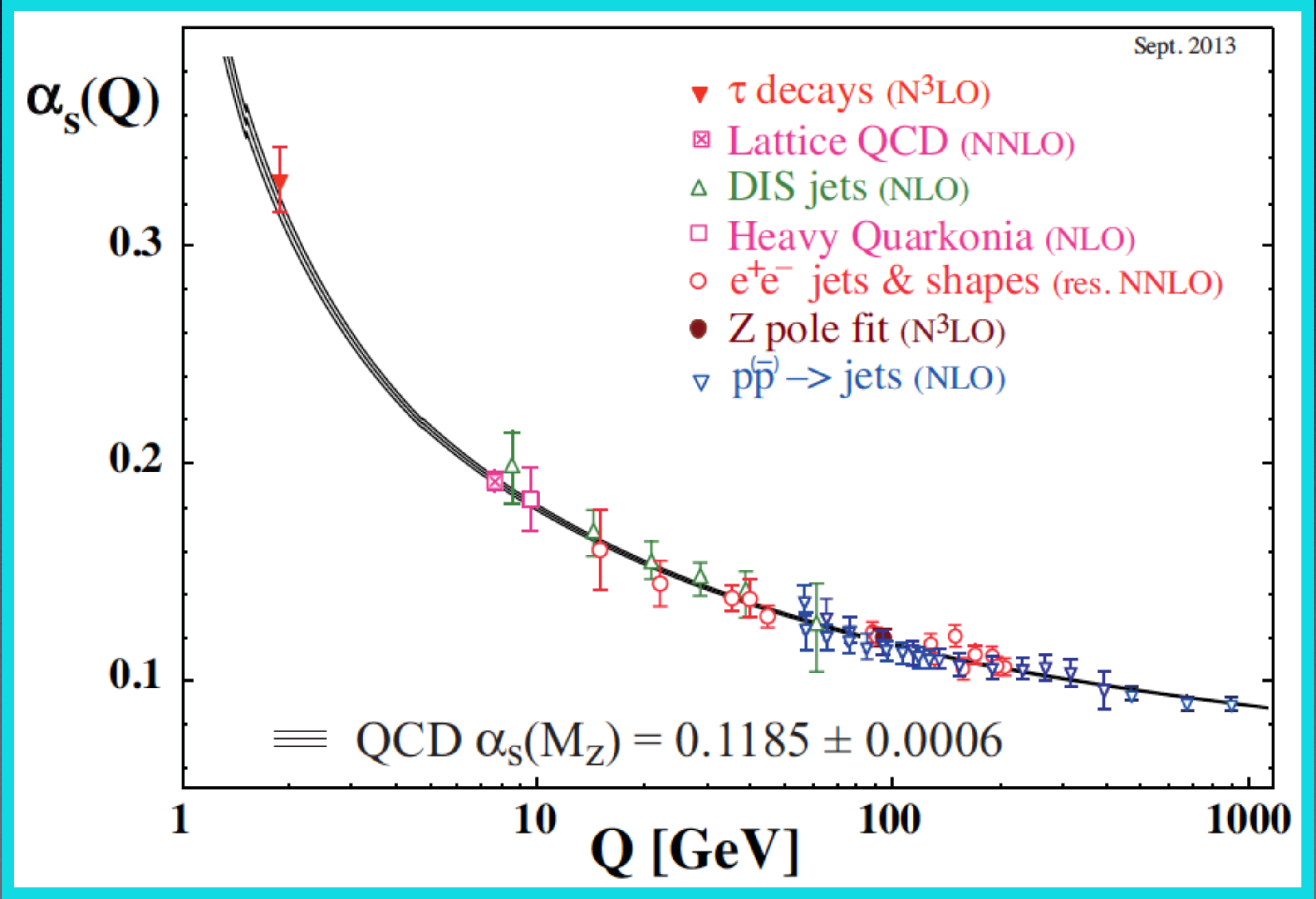

The running coupling

Asymptotic freedom:

$$\alpha_s(Q^2) = \frac{\alpha_s(Q_0^2)}{1 + b_0 \alpha_s(Q_0^2) \ln \frac{Q^2}{Q_0^2}} = \frac{1}{b_0 \ln \frac{Q^2}{\Lambda^2}}$$

note the sign change compared to QED

- Λ, often called Λ_{QCD}, is the fundamental scale of QCD at which the coupling blows up. $\Lambda \simeq 0.2$GeV.
- Perturbative expansions are valid for scales $Q \gg \Lambda$.

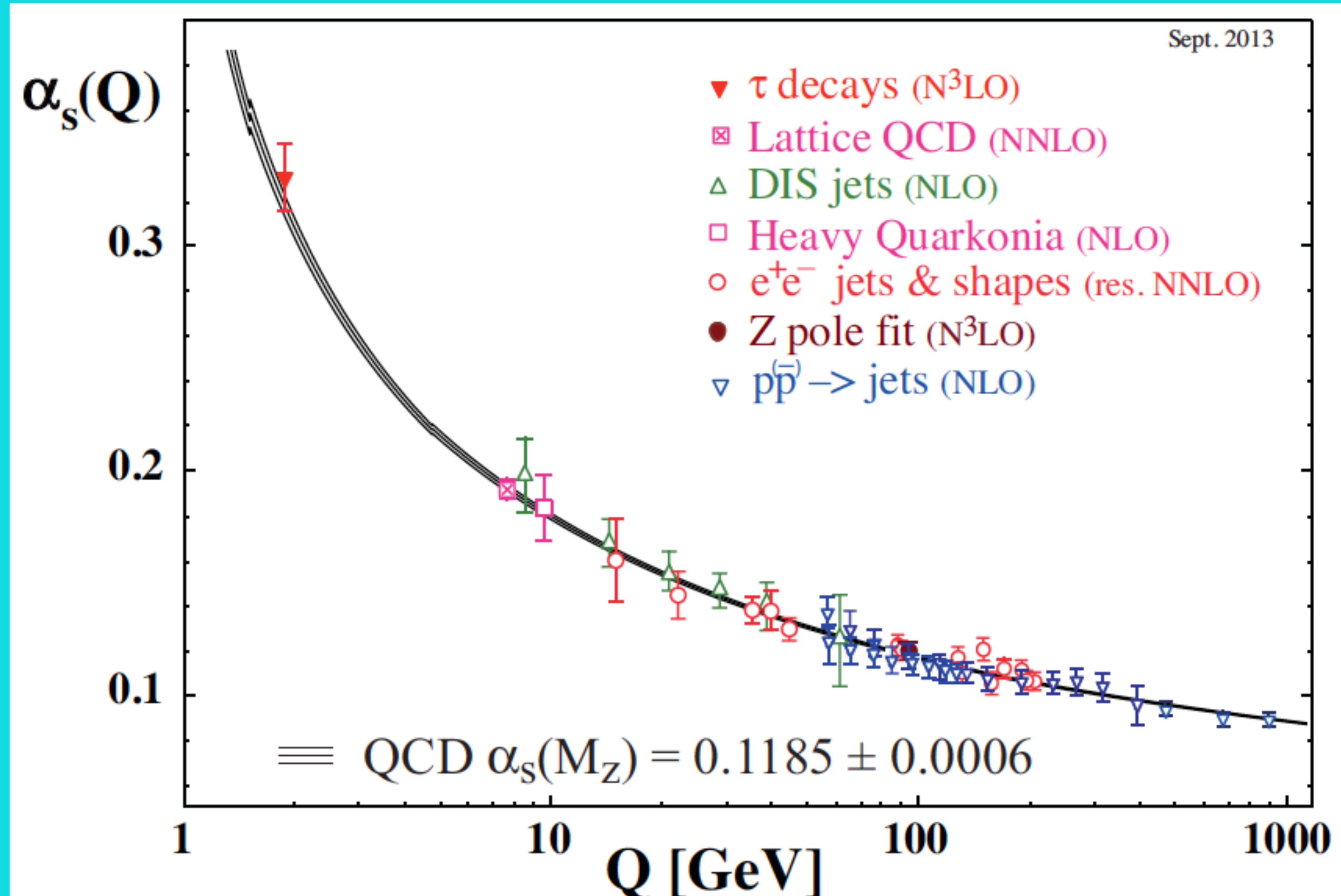

Confinement in QCD

- QCD becomes strongly coupled at low energies. We *think* this leads to the experimentally observed confinement of quarks and gluons into hadrons.

- It is assumed that confinement always holds, although we have no rigorous proof of that.

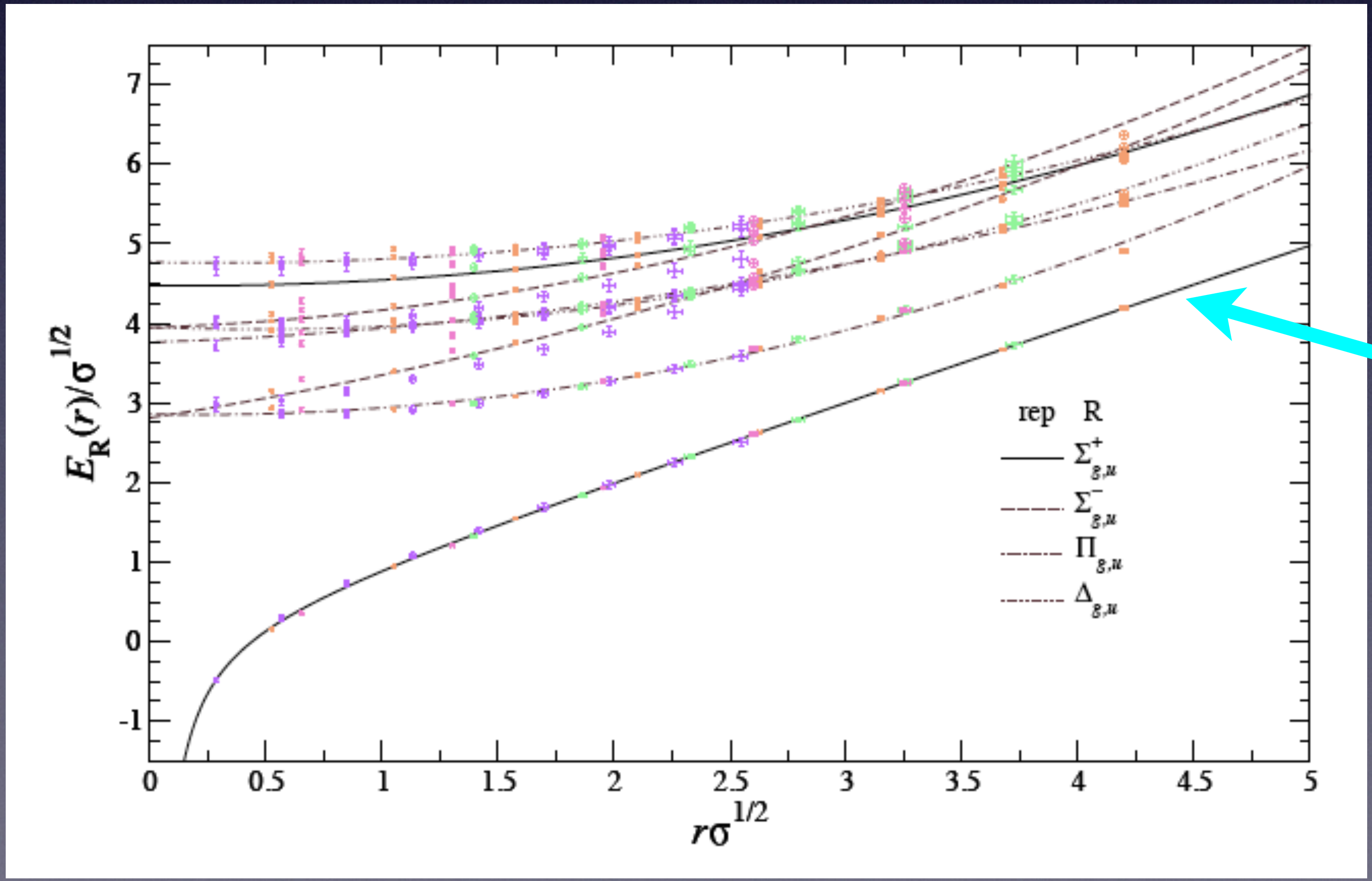

quark-antiquark potential grows linearly at large separation, suggesting confinement

Juge, Kuti, Morningstar; review by Kronfeld, 1203.1204

QCD and hadronic collisions

Hadronization at Λ_{QCD}

Hadron decays

Multiple parton interactions

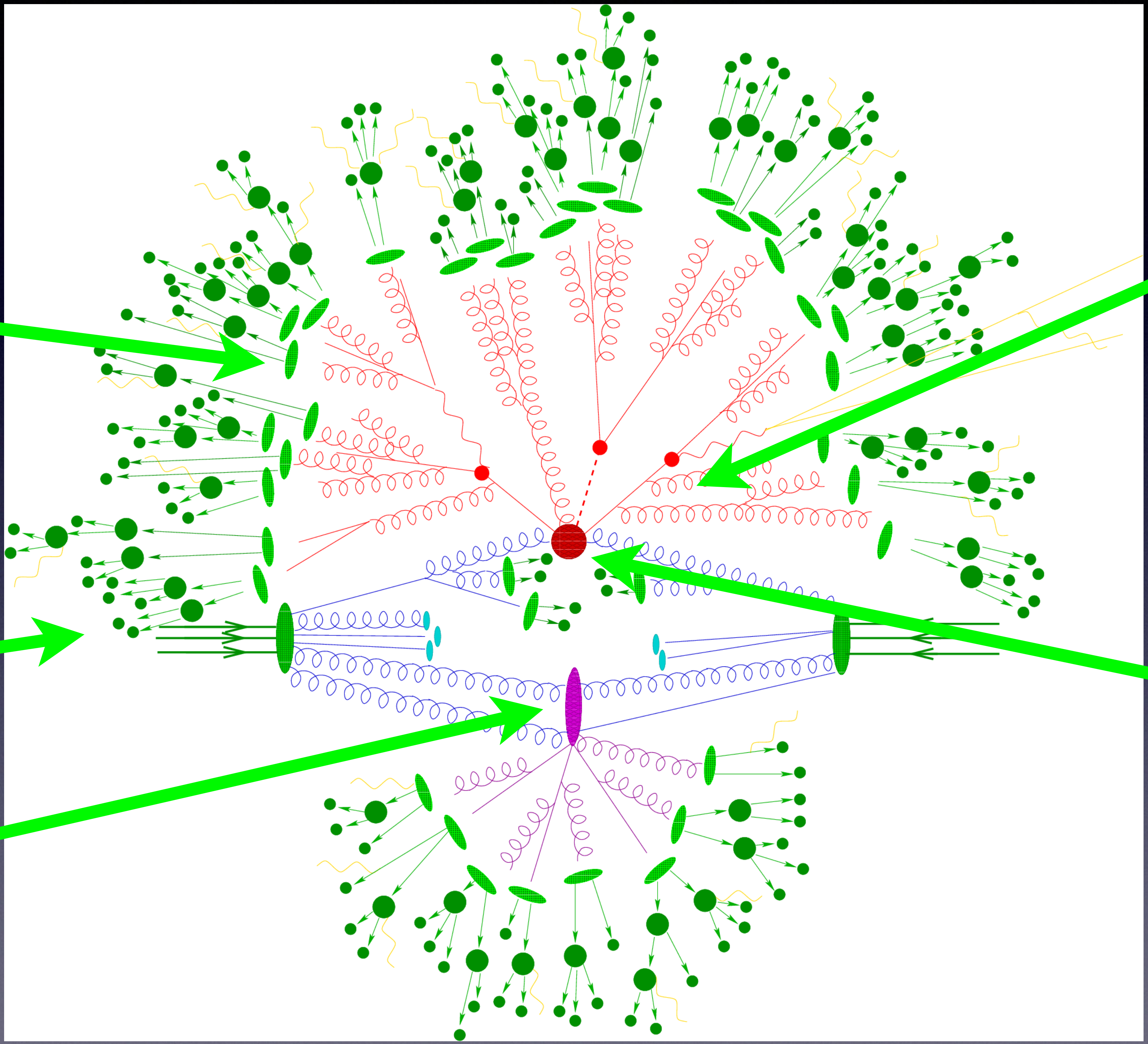

Parton-shower evolution to low energies

Hard collision (Higgs production) at short distances/ high energies

How does theory allow us to peer into the inner "hard-scattering" in this mess?

The concept of factorization

- The cross section for a hadronic process can be separated into a perturbative and a non-perturbative part in the following way:

renormalization scale

$$d\sigma = \sum_{a,b} \int dx_1 dx_2 \;\; f_a(x_1,\mu_F) f_b(x_2,\mu_F) \; d\hat{\sigma}_{ab\to X}(\hat{s},\mu_F,\mu_R)$$

Parton density functions

Parton-level (differential) cross section

factorization scale

- The two ingredients are the **partonic cross section** (for which we will do few perturbative calculations) and the Parton Distribution Functions (PDFs) which are non-perturbative quantities that define the distribution of partons inside the proton. They are determined from data together with some theory input.

Note: this formula is correct up to some power corrections that scale like (Λ_{QCD}/Q)^n where Q is the hard scale of the studied process and n is a process dependent factor.

The concept of factorization

- The cross section for a hadronic process can be separated into a perturbative and a non-perturbative part in the following way:

$$d\sigma = \sum_{a,b} \int dx_1 dx_2 \;\; \underbrace{f_a(x_1, \mu_F) f_b(x_2, \mu_F)}_{\text{Parton density functions}} \; \underbrace{d\hat{\sigma}_{ab\to X}(\hat{s}, \mu_F, \mu_R)}_{\text{Parton-level (differential) cross section}}$$

- We can see how the factorization of cross sections into hard and soft parts appears in a simple example: the **R-ratio** in $e^+e^- \to$ hadrons. We will explicitly calculate this quantity in perturbative QCD to next-to-leading order in the strong coupling constant.

The R-ratio in e+e-

- The R-ratio is defined in the following way:

$$R \equiv \frac{\sigma(e^+e^- \to \text{hadrons})}{\sigma(e^+e^- \to \mu^+\mu^-)}$$

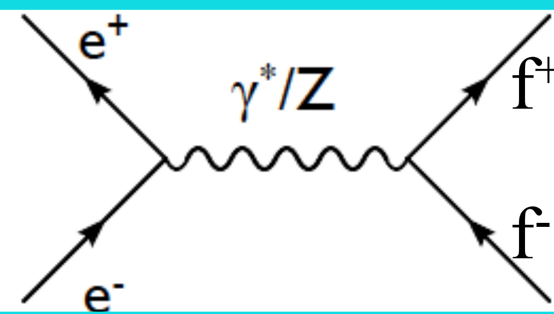

- At lowest order in perturbation theory we have:

$$\sigma(e^+e^- \to \text{hadrons}) = \sigma_0(e^+e^- \to q\bar{q})$$

- Since hadronization happens at much longer time scales than the production of quarks which happens at high energies (short time scale), we can replace hadrons with partons.
  - Time scale for f^+f^- production: $\tau \sim 1/Q$
  - Time scale for hadronization: $\tau \sim 1/\Lambda$

The R-ratio in e+e-

- The R-ratio is defined in the following way:

$$R \equiv \frac{\sigma(e^+e^- \to \text{hadrons})}{\sigma(e^+e^- \to \mu^+\mu^-)}$$

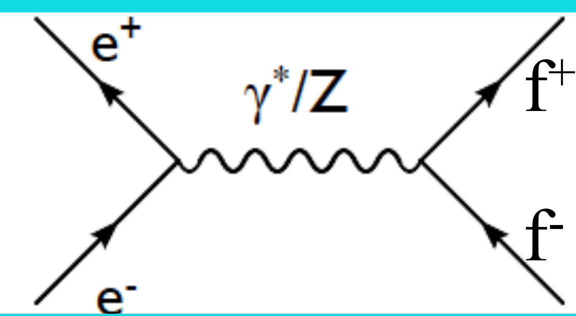

- At lowest order in perturbation theory we have:

$$\sigma(e^+e^- \to \text{hadrons}) = \sigma_0(e^+e^- \to q\bar{q})$$

- Since hadronization happens at much longer time scales than the production of quarks which happens at high energies (short time scale), we can replace hadrons with partons.

- At lowest order, the R-ratio is simple (common factors cancel in the ratio):

$$R_0 = \frac{\sigma_0(\gamma^* \to \text{hadrons})}{\sigma_0(\gamma^* \to \mu^+\mu^-)} = N_c \sum_f q_f^2$$

electric charge of the quarks

The R-ratio in e+e-

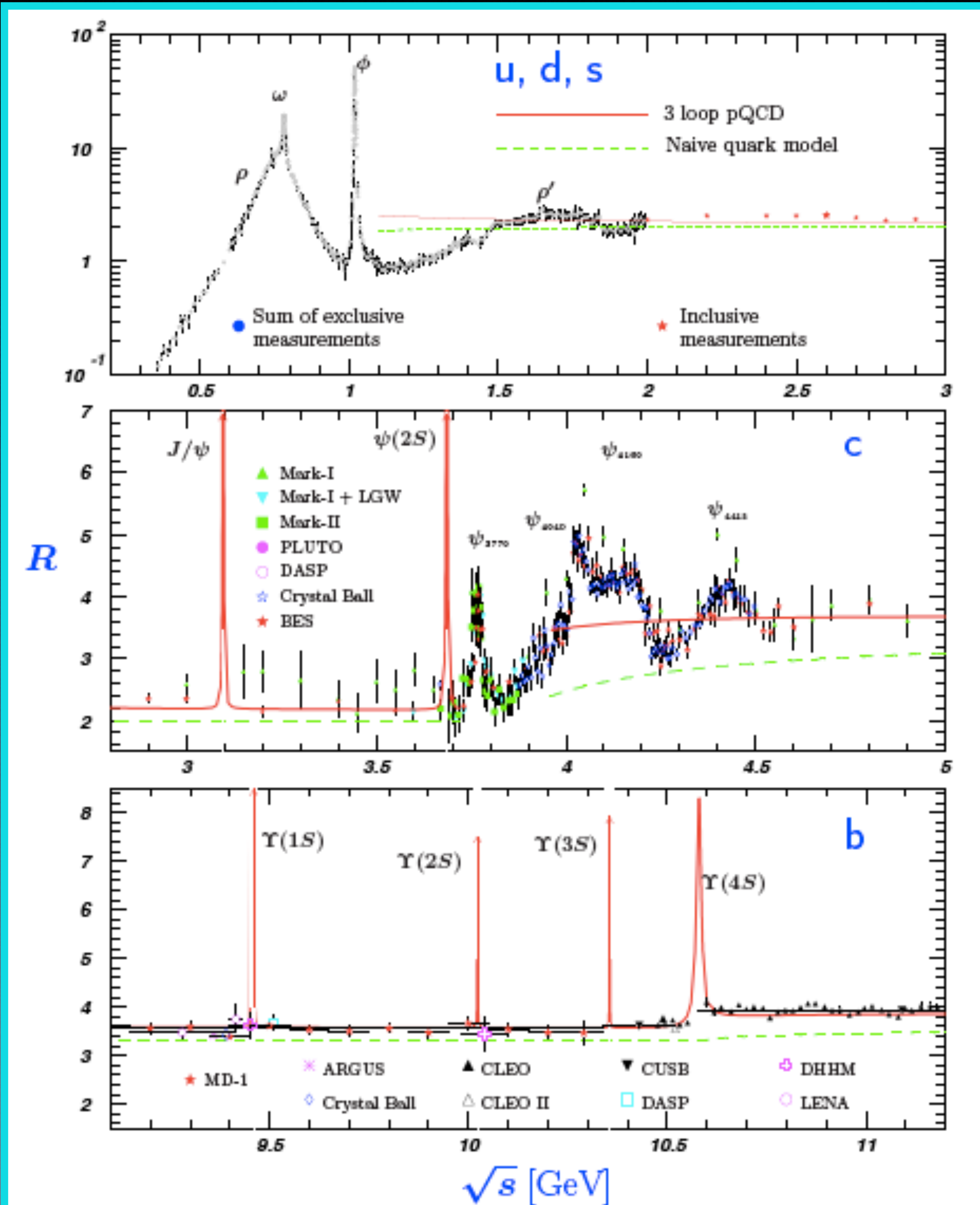

$$3 \times \left\{ \left(\frac{2}{3}\right)^2 + 2\left(\frac{1}{3}\right)^2 \right\} = 2$$

$$3 \times \left\{ 2\left(\frac{2}{3}\right)^2 + 2\left(\frac{1}{3}\right)^2 \right\} = \frac{10}{3}$$

$$3 \times \left\{ 2\left(\frac{2}{3}\right)^2 + 3\left(\frac{1}{3}\right)^2 \right\} = \frac{11}{3}$$

The R-ratio in e+e-

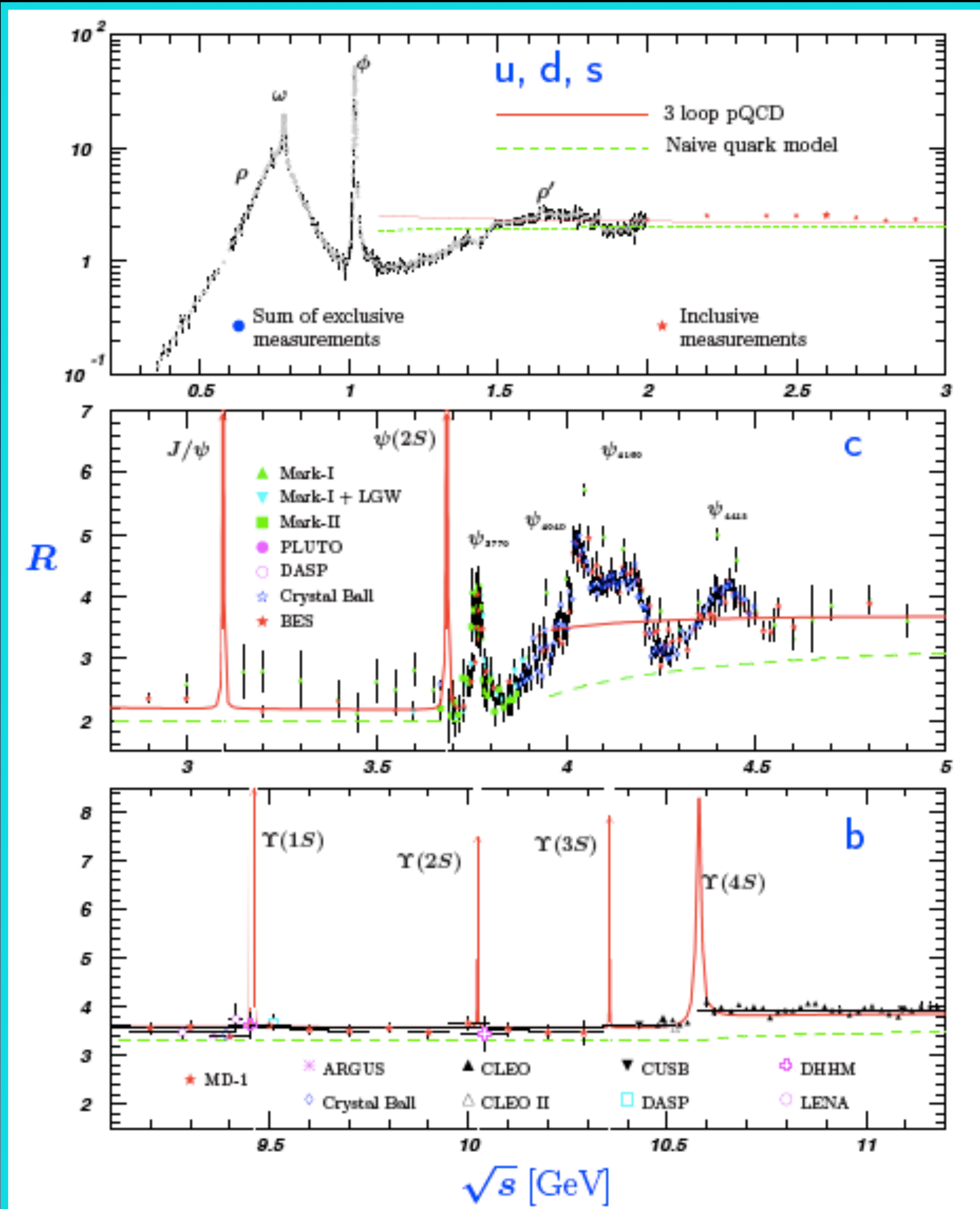

- Simple leading-order QCD (the green line) roughly describes the data.
- QCD at higher orders in the strong coupling (the red line, through N^3LO) does a very good job in describing the data (away from the resonance regions). We will calculate the QCD predictions through NLO.
- There are technical details associated with describing the resonances that we will not discuss in these lectures.

Example 1: e^+e^- to hadrons at NLO

(on the blackboard)

e^+e^- to hadrons at NLO: recap

- We have learned many interesting aspects of QCD by calculating the R-ratio at NLO in QCD.
- Both real and virtual corrections to the R-ratio have IR soft and collinear singularities that cancel in the sum (satisfying the KLN theorem).
- Regulating these singularities at intermediate steps was done by using dimensional regularization (work in $d=4-2\epsilon$). IR singularities appeared as double/single poles in ϵ. Dimensional regularization regulates both IR and UV singularities without introducing new scales to the calculation, while maintaining gauge symmetry.
- Only IR-safe observables can be calculated in perturbation theory.

Scale dependence

- If we calculate the R-ratio to $O(\alpha_s^2)$ we would find the following result:

$$\boxed{R = R_0(1 + \alpha_s/\pi + (\alpha_s/\pi)^2(c + \pi b_0 \ln \frac{\mu^2}{Q^2}) + \mathcal{O}(\alpha_s^3))}$$

where b_0 and c are μ-independent constants, $Q = \sqrt{s}$

- R is a physical observable that should not depend on the arbitrary scale μ. Given the log dependence on μ, R is only independent of μ if α_s is μ dependent.

$$\boxed{R = R_0(1 + \alpha_s(\mu)/\pi + (\alpha_s(\mu)/\pi)^2(c + \pi b_0 \ln \frac{\mu^2}{Q^2}) + \mathcal{O}(\alpha_s^3(\mu)))}$$

Renormalization group equations

- We can use the independence of R from μ to derive the renormalization group equation (RGE) for the R-ratio:

$$\boxed{\frac{dR(\mu^2,\alpha_s(\mu^2))}{d\mu^2} = 0 \;\Rightarrow\; \mu^2\frac{\partial R}{\partial \mu^2} + \beta_{QCD}(\alpha_s)\frac{\partial R}{\partial \alpha_s} = 0}$$

$$\beta_{QCD}(\alpha_s) = \mu^2\frac{\partial \alpha_s}{\partial \mu^2}$$

- We can use this equation to predict the μ dependence at higher orders:

$$\mu^2\frac{\partial R^{(2)}}{\partial \mu^2} = \frac{\beta_0}{4\pi}\alpha_s^2\frac{\partial R^{(1)}}{\partial \alpha_s}$$

(β0=b0); $\beta(\alpha_s) = -\alpha_s^2(b_0 + b_1\alpha_s + b_2\alpha_s^2 + \dots)$

$$\Rightarrow \quad R^{(2)} = \frac{\beta_0}{4}\left(\frac{\alpha_s}{\pi}\right)^2 R^{(0)}\ln\frac{\mu^2}{s} + \dots$$

terms without $\ln(\mu^2/s)$ that are not predicted by RGE

The beta function

- As we have seen earlier, the beta function has a perturbative expansion in αs:

$$\boxed{\beta = -\alpha_s^2(\mu)\sum_i b_i \alpha_s^i(\mu)}$$

$$b_0 = \frac{11N_c - 4n_f T_R}{12\pi};$$

$$b_1 = \frac{17N_c^2 - 5N_c n_f - 3C_F nf}{24\pi^2}$$

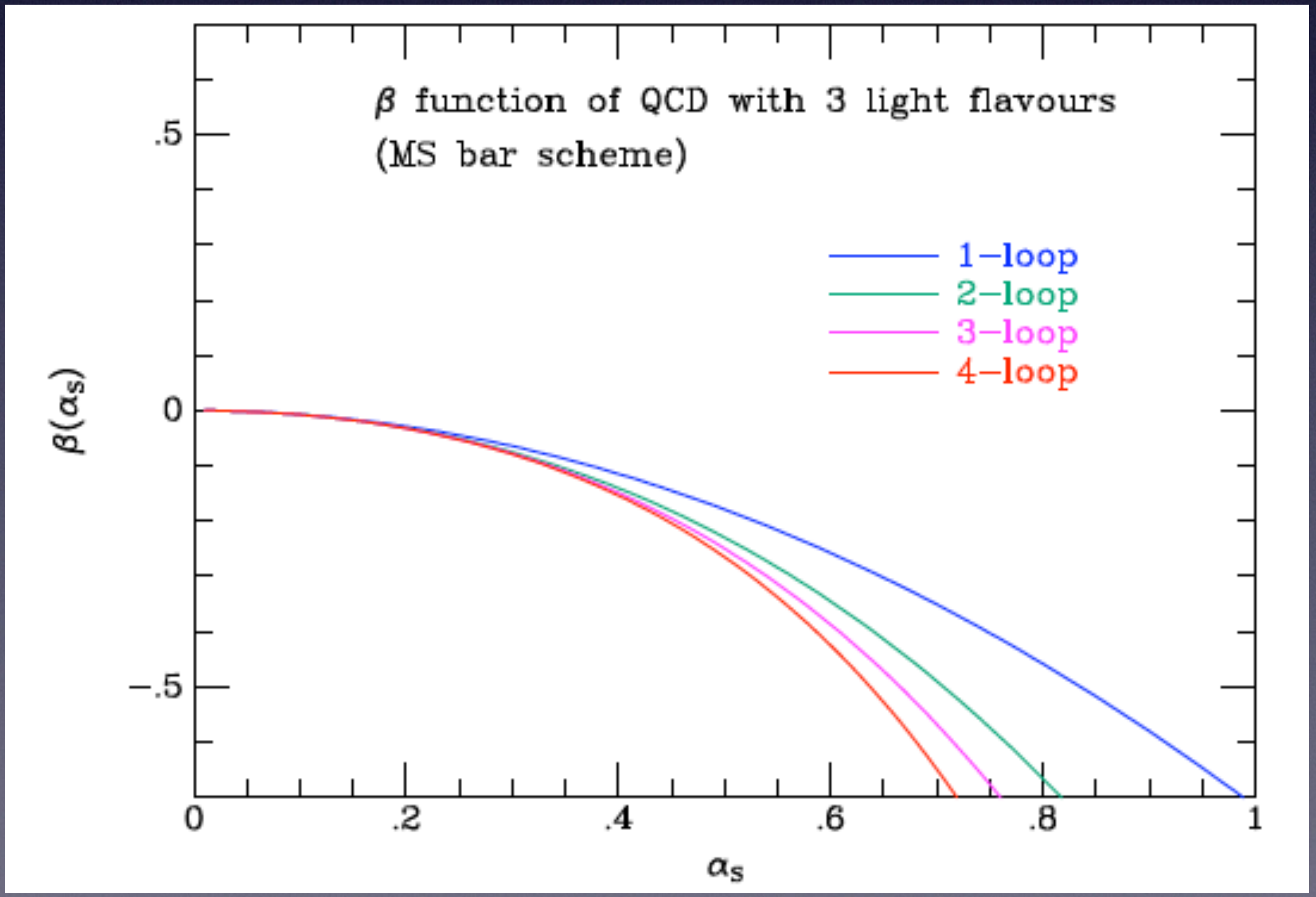

- nf is the number of active flavors, it depends on the scale Q
- Today, the beta function is known completely to 4-loops and partially at 5-loops.

Theoretical uncertainty

- Variation of the scale μ in some specified range is often used as an estimate of theoretical uncertainty. If our cross section was calculated to all orders, this dependence would vanish.

- The scale dependence is much flatter at NNLO than at NLO, leading to smaller uncertainty.

- The scale variation is only a rough guide to the uncertainty associated with the terms neglected in our perturbative expansion (ie missing higher order corrections).

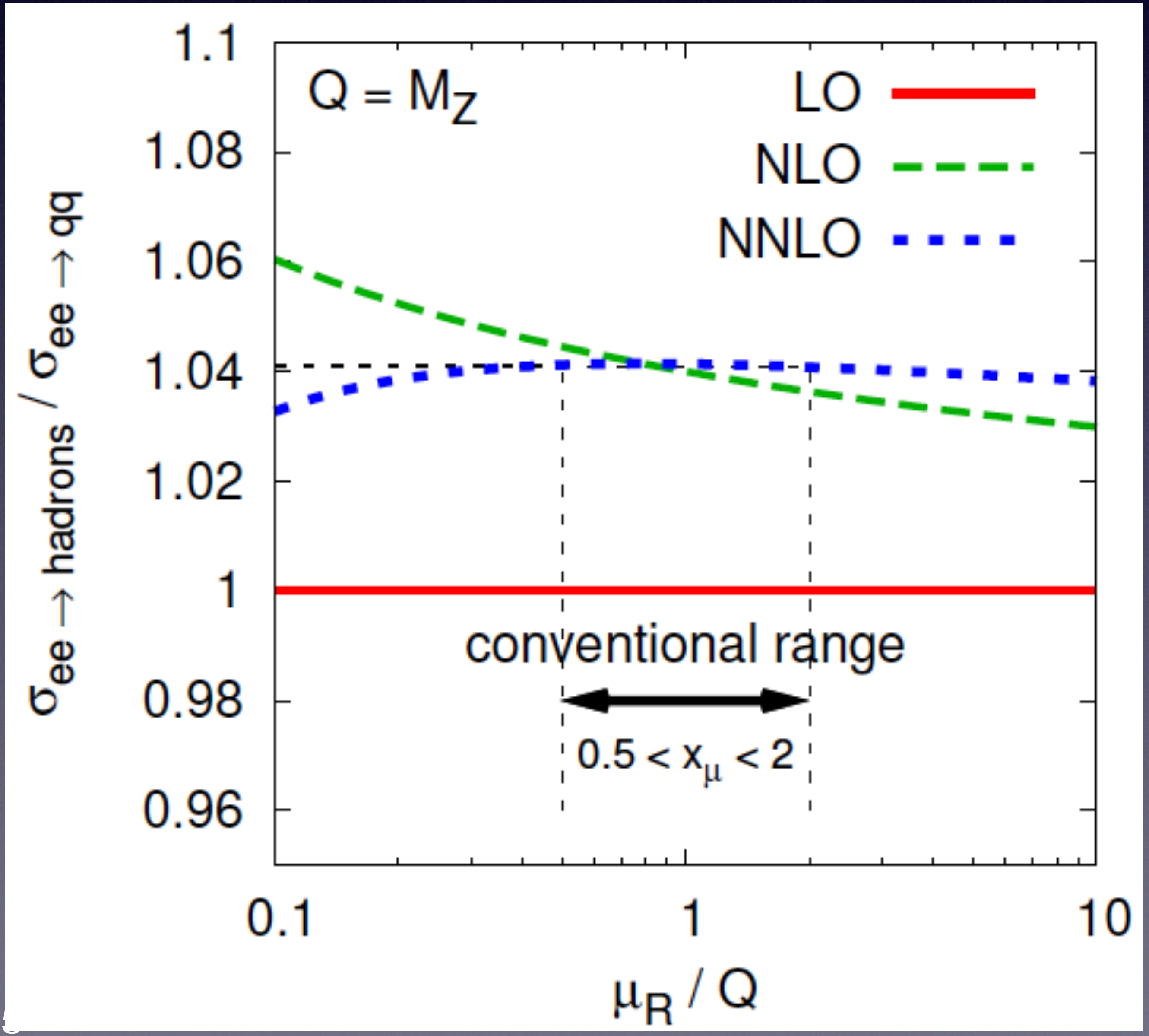

Eikonal approximation

- It is useful to have diagnostic tools to check pieces of a calculation. The eikonal approximation for soft gluons allows us to get the double pole.

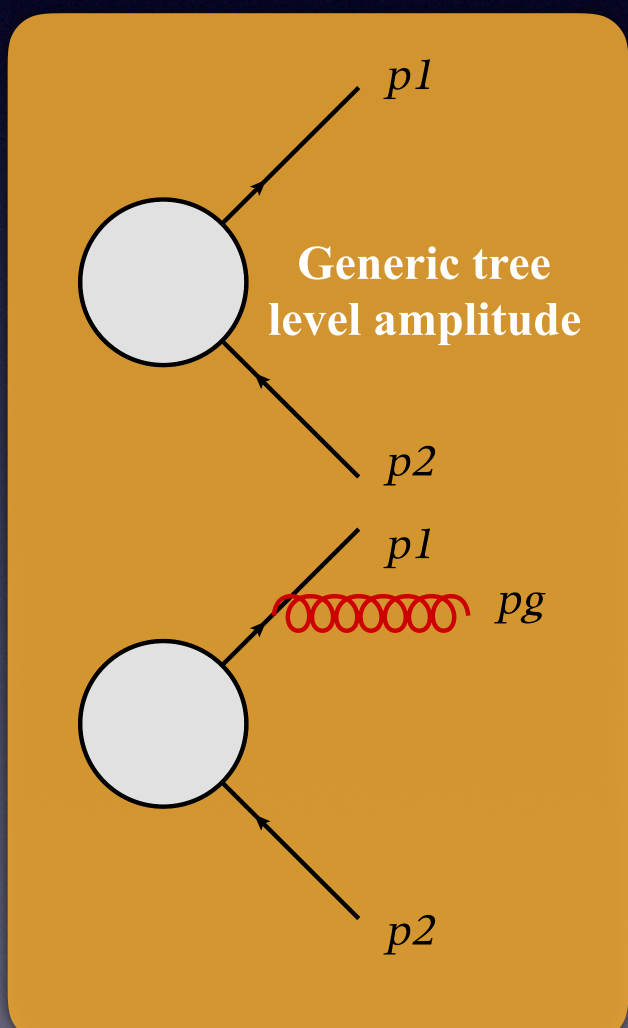

$$= \bar{u}^i(p_1)\left[i\mathcal{M}_0^{ij}\right] v^j(p_2)$$

i,j: color indices in the fundamental representation

$$\begin{aligned} &= \quad \bar{u}^i(p_1)\left\{ i g_s\, \not{\epsilon}_g^a T^a_{ij} \frac{i(\not{p}_1 + \not{p}_g)}{(p_1+p_g)^2}\left[i\mathcal{M}_0^{jk}\right]\right\} v^k(p_2) \\ &\approx \quad -g_s \frac{p_1\cdot\epsilon_g^a}{p_1\cdot p_g}\bar{u}^i(p_1)\left\{T^a_{ij}\left[i\mathcal{M}_0^{jk}\right]\right\} v^k(p_2) \end{aligned}$$

(drop p_g in the numerator and p_g^2 in the denominator)

- Real radiation amplitude is proportional to the lower-order amplitude, with a color correlation. Emission off the other leg also simplifies

Eikonal approximation

- It is useful to have diagnostic tools to check pieces of a calculation. The eikonal approximation for soft gluons allows us to get the double pole.

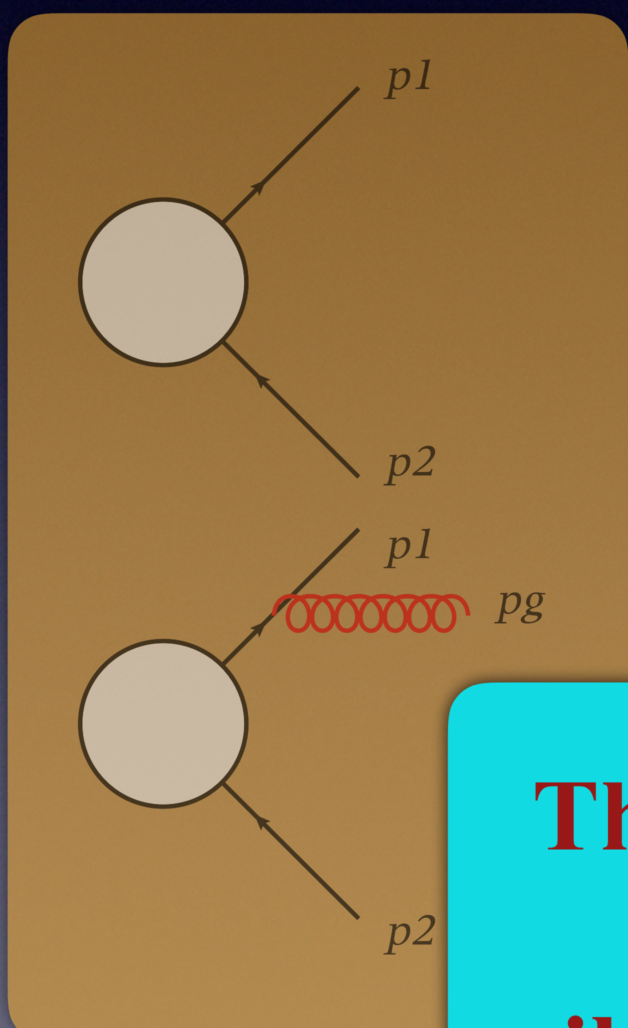

$$= \bar{u}^i(p_1)\left[i\mathcal{M}_0^{ij}\right] v^j(p_2)$$

i,j: color indices in the fundamental representation

$$= \bar{u}^i(p_1)\left\{ i g_s\, \not{\epsilon}_g^a T^a_{ij} \frac{i(\not{p}_1+\not{p}_g)}{(p_1+p_g)^2} \left[i\mathcal{M}_0^{jk}\right]\right\} v^k(p_2)$$

The real emission amplitude has *factorized* into the tree-level amplitude times an eikonal factor, with non-trivial correlations in color-space, in the soft limit

Eikonal approximation

- Phase space also factorizes, into the soft-gluon component times the remainder. Can derive simplified expressions for the cross section in this limit. For an arbitrary process:

sum over the hard colored states

$$d\sigma_s = \left[\frac{\alpha_s}{2\pi}\frac{\Gamma(1-\epsilon)}{\Gamma(1-2\epsilon)}\left(\frac{4\pi\mu^2}{s_{12}}\right)^{\epsilon}\right]\sum_{f,f'} d\sigma^0_{ff'}\int dS\,\frac{-p_f\cdot p_{f'}}{p_f\cdot p_s p_{f'}\cdot p_s}$$

p_s: momentum of soft gluon

partonic CM energy squared

from Harris & Owens hep-ph/0102128, a useful reference for relevant formulae

$$dS = \frac{1}{\pi}\left(\frac{4}{s_{12}}\right)^{-\epsilon}\int_0^{\delta_s\sqrt{s_{12}}/2} dE_s\, dc_\theta\, d\phi\, E_s^{1-2\epsilon} s_\theta^{-2\epsilon} s_\phi^{-2\epsilon}$$

δ_s restricts gluon energy to the soft region, it is a small number

Note that the cutoff δ_s restricts only the gluon energy. We are however integrating over all angles, and therefore collinear singularities can be present.

Eikonal approximation

- Phase space also factorizes, into the soft-gluon component times the remainder. Can derive simplified expressions for the cross section in this limit. For an arbitrary process:

sum over the hard colored states

$$d\sigma_s = \left[\frac{\alpha_s}{2\pi}\frac{\Gamma(1-\epsilon)}{\Gamma(1-2\epsilon)}\left(\frac{4\pi\mu^2}{s_{12}}\right)^{\epsilon}\right]\sum_{f,f'} d\sigma^0_{ff'}\int dS\,\frac{-p_f\cdot p_{f'}}{p_f\cdot p_s p_{f'}\cdot p_s}$$

p_s: momentum of soft gluon

partonic CM energy squared

from Harris & Owens **hep-ph/0102128**, a useful reference for relevant formulae

$$dS = \frac{1}{\pi}\left(\frac{4}{s_{12}}\right)^{-\epsilon}\int_0^{\delta_s\sqrt{s_{12}}/2} dE_s\, dc_\theta\, d\phi\, E_s^{1-2\epsilon} s_\theta^{-2\epsilon} s_\phi^{-2\epsilon}$$

δ_s restricts gluon energy to the soft region, it is a small number

$$|\mathcal{M}_{ff'}|^2 = \left[\mathcal{M}_{c_1\ldots b_f\ldots b_{f'}\ldots c_n}\right]^* T^a_{b_f d_f} T^a_{b_{f'} d_{f'}} \mathcal{M}_{c_1\ldots d_f\ldots d_{f'}\ldots c_n}$$

general structure of the factorized real emission amplitude squared

Eikonal approximation

- Applying the eikonal approximation to the current process yields:

$$R^{q\bar{q}g}_{1,soft} = R_0 \times \frac{\alpha_s C_F}{\pi} \frac{\Gamma(1-\epsilon)}{\Gamma(1-2\epsilon)} \left(\frac{s}{4\pi\mu^2}\right)^{-\epsilon} \left\{ \frac{1}{\epsilon^2} - \frac{2}{\epsilon} \ln \delta_s + 2 \ln^2 \delta_s + \text{finite} \right\}$$

agrees with our full calculation

Cutoff dependence must cancel against other regions of gluon phase space

- The $1/\varepsilon^2$ must cancel against virtual corrections.

- The cutoff dependence must cancel against the collinear and hard regions. We will write down the collinear approximation. The hard region can be calculated numerically as it is finite.

Collinear approximation

- Another singular region to consider is collinear gluon emission. We can study the region $p_1 || p_g$ using a sudakov parametrization of the momenta (see Catani-Grazzini, hep-ph/9810389):

$$p_1^\mu = zp^\mu + k_\perp^\mu - \frac{k_\perp^2}{z}\frac{n^\mu}{2p\cdot n},$$
$$p_g^\mu = (1-z)p^\mu - k_\perp^\mu - \frac{k_\perp^2}{1-z}\frac{n^\mu}{2p\cdot n}$$

p: collinear direction; $k_\perp$: transverse momentum to p

$$z = \frac{E_1}{E_1+E_g}, \quad s_{1g} = -\frac{k_\perp^2}{z(1-z)}$$

- S_{1g} vanishes when $k_\perp \to 0$, this is the singular limit. p and n are light-like vectors satisfying $p.k_\perp = 0 = n.k_\perp$. The amplitude simplifies in this limit:

$$|\mathcal{M}_1(p_1,p_2,p_g)|^2 \approx \frac{2}{s_{1g}} g_s^2 \mu^{2\epsilon} P_{qq}(z,\epsilon)\, |\mathcal{M}_0(p_1+p_g,p_2)|^2$$
$$P_{qq}(z,\epsilon) = C_F\left[\frac{1+z^2}{1-z} - \epsilon(1-z)\right]$$

Collinear approximation

- The phase space also simplifies in this limit. We get the following contribution to the NLO R-ratio from the $p_1||p_g$ region:

$$R^{q\bar{q}g}_{1,1||g} = R_0 \times \frac{\alpha_s}{2\pi}\frac{C_F}{\Gamma(1-\epsilon)}\left[\frac{s}{4\pi\mu^2}\right]^{-\epsilon}\int_{1-\delta_c}^{1} dx_2\,(1-x_2)^{-1-\epsilon}\int_0^{1-\delta_s} dz\,[z(1-z)]^{-\epsilon}\,P_{qq}(z,\epsilon)$$

$$= R_0 \times \frac{\alpha_s}{2\pi}\frac{C_F}{\Gamma(1-\epsilon)}\left[\frac{s}{4\pi\mu^2}\right]^{-\epsilon}\left\{\frac{1}{\epsilon}\left(\frac{3}{2}+2\ln\delta_s\right)-\ln^2\delta_s-\frac{3}{2}\ln\delta_c-2\ln\delta_s\ln\delta_c+\text{finite}\right\}$$

agrees with our full calculation

$\cos(\theta) = 2\,x_2 - 1$

δc is a cutoff that restricts the integration to the collinear region $p_1||p_g$. The z integral is restricted at $1-\delta s$ to prevent the gluon energy from extending into the soft region; we don't want to double-count the contribution from the soft gluons already included in the eikonal approximation.

Collinear approximation

- The phase space also simplifies in this limit. We get the following contribution to the NLO R-ratio from the $p_1||p_g$ region:

$$R^{q\bar{q}g}_{1,1||g} = R_0 \times \frac{\alpha_s}{2\pi}\frac{C_F}{\Gamma(1-\epsilon)}\left[\frac{s}{4\pi\mu^2}\right]^{-\epsilon}\int_{1-\delta_c}^{1} dx_2\,(1-x_2)^{-1-\epsilon}\int_0^{1-\delta_s} dz\,[z(1-z)]^{-\epsilon}\,P_{qq}(z,\epsilon)$$

$$= R_0 \times \frac{\alpha_s}{2\pi}\frac{C_F}{\Gamma(1-\epsilon)}\left[\frac{s}{4\pi\mu^2}\right]^{-\epsilon}\left\{\frac{1}{\epsilon}\left(\frac{3}{2}+2\ln\delta_s\right)-\ln^2\delta_s-\frac{3}{2}\ln\delta_c-2\ln\delta_s\ln\delta_c+\text{finite}\right\}$$

agrees with our full calculation

- There is an identical contribution from the region $p_2||p_g$, so we just multiply the above result by a factor of 2.
- Adding the collinear contributions to the soft region cancels the cutoff dependence in the poles and reproduces the poles of the full result.
- The remaining cutoff dependence cancels against the hard region of the phase space which is finite and can be handled numerically in 4 dimensions.

Subtraction Schemes @ NLO

- The splitting functions and eikonal factors are universal. They can be used to predict the poles for any process. This forms the basis for various subtraction schemes that handle IR singularities.

Phase-space slicing, Harris, Owens hep-ph/0102128;

Dipole subtraction, Catani, Seymour hep-ph/9605323;

FKS, Frixione, Kunszt, Signer hep-ph/9512328

Where to next?

We have so far focused on aspects of QCD in the final state, for processes with leptonic initial state. What happens when we have more complicated initial states involving hadrons?

Hadronic cross sections

- We have shown earlier the factorization formula for a hard process in hadron-hadron collisions:

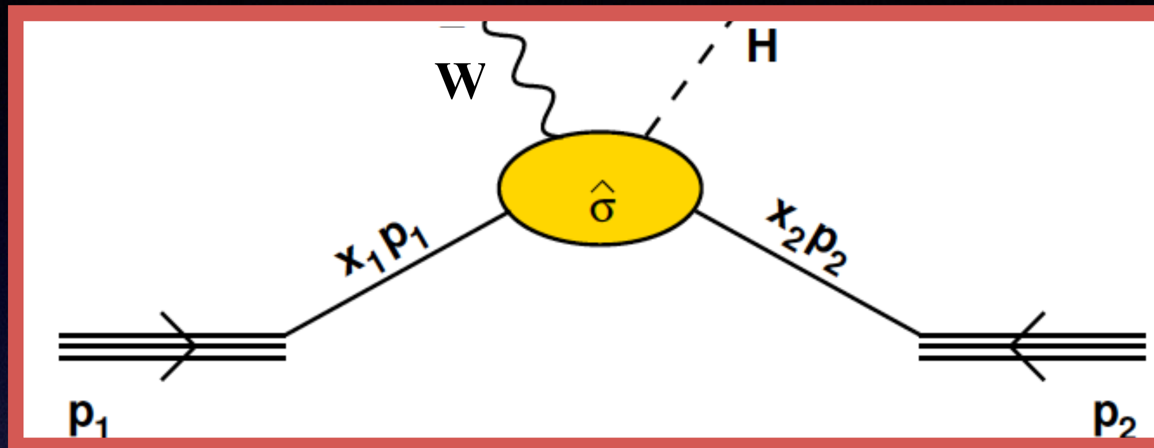

$$\sigma = \sum_{i,j} \int dx_1 f_{i/p}(x_1, \mu_F^2) \int dx_2 f_{\bar{j}/\bar{p}}(x_2, \mu_F^2)\, \hat{\sigma}_{ij}(\hat{s}, \mu_R^2, \mu_F^2)\,, \quad \hat{s} = x_1 x_2 s$$

PDFs: universal, extracted from data

partonic cross section: process dependent, calculated perturbatively

- Knowing the PDFs allows us to compare the predicted hadronic cross section with the measured one. This would also be a test of our framework for computing the partonic cross section.

Hadronic cross sections

- We have shown earlier the factorization formula for a hard process in hadron-hadron collisions:

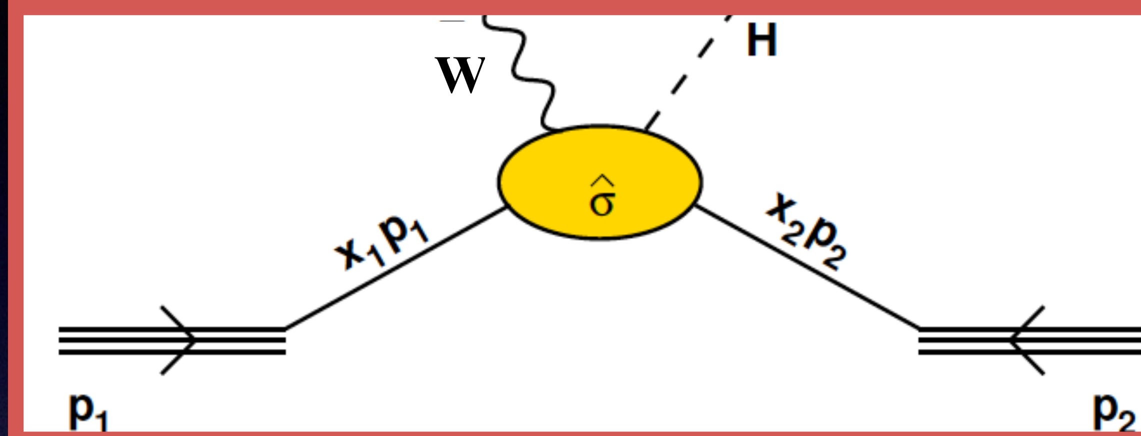

$$\sigma = \sum_{i,j} \int dx_1 f_{i/p}(x_1, \mu_F^2) \int dx_2 f_{\bar{j}/\bar{p}}(x_2, \mu_F^2)\, \hat{\sigma}_{ij}(\hat{s}, \mu_R^2, \mu_F^2)\,, \qquad \hat{s} = x_1 x_2 s$$

PDFs: universal, extracted from data

partonic cross section: process dependent, calculated perturbatively

- Kn … nic cro … st of ou …

How do we extract the PDFs from data?

Deep Inelastic Scattering

- To understand this aspect, lets look at a simpler process with just one hadronic initial state: DIS - the scattering of a lepton on a proton.
- DIS is still one of the most important processes to extract information about PDFs (ep at DESY).

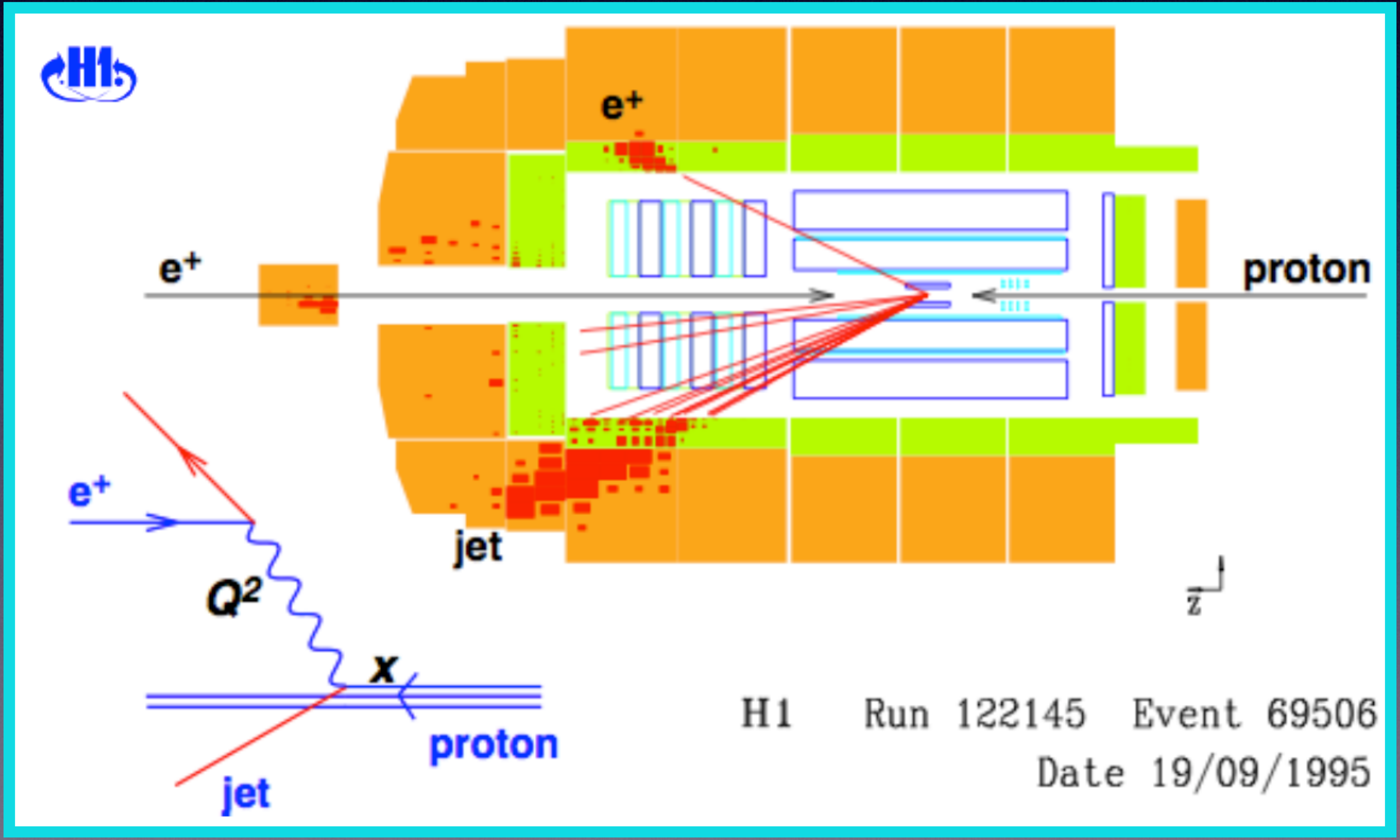

Deep Inelastic Scattering

- To understand this aspect, lets look at a simpler process with just one hadronic initial state: DIS - the scattering of a lepton on a proton.
- DIS is still one of the most important processes to extract information about PDFs (ep at DESY).

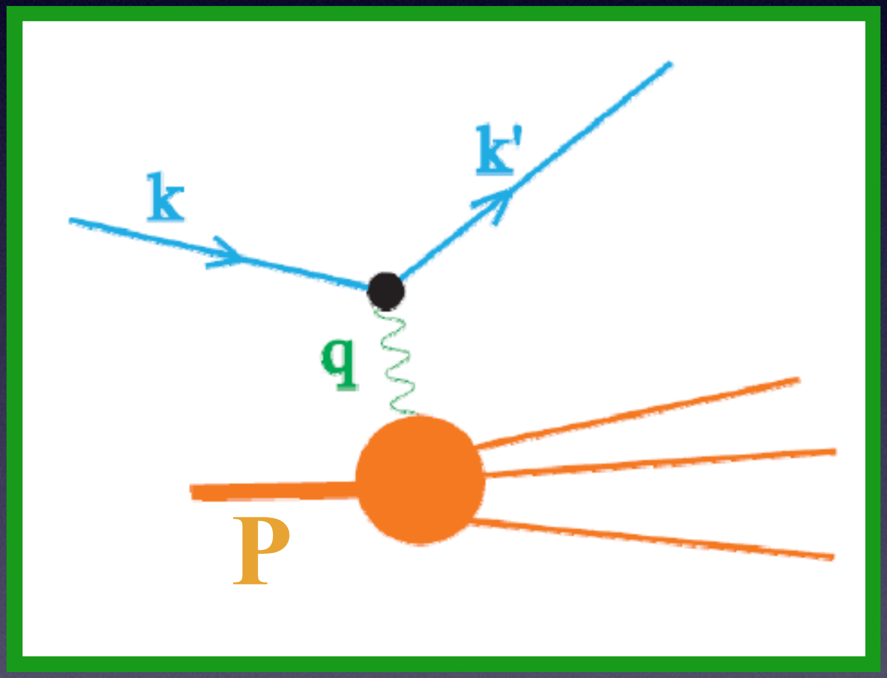

$$
\begin{aligned}
q^\mu &= k^\mu - k'^\mu \\
Q^2 &= -q^2 \\
x &= \frac{Q^2}{2P\cdot q} \\
y &= \frac{P\cdot q}{P\cdot k} \overset{lab}{=} \frac{E-E'}{E}
\end{aligned}
$$

P: proton momentum

Q^2: photon virtuality, ie transverse resolution at which it probes proton structure

x: longitudinal momentum fraction of struck parton in proton

y: momentum fraction lost by the electron (in proton rest frame)

Deep Inelastic Scattering

- To understand this aspect, lets look at a simpler process with just one hadronic initial state: DIS - the scattering of a lepton on a proton.
- DIS is still one of the most important processes to extract information about PDFs (ep at DESY).

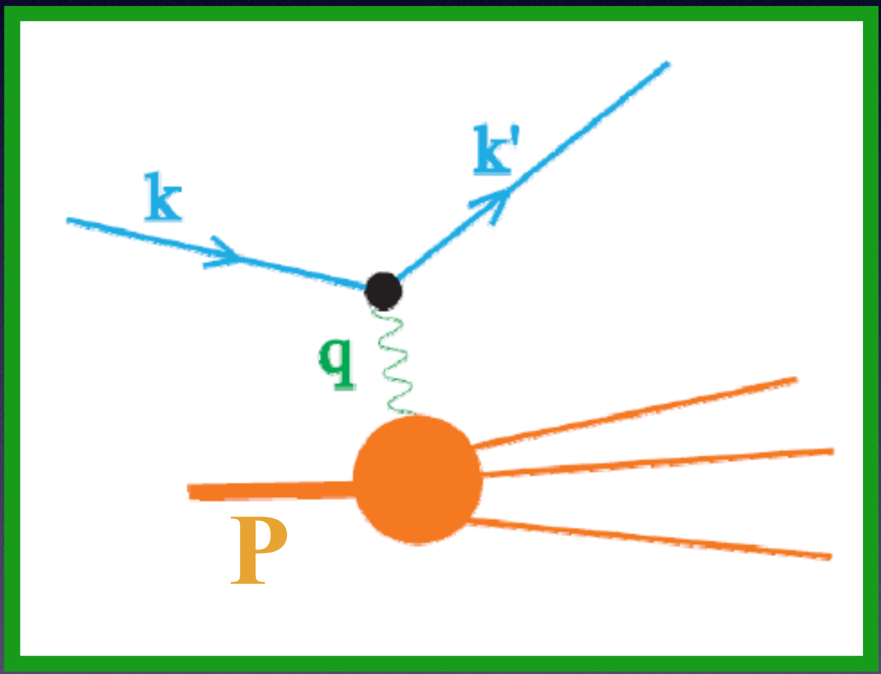

$$\begin{aligned} q^\mu &= k^\mu - k'^\mu \\ Q^2 &= -q^2 \\ x &= \frac{Q^2}{2P\cdot q} \\ y &= \frac{P\cdot q}{P\cdot k} \stackrel{lab}{=} \frac{E-E'}{E} \end{aligned}$$

$$d\sigma = \frac{4\alpha^2}{s}\frac{d^3\vec{k}'}{2|\vec{k}'|}\frac{1}{Q^4}L^{\mu\nu}(k,q)W_{\mu\nu}(p,q)$$

phase space scat. lepton

photon propagator²

leptonic tensor

hadronic tensor contains information about hadronic structure

s : C.M.E^2

$L_{\mu\nu}$: QED leptonic tensor

(obtained from squaring the upper part of the Feynman diagram)

DIS: hadronic tensor

- Hermiticity ($W_{\mu\nu}^\dagger = W_{\mu\nu}$), current conservation ($q^\mu W_{\mu\nu} = 0$) and parity invariance (in this case absence of $\varepsilon_{\mu\nu\rho\sigma}$) allow us to simplify $W_{\mu\nu}$:

$$W_{\mu\nu} = \left\{ g_{\mu\nu} - \frac{q_\mu q_\nu}{q^2} \right\} F_1(x, Q^2) + \left\{ P_\mu + \frac{q_\mu}{2x} \right\} \left\{ P_\nu + \frac{q_\nu}{2x} \right\} \frac{F_2(x, Q^2)}{P \cdot q}$$

Structure functions

$$\frac{d\sigma}{dx\, dQ^2} = \frac{4\pi\alpha^2}{Q^4} \left\{ \left[1 + (1-y)^2\right] F_1 + \frac{1-y}{x} \left[F_2 - 2x\, F_1\right] \right\}$$

- Parton model: electromagnetic (EM) current interacts with proton via point-like interactions with partons inside the proton ($p_{parton} = \xi P$).

DIS: hadronic tensor

- Hermiticity ($W_{\mu\nu}^\dagger = W_{\mu\nu}$), current conservation ($q^\mu W_{\mu\nu} = 0$) and parity invariance (in this case absence of $\varepsilon_{\mu\nu\rho\sigma}$) allow us to simplify $W_{\mu\nu}$:

$$W_{\mu\nu} = \left\{ g_{\mu\nu} - \frac{q_\mu q_\nu}{q^2} \right\} F_1(x, Q^2) + \left\{ P_\mu + \frac{q_\mu}{2x} \right\} \left\{ P_\nu + \frac{q_\nu}{2x} \right\} \frac{F_2(x, Q^2)}{P \cdot q}$$

Structure functions

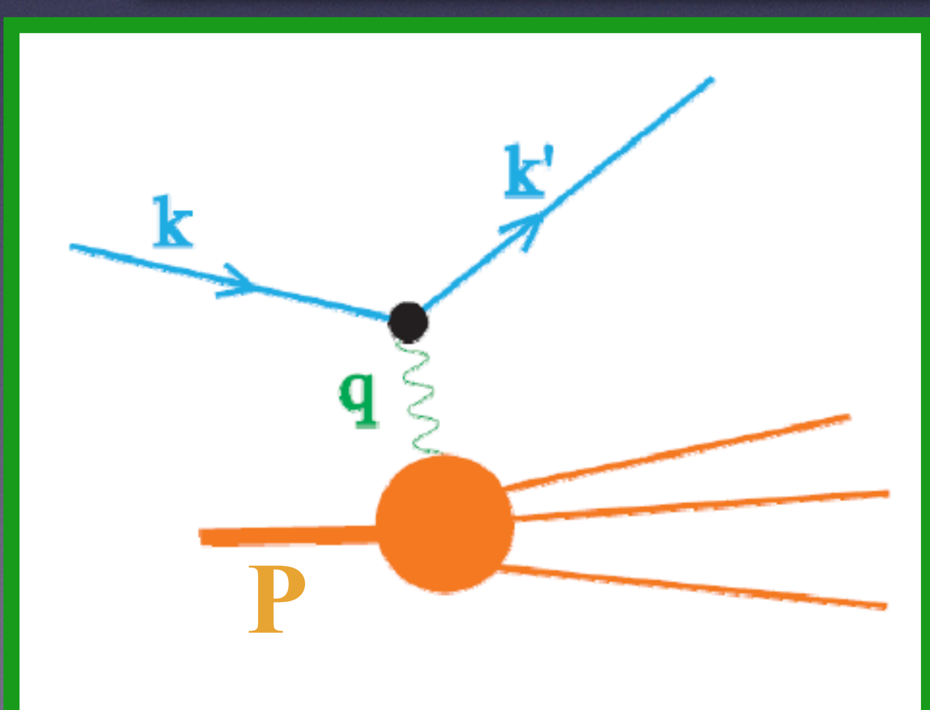

$1 + (1 - y)^2]\ F_1 + \frac{1}{}$

Parton model

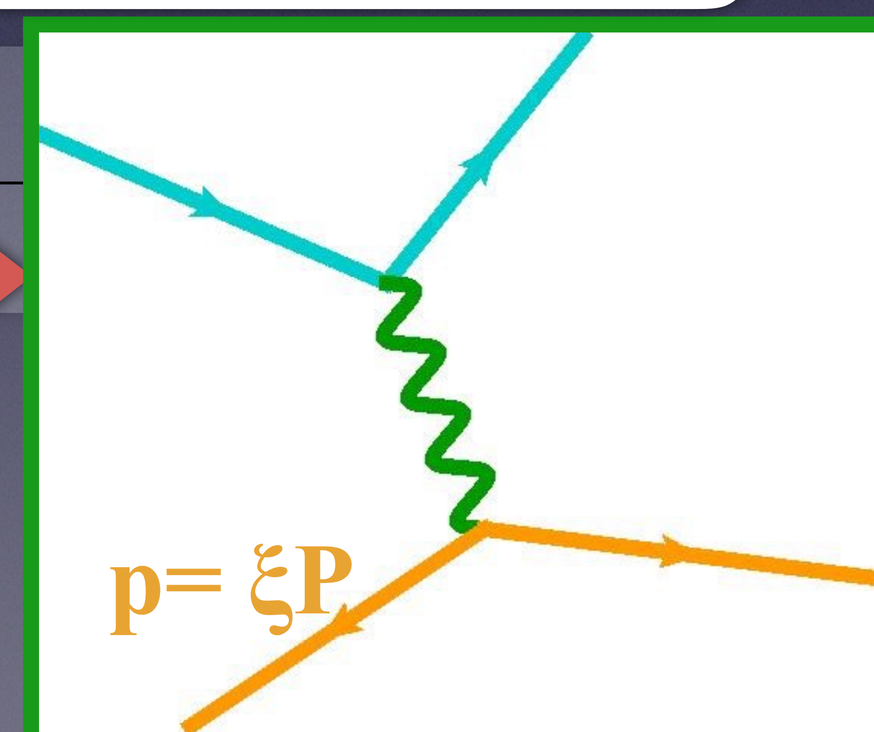

DIS: hadronic tensor

- Hermiticity ($W_{\mu\nu}^{\dagger} = W_{\mu\nu}$), current conservation ($q^{\mu} W_{\mu\nu} = 0$) and parity invariance (in this case absence of $\varepsilon_{\mu\nu\rho\sigma}$) allow us to simplify $W_{\mu\nu}$:

$$W\mu\nu = \left\{ g_{\mu\nu} - \frac{q_\mu q_\nu}{q^2} \right\} F_1(x, Q^2) + \left\{ P_\mu + \frac{q_\mu}{2x} \right\} \left\{ P_\nu + \frac{q_\nu}{2x} \right\} \frac{F_2(x, Q^2)}{P \cdot q}$$

Structure functions

F1(x,Q^2) and F2(x,Q^2) are related through the Callan-Gross relation which is valid in the parton model:

$$2\, x\, F1(x,\ Q\char`^2) = F2(x,Q\char`^2)$$

Calculating the structure function F_2

- We will calculate the structure function F2. We can obtain it by applying the following projection operator to $W_{\mu\nu}$

$$
\begin{aligned}
F_2 &= R^{\mu\nu} W_{\mu\nu} \\
R^{\mu\nu} &= \frac{2x}{d-2} \left\{ g^{\mu\nu} - 4\,(d-1)\,\frac{x^2}{Q^2} P^\mu P^\nu \right\}
\end{aligned}
$$

- We just need to calculate the following LO diagram (single quark in the final state):

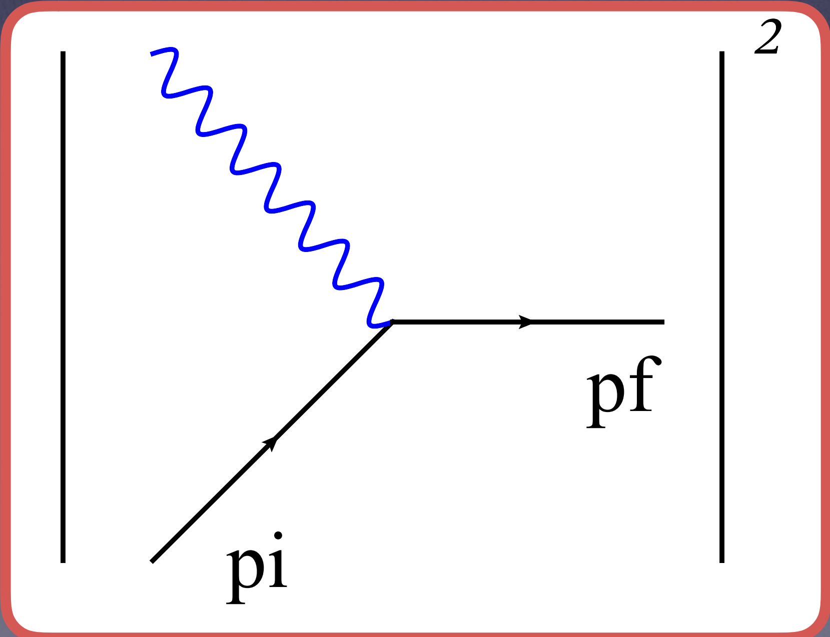

Momenta parametrization (Breit frame)

$$
\begin{aligned}
P^\mu &= \frac{Q}{2x}\left(1, \vec{0}, 1\right) \\
p_i^\mu = p^\mu &= \frac{\xi Q}{2x}\left(1, \vec{0}, 1\right) \\
q^\mu &= \left(0, \vec{0}, -Q\right)
\end{aligned}
$$

Calculating the structure function F_2

- We will calculate the structure function F2. We can obtain it by applying the following projection operator to $W_{\mu\nu}$

$$
\begin{aligned}
F_2 &= R^{\mu\nu} W_{\mu\nu} \\
R^{\mu\nu} &= \frac{2x}{d-2} \left\{ g^{\mu\nu} - 4\,(d-1)\,\frac{x^2}{Q^2} P^\mu P^\nu \right\}
\end{aligned}
$$

- We just need to calculate the following LO diagram (single quark in the final state):

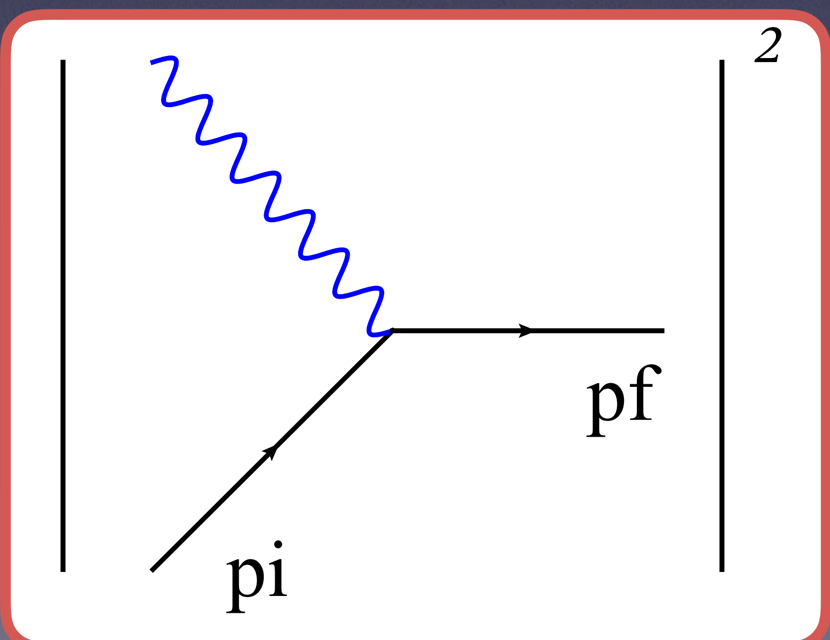

- Derive the following phase-space expression:

$$
\begin{aligned}
PS &= \int \frac{d^d p_f}{(2\pi)^{d-1}} \delta(p_f^2)(2\pi)^d \delta^{(d)}(q + p - p_f) \\
&= \frac{2\pi}{Q^2} \delta\left(1 - \frac{x}{\xi}\right)
\end{aligned}
$$

Note: virtual corrections will have the same phase-space. Needed later.

Calculating the structure function F_2

- We will calculate the structure function F2. We can obtain it by applying the following projection operator to $W_{\mu\nu}$

$$\boxed{\begin{aligned} F_2 &= R^{\mu\nu} W_{\mu\nu} \\ R^{\mu\nu} &= \frac{2x}{d-2}\left\{ g^{\mu\nu} - 4\,(d-1)\frac{x^2}{Q^2} P^\mu P^\nu \right\} \end{aligned}}$$

- We just need to calculate the following LO diagram (single quark in the final state):

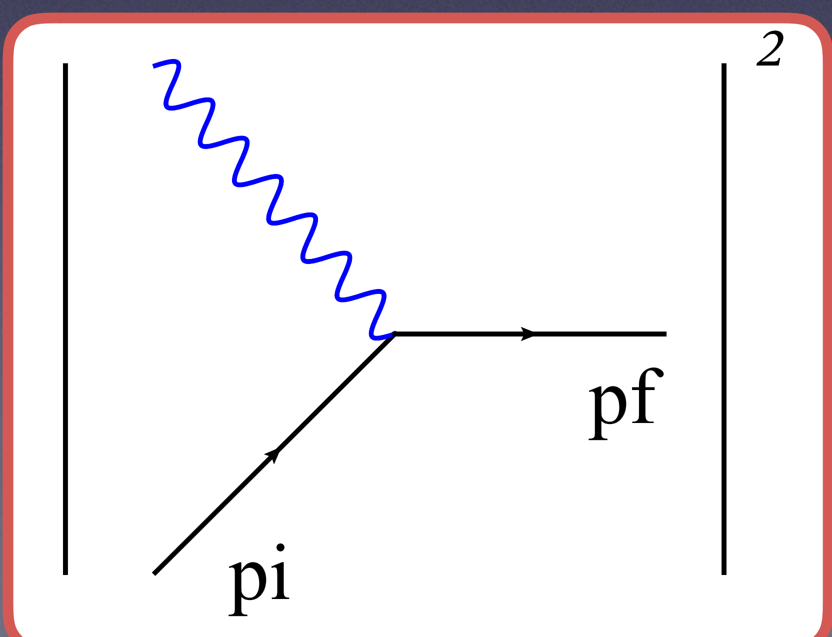

- Obtain the structure function:

$$F_2 = \frac{1}{4\pi}\int \frac{d\xi}{\xi} \sum_q f_q(\xi) \times \frac{PS}{2N} \times R^{\mu\nu} \times W_{\mu\nu}$$

$$= \sum_q e^2 Q_q^2 \int d\xi\, f_q(\xi)\, \xi\, \delta(x-\xi)$$

$$= \sum_q e^2 Q_q^2\, x\, f_q(x)$$

color+spin averaging for initial state quark. N=3

Scaling

$$\boxed{F_2(x) = \sum_q e^2 Q_q^2 \, x \, f_q(x)}$$

The LO prediction we have calculated shows no dependence on the virtuality of the photon Q^2. Is this consistent with data?

Scaling

$$\boxed{F_2(x) = \sum_q e^2 Q_q^2\, x\, f_q(x)}$$

The LO prediction we have calculated shows no dependence on the virtuality of the photon Q^2. Is this consistent with data?

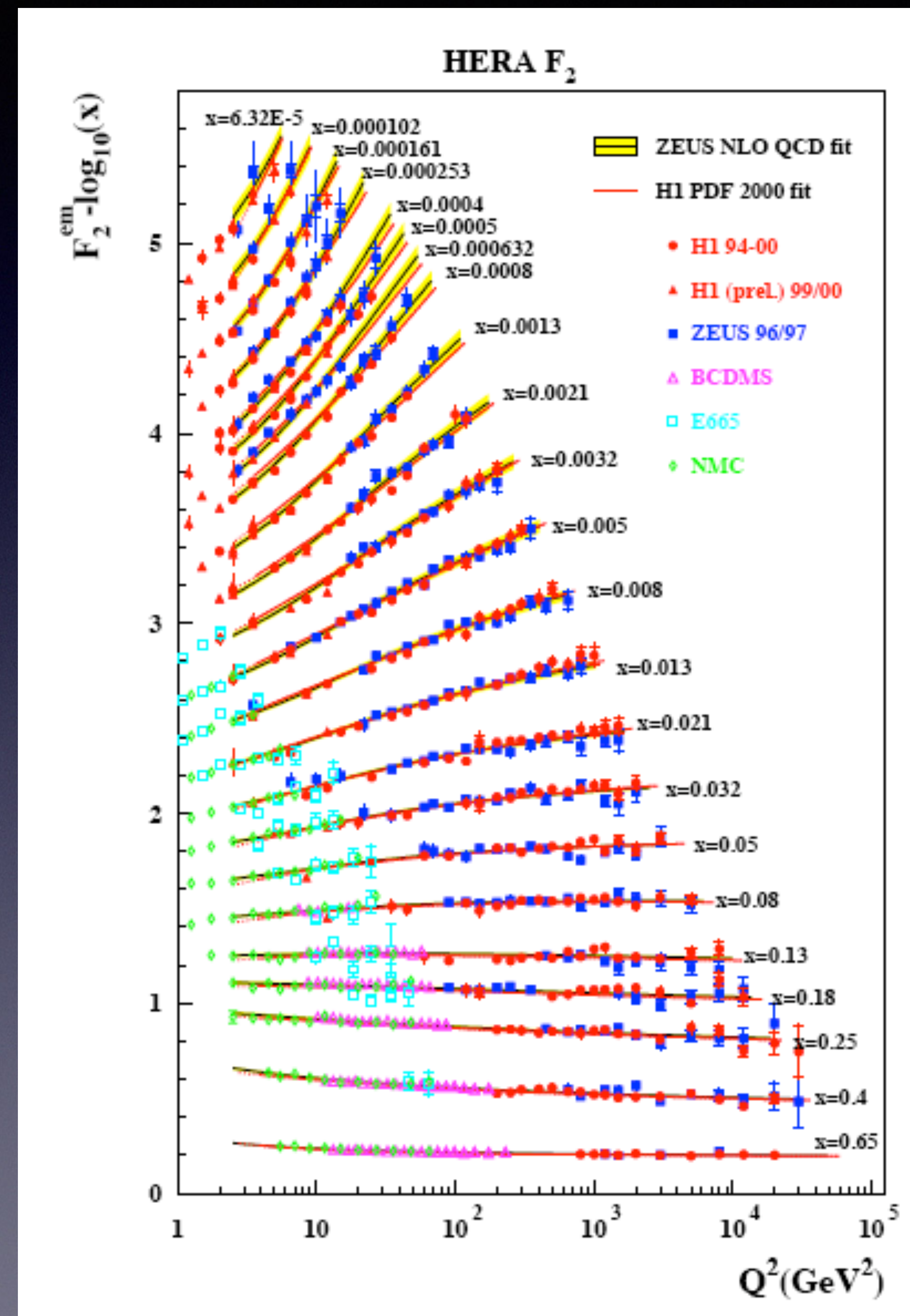

Scaling

$$\boxed{F_2(x) = \sum_q e^2 Q_q^2 \, x \, f_q(x)}$$

The LO prediction we have calculated shows no dependence on the virtuality of the photon Q^2. Is this consistent with data?

No. Data shows variation of F_2 with Q^2. Can higher order QCD predict this behavior?

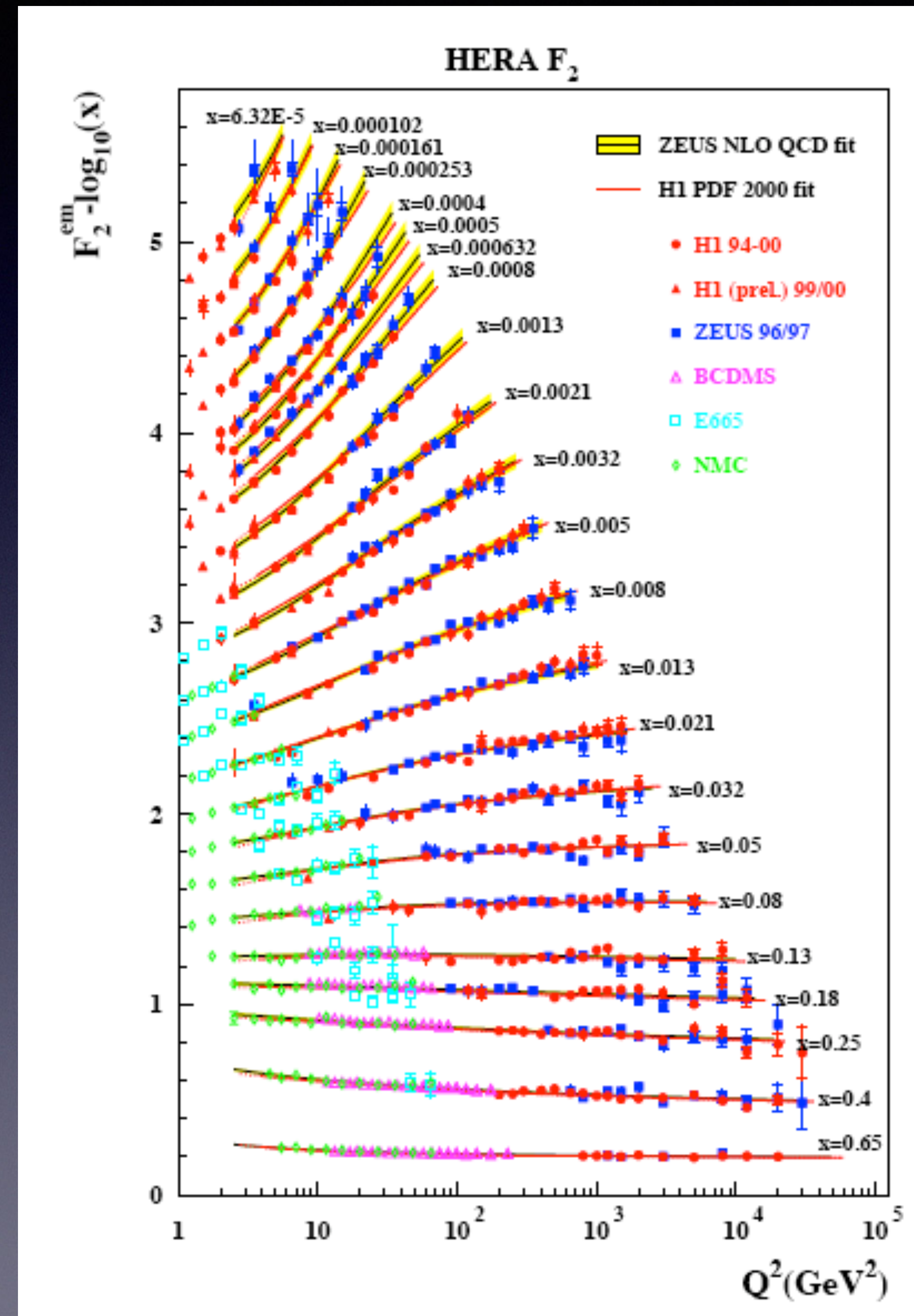

Real-emission phase space for F_2

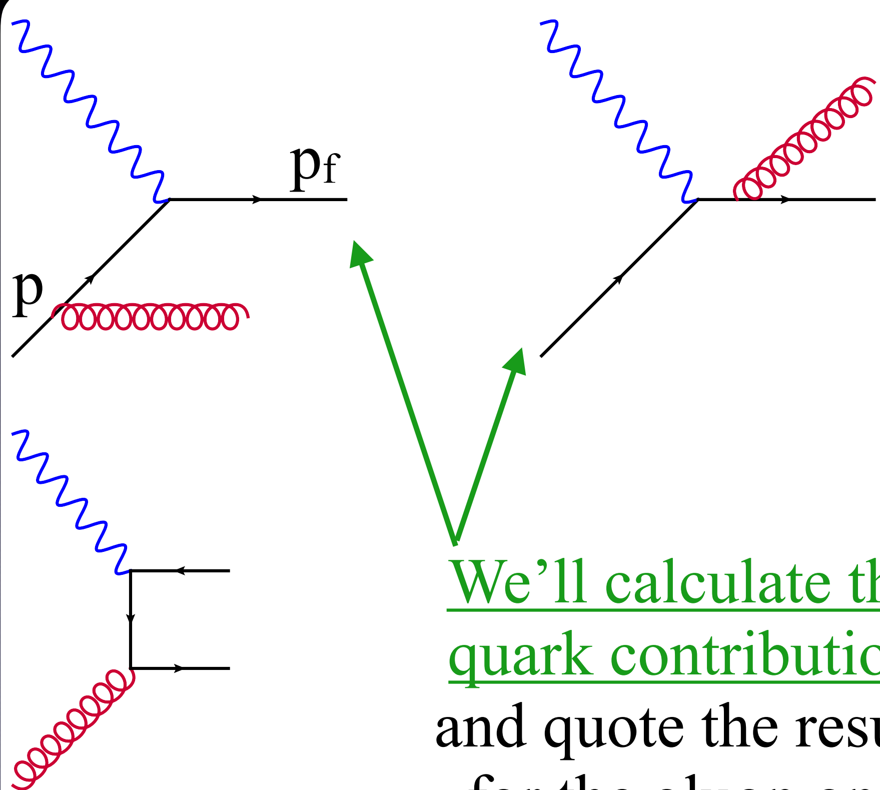

We'll calculate the quark contribution and quote the result for the gluon one

$$PS = \frac{1}{(2\pi)^{d-2}} \int d^d p_f d^d p_g \delta(p_g^2)\delta(p_f^2)\delta^{(d)}(q+p-p_f-p_g)$$
$$= \frac{1}{(2\pi)^{d-2}} \int ds_{pg} \int d^d p_f d^d p_g \delta(p_g^2)\delta(p_f^2)\delta(s_{pg}+2p\cdot p_g)\delta^{(d)}(q+p-p_f-p_g)$$

parametrize p_g as $p_g = (E, pT, 0, k)$; use delta functions to remove the E, pT and k integrations.

Set $s_{pg} = -Q^2 \xi z/x$, which defines z, to derive:

$$PS = \frac{\Omega(d-2)}{4(2\pi)^{d-2}} \int_0^1 dz \left[Q^2 z(1-z)\frac{\xi}{x}\left(1-\frac{x}{\xi}\right)\right]^{-\epsilon}$$
$$p\cdot p_g = \frac{\xi}{2x} Q^2 z$$
$$p_f\cdot p_g = \frac{\xi}{2x} Q^2 \left(1-\frac{x}{\xi}\right)$$

Real-emission matrix elements for F_2

- The spin, color summed/averaged + projected matrix elements:

$$|\bar{\mathcal{M}}|^2 = 4\, C_F\, e^2 Q_q^2\, g_s^2 \mu^{2\epsilon} \left\{ \frac{p_f \cdot p_g}{p \cdot p_g} + \frac{p \cdot p_g}{p_f \cdot p_g} + \frac{Q^2 p \cdot p_f}{p_f \cdot p_g\, p \cdot p_g} + \underbrace{\ldots}_{\text{finite terms}} \right\}$$

- The real emission contribution of quark diagrams is then:

$$\begin{aligned} F_{2,q}^{(1),real} &= e^2 Q_q^2\, x\, \frac{\alpha_s}{2\pi} \frac{1}{\Gamma(1-\epsilon)} \left[\frac{Q^2}{4\pi\mu^2}\right]^{-\epsilon} \int_x^1 \frac{d\xi}{\xi} f_q(\xi) \\ &\times \left(\frac{x}{\xi}\right)^{\epsilon} \left(1 - \frac{x}{\xi}\right)^{-\epsilon} \left\{ -\frac{C_F}{\epsilon} \frac{1 + (x/\xi)^2}{1 - x/\xi} - 2C_F \frac{x/\xi}{1 - x/\xi} + \ldots \right\} \end{aligned}$$

This term is bad news, no way it can cancel against virtual correction, which go like $\delta(x-\xi)$

Looks like P_{qq} $\Rightarrow$ collinear singularity

Notice the singularity when $x = \xi \Rightarrow$ soft singularity

Factorization of IR singularities

- The $1/\epsilon$ pole that is not proportional to $\delta(x-\xi)$ originates from initial-state collinear emission. This pole needs to be absorbed into the PDF. We need to redo the calculation replacing the PDF function f_q with the bare one $f_{q,0}$. Choose the bare PDF to remove the $1/\varepsilon$ pole.

- Make soft singularity at $x=\xi$ manifest with plus distribution expansion. This expansion leads to a double pole in the real emission.

- Must also add virtual corrections, this removes the double pole in the real emission.

$$\boxed{\left(1-\frac{x}{\xi}\right)^{-1-\epsilon} = -\frac{1}{\epsilon}\delta\left(1-\frac{x}{\xi}\right)+\frac{1}{[1-x/\xi]_+}+\mathcal{O}(\epsilon)}$$

Factorization of IR singularities

- We will perform this \`mass factorization' step-by-step. First we define a *plus distribution*

$$\int_0^1 dx\, f(x)\, [g(x)]_+ = \int_0^1 dx\, g(x)\, [f(x) - f(0)]$$

if g(x)=1/x, it removes singularities at x=0

- After adding virtual corrections (which can be obtained from e+e- virtual corrections upon crossing symmetry) and rearranging terms, our result for the divergent part of F_2 is:

$$F_{2,q} = e^2 Q_q^2\, x \int_x^1 \frac{d\xi}{\xi} f_{q,0}(\xi) \left\{ \delta(1 - x/\xi) + \frac{\alpha_s}{2\pi\Gamma(1-\epsilon)} \left[\frac{Q^2}{4\pi\mu^2}\right]^{-\epsilon} \left[-\frac{1}{\epsilon} P_{qq}(x/\xi) + \text{finite} \right] \right\}$$

$$P_{qq}(x) = C_F \left[\frac{1+x^2}{[1-x]_+} + \frac{3}{2}\delta(1-x) \right]$$

Factorization of IR singularities

- We will perform this 'mass factorization' step-by-step. First we define a *plus distribution*

$$\int_0^1 dx\, f(x)\, [g(x)]_+ = \int_0^1 dx\, g(x)\, [f(x) - f(0)]$$

if g(x)=1/x, it removes singularities at x=0

- Redefine PDF according to:

$$f_q(x,\mu^2) = f_{q,0}(x) + \frac{\alpha_s}{2\pi}\int_x^1 \frac{d\xi}{\xi} f_{q,0}(\xi)\left\{-\frac{1}{\epsilon}P_{qq}(x/\xi) + C(x/\xi)\right\}$$

In MSbar: C chosen to remove ln(4π)-γ_E

- Arrive at the structure function:

$$F_{2,q} = e^2 Q_q^2\, x \int_x^1 \frac{d\xi}{\xi} f_q(\xi,\mu^2)\left\{\delta(1-x/\xi) + \frac{\alpha_s}{2\pi}\left[P_{qq}(x/\xi)\ln\frac{Q^2}{\mu^2} + \text{finite}\right]\right\}$$

☛ ln(Q^2) dependence of $F_2 \Rightarrow$ **explains the observed scaling violation**

Scale variation and DGLAP

- Pole turns into a $\ln(\mu^2)$ dependence ⇒ F_2 must be independent of this arbitrary *factorization scale*, which leads to an evolution equation for the PDF.

$$\boxed{\frac{d\, f_q(x,\mu^2)}{d\ln\mu^2} = \frac{\alpha_s}{2\pi}\int_x^1 \frac{d\xi}{\xi} f_q(\xi,\mu^2) P_{qq}(x/\xi)}$$

DGLAP equation

- Inclusion of gluon-initiated partonic processes:

$$\begin{aligned} F_{2,q} &= e^2 Q_q^2\, x \int_x^1 \frac{d\xi}{\xi} f_q(\xi,\mu^2)\left\{\delta(1-x/\xi) + \frac{\alpha_s}{2\pi}\left[P_{qq}(x/\xi)\ln\frac{Q^2}{\mu^2} + \text{finite}\right]\right\} \\ &+ e^2 Q_q^2\, x \int_x^1 \frac{d\xi}{\xi} f_g(\xi,\mu^2)\left\{\frac{\alpha_s}{2\pi}\left[P_{qg}(x/\xi)\ln\frac{Q^2}{\mu^2} + \text{finite}\right]\right\} \end{aligned}$$

$$\frac{d}{d\ln\mu^2}\begin{pmatrix} f_q(x,\mu^2) \\ f_g(x,\mu^2)\end{pmatrix} = \frac{\alpha_s}{2\pi}\int_x^1 \frac{d\xi}{\xi}\begin{pmatrix} P_{qq}(x/\xi) & P_{qg}(x/\xi) \\ P_{gq}(x/\xi) & P_{gg}(x/\xi)\end{pmatrix}\begin{pmatrix} f_q(x,\mu^2) \\ f_g(x,\mu^2)\end{pmatrix}$$

PDFs

- We get much of our knowledge of PDFs from the DIS process
- PDFs enter every hadron collider prediction, so we'd better know them well. They are non-perturbative objects with perturbative evolution.
- The Q^2 dependence of the PDF $f(x, Q^2)$ is calculable in perturbative QCD through the DGLAP equation, while the x dependence is extracted from data.
- Several groups are working on extracting the PDFs and improving their uncertainties: CTEQ, NNPDF, ABM, MMHT, HERAPDF, JR
- Basic idea:

$$\underbrace{\text{Hadronic cross section}}_{\text{measure}} = \underbrace{\text{PDFs}}_{\text{extract}} \otimes \underbrace{\text{partonic cross section}}_{\text{calculate}}$$

Parton density coverage

Simple LO solution of the DGLAP equation for a single quark:

$$f_q(x,\mu^2) = f(x,Q_0^2) + \frac{\alpha_s(Q_0^2)}{2\pi}\,\mathrm{Log}\frac{\mu^2}{Q_0^2} \times \int_x^1 \frac{d\xi}{\xi} f_q(\xi,Q_0^2) P_{qq}\left(\frac{x}{\xi}\right)$$

PDF at lower x

PDF at higher x

DGLAP evolution moves PDFs down in x in addition to changing Q

- 100 GeV physics at LHC: probes small-x, sea partons
- TeV physics: probes large-x

NNPDF3.1, 1706.00428

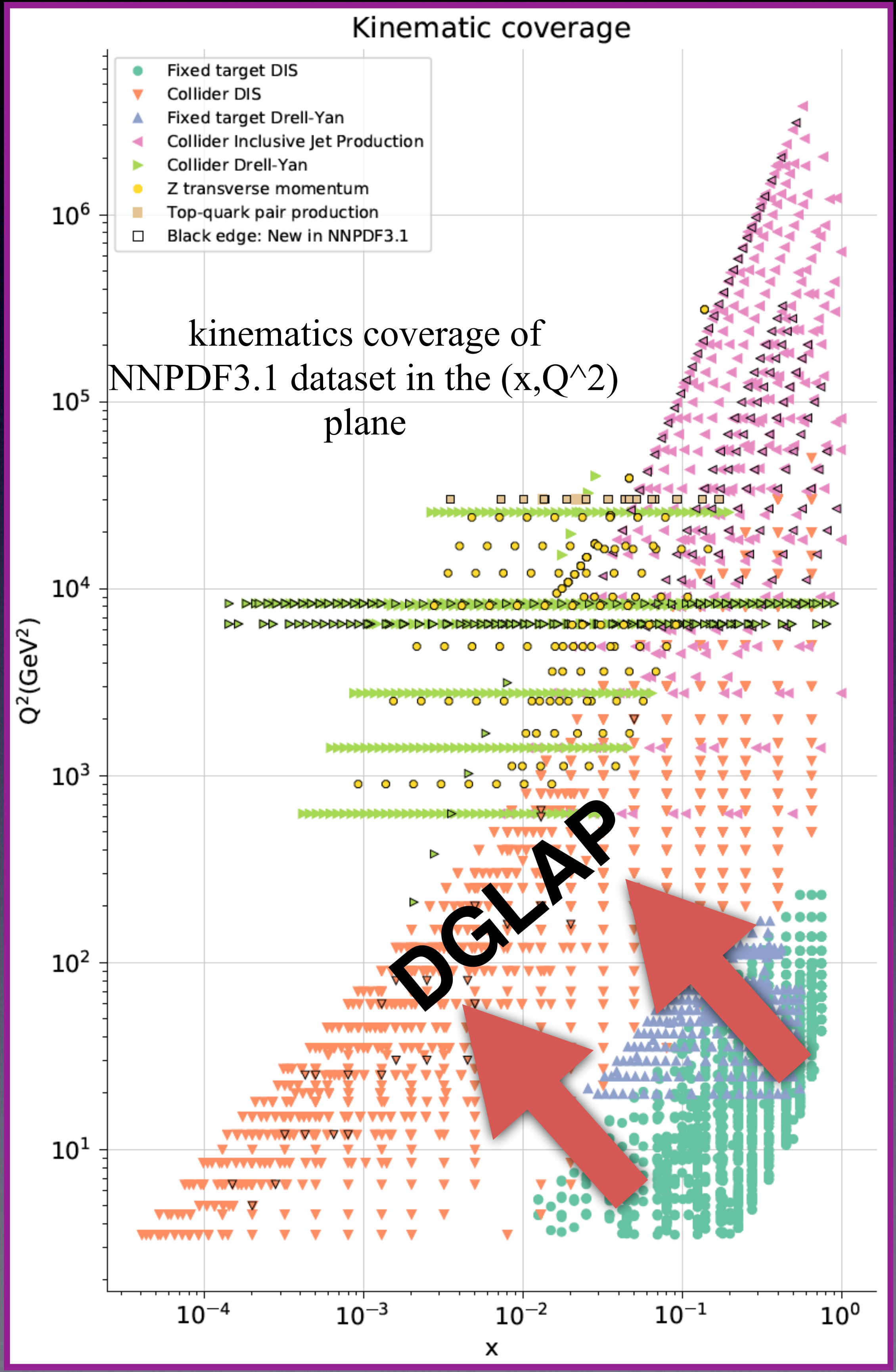

Precision of today's PDFs

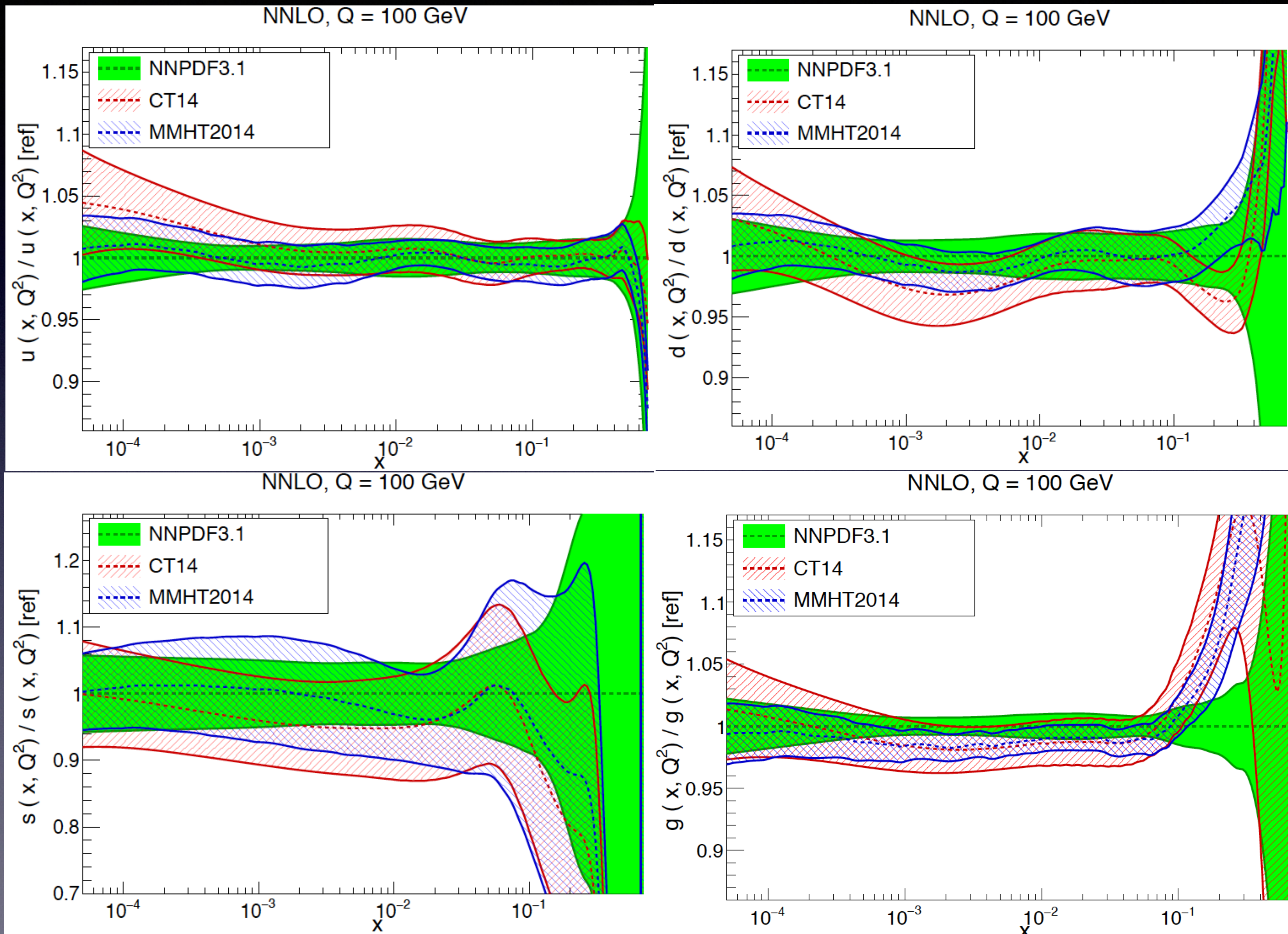

Precision of today's PDFs

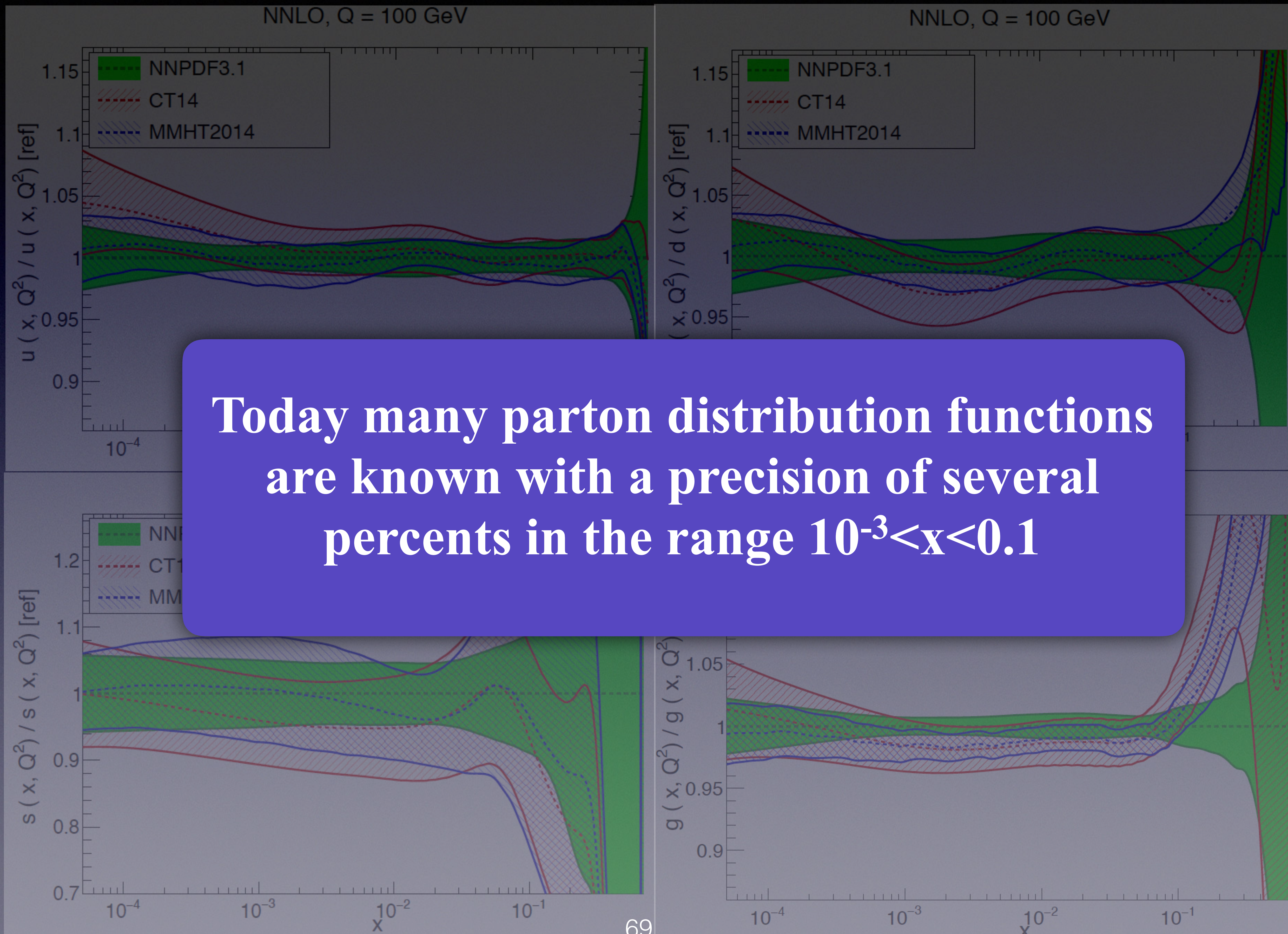

Today many parton distribution functions are known with a precision of several percents in the range $10^{-3}<x<0.1$

Benchmark processes for PDFs

- Impact of uncertainties from PDFs on benchmark processes

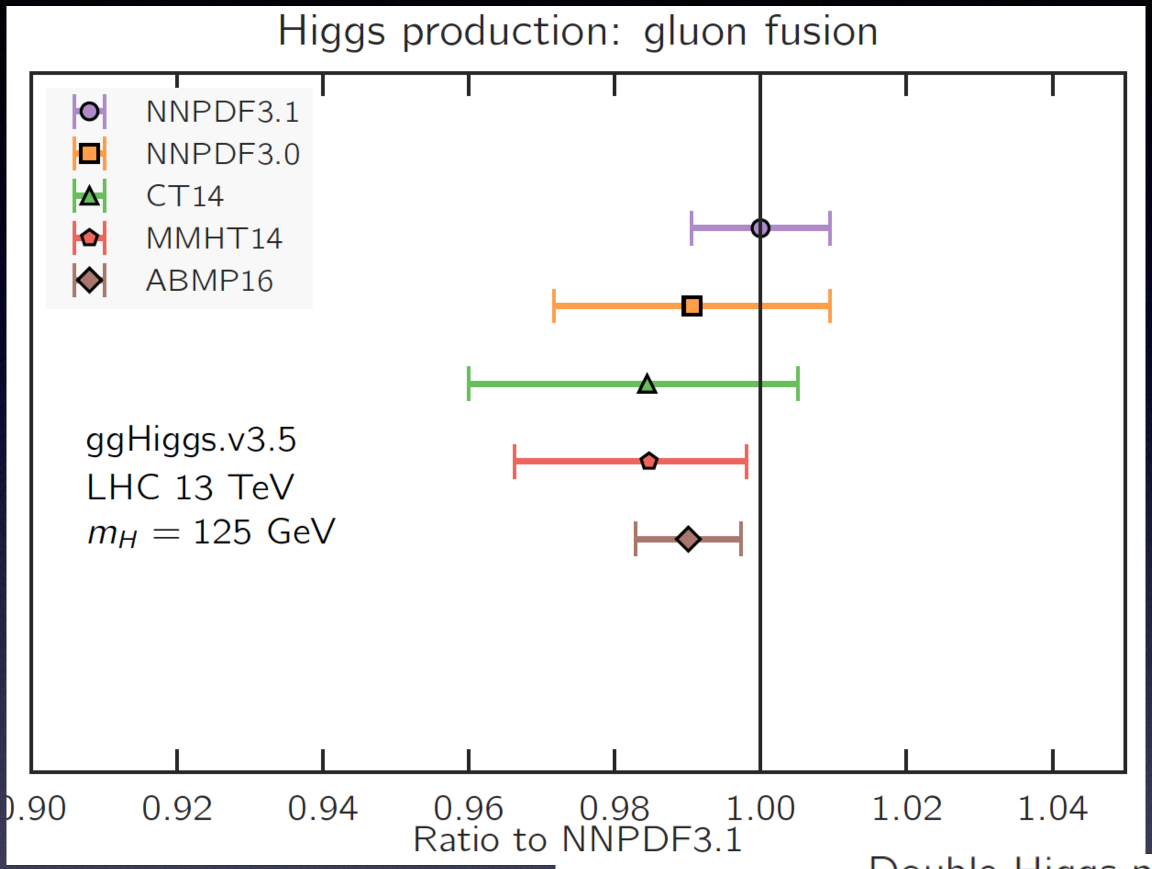

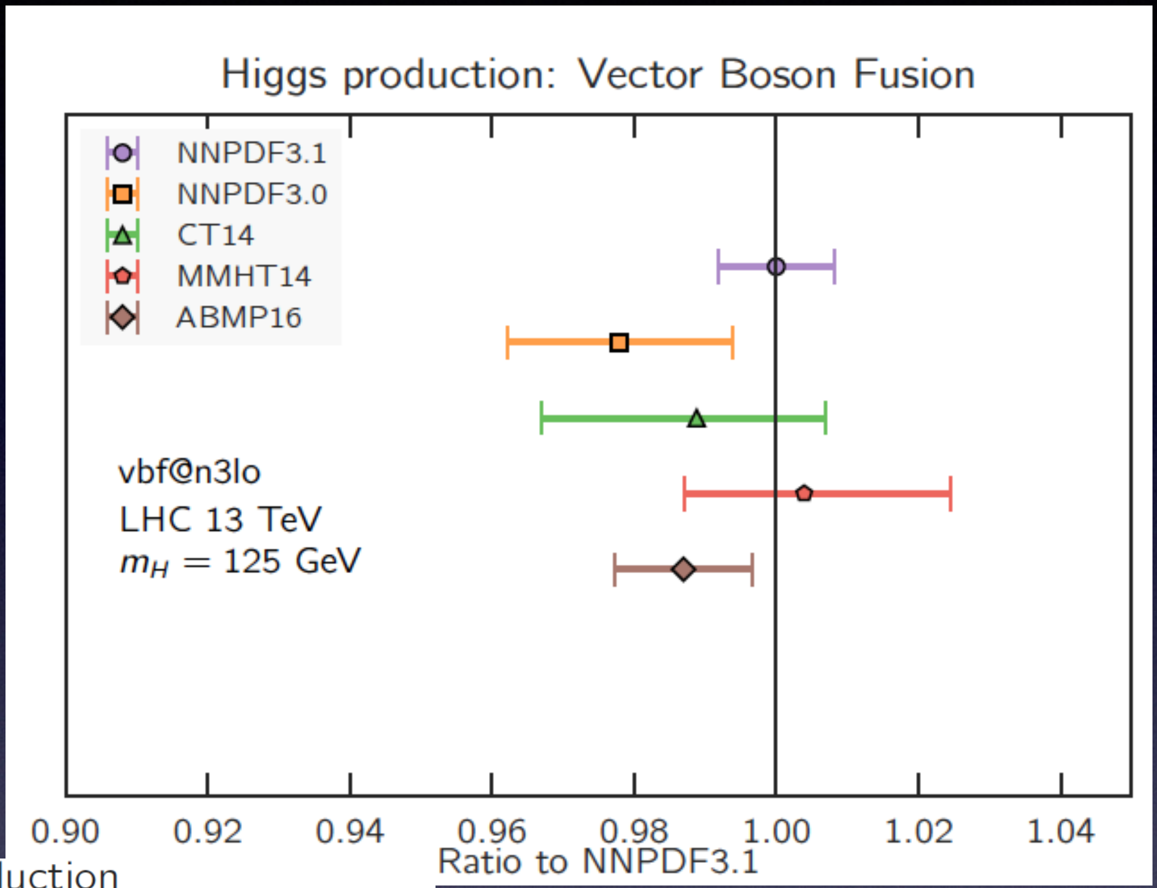

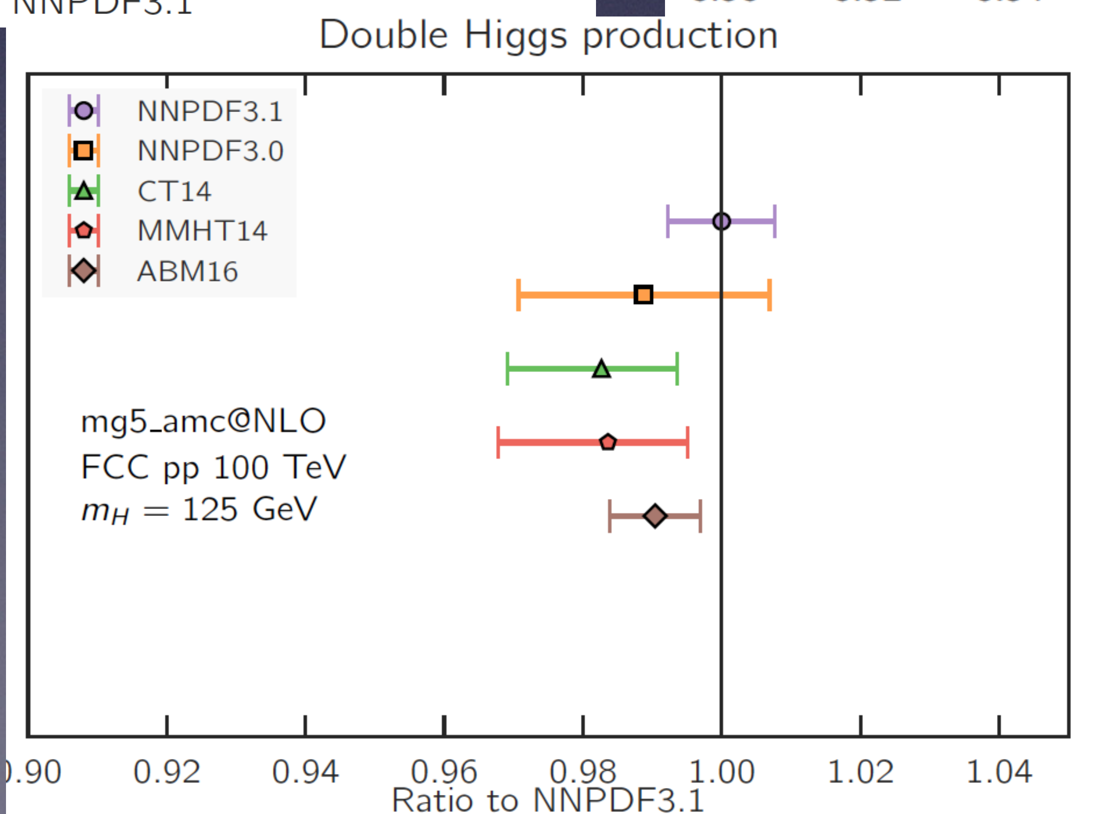

1706.00428

Benchmark processes for PDFs

- Impact of uncertainties from PDFs on benchmark processes

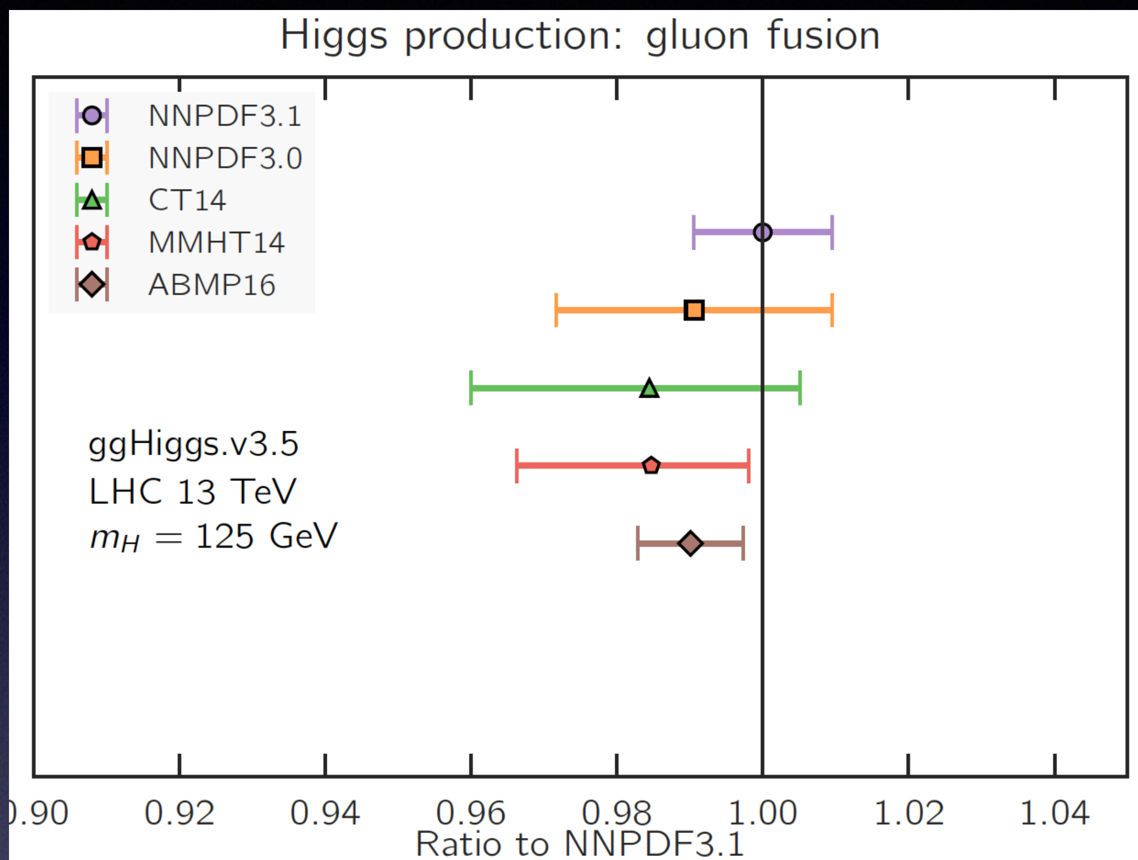

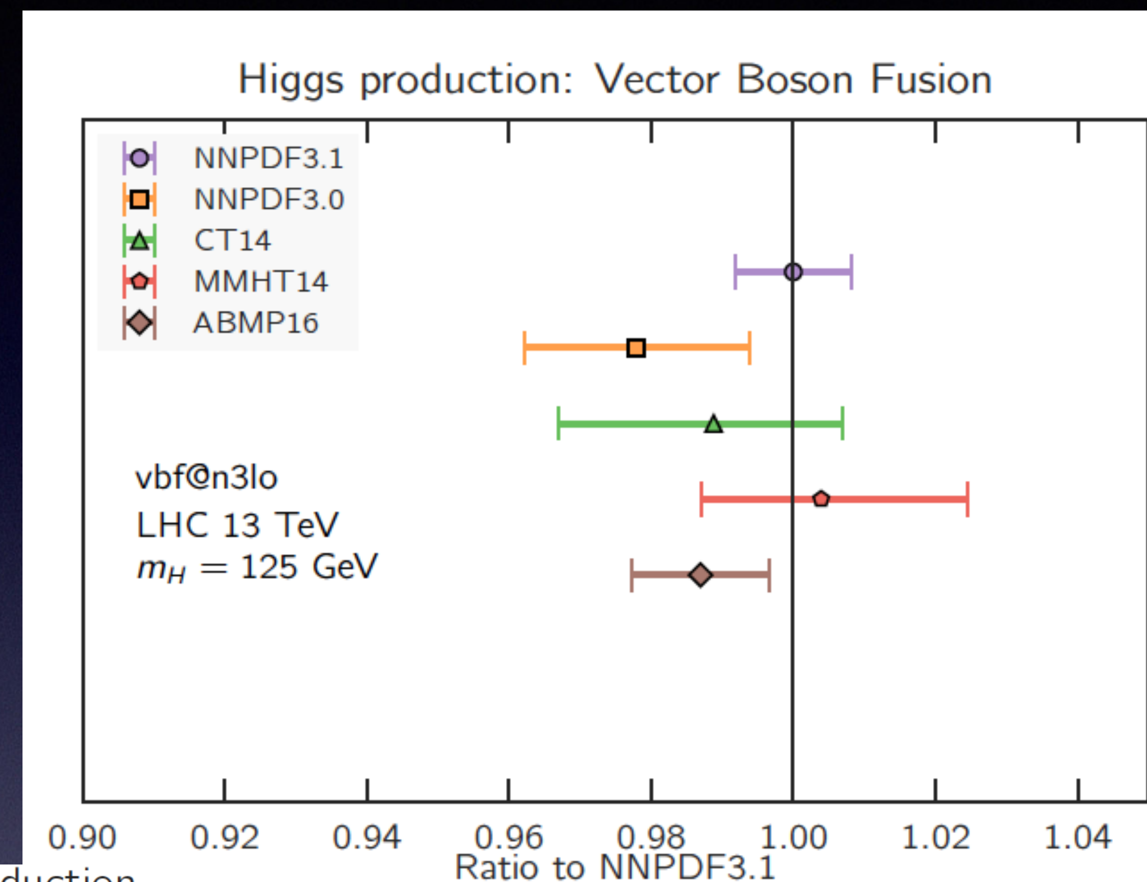

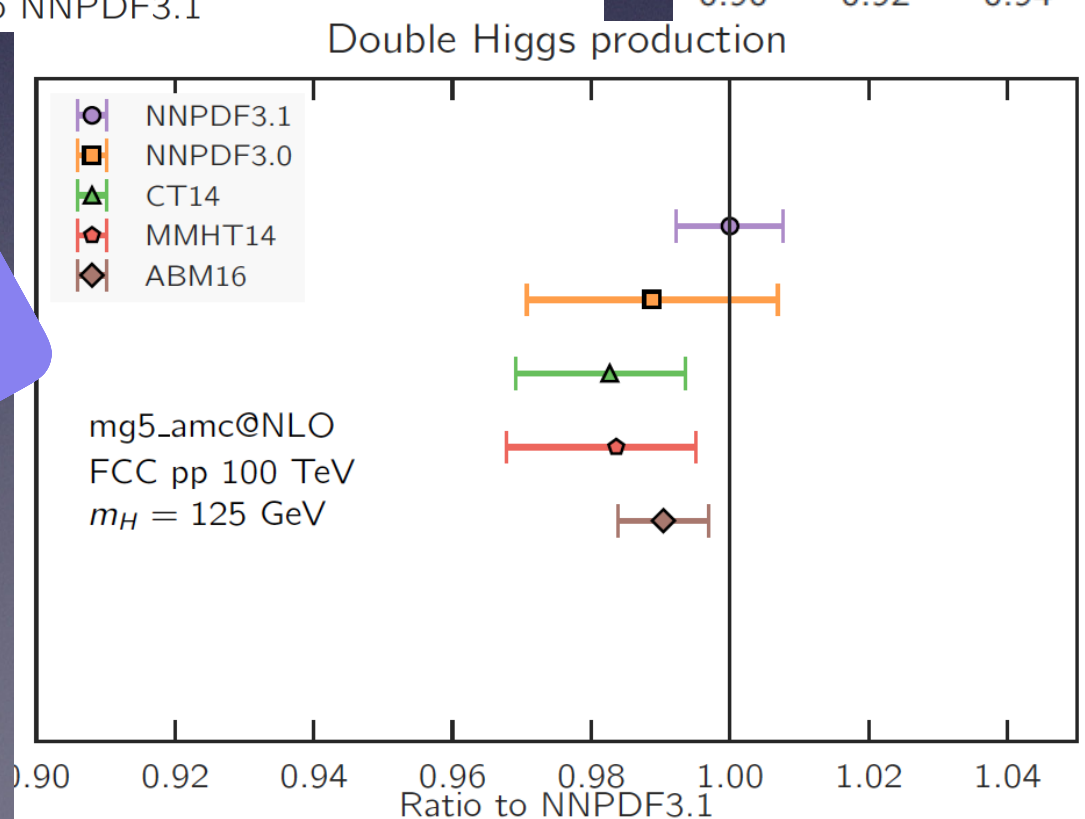

Estimated errors on benchmark processes within a given set are at the ±2% level

Differences between central values predicted by different groups 2% or less

PDF errors

- Published PDF sets come with errors. what could induce an error in a PDF?
    - Data set choice: different groups use different data sets.
    - Parametrization choices for the PDF functional form
    - Order of perturbation theory for the hard cross section (leads to a different scale uncertainty)
    - Errors on data sets.

PDF errors

- Published PDF sets come with errors. what could induce an error in a PDF?
    - Data set choice: different groups use different data sets.
    - Parametrization choices for the PDF functional form
    - Order of perturbation theory for the hard cross section (leads to a different scale uncertainty)
    - Errors on data sets ☛ ***the only error included in the current fits***

DIS& PDFs: Recap

- Factorization of long and short distance effects in QCD is key to our ability to calculate hadronic cross sections. Understanding PDFs is very important in achieving reliable predictions.
- DIS data has played an important role in our probe of the proton structure. LHC and Tevatron data have allowed to further constrain other kinematic range for Bjorken x.
- Today's precision of PDFs has improved significantly, with some PDF determinations approaching the percent level precision. This is crucial for Higgs precision prospects. However there is still room for further improvements in their uncertainty.

Two Hadronic Initial States: Drell-Yan Production

The Drell-Yan Process

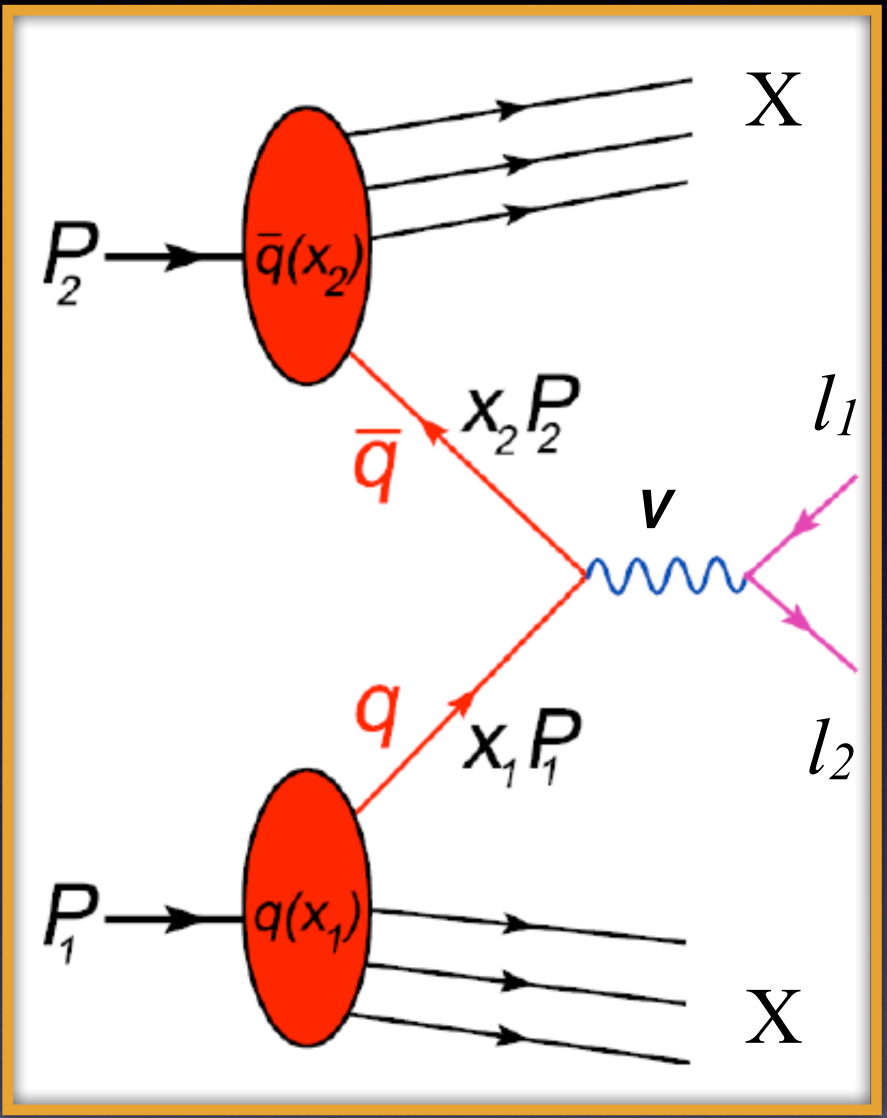

- Drell-Yan is the production of lepton pairs in the s-channel. Drell-Yan like processes include:

$$h(P_1) + h'(P_2) \to (\gamma^*, Z \to l^+l^-)X \ \text{ with } \ l = e,\mu$$

$$h(P_1) + h'(P_2) \to (W \to l\nu)X$$

$$h(P_1) + h'(P_2) \to V_{BSM}X; \quad V = Z', \ldots$$

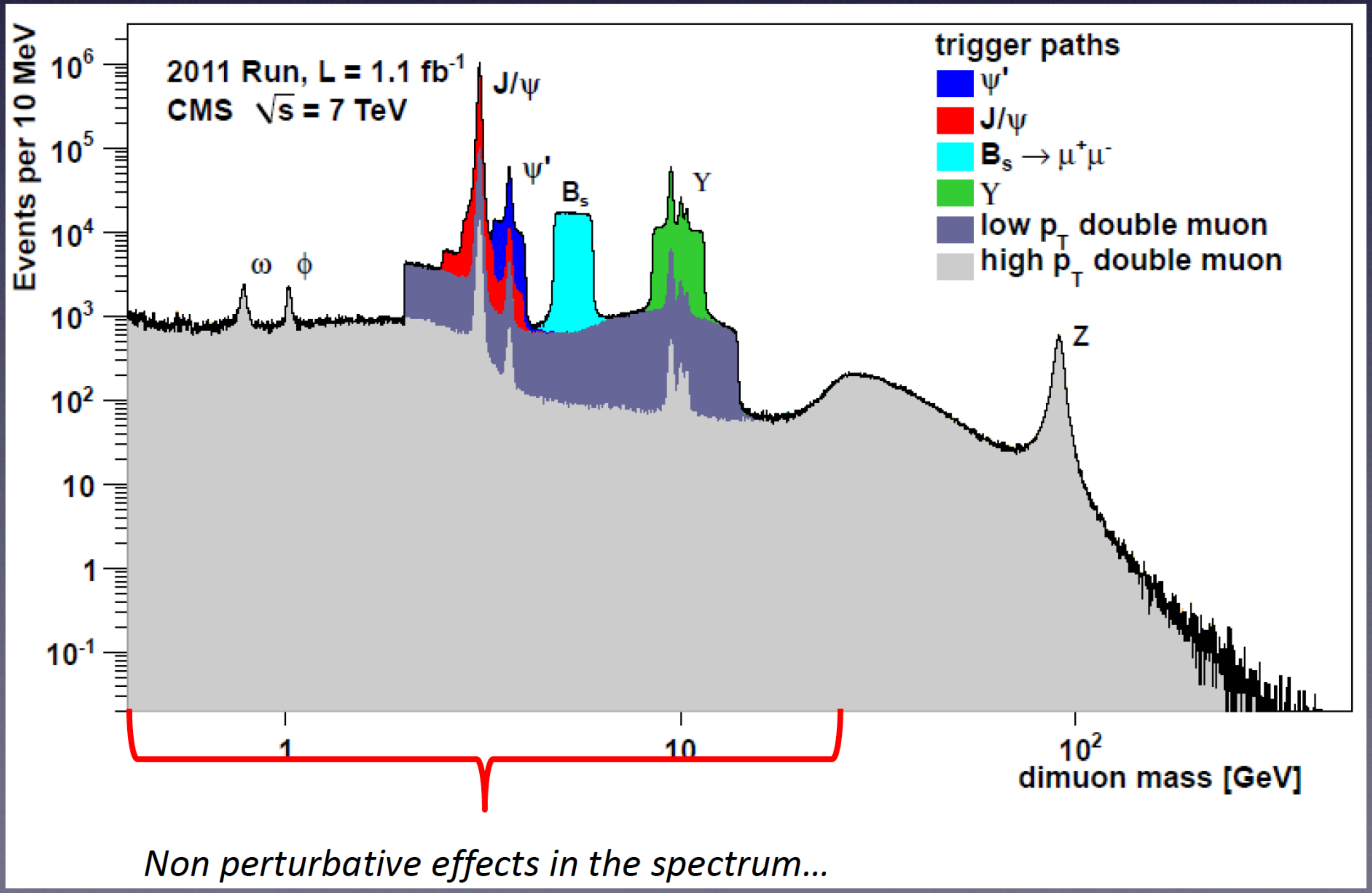

Facts about Drell-Yan

- Clean signal at hadron colliders, since the lepton pair does not interact strongly
- One of the best theoretically studied processes at a hadron collider with uncertainties at the few percent level
- Factorization is proved to all orders in QCD perturbation theory (Collins-Soper-Stermann)
- Standard Candle for detector calibration (eg. detector response to lepton energy)

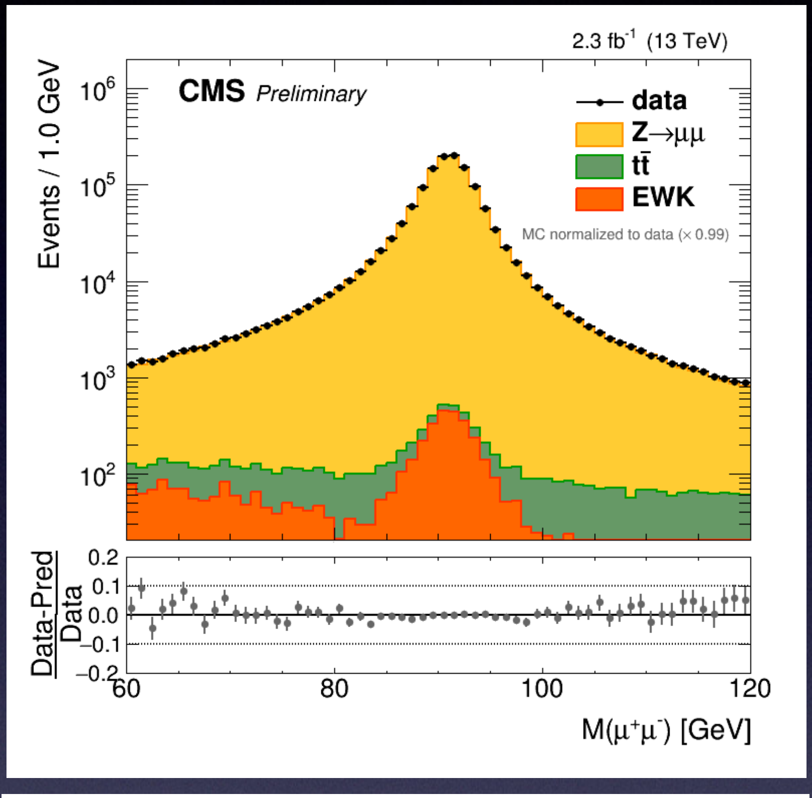

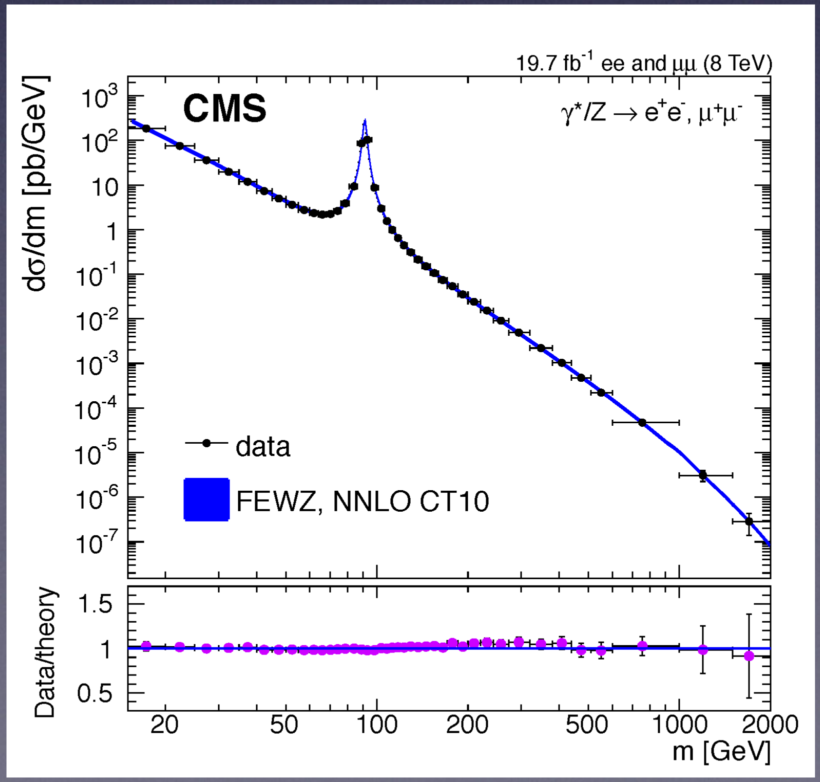

Historical importance

- Study of the Drell-Yan process was critically important in establishing QCD as a quantitative theory

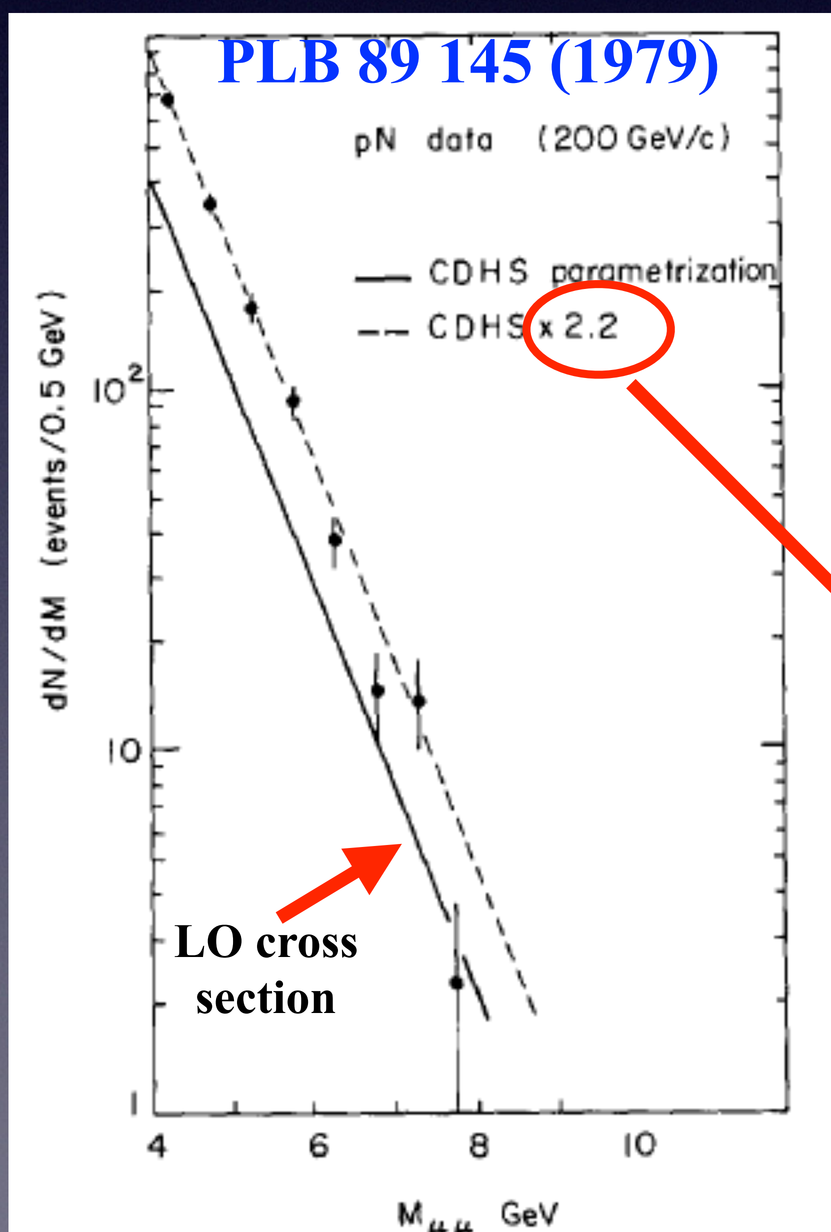

Comparison of di-muon invariant mass data from the NA3 experiment at CERN in 1979:

In all the channels studied the experimental cross section is significantly larger by a factor of 2.3 ± 0.5 than expected

The first introduction of a “K-factor” to explain discrepancies between theory and data

$K = (d^2\sigma/dx_1dx_2)_{exp}/(d^2\sigma/dx_1dx_2)_{DY\ model}$.

Reaction	pN	$\bar{p}$N
K	2.2 ± 0.4	2.4 ± 0.5

Historical importance

- Study of the Drell-Yan process was critically important in establishing QCD as a quantitative theory

TOT= sum of all partonic channels @ NLO

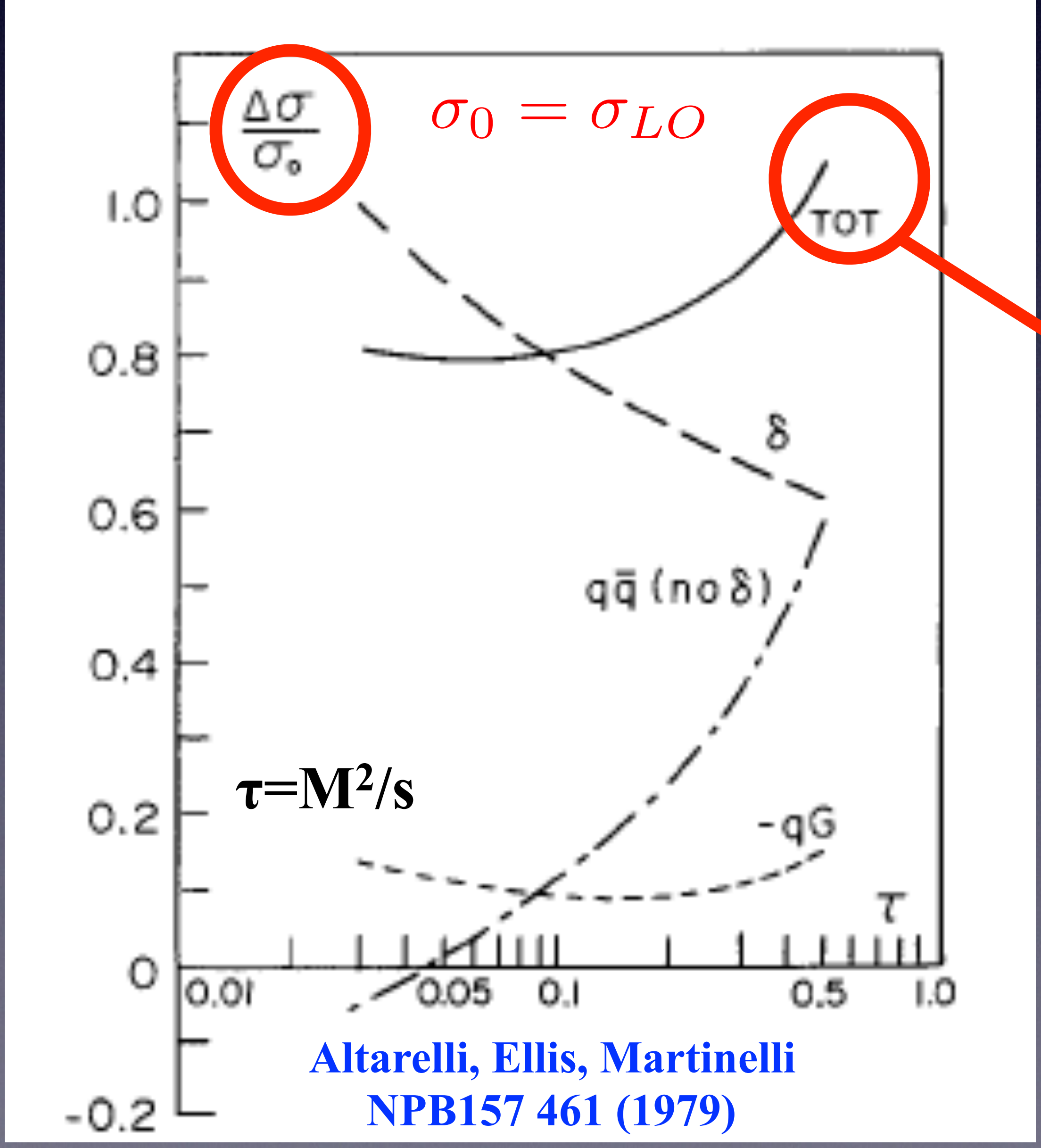

$$\Delta\sigma_{TOT}/\sigma_0 \sim 0.8 - 1.0$$

$\Delta\sigma =$ **pure NLO coefficient**

$$\sigma_{NLO} = \sigma_0 + \Delta\sigma_{TOT}$$

NLO QCD corrections reach nearly a factor of 2, greatly reducing tension between theory and experiment

Discrepancy resolved by next-to-leading order QCD!

Historical importance

- Understanding of vector boson production through the Drell-Yan process has required continued advances in our ability to understand QCD precisely, with data from the Tevatron and the LHC requiring NNLO corrections

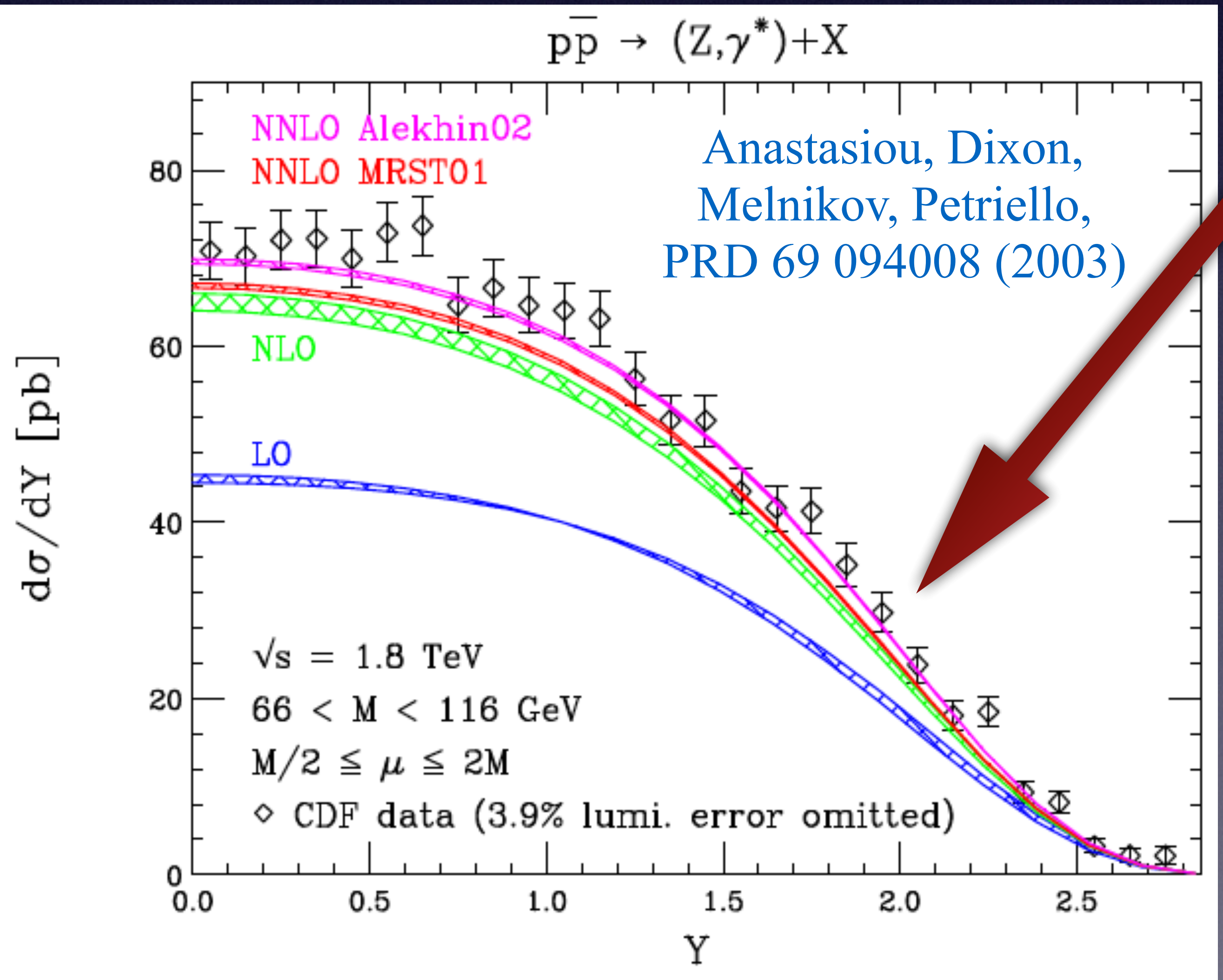

- Drell-Yan data and predictions can be used to to improve our understanding of proton structure

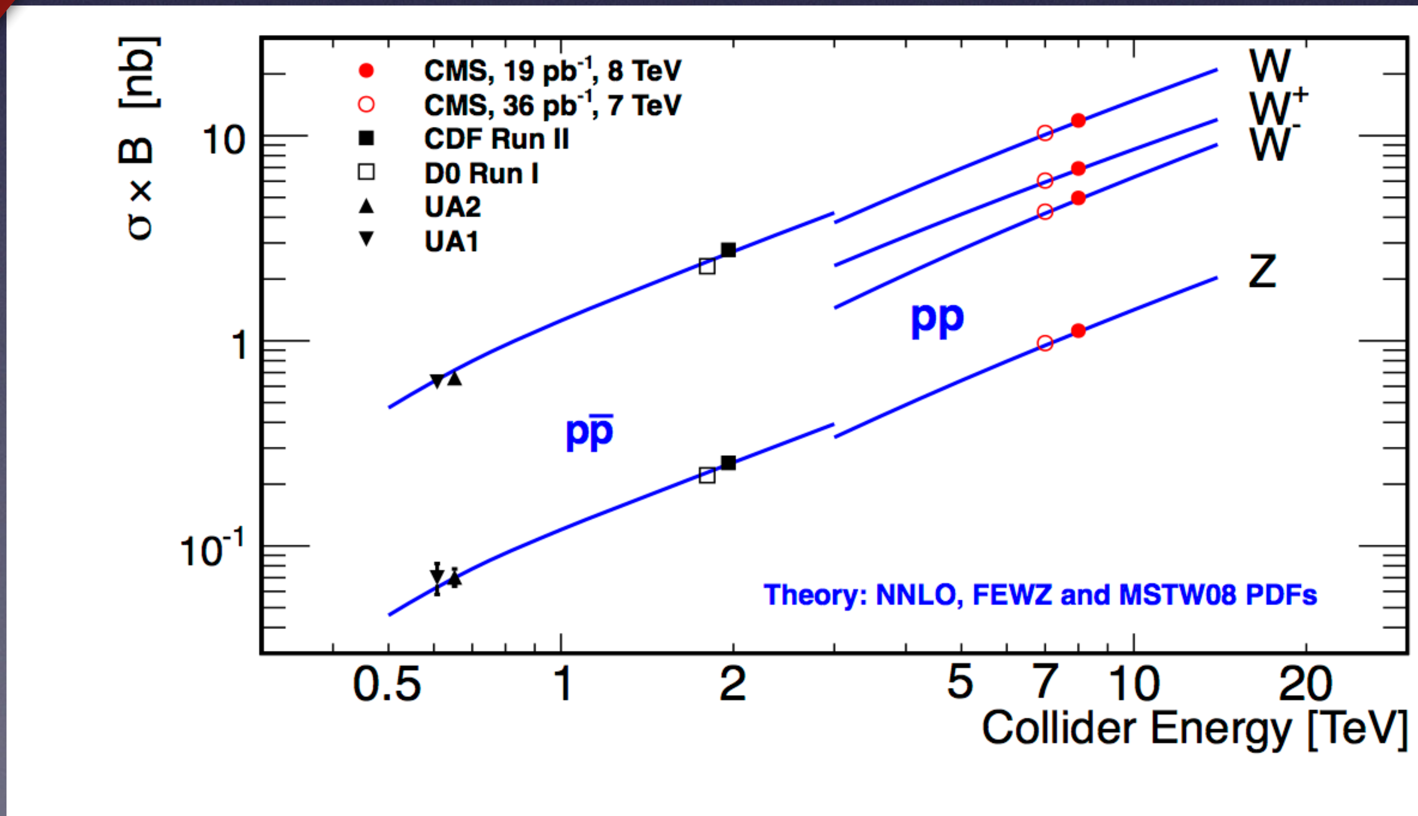

Historical importance

- The Drell-Yan process has been an important discovery mode throughout the modern history of high energy physics

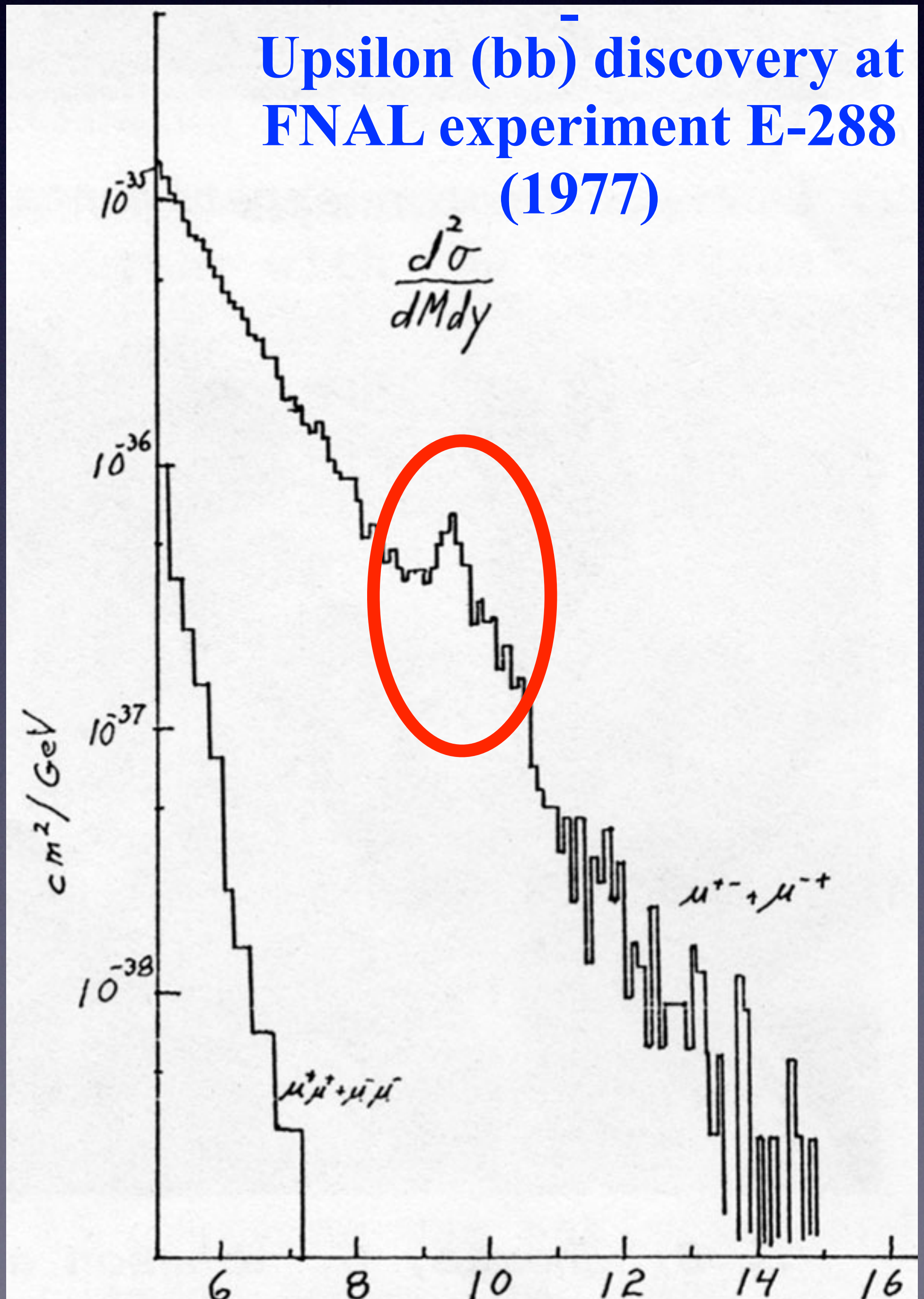

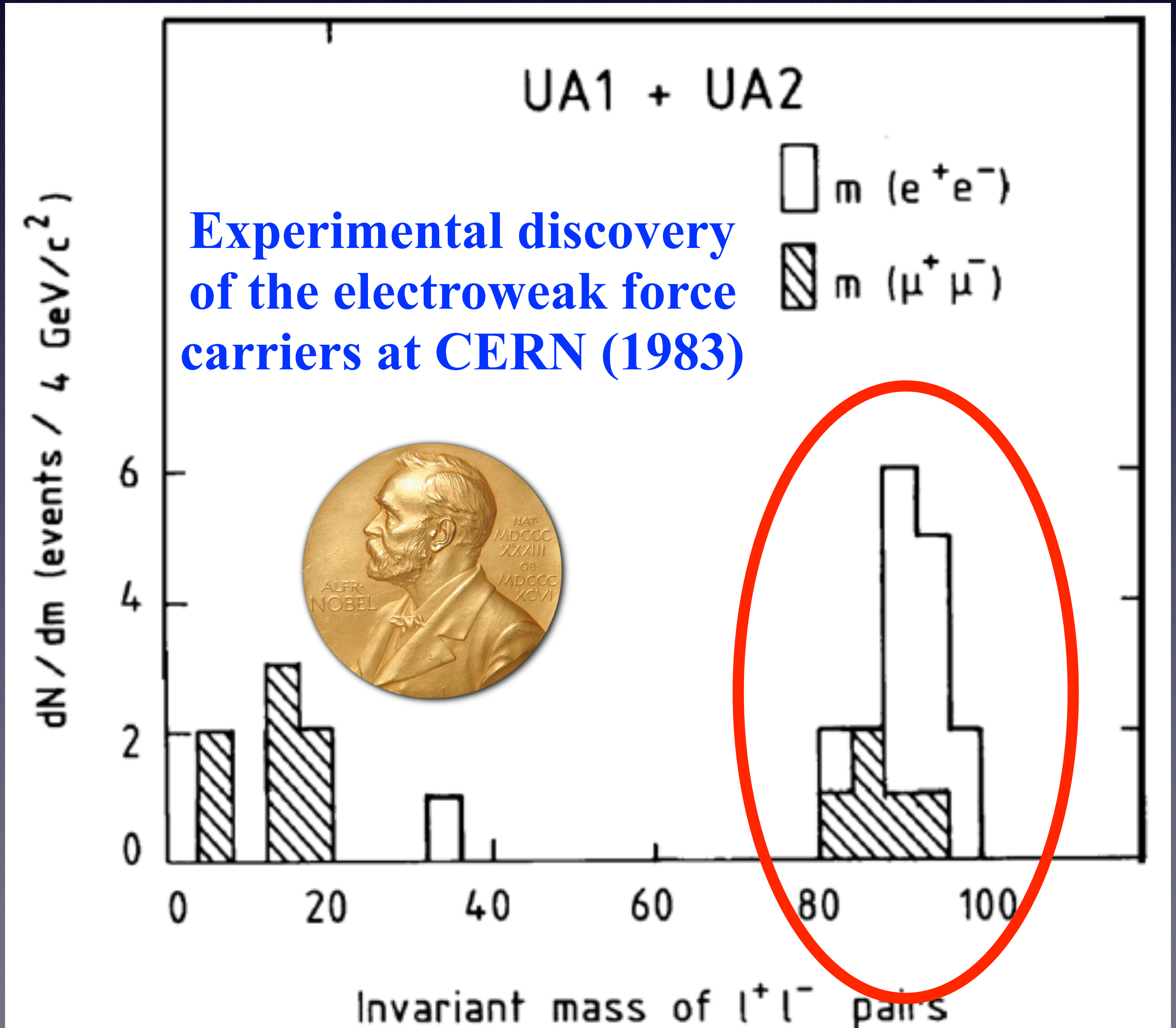

Historical importance

- The Drell-Yan production of vector bosons has also played a prominent role in famous non-discoveries in particle physics…

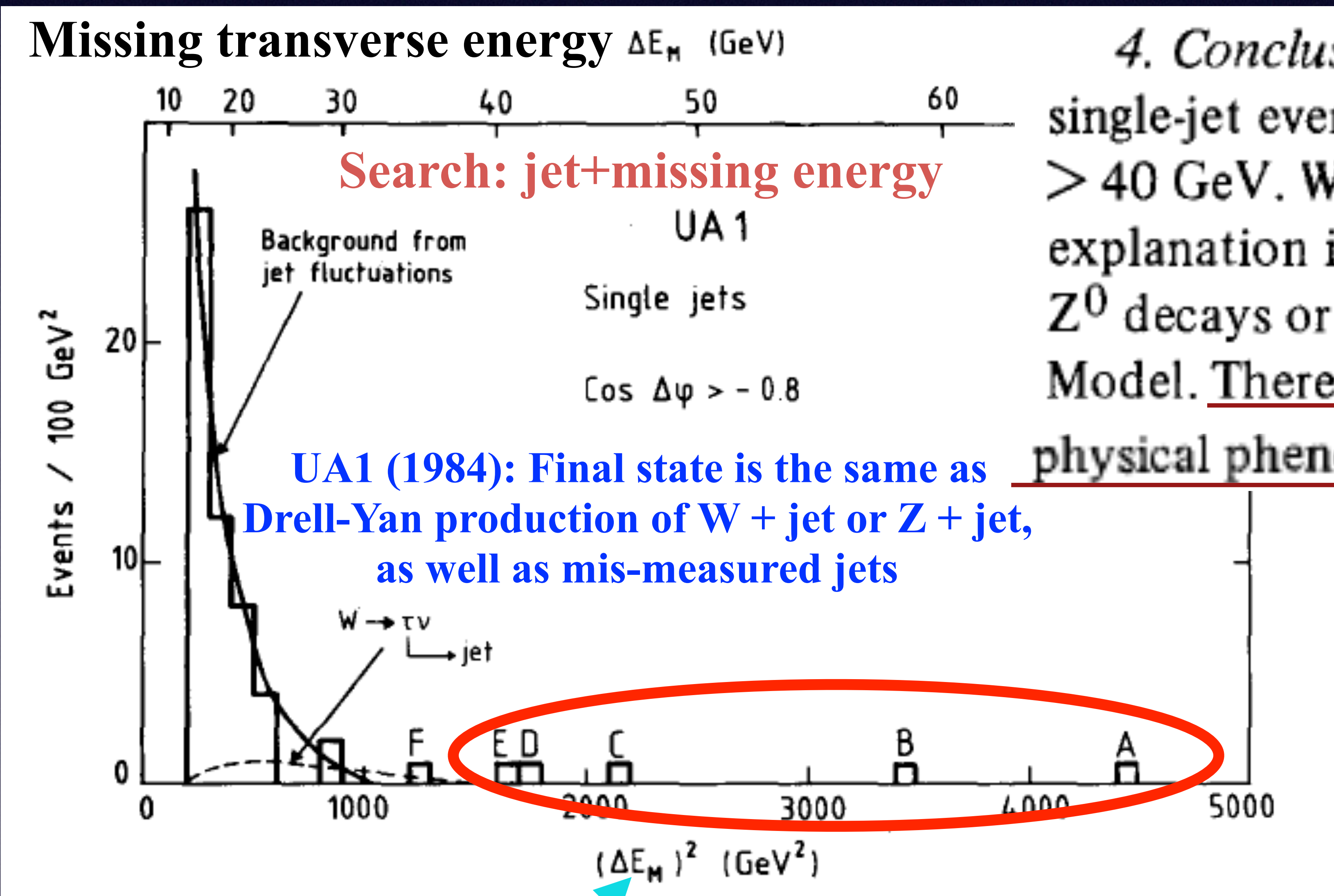

missing transverse energy

4. Conclusions. We have presented a sample of five single-jet events and two "photon" events with $\Delta E_M > 40$ GeV. We have been unable to find a reasonable explanation in terms of background including W and Z^0 decays or within the expectation of the Standard Model. Therefore we believe they are due to some new physical phenomenon.

Historical importance

- The Drell-Yan production of vector bosons has also played a prominent role in famous non-discoveries in particle physics…

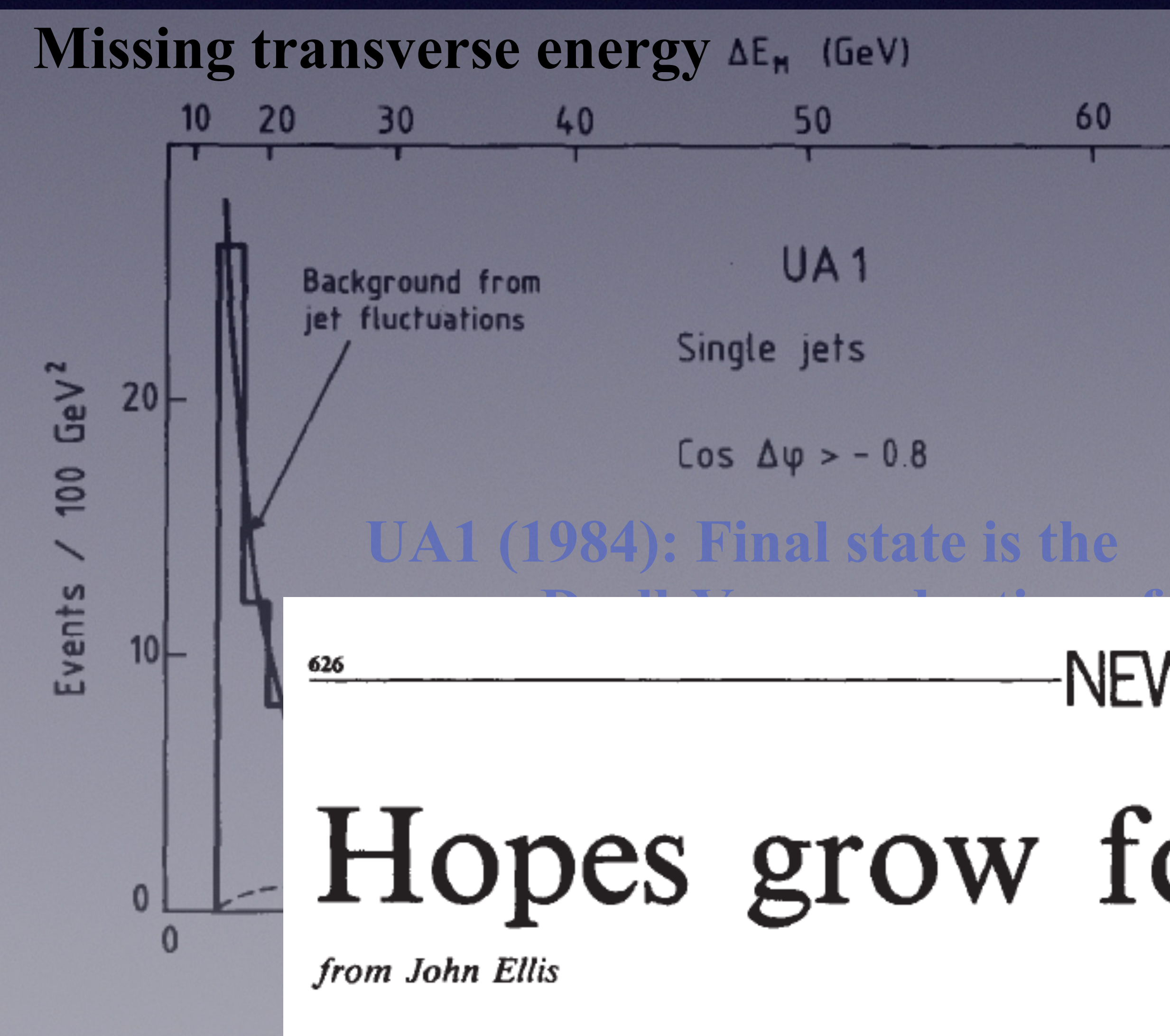

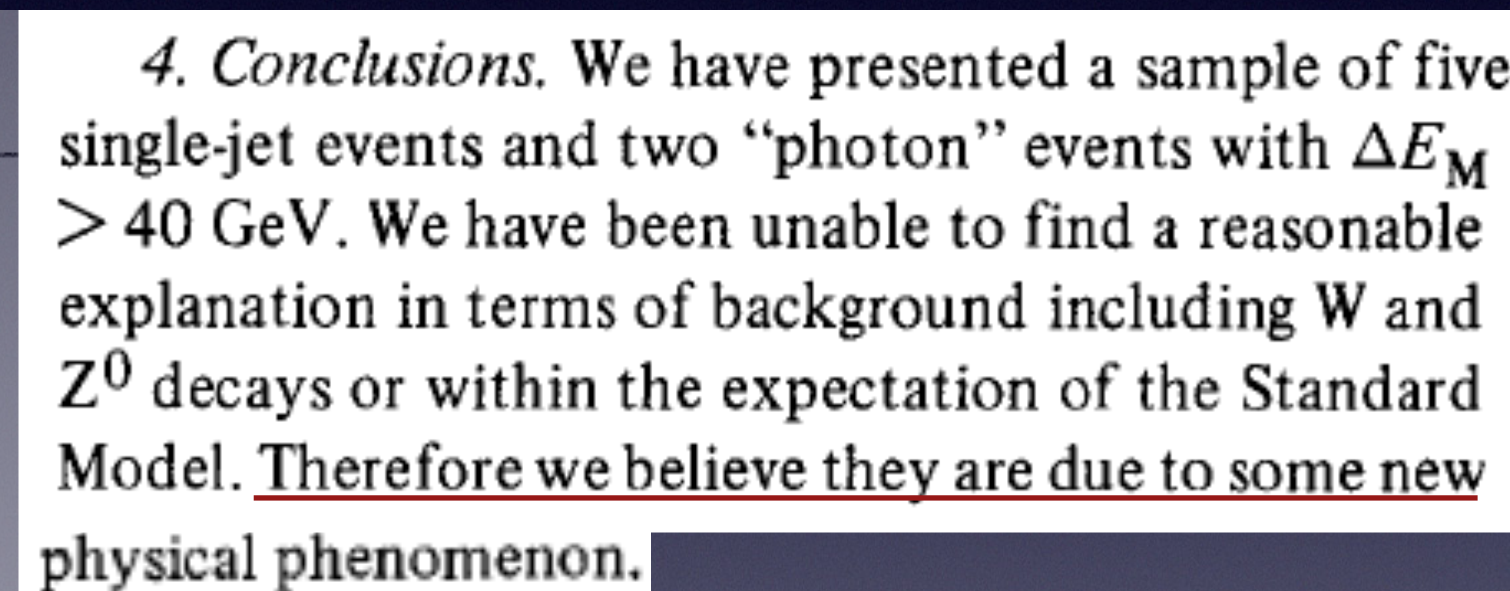

4. *Conclusions.* We have presented a sample of five single-jet events and two "photon" events with $\Delta E_M > 40$ GeV. We have been unable to find a reasonable explanation in terms of background including W and Z^0 decays or within the expectation of the Standard Model. Therefore we believe they are due to some new physical phenomenon.

626 NEWS AND VIEWS NATURE VOL. 313 21 FEBRUARY 1985

1985

Hopes grow for supersymmetry

from John Ellis

High-energy collisions between protons and antiprotons produce strange events in which momentum fails to balance. Missing momentum may be carried by photinos, super-partners of the photon.

Historical importance

- The Drell-Yan production of vector bosons has also played a prominent role in famous non-discoveries in particle physics…

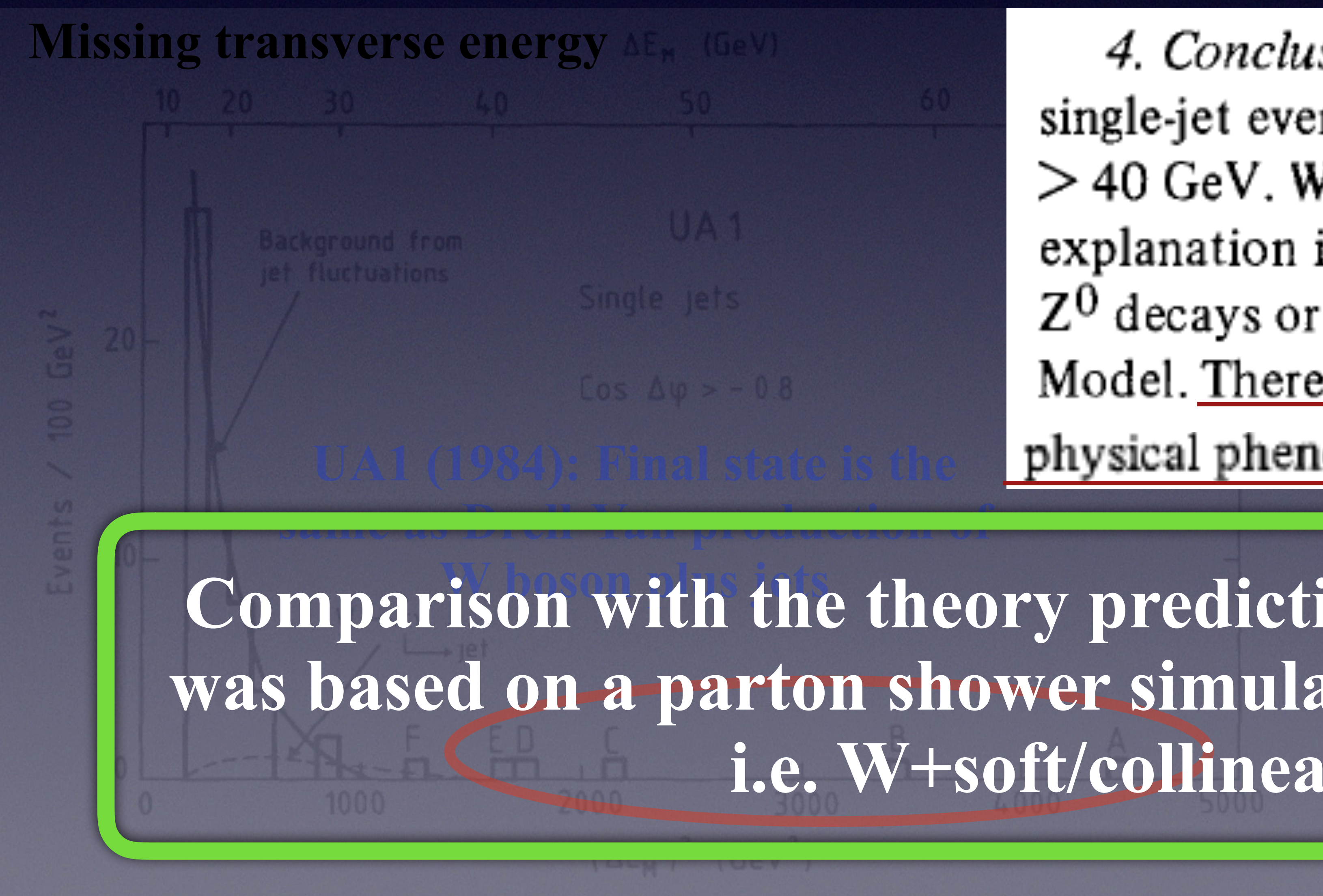

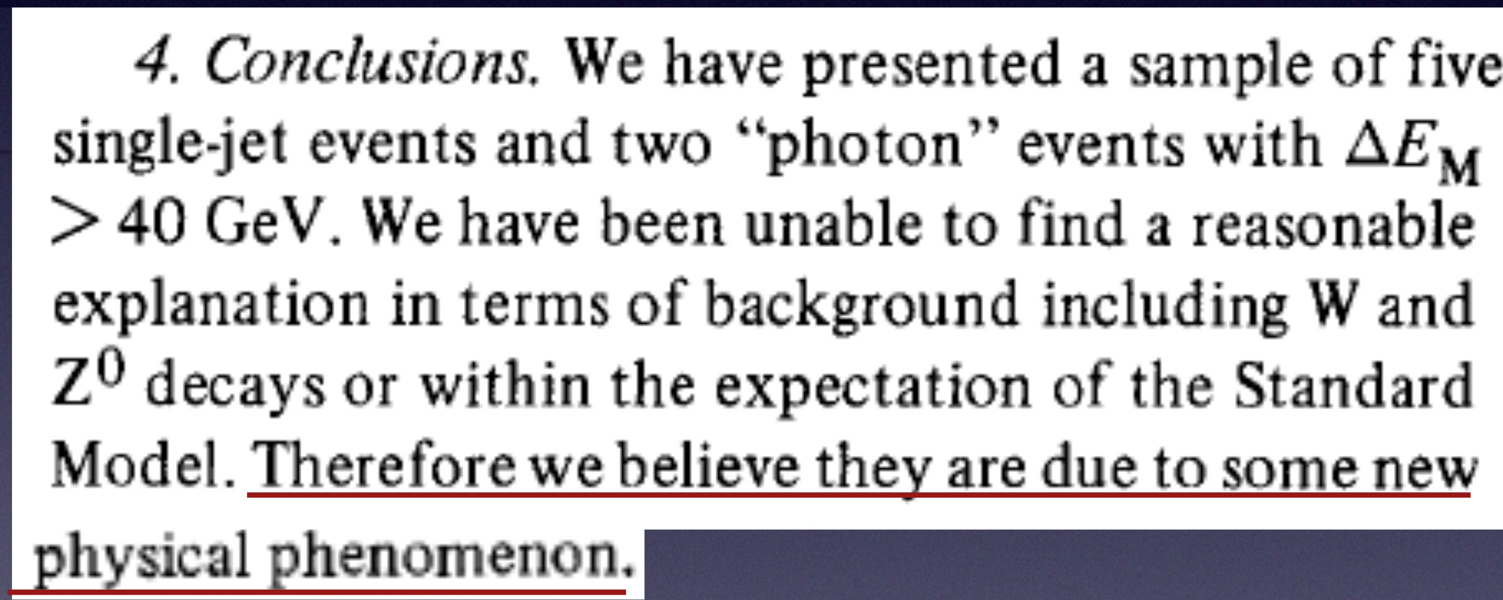

4. *Conclusions.* We have presented a sample of five single-jet events and two "photon" events with $\Delta E_M > 40$ GeV. We have been unable to find a reasonable explanation in terms of background including W and Z^0 decays or within the expectation of the Standard Model. Therefore we believe they are due to some new physical phenomenon.

Comparison with the theory prediction for the background was based on a parton shower simulation for W-production, i.e. W+soft/collinear jets

Historical importance

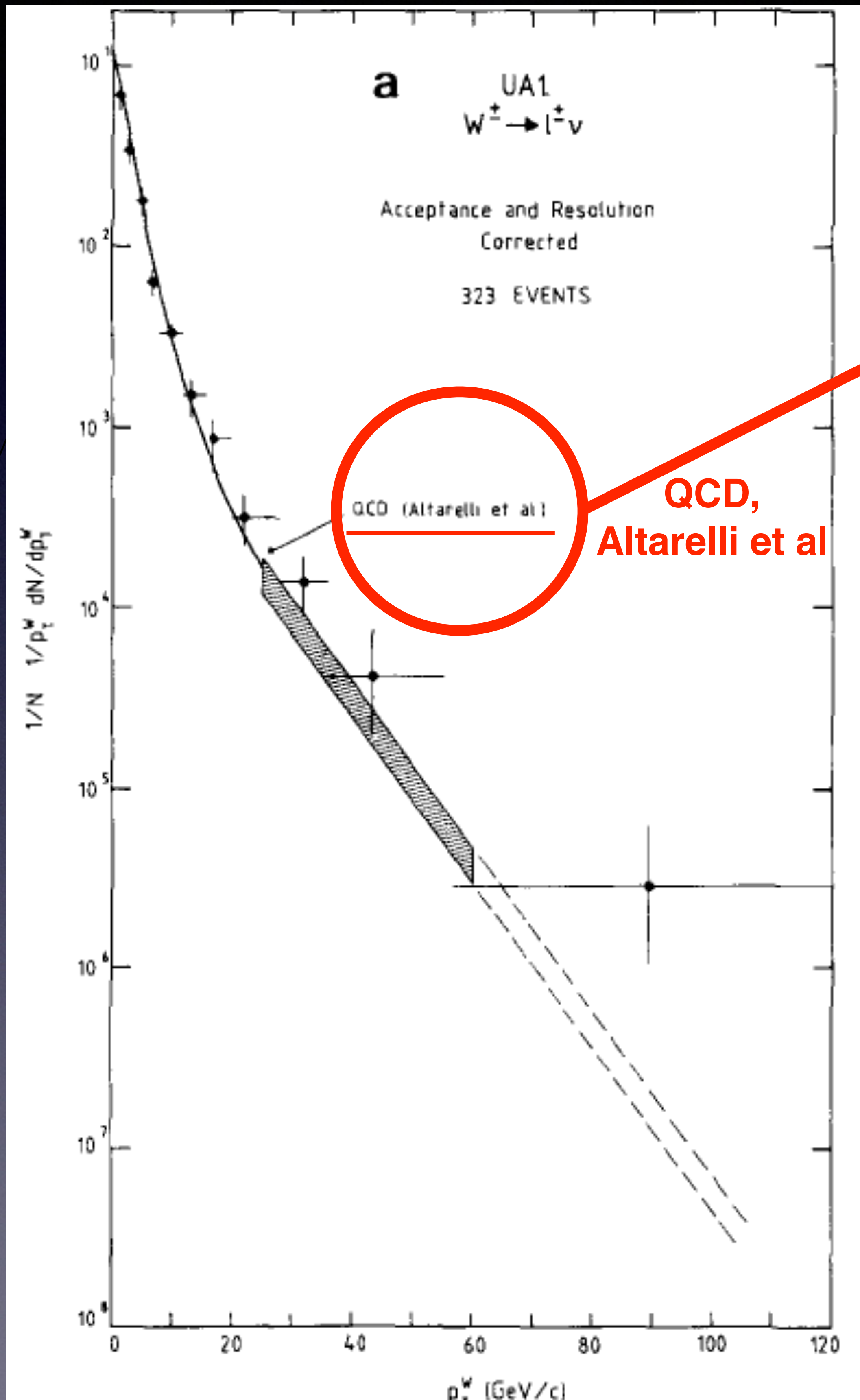

A proper SM prediction for the background requires W+hard jet emissions. This explained the discrepancy, not SUSY!

Parton showers (without matching to exact tree level matrix elements) do not explain hard emissions correctly

UA1 CM energy = 540 GeV $\Longrightarrow$ 40 GeV missing energy is hard, not soft !

From Drell-Yan Yesterday to Drell-Yan Today

Modern applications

- The W-boson mass is an important observable in the global fit to electroweak precision data. The agreement between the direct M_W measurement and the indirect determination from fitting other data is a powerful constraint on Standard Model extensions.

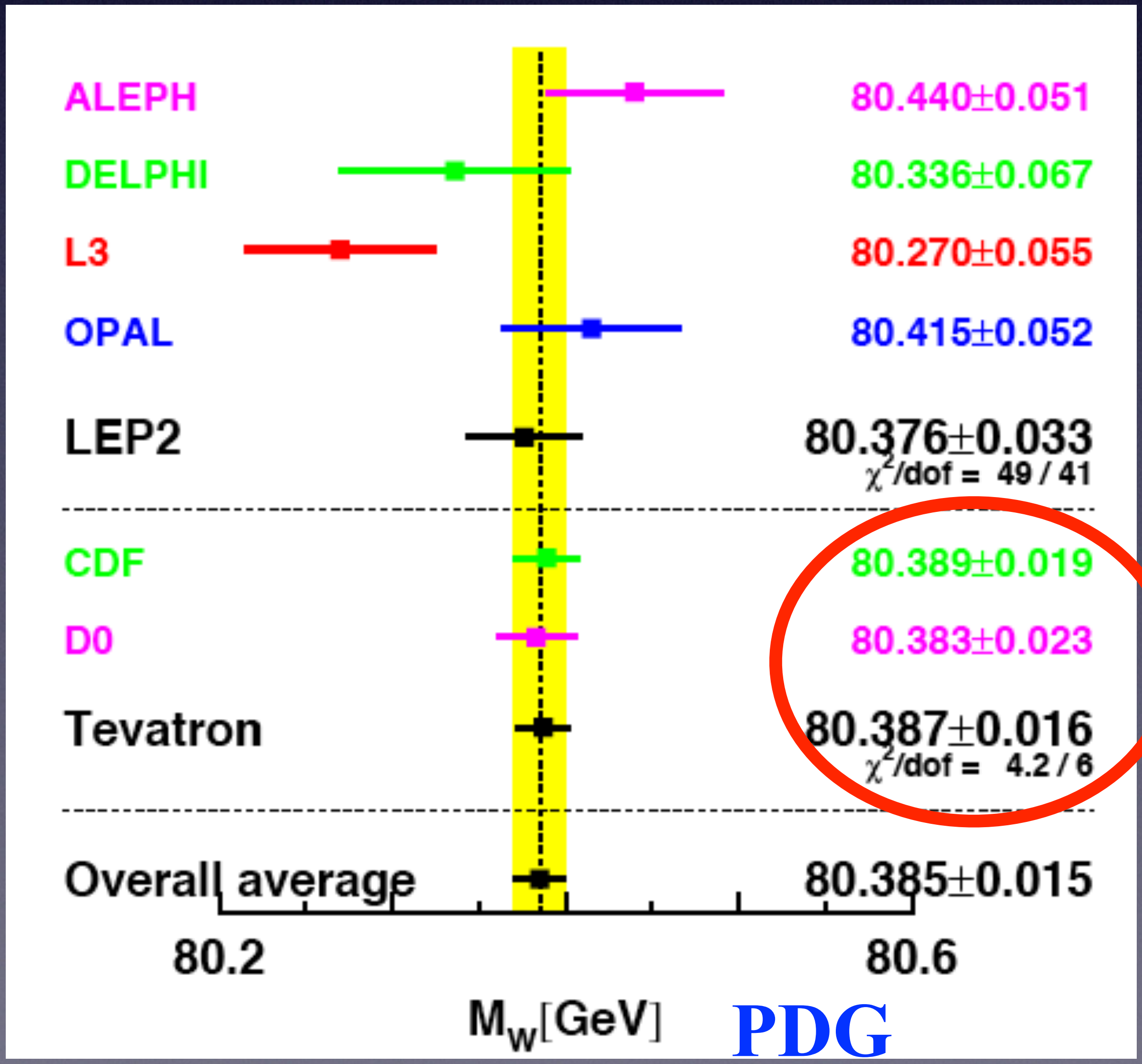

Direct measurement

Most precise determinations of M_W are from Drell-Yan production at the Tevatron

Modern applications

- The W-boson mass is an important observable in the global fit to electroweak precision data. The agreement between the direct M_W measurement and the indirect determination from fitting other data is a powerful constraint on Standard Model extensions.

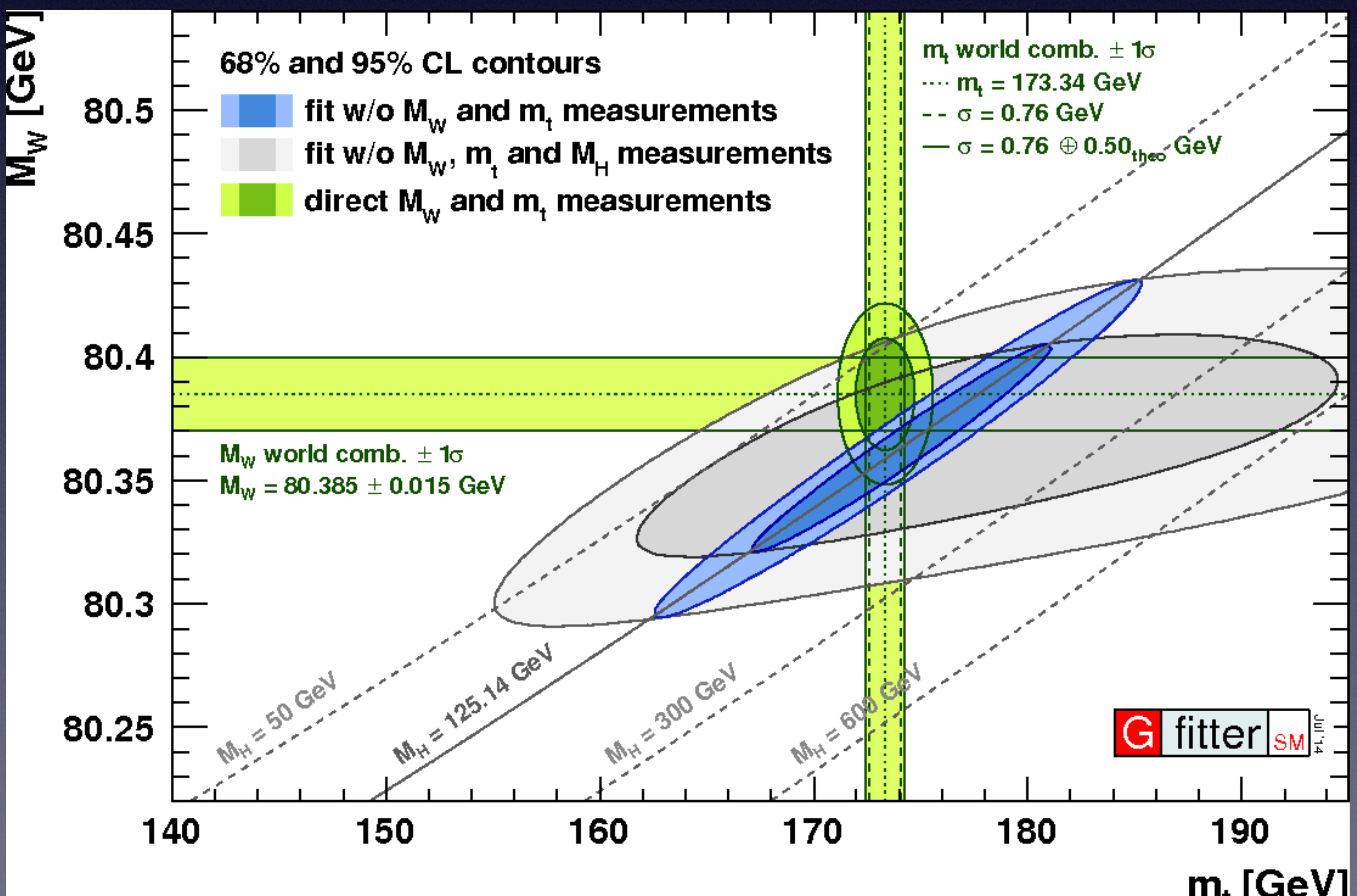

Indirect measurement

✳ All fits: use primarily LEP data (eg. forward-backward asymmetries in lepton pair production, total hadronic cross section, etc)

✳ Blue fit: uses in addition LHC Higgs measurements

✳ Grey fit: does not use LHC Higgs measurements

Good agreement between direct and indirect measurements

Measuring the W mass

- The W→lν contains final-state missing energy; cannot reconstruct the W mass peak

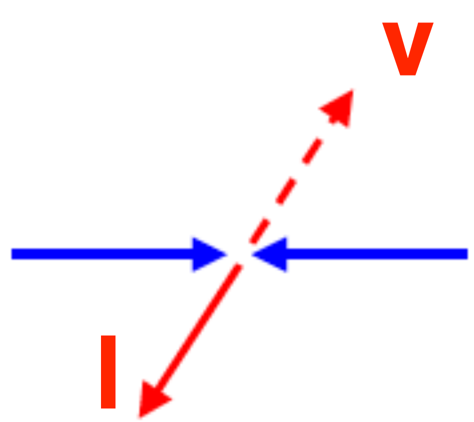

In the W rest frame:

- $|\vec{p}_\ell| = |\vec{p}_\nu| = \frac{M_W}{2}$
- $|p_\ell^T| \leq \frac{M_W}{2}$

$$\frac{d\sigma}{dp_T^e} = \underbrace{\left|\frac{d\cos\theta_*}{dp_T^e}\right|}_{\text{Jacobian}} \frac{d\sigma}{d\cos\theta_*} = \frac{1}{\sqrt{1-\left(\frac{2p_T^e}{M_W}\right)^2}} \frac{4p_T^e}{M_W^2} \frac{d\sigma}{d\cos\theta_*}$$

This is a smooth function (can write it in terms of spherical harmonics)

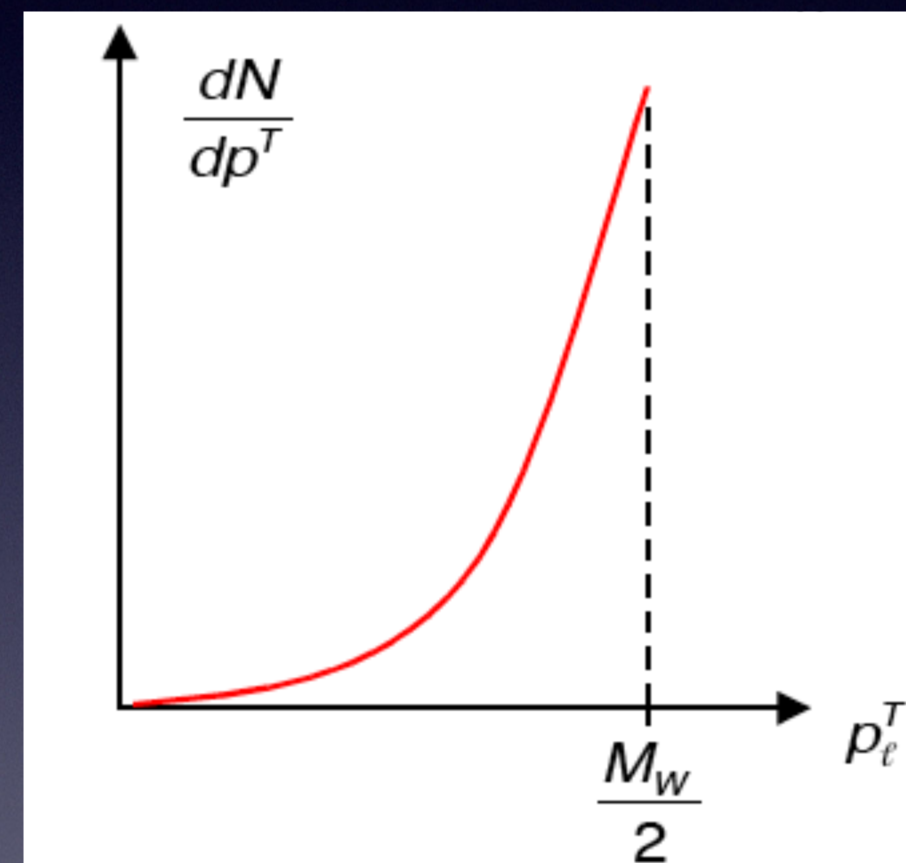

Predict a sharp drop at $M_W/2$; this distribution sensitive to W mass! Called a “Jacobian peak”

Measuring the W mass

- Sensitivity to M_W reduced by several effects: width of the W boson, addition of finite p_{TW} (the previous derivation was valid for p_{TW}=0), detector smearing

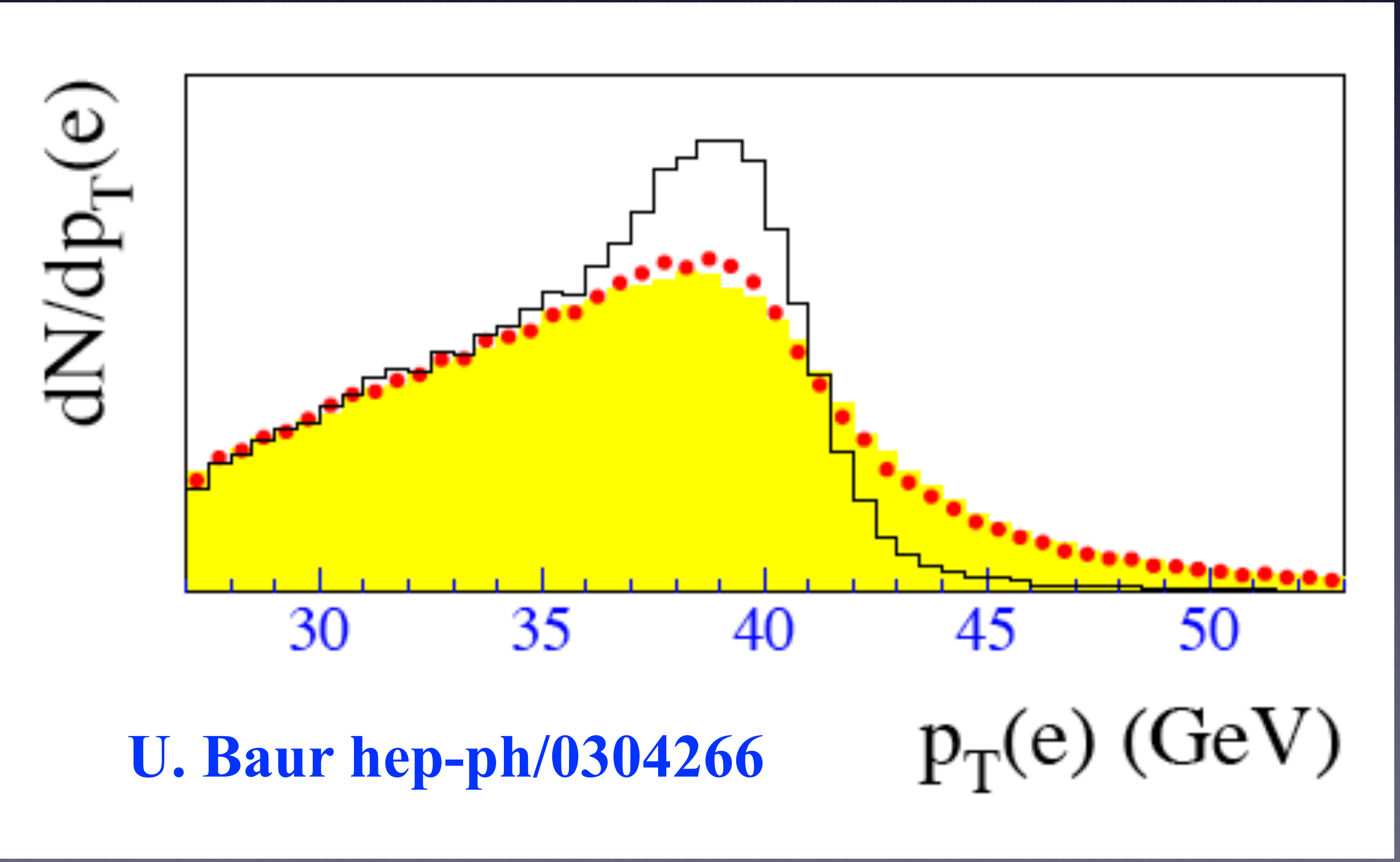

* Black histogram: shows the effect of the width Γ_W
* Red dots: show the effect of a non-zero p_{TW} due to the hadronic radiation
* Yellow histogram: shows the effect of detector smearing

Measuring the W mass

- Can construct the transverse mass, which is less sensitive our theoretical understanding of p_{TW}

$$M_T = \sqrt{2p_T(\ell)p_T(\nu)(1-\cos(\phi_{\ell,\nu}))}$$

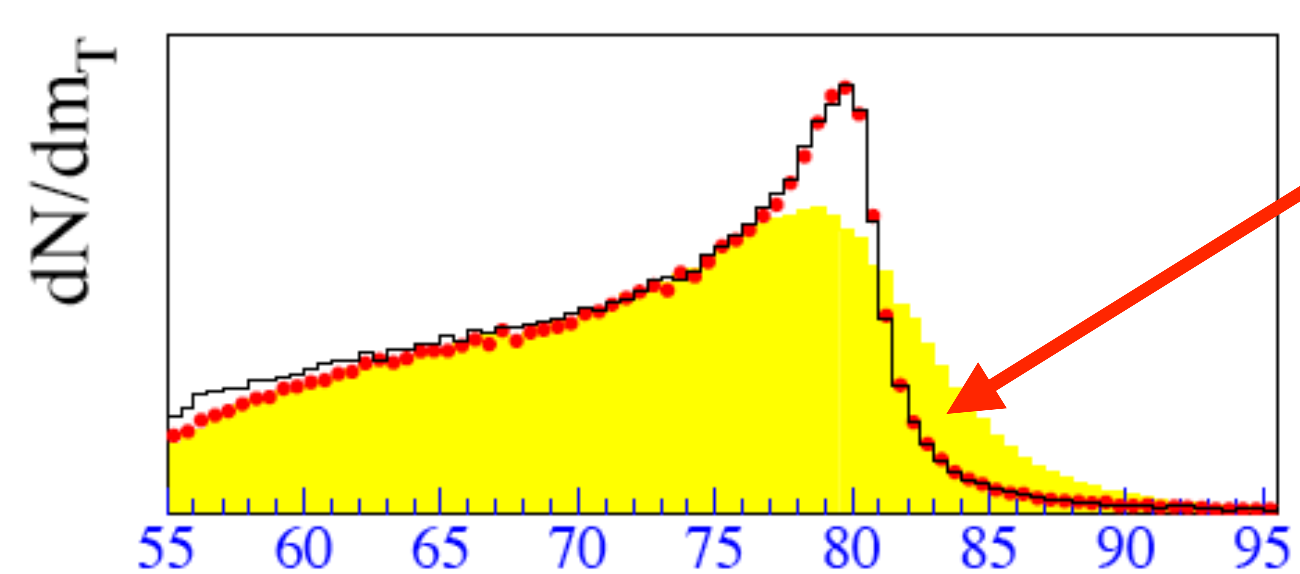

U. Baur hep-ph/0304266

- Finite-p_{TW} corrections to the m_T distribution are suppressed by p_{TW}^2/M_W^2
- However, it is still sensitive to detector smearing
- In practice, m_T and p_T of both the electron and missing energy are used

Distribution	W-boson mass (MeV)	χ^2/dof
$m_T(e,\nu)$	$80\ 408 \pm 19_{\text{stat}} \pm 18_{\text{syst}}$	52/48
$p_T^{\ell}(e)$	$80\ 393 \pm 21_{\text{stat}} \pm 19_{\text{syst}}$	60/62
$p_T^{\nu}(e)$	$80\ 431 \pm 25_{\text{stat}} \pm 22_{\text{syst}}$	71/62

CDF, PRL 108 151803 (2012)

Measuring the W mass

- Sensitivity to M_W reduced by several effects: width of the W boson, addition of finite p_{TW} (the previous derivation was valid for $p_{TW}=0$), detector smearing

All these effects make the precise extraction of M_W a complicated task!

First LHC measurement appeared recently!

U. Baur hep-ph/0304266

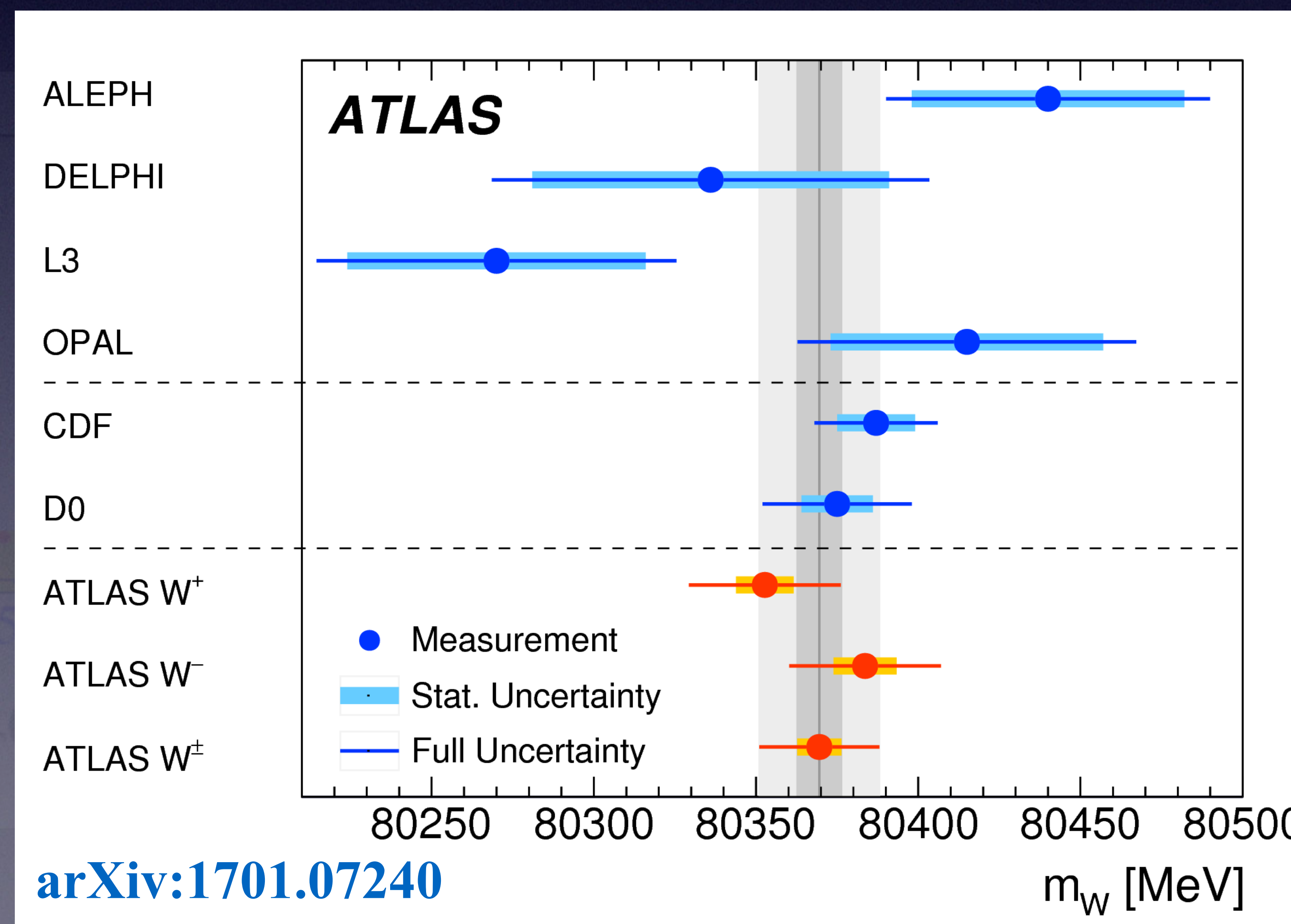

Modern applications

- Drell-Yan is the primary search mode for W’ and Z’ bosons that would signal an extension of the Standard Model gauge group

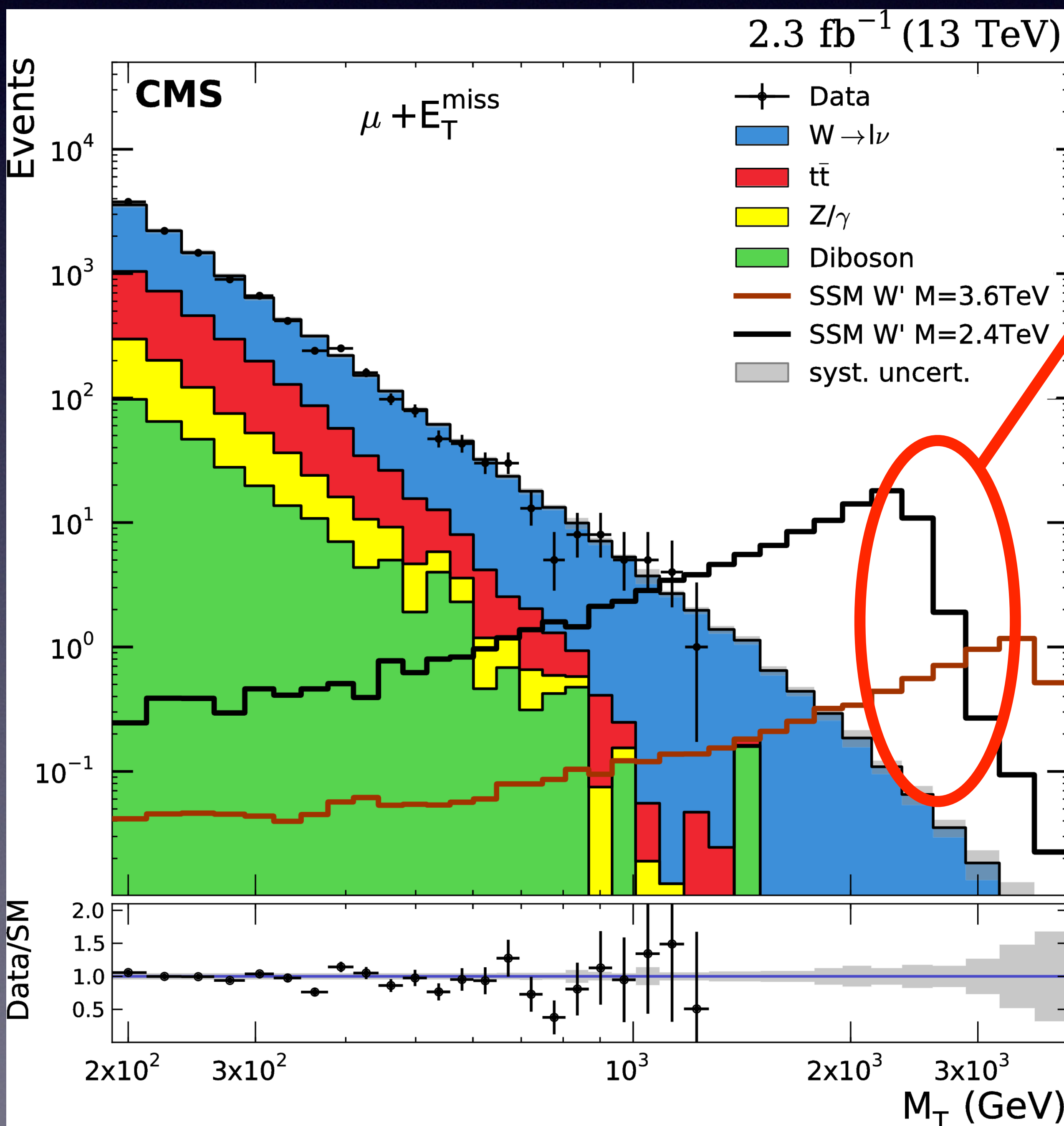

- Hypothetical signature of a W’ boson with fermionic couplings identical to the Standard Model W couplings in the muon+missing transverse energy channel in CMS
- Probes extensions of the Standard Model to several TeV
- Note the Jacobian peak that appears for $M_T = M_{W'}$; same structure that appears for the Standard Model W

Modern applications (PDFs)

- Drell-Yan production, at both collider energies and fixed-target energies, provides invaluable information on PDFs

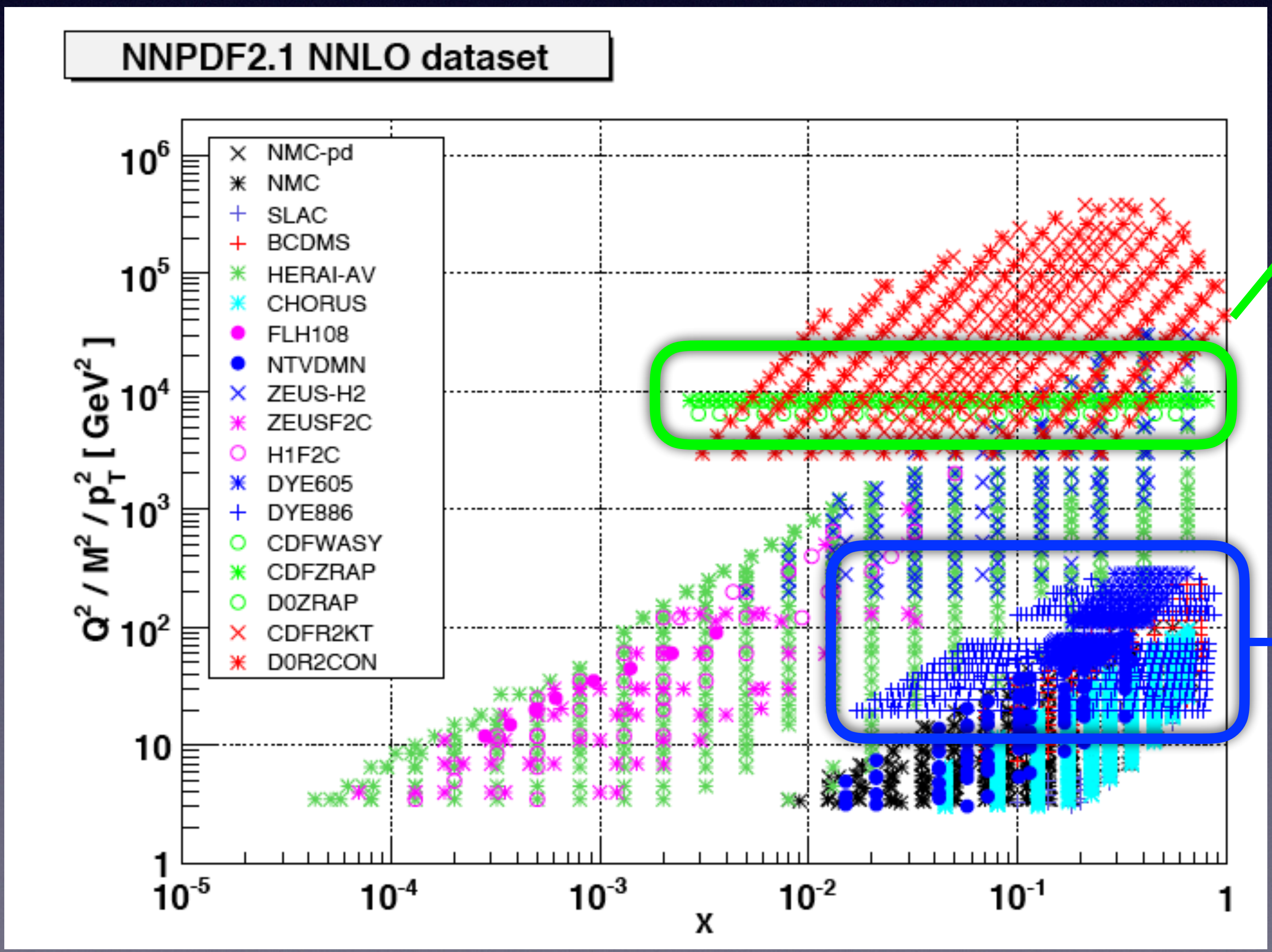

Tevatron W and Z production probe quark PDFs down to x~10^{-3} (**CDFWASY, CDFZRAP, D0ZRAP**)

Important constraints on quark/anti-quark PDFs at higher-x from fixed-target Drell-Yan (**DYE605, DYE866**)

Modern applications (PDFs)

- Drell-Yan production, at both collider and fixed-target energies, provides invaluable information on PDFs

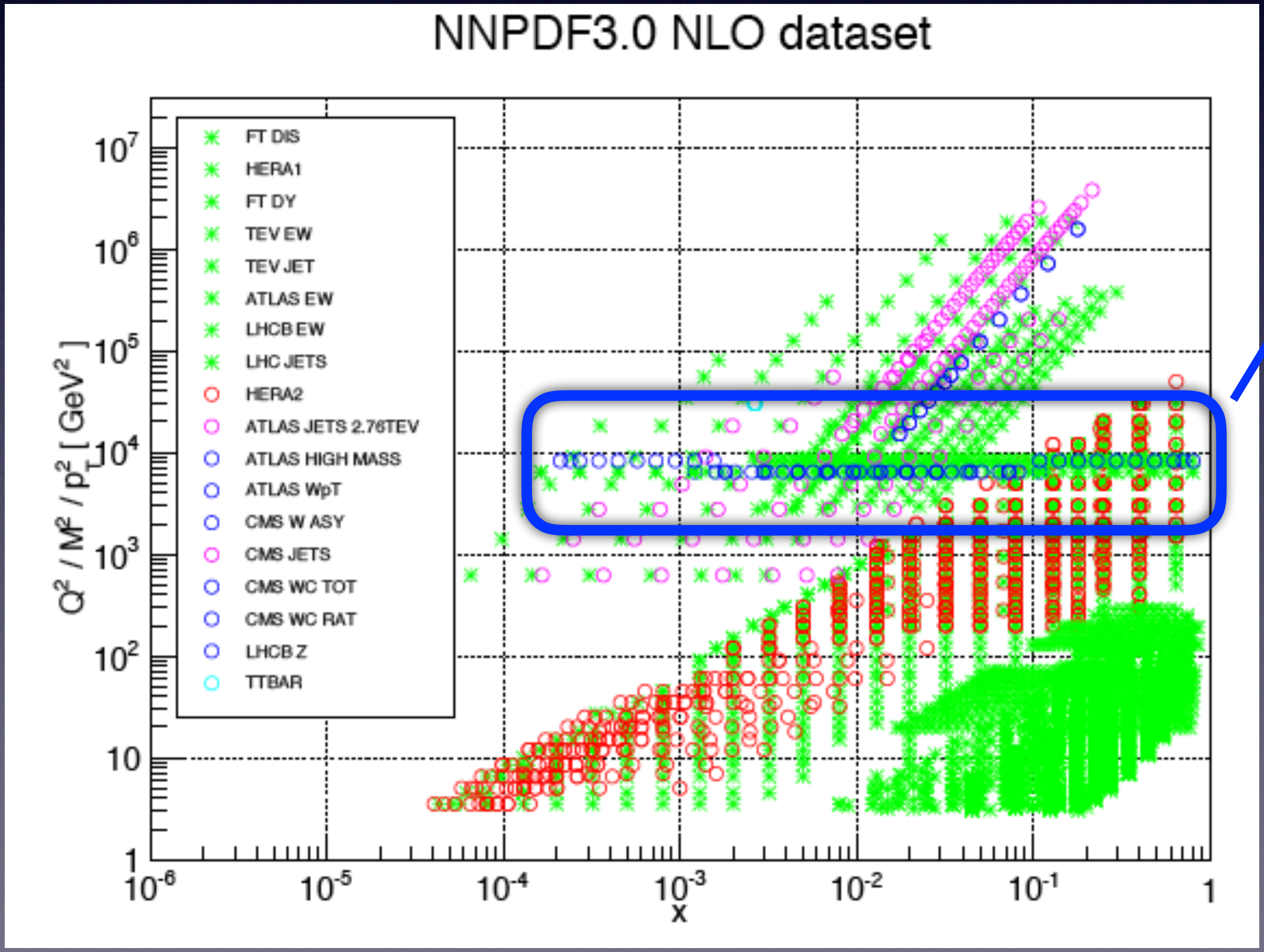

High-precision LHC data on W/Z production increasingly becoming an important element of modern PDF fits (eg. CMS W ASY)

Flavor separation of sea quarks

- Measuring Drell-Yan on a variety of nuclear targets probes differences in sea-quark PDFs

σ_{pd}: proton-deuterium xsection

deuterium has 1 proton and 1 neutron

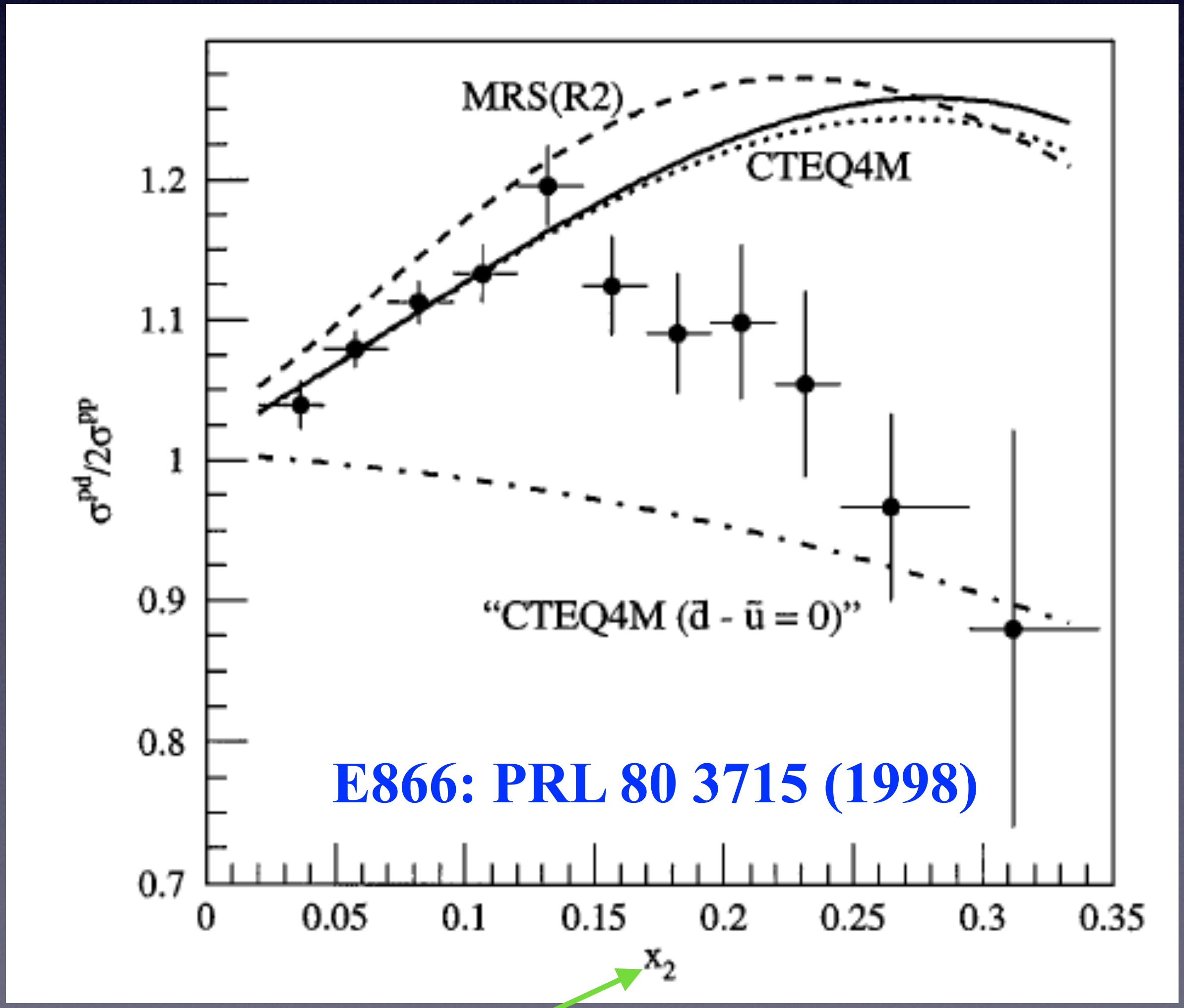

momentum fraction of the target quark

Historically important in ensuring an appropriate parameterization of the sea quarks in the high-x region

Accounting for E866 in CTEQ5:

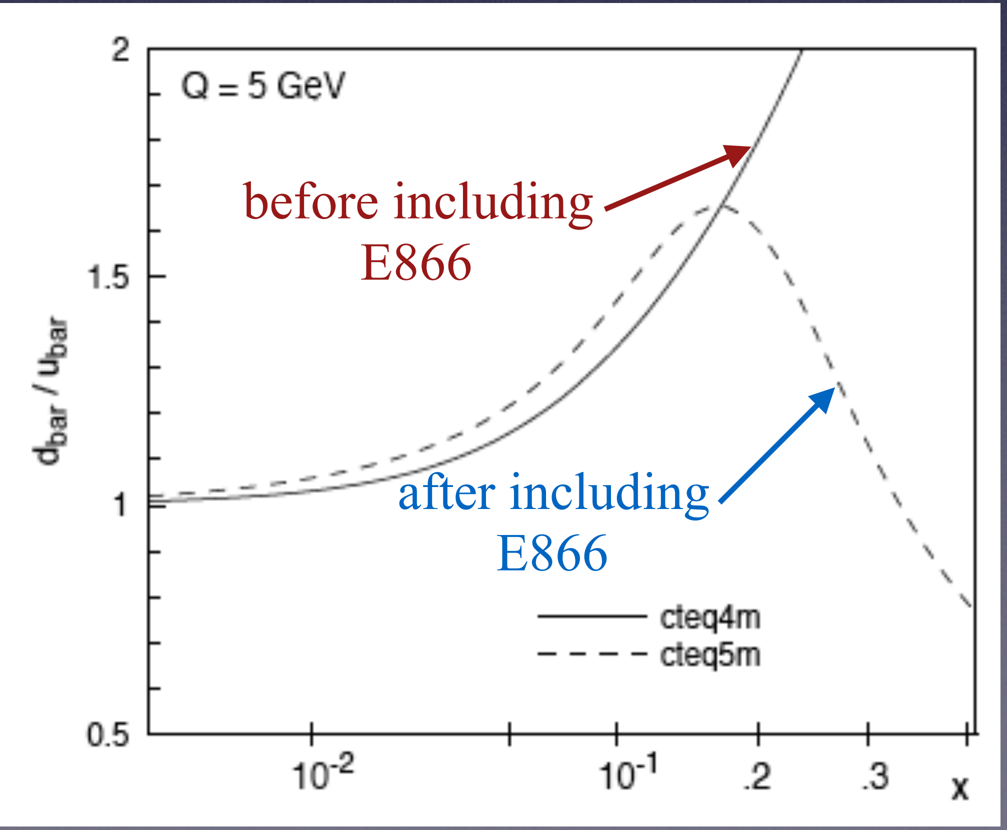

Flavor separation of valence quarks

- Tevatron measurements of the W-boson charge asymmetry probes the flavor separation of the up/down valence quark ratio

$$A_{ch}(y_W) = \frac{\frac{d\sigma^{W^+}}{dy_W} - \frac{d\sigma^{W^-}}{dy_W}}{\frac{d\sigma^{W^+}}{dy_W} + \frac{d\sigma^{W^-}}{dy_W}} \approx \frac{\frac{u(x_A)}{d(x_A)}\frac{\bar{d}(x_B)}{\bar{u}(x_B)} - 1}{\frac{u(x_A)}{d(x_A)}\frac{\bar{d}(x_B)}{\bar{u}(x_B)} + 1}$$

$$x_A = \frac{M_W}{\sqrt{s}} e^{y_W}; \quad x_B = \frac{M_W}{\sqrt{s}} e^{-y_W}$$

Assuming born kinematics and valence quarks domination of the cross section

- As y_W goes to its maximum value (large rapidity), x_B becomes small (while $x_A \rightarrow 1$) and the ratio dbar/ubar $\rightarrow$ 1. This allows us to constrain $u(x_A)/d(x_A)$.

Flavor separation of valence quarks

- Tevatron measurements of the W-boson charge asymmetry probes the flavor separation of the up/down valence quark ratio

electron charge asymmetry predicted using different codes and PDF sets

The intermediate rapidity range ($y_W \sim 1$) shows differences between MSTW and NNPDF when using the same code **(MC@NLO)**

The charge asymmetry dataset is needed to better determine the proton structure

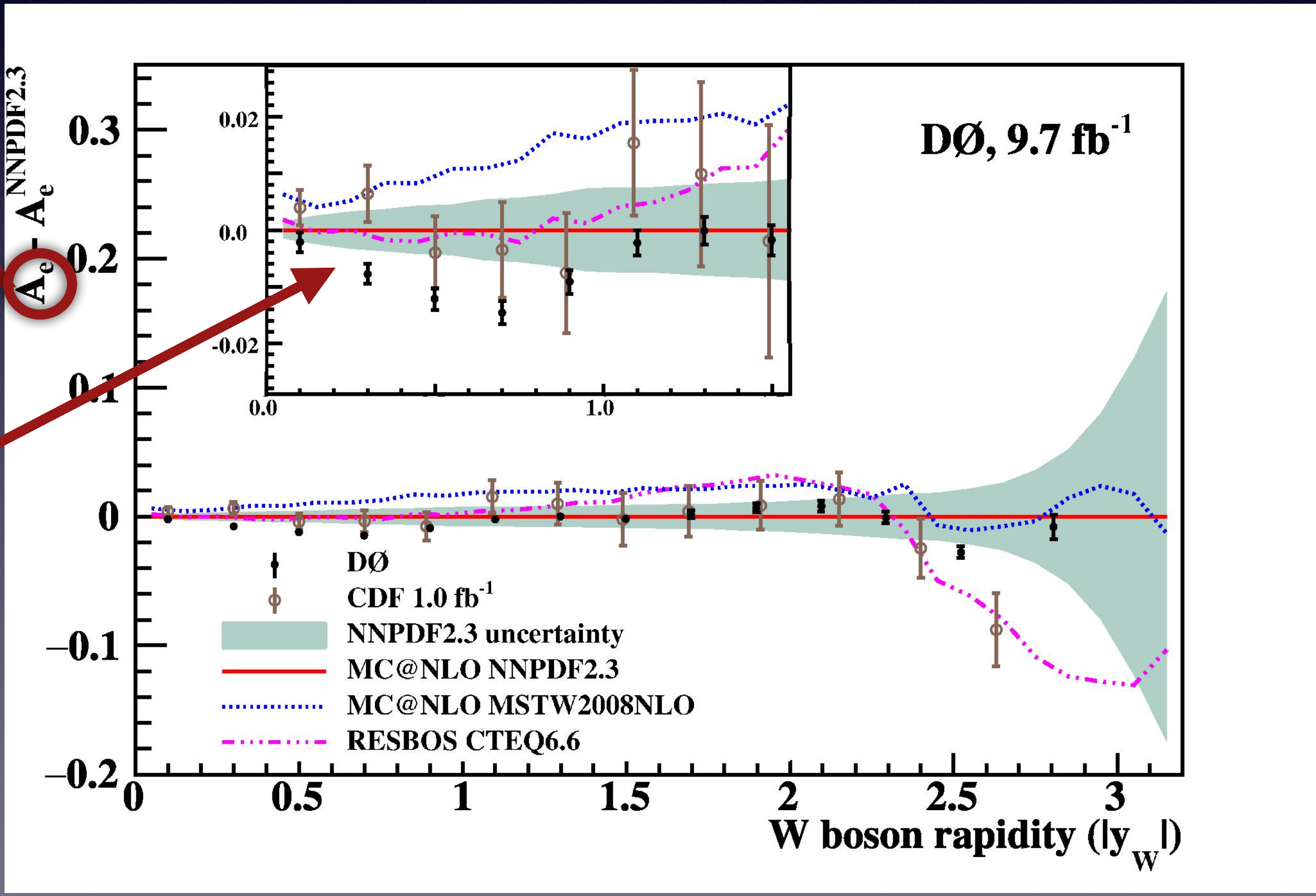

Gluon PDF from Z p_T

- New development: can constrain the intermediate-x gluon relevant for Higgs production using the Z-boson p_T spectrum

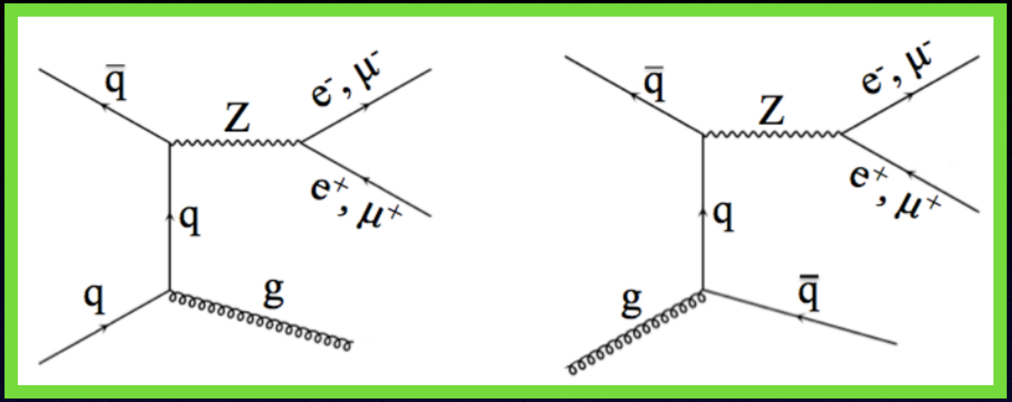

RB, Guffanti, Petriello, Ubiali 1705.00343

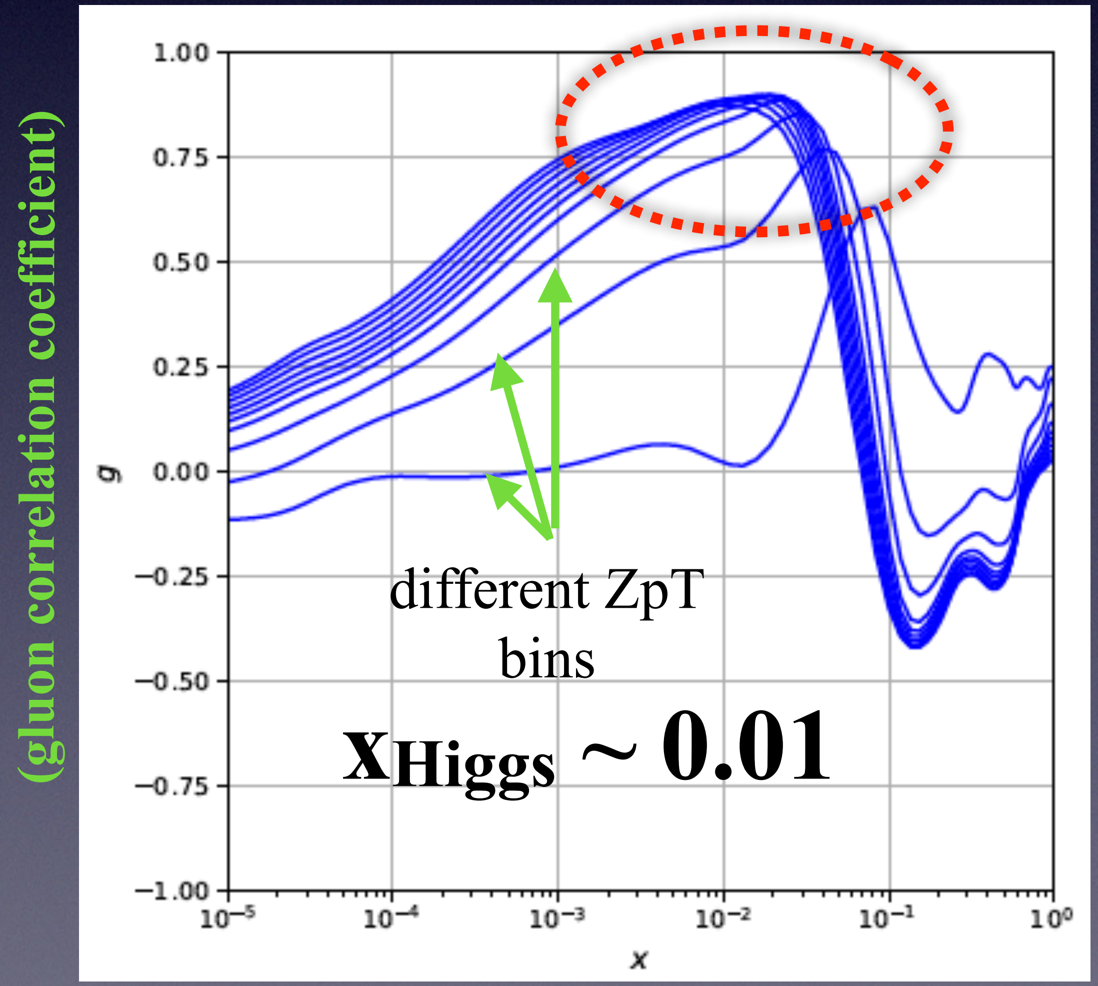

Z p_T is highly-correlated with gluon in x-region for Higgs

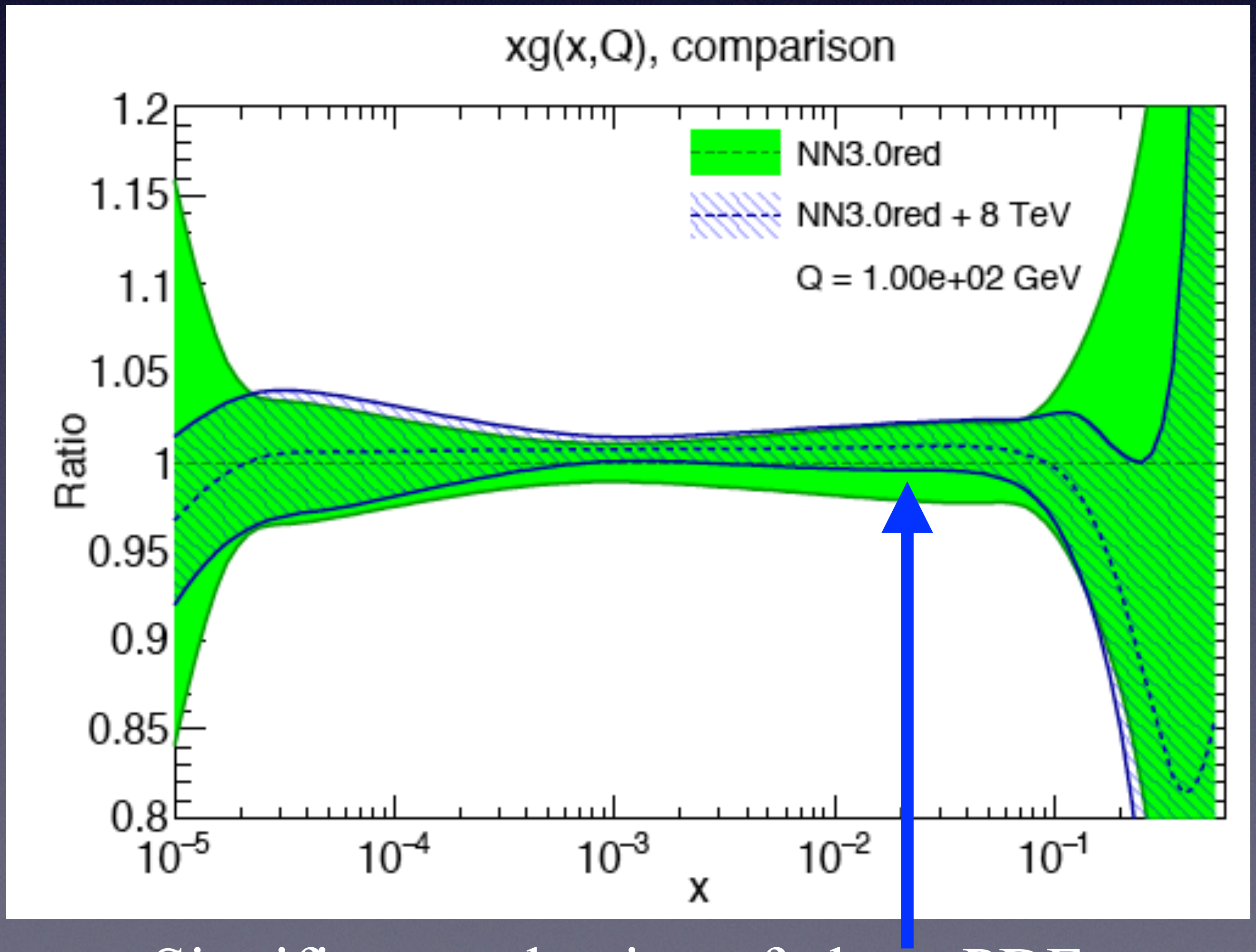

Significant reduction of gluon PDF error after including Z p_T

Predicting Drell-Yan in QCD Perturbation Theory

Drell-Yan @ LO

Drell-Yan @ LO

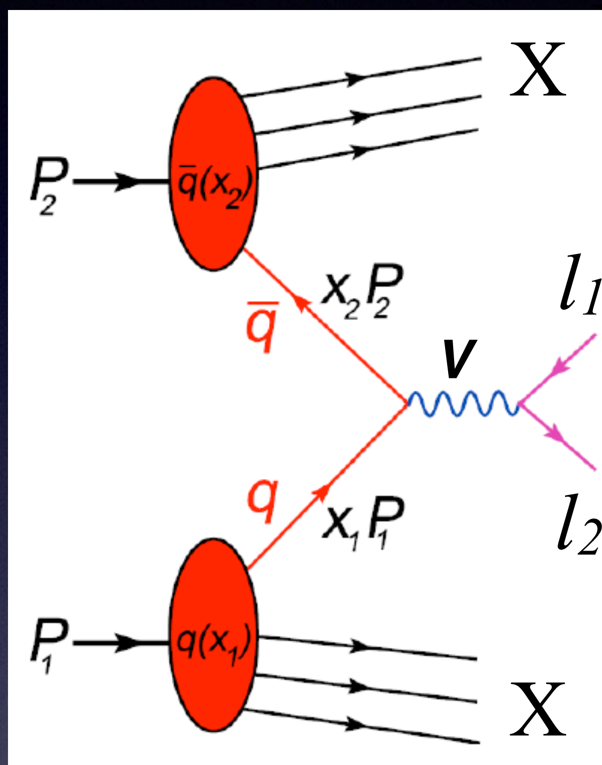

$$h(P_1) + h'(P_2) \to W^+(\to e^+\nu_e)X$$

$$\hat{s} = S\,x_1\,x_2 = M^2_{l_1 l_2}$$

partonic s

hadronic s = $(P_1+P_2)^2$

Drell-Yan @ LO

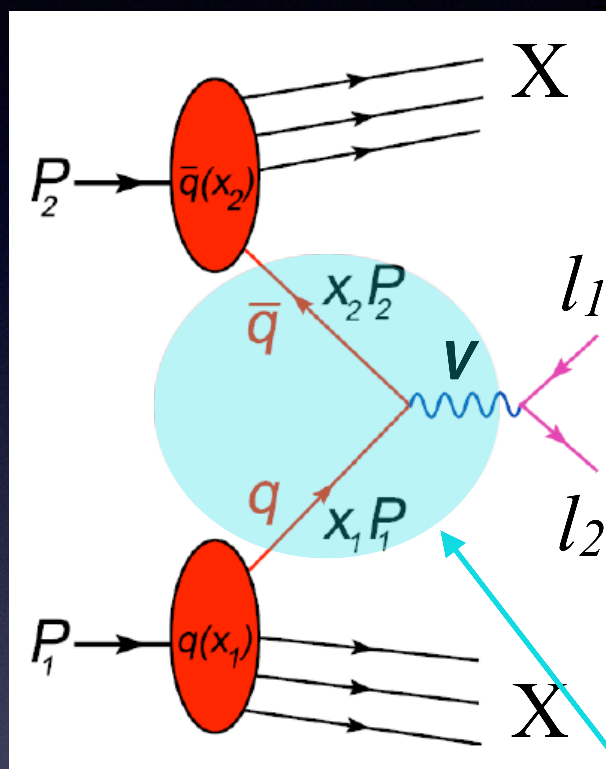

$$h(P_1) + h'(P_2) \to W^+(\to e^+\nu_e)X$$

$$\hat{s} = S\, x_1\, x_2 = M^2_{l_1 l_2}$$

partonic s

hadronic s = $(P_1+P_2)^2$

- LO partonic cross section:

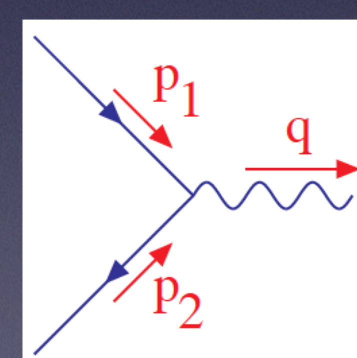

$p_1 = x_1 P_1,\ p_2 = x_2 P_2$

$$\hat{\sigma}_{q\bar{q}'} = \frac{1}{2\hat{s}} \int \frac{d^3q}{(2\pi)^3 2q_0} (2\pi)^4 \delta^4(p_1 + p_2 - q) \cdot \overline{|\mathcal{M}|}^2$$

Drell-Yan @ LO

- LO partonic cross section:

$$\hat{\sigma}_{q\bar{q}'} = \frac{1}{2\hat{s}} \int \frac{d^3q}{(2\pi)^3 2q_0} (2\pi)^4 \delta^4(p_1 + p_2 - q) \cdot \overline{|\mathcal{M}|}^2$$

where

$$\overline{|\mathcal{M}|}^2 = \underbrace{\left(\frac{1}{3} \cdot \frac{1}{3}\right) \left(\frac{1}{2} \cdot \frac{1}{2}\right)}_{\text{average color and spin}} \sum_{spin} \sum_{color}$$

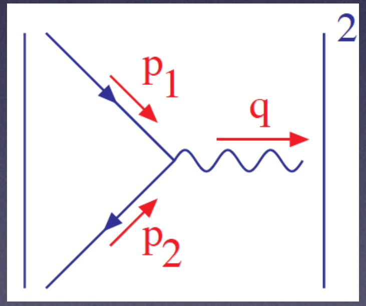

and

$$-i\mathcal{M}_\mu = \bar{v}(p_2) \frac{ig_w}{\sqrt{2}} \gamma_\mu \frac{1}{2}(1 - \gamma_5) u(p_1)$$

Drell-Yan @ LO

- LO *partonic* cross section (for on-shell W):

$$\boxed{\hat{\sigma}_{q\bar{q}',LO} = \frac{\pi}{12\,\hat{s}} g_w^2\, \delta(1-z)} \qquad z = \frac{M_{l\nu}^2}{\hat{s}}$$

- LO *hadronic* cross section:

$$\sigma_{q\bar{q}',LO} = \int_0^1 dx_1 dx_2 \underbrace{\sum_q \left(q(x_1)\bar{q}'(x_2) + \bar{q}(x_1)q'(x_2)\right)}_{\text{quark PDFs}} \hat{\sigma}(\hat{s}, z)$$

Drell-Yan @ NLO in QCD

Drell-Yan @ NLO in QCD

- Several ingredients contribute to the NLO QCD cross section for Drell-Yan:
  - Virtual corrections for the $q\bar{q}'$ channel:

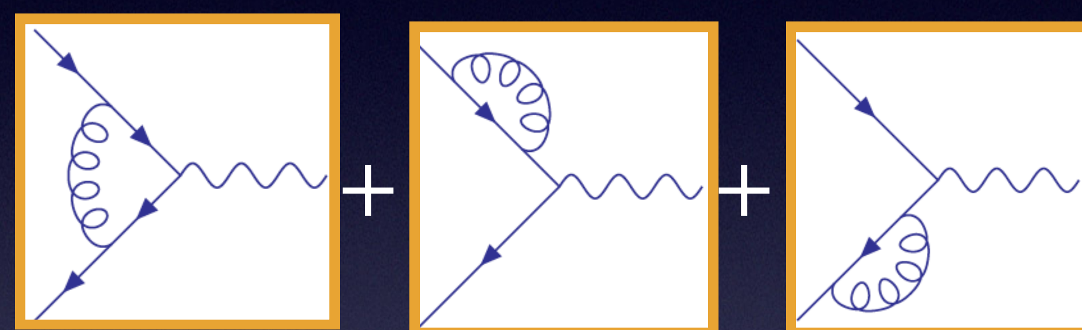

  - Real corrections for the $q\bar{q}'$ channel:

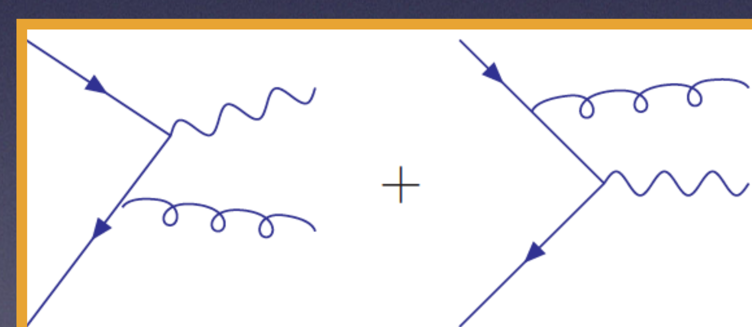

  - Real corrections for the qg and $g\bar{q}'$ channel:

These are new channels that appear for the first time at NLO!

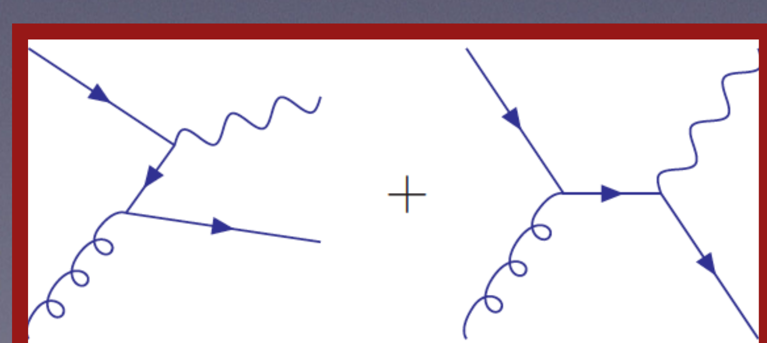

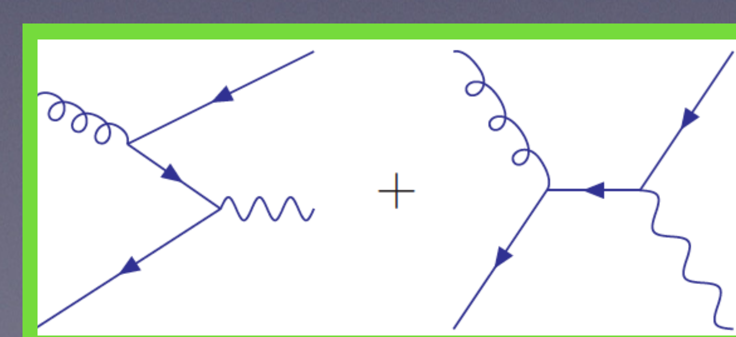

Drell-Yan @ NLO in QCD

- Feynman rules:

Quark-propagator

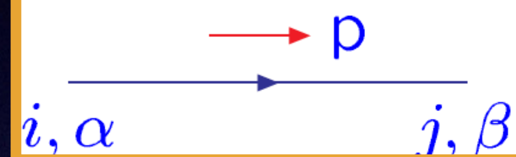

$$\frac{i(\not{p}+m)_{\beta\alpha}}{p^2-m^2+i\epsilon}\delta_{ij}$$

$i,j=1,..3$

Gluon-propagator

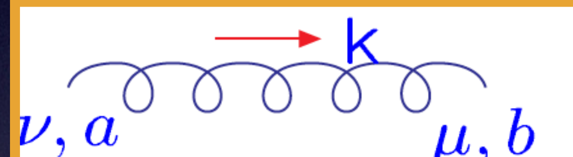

$$\frac{i(-g_{\mu\nu})}{k^2+i\epsilon}\delta_{ab}$$

$a,b=1,..8$

Quark-W vertex

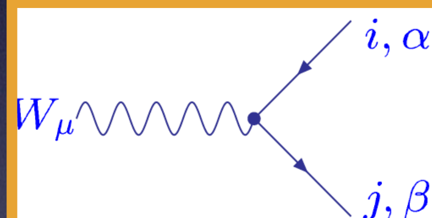

$$i\frac{g_W}{\sqrt{2}}(\gamma_\mu)_{\beta\alpha}\frac{(1-\gamma_5)}{2}\delta_{ij}$$

$g_w = \frac{e}{\sin\theta_w}$, weak coupling

Quark-gluon vertex

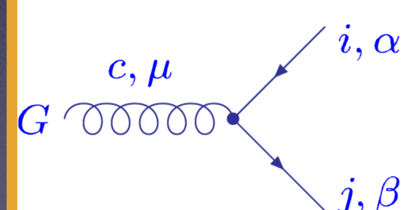

$$-ig\,(t_c)_{ji}\,(\gamma_\mu)_{\beta\alpha}$$

t_c is the $SU(N)_{N\times N}$ generator

Color generators for the quarks

$$[t_a, t_b] = i f_{abc} t_c$$

$$\sum_c t_c^2 = C_F\, I_{N\times N}$$

$$C_F = \frac{N^2-1}{2N} = \frac{4}{3}\ , \quad (N=3)$$

$$Tr(\sum_c t_c^2) = N\, C_F$$

Drell-Yan @ NLO in QCD

- In **d = 4-2$\boldsymbol{\epsilon}$** the LO partonic cross section becomes:

$$\boxed{\hat{\sigma}_{q\bar{q}',LO} = \frac{\pi}{12\,\hat{s}} g_w^2\,(1-\epsilon)\,\delta(1-z)} \qquad z = M_{l\nu}^2/\hat{s}$$

can rewrite it as: $\hat{\sigma}_{q\bar{q}',LO} = \sigma_0\,\delta(1-z)$

- In d-dimensions, the strong coupling constant has a mass dimension, i.e.$[g_s] \sim \mu^{\epsilon}$ when $\boldsymbol{\epsilon}$ is not 0. The Feynamn rules should read $g_s \to g_s\,\mu^{\epsilon}$

  Fermion field: $[\psi] \sim \mu^{\frac{d-1}{2}}$ gluon field: $[G] \sim \mu^{\frac{d-2}{2}}$

- In d-dimensions, gluons have d-2 = 2-2$\boldsymbol{\epsilon}$ polarizations. This changes the spin averaging over the initial state, which is relevant for the qg and gq channels. The number of quark polarizations is 2.

Drell-Yan @ NLO in QCD

- The virtual corrections for the $q\bar{q}'$ channel:

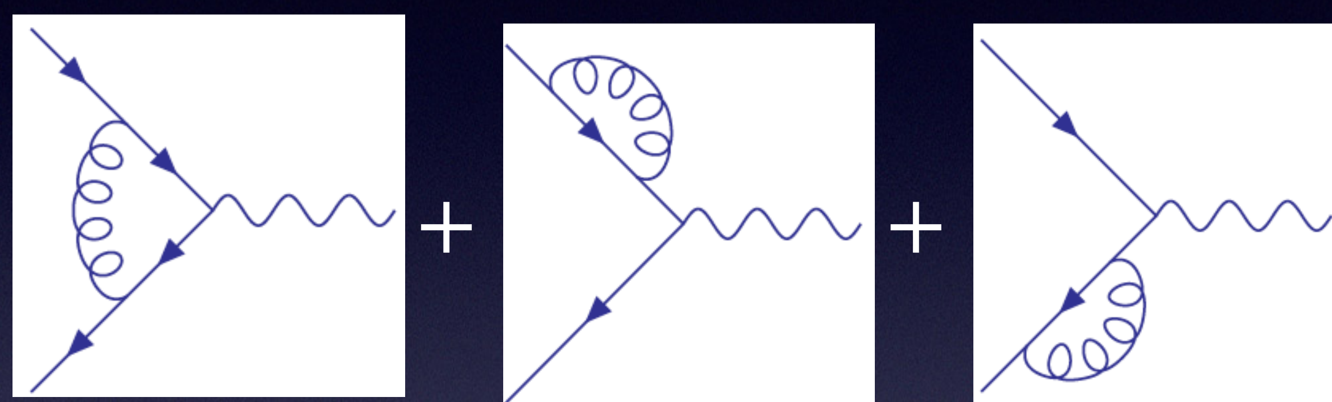

- In dimensional regularization, external self-energy diagrams vanish for massless quarks as the corresponding integral is scaleless:

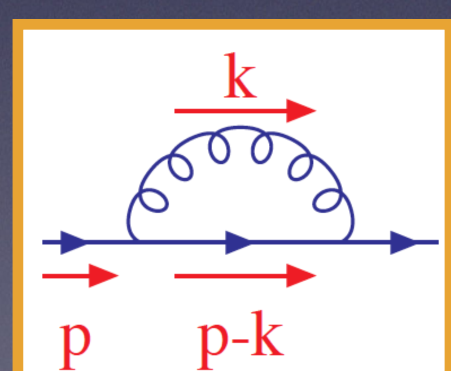

$= 0$ (prove this as an exercise)

- We therefore need to consider the vertex 1-loop diagram only

Drell-Yan @ NLO in QCD

- The virtual vertex corrections for the $q\bar{q}'$ channel taking only $O(g_s{}^2)$:

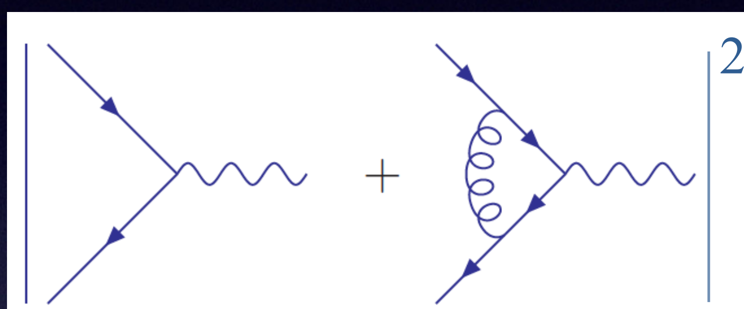

$\rightarrow 2\,Re\,($ $\{$ 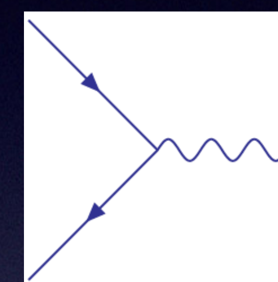 $\}^*$ x 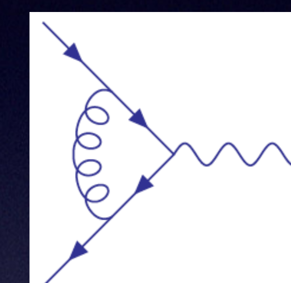 $)$

- Let's work on the $O(g_s{}^2)$ vertex:

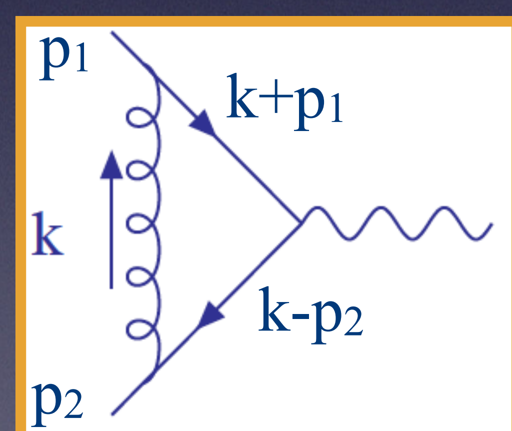

$= V_{q\bar{q}'}$

$$V_{q\bar{q}'} = -\frac{g_w}{2\sqrt{2}} g_s^2 \mu^{2\epsilon} \int \frac{d^d k}{(2\pi)^d} \frac{\bar{v}(p_2)\gamma^\mu(\not{k} - \not{p}_2)\ \not{\epsilon}_w(1-\gamma_5)(\not{k} + \not{p}_1)\gamma_\mu u(p_1)}{k^2(k+p_1)^2(k-p_2)^2}$$

Drell-Yan @ NLO in QCD

- Combine the denominators using the following Feynman parametrization, then shift the momentum $k \to k - xp_1 + yp_2$

$$\frac{1}{a\,b\,c} = 2\int_0^1 dx\,dy\,dz\,\delta(1-x-y-z)\;\frac{1}{[x\,a+y\,b+c\,z]^3}$$

- The shift leads to the simplified integral:

abbreviated numerator

$$V_{q\bar{q}'} = -\frac{g_w}{2\sqrt{2}} g_s^2 \mu^{2\epsilon} \int_0^1 dx\,dy\,dz\,\delta(1-x-y-z)\;\int \frac{d^d k}{(2\pi)^d}\frac{N}{(k^2+x\,y\,\hat{s})^3}$$

- Applying the same shift to the numerator, keeping in mind that terms odd in k^μ integrate to zero, and using on-shell conditions leads to the following numerator:

$$N = -2(1-\epsilon)\,\frac{2-d}{d}\,k^2\,\bar{v}(p_2)\;\not{\epsilon}_w(1-\gamma_5)\,u(p_1)$$
$$-2\hat{s}\,\bar{v}(p_2)\;\not{\epsilon}_w(1-\gamma_5)\,u(p_1)\;((1-x)(1-y)-\epsilon xy)$$

Drell-Yan @ NLO in QCD

- Our integral now becomes:

$$V_{q\bar{q}'} = -iM_{LO}\, 2\, g_s^2\, \mu^{2\epsilon} \int_0^1 dx\, dy\, dz\, \delta(1-x-y-z) \int \frac{d^d k}{(2\pi)^d} \frac{1}{(k^2+x\, y\, \hat{s})^3}$$
$$\times \left[\frac{4\,(1-\epsilon)^2\, k^2}{d} - 2\hat{s}\,((1-x)(1-y) - \epsilon xy)\right]$$

with $$\boxed{-iM_{LO} = -\frac{g_w}{2\sqrt{2}}\, \bar{v}(p_2)\, \not{\epsilon}_w (1-\gamma_5)\, u(p_1)}$$

- It remains to do the loop integral. We use the following results:

$$\int \frac{d^d k}{(2\pi)^d} \frac{1}{[k^2-\Delta]^3} = -i\, \frac{\Gamma[1+\epsilon]}{2\,(4\pi)^{d/2}}\, \Delta^{-1-\epsilon}$$

$$\int \frac{d^d k}{(2\pi)^d} \frac{k^2}{[k^2-\Delta]^3} = i\, \frac{d}{4}\, \frac{\Gamma[1+\epsilon]}{\epsilon}\, \frac{\Delta^{-\epsilon}}{(4\pi)^{d/2}}$$

UV-divergence

and get:

$$V_{q\bar{q}'} = -iM_{LO}\, g_s^2\, \mu^{2\epsilon}\, \frac{\Gamma(1+\epsilon)}{(4\pi)^{d/2}}\, i \int_0^1 dx\, dy\, dz\, (-x\, y\, \hat{s})^{-\epsilon}\, \delta(1-x-y-z) \left\{\frac{2\,(1-\epsilon)^2}{\epsilon} + \frac{2\hat{s}\,((1-x)(1-y)-\epsilon\, x\, y)}{(-x\, y\, \hat{s})}\right\}$$

Soft+Collinear divergences

Drell-Yan @ NLO in QCD

- Doing the parametric integrals, adding the color structure $[T^aT^a]_{ij}$ (i and j are the quark color indices), and taking the *2 Re*$(V_{q\bar{q}'} M^*_{LO})$:

$$2Re(V_{q\bar{q}'}\, M^*_{LO}) = |M_{LO}|^2\, C_F\, \left(\frac{\alpha_s}{2\pi}\right) \left(\frac{\hat{s}}{4\pi\mu^2}\right)^{-\epsilon} \frac{\Gamma(1-\epsilon)}{\Gamma(1-2\epsilon)} \left(\frac{-2}{\epsilon^2} - \frac{3}{\epsilon} + \frac{2\pi^2}{3} - 8\right)$$

$$\boxed{\sigma^{\text{virtual}}_{NLO,q\bar{q}'} = \sigma_{LO}\, C_F\, \left(\frac{\alpha_s}{2\pi}\right) \left(\frac{\hat{s}}{4\pi\mu^2}\right)^{-\epsilon} \frac{\Gamma(1-\epsilon)}{\Gamma(1-2\epsilon)} \left(\frac{-2}{\epsilon^2} - \frac{3}{\epsilon} + \frac{2\pi^2}{3} - 8\right)}$$

- Need the real radiation contributions as well:

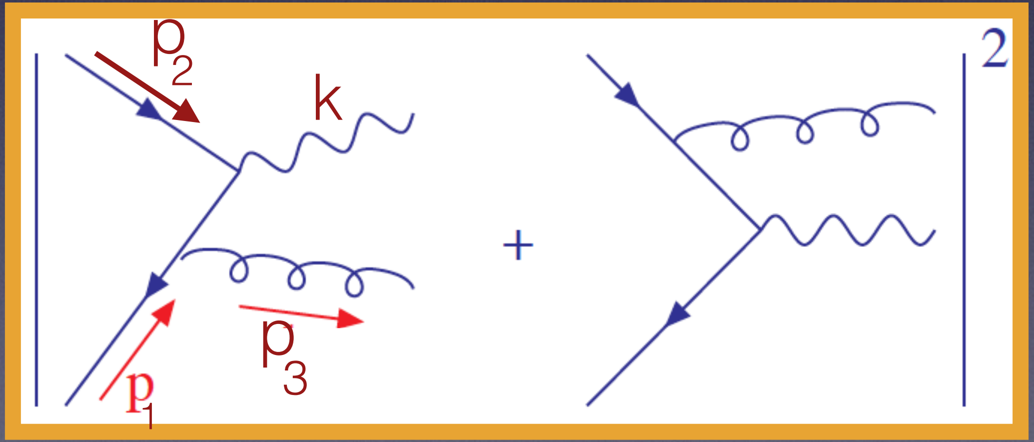

$$\hat{\sigma} = \frac{1}{2\,\hat{s}} \overline{|\mathcal{M}|}^2 \cdot \mathcal{PS}_2 \quad \text{and} \quad \begin{aligned} \hat{s} &= (p_1 + p_2)^2 = 2\, p_1 \cdot p_2 \\ \hat{t} &= (p_1 - p_3)^2 = -2\, p_1 \cdot p_3 \\ \hat{u} &= (p_2 - p_3)^2 = -2\, p_2 \cdot p_3 \end{aligned}$$

Drell-Yan @ NLO in QCD

$$\overline{|\mathcal{M}_{q\bar{q}'}|}^2 = -\underbrace{\left(\frac{1}{2}\cdot\frac{1}{2}\right)}_{\text{spin avg.}}\underbrace{\left(\frac{1}{3}\cdot\frac{1}{3}\right)}_{\text{color avg.}}\cdot Tr(T^aT^a)\cdot(g\mu^\epsilon)^2\cdot g_w^2\cdot 2(1-\epsilon)$$

$$\cdot\left((1-\epsilon)\left(-\frac{\hat{u}}{\hat{t}}-\frac{\hat{t}}{\hat{u}}\right)-\frac{2\hat{s}M^2}{\hat{t}\hat{u}}+2\epsilon\right)$$

$$PS_2 = \frac{1}{8\pi}\left(\frac{4\pi}{M^2}\right)^\epsilon\frac{1}{\Gamma(1-\epsilon)}z^\epsilon(1-z)^{1-2\epsilon}\int_0^1 dy(y(1-y))^{-\epsilon}$$

with

$$y = \tfrac{1}{2}\left(1+cos\theta\right)$$
$$\hat{t} = -\hat{s}\left(1-\tfrac{M^2}{\hat{s}}\right)(1-y)$$
$$\hat{u} = -\hat{s}\left(1-\tfrac{M^2}{\hat{s}}\right)y$$

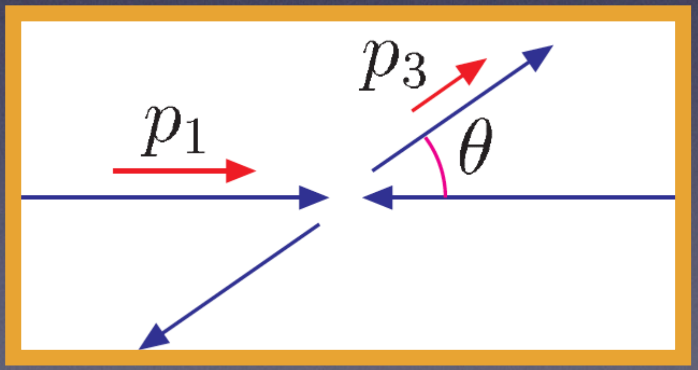

partonic CM frame

and $\int_0^1 dy\, y^\alpha\,(1-y)^\beta = \frac{\Gamma(1+\alpha)\,\Gamma(1+\beta)}{\Gamma(2+\alpha+\beta)}$, $z = M^2/\hat{s}$ and $M{=}M_W$

Drell-Yan @ NLO in QCD

- The result for the real radiation contribution for the $q\bar{q}'$ is:

$$\hat{\sigma}^{R}_{q\bar{q}',NLO} = \sigma_0\, C_F\, \left(\frac{\alpha_s}{2\pi}\right) \left(\frac{\hat{s}}{4\pi\mu^2}\right)^{-\epsilon} \frac{\Gamma(1-\epsilon)}{\Gamma(1-2\epsilon)} \left\{ \frac{2}{\epsilon^2}\delta(1-z) - \frac{2}{\epsilon}\frac{1+z^2}{(1-z)_+} + 4(1+z^2)\left[\frac{\ln(1-z)}{1-z}\right]_+ \right\}$$

You will need to use the plus-distribution expansion defined through the following formulae:

$$\frac{1}{(1-z)^{1+2\epsilon}} = -\frac{1}{2\epsilon}\delta(1-z) + \frac{1}{(1-z)_+} - 2\epsilon\left[\frac{\ln(1-z)}{(1-z)}\right]_+ + \ldots$$

$$\int_0^1 dz \left[\frac{\ln^n(1-z)}{1-z}\right]_+ f(z) = \int_0^1 dz\, \frac{\ln^n(1-z)}{1-z}\left(f(z) - f(1)\right)$$

- Combining this result with the virtual corrections one shown on a previous slide leads to:

$$\hat{\sigma}_{q\bar{q}',NLO} = \sigma_0\, C_F\, \left(\frac{\alpha_s}{2\pi}\right) \left(\frac{\hat{s}}{4\pi\mu^2}\right)^{-\epsilon} \frac{\Gamma(1-\epsilon)}{\Gamma(1-2\epsilon)} \left\{ \frac{-2}{\epsilon} P_{qq}(z) + \left(\frac{2\pi^2}{3} - 8\right)\delta(1-z) + 4(1+z^2)\left[\frac{\ln(1-z)}{1-z}\right]_+ \right\}$$

where $\quad P_{qq}(z) = \frac{3}{2}\,\delta(1-z) + \frac{1+z^2}{(1-z)_+}$

- While the leading pole cancels in the sum of real and virtual corrections for the $q\bar{q}'$ channel, the left over $1/\epsilon$ pole (from initial state collinear singularity) requires subtraction to obtain a finite cross section.

Drell-Yan @ NLO in QCD

- Absorb remaining initial-state collinear singularities into PDFs, which amounts to adding the following counterterm:

One for each PDF

$$2 \times \frac{\alpha_s}{2\pi} \left(\frac{4\pi}{e^\gamma}\right)^\epsilon \frac{1}{\epsilon} P_{qq} \bigotimes \hat{\sigma}_{LO}(z) \quad \text{where} \quad f \bigotimes g(z) = \int_0^1 dx\, dy\, f(x)\, g(y)\, \delta(z - xy)$$

$$2 \times \frac{\alpha_s}{2\pi} \left(\frac{4\pi}{e^\gamma}\right)^\epsilon \frac{1}{\epsilon} P_{qq} \bigotimes \hat{\sigma}_{LO}(z) = 2 \times \frac{\alpha_s}{2\pi} \left(\frac{4\pi}{e^\gamma}\right)^\epsilon \frac{C_F}{\epsilon} \sigma_{LO}\, P_{qq}(z)$$

- Arrive at the final result (we have switched to the MSbar scheme):

$$\boxed{\hat{\sigma}_{q\bar{q}',NLO} = \sigma_0\, C_F \left(\frac{\alpha_s}{2\pi}\right) \left\{2 \ln\left(\frac{\hat{s}}{\mu^2}\right) P_{qq}(z) + \left(\frac{2\pi^2}{3} - 8\right)\delta(1-z) + 4(1+z^2)\left[\frac{\ln(1-z)}{1-z}\right]_+\right\}}$$

Drell-Yan @ NLO in QCD

- The $g\bar{q}$' channel:

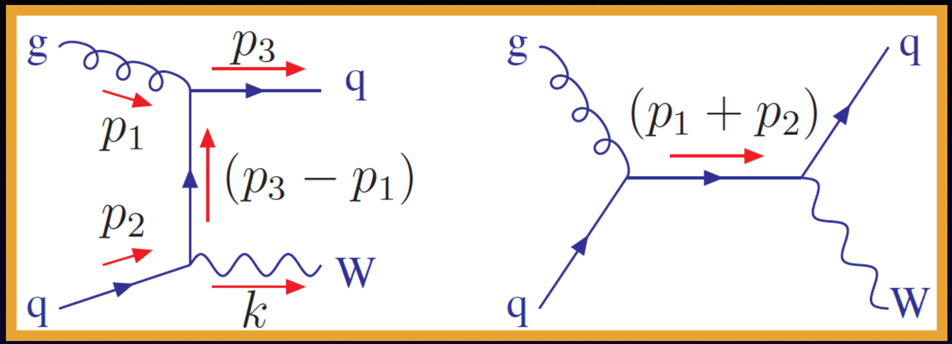

$$\hat{\sigma} = \frac{1}{2\,\hat{s}} \overline{|\mathcal{M}|}^2 \cdot \mathcal{PS}_2 \quad \text{and} \quad \begin{array}{l} \hat{s} = (p_1 + p_2)^2 = 2\,p_1 \cdot p_2 \\ \hat{t} = (p_1 - p_3)^2 = -2\,p_1 \cdot p_3 \\ \hat{u} = (p_2 - p_3)^2 = -2\,p_2 \cdot p_3 \end{array}$$

$$\overline{|\mathcal{M}|}^2 = \underbrace{\left(\frac{1}{2\,(1-\epsilon)}\frac{1}{2}\right)}_{\text{spin avg.}} \underbrace{\left(\frac{1}{3}\cdot\frac{1}{8}\right)}_{\text{color avg.}} \cdot Tr(t^a t^a) \cdot (g_s \mu^\epsilon)^2 \cdot g_w^2 \cdot 2(1-\epsilon)$$

$$\cdot \left((1-\epsilon)\left(-\frac{\hat{s}}{\hat{t}} - \frac{\hat{t}}{\hat{s}}\right) - \frac{2\hat{u}M^2}{\hat{t}\hat{s}} + 2\epsilon \right)$$

$$PS_2 = \frac{1}{8\pi}\left(\frac{4\pi}{M^2}\right)^\epsilon \frac{1}{\Gamma(1-\epsilon)} z^\epsilon (1-z)^{1-2\epsilon} \int_0^1 dy (y(1-y))^{-\epsilon}$$

Drell-Yan @ NLO in QCD

- The $g\bar{q}$' channel:

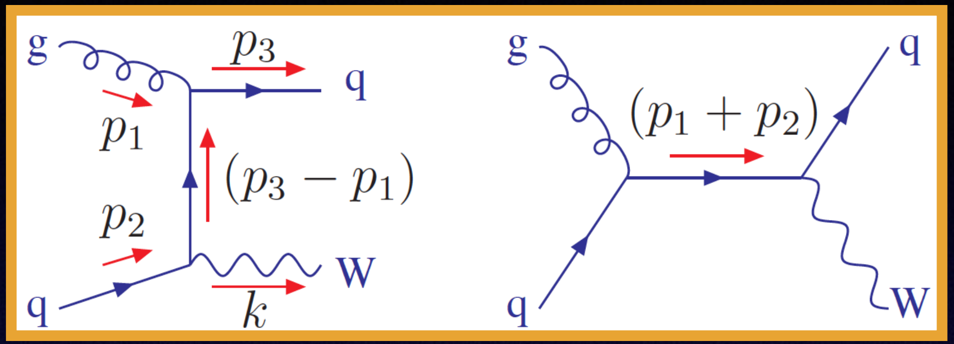

$$\hat{\sigma}_{gq'} = \sigma_0 \, \frac{\alpha_s}{2\pi} \cdot \left\{ 2 \cdot \underbrace{\left(\frac{1}{2} (z^2 + (1-z)^2) \right)}_{P_{gq}^{(0)}(z)} \cdot \left[\ln\left(\frac{M^2}{\mu^2} \right) + \ln\left(\frac{(1-z)^2}{z} \right) \right] + \frac{3}{4} + \frac{z}{2} - \frac{3}{4} z^2 \right\}$$

- The cross section for the qg channel is identical to the $g\bar{q}$' cross section since we are integrating inclusively over the final state.

$$\hat{\sigma}_{qg} = \hat{\sigma}_{g\bar{q}'}$$

Future High Energy Colliders

A future 100 TeV machine?

- There is growing interest in the HEP community to build a future high-energy pp machine with CM energy ~100 TeV
- Initial discussions regarding CERN, Chinese sites. This would possibly be after an e+e- Higgs factory is constructed.

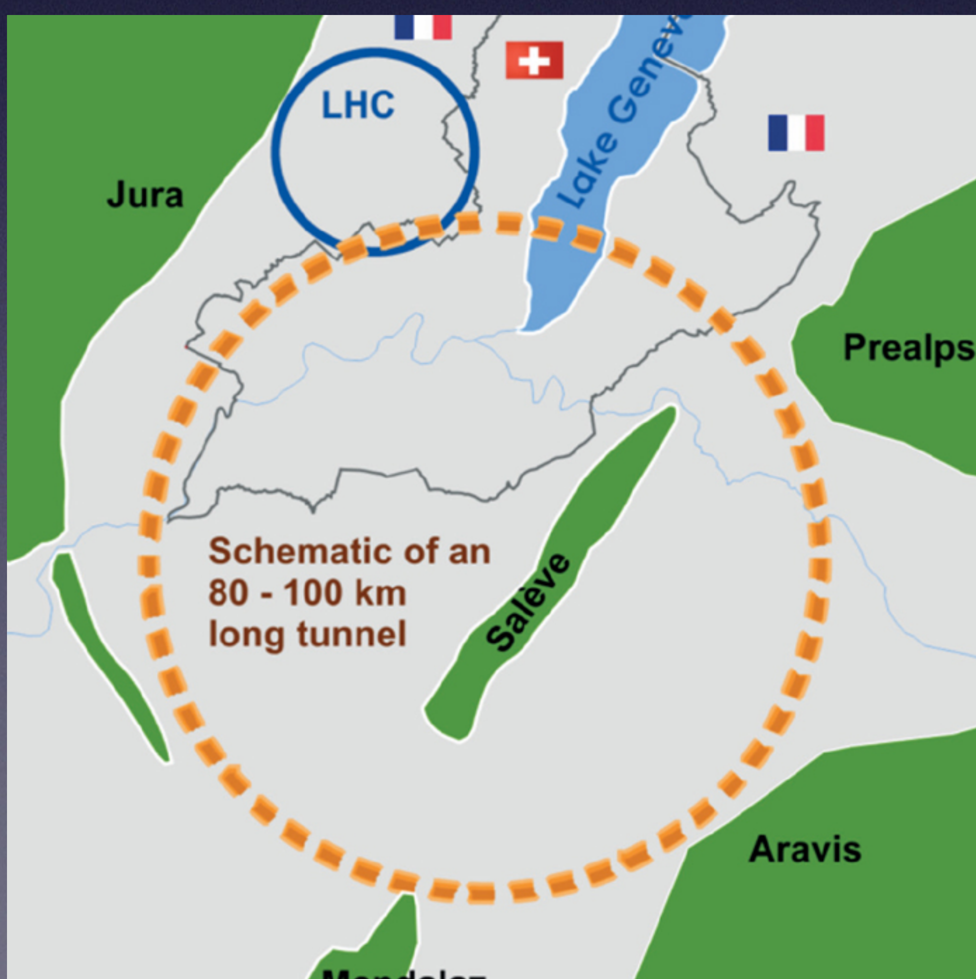

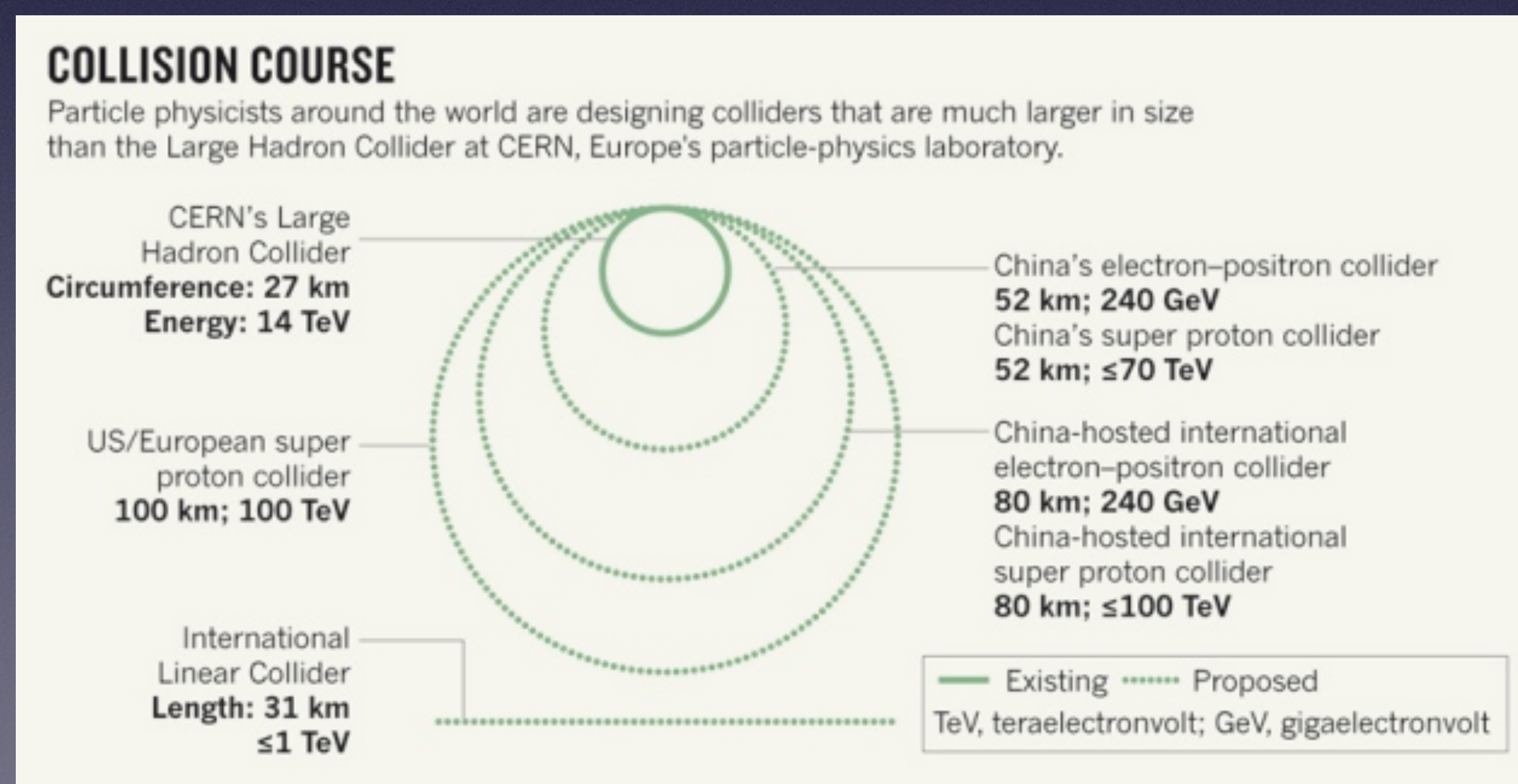

Drell-Yan in the future

- Drell-Yan will continue to play an integral role of the physics program at such future machines.

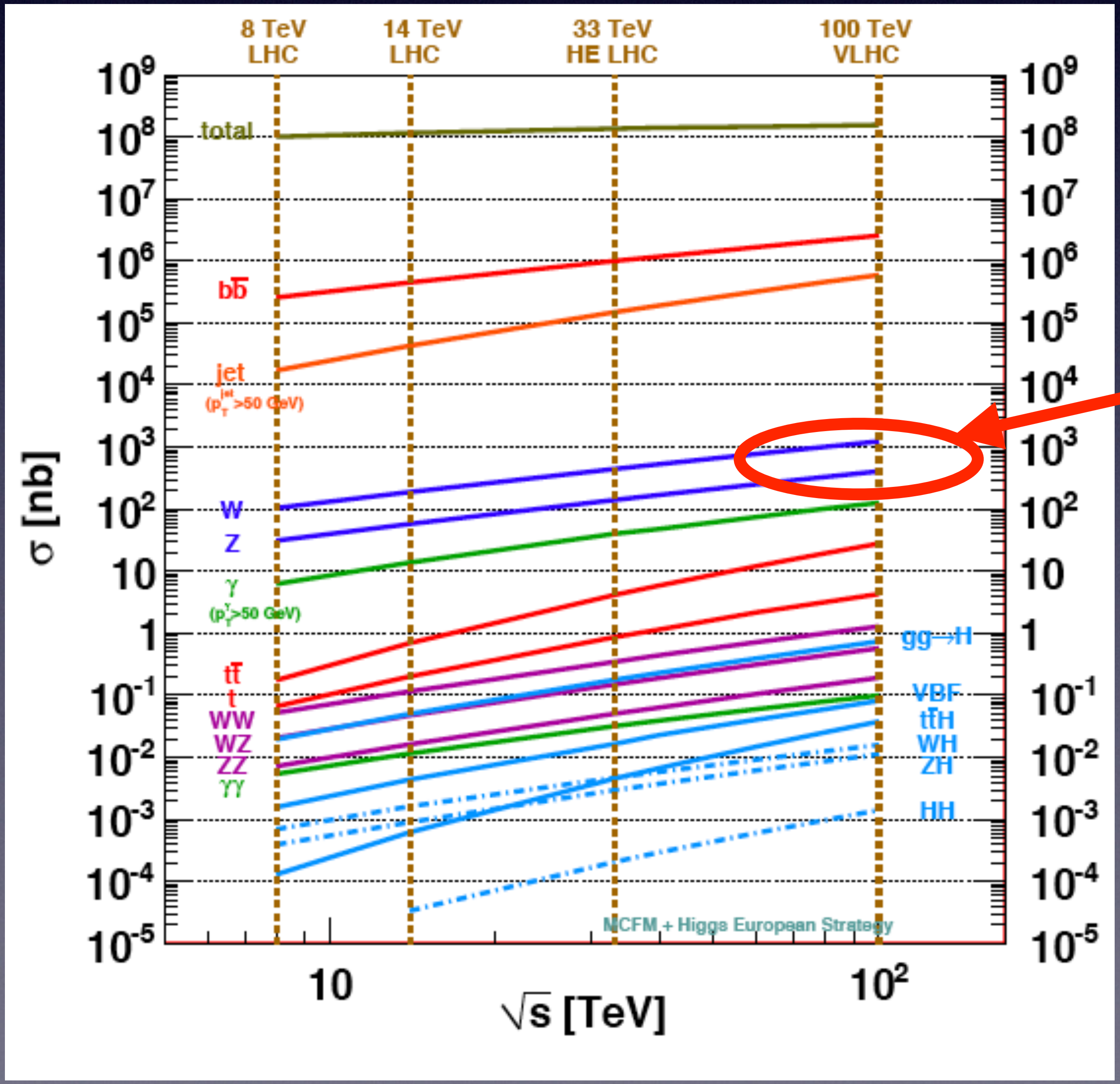

Large production rates for W and Z boson production via Drell-Yan at 100 TeV; will remain an important background to any searches at high energies

Drell-Yan in the future

- Drell-Yan will continue to play an integral role of the physics program at such future machines

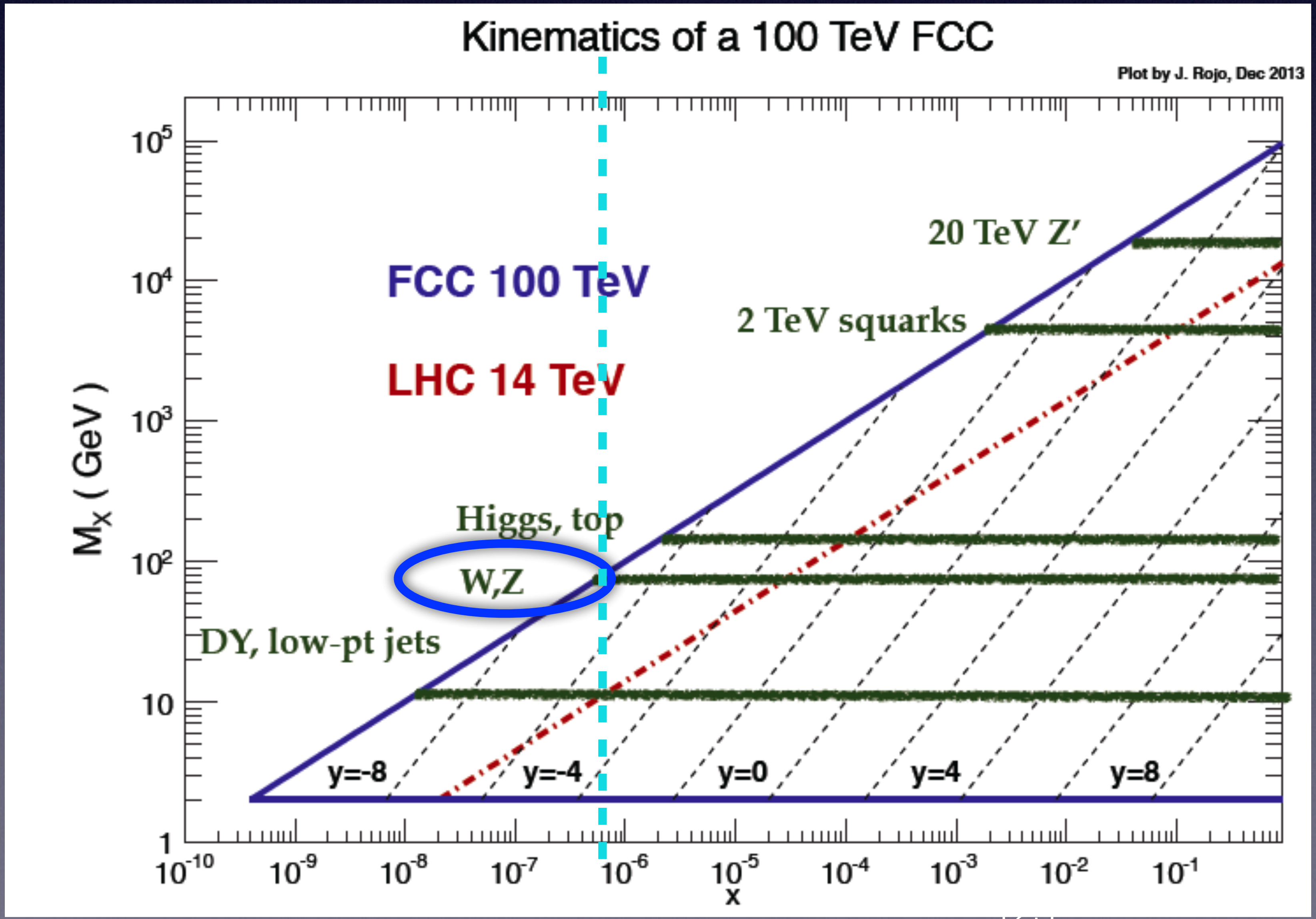

New kinematic regions probed; W/Z production down to Bjorken x~10^{-6}, more than an order of magnitude lower than LHC 14 TeV coverage

New gauge bosons at 100 TeV

- Unmatched reach for new gauge bosons which would indicate new forces of Nature beyond SU(3)xSU(2)xU(1)

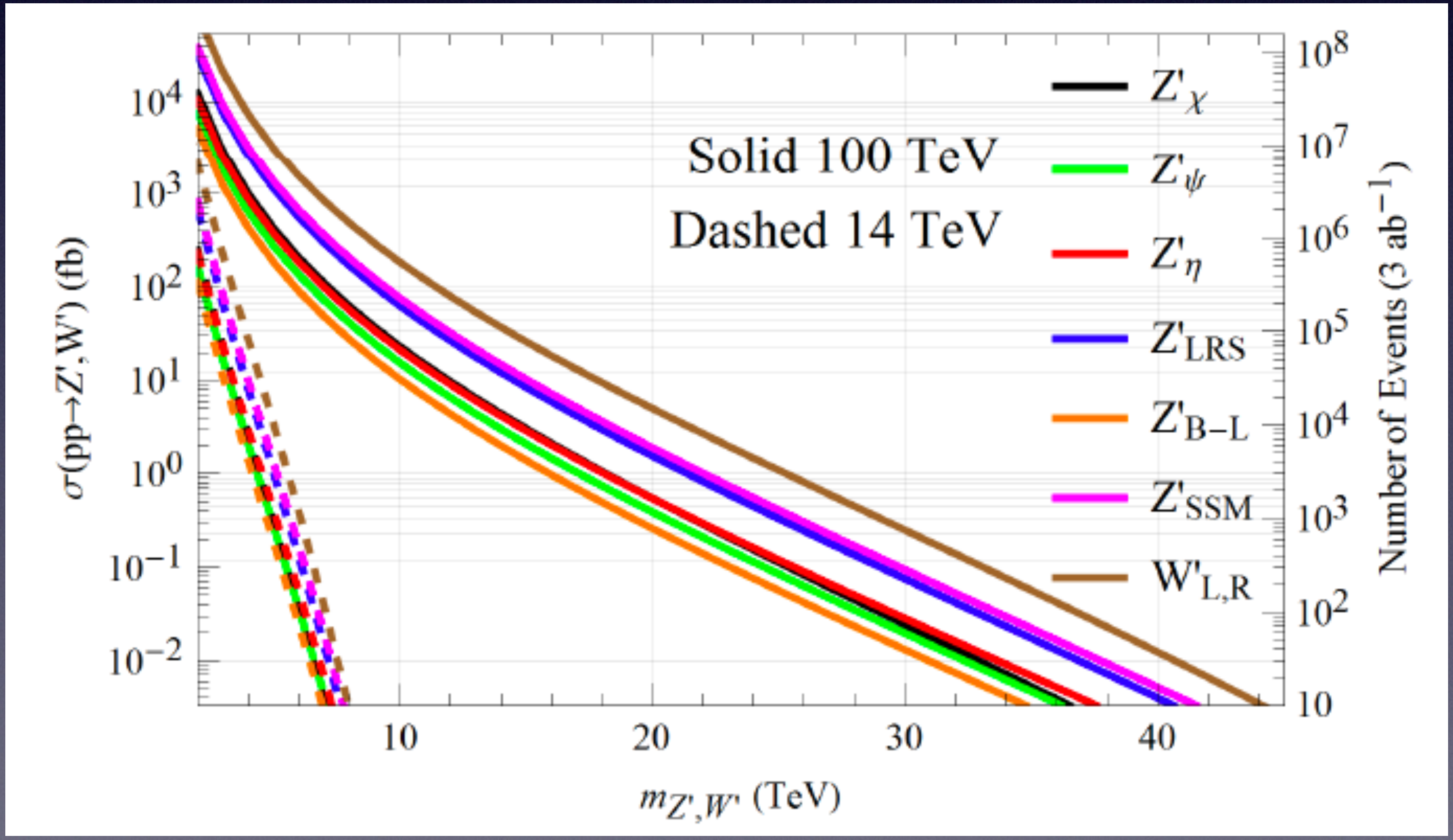

1511.06495

- Ultimate LHC reach in mass is ~7-8 TeV
- A 100 TeV machine extends this out to 35 TeV or beyond, depending on the model

Drell-Yan: Recap

- Drell-Yan is an important precision tool at hadron colliders
- This is the only process for which we are approaching percent level precision both experimentally and theoretically
- Proven track record for discovery (Z/W-boson, several resonances, etc). Plays an important role in understanding proton structure (PDFs)
- It will continue to play an important role at future hadron colliders

Highlights of Methods and Recent Results for NNLO Calculations

The need for NNLO

Benchmark processes measured with high precision, eg.: Drell-Yan, Z+jet, …

Background to Higgs studies, eg.:di-boson; Input to PDFs, eg.:V+jet, dijet, ttbar,…

NNLO important for:

When NLO corrections are large, NNLO is needed to test perturbative behavior, eg.: gg → Higgs

Ingredients for NNLO calculations

- Three basic ingredients for NNLO calculations:

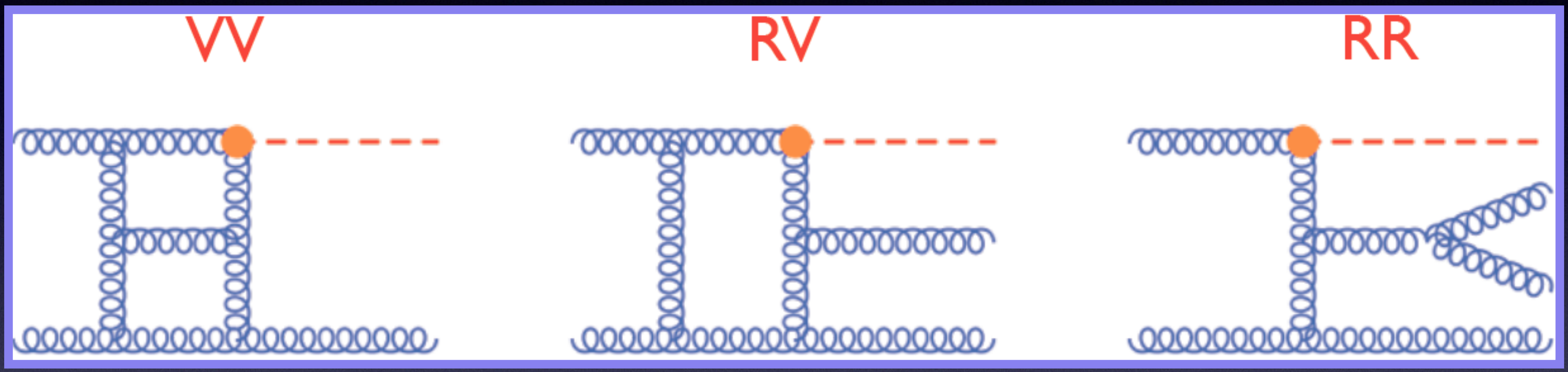

- IR singularities cancel in the sum of real and virtual corrections and mass factorization counterterms but only after phase space integration for real radiations

- Virtual corrections have explicit IR poles, whereas real corrections have implicit IR poles that need to be extracted.

Ingredients for NNLO calculations

- Three basic ingredients for NNLO calculations:

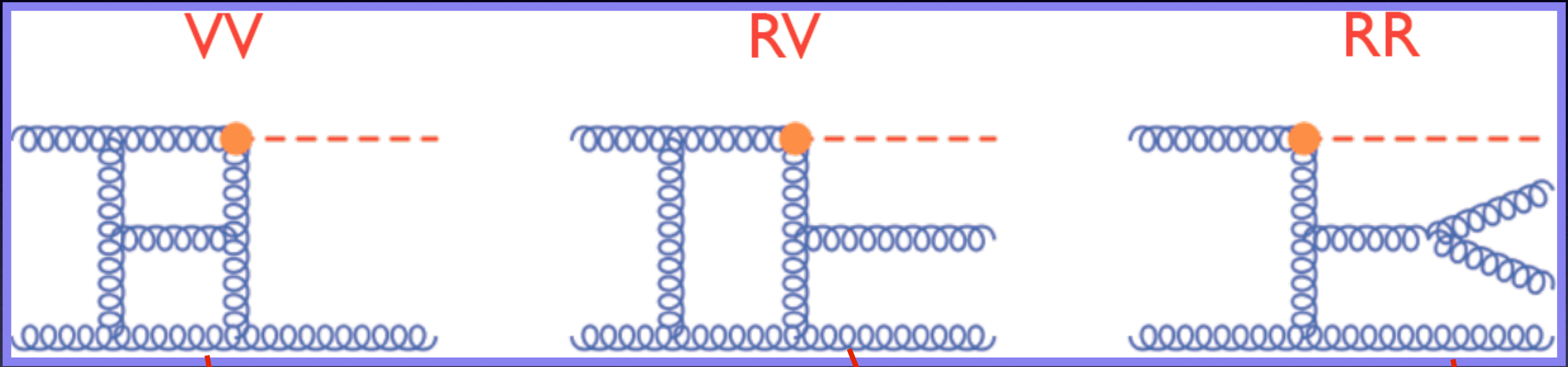

- IR singularities cancel in the sum of real and virtual corrections and mass factorization counterterms but only after phase space integration for real radiations

- Virtual corrections have explicit IR poles, whereas real corrections have implicit IR poles that need to be extracted.

$$\int \left[\frac{vv_4}{\epsilon^4} + \frac{vv_3}{\epsilon^3} + \frac{vv_2}{\epsilon^2} + \frac{vv_1}{\epsilon} + vv_0\right] \, d\Phi_2 \qquad \int \left[\frac{rv_2}{\epsilon^2} + \frac{rv_1}{\epsilon} + rv_0\right] \, d\Phi_3 \qquad \int \left[rr_0\right] \, d\Phi_4$$

Ingredients for NNLO calculations

- Three basic ingredients for NNLO Calculations:

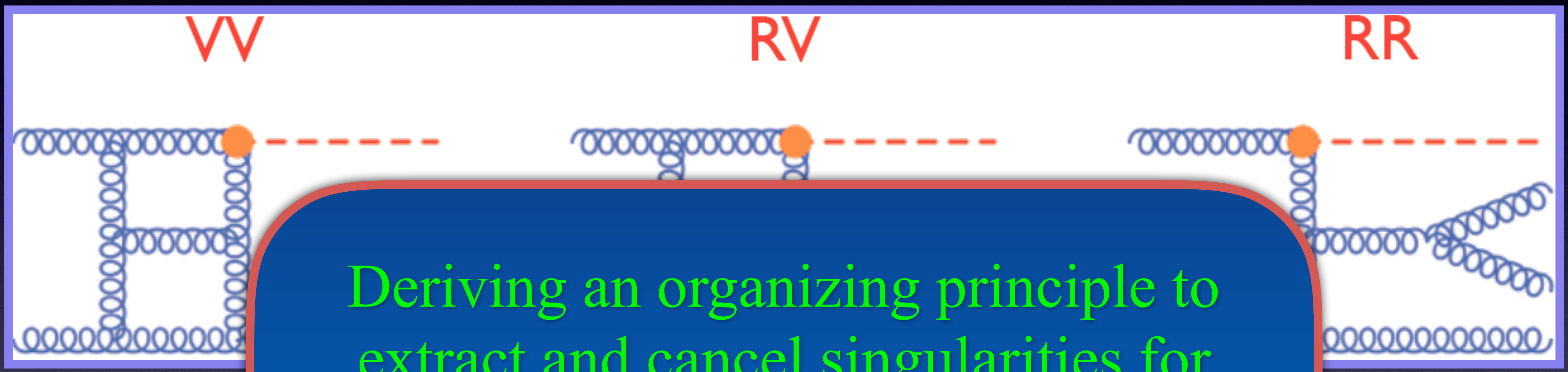

- IR singul[...] factorizatio[...] radiations [...]ns and mass [...]n for real

Deriving an organizing principle to extract and cancel singularities for arbitrary observables was the major obstacle in obtaining NNLO predictions

- Virtual corrections have explicit IR poles, whereas real corrections have implicit IR poles that need to be extracted.

Breaking through to NNLO

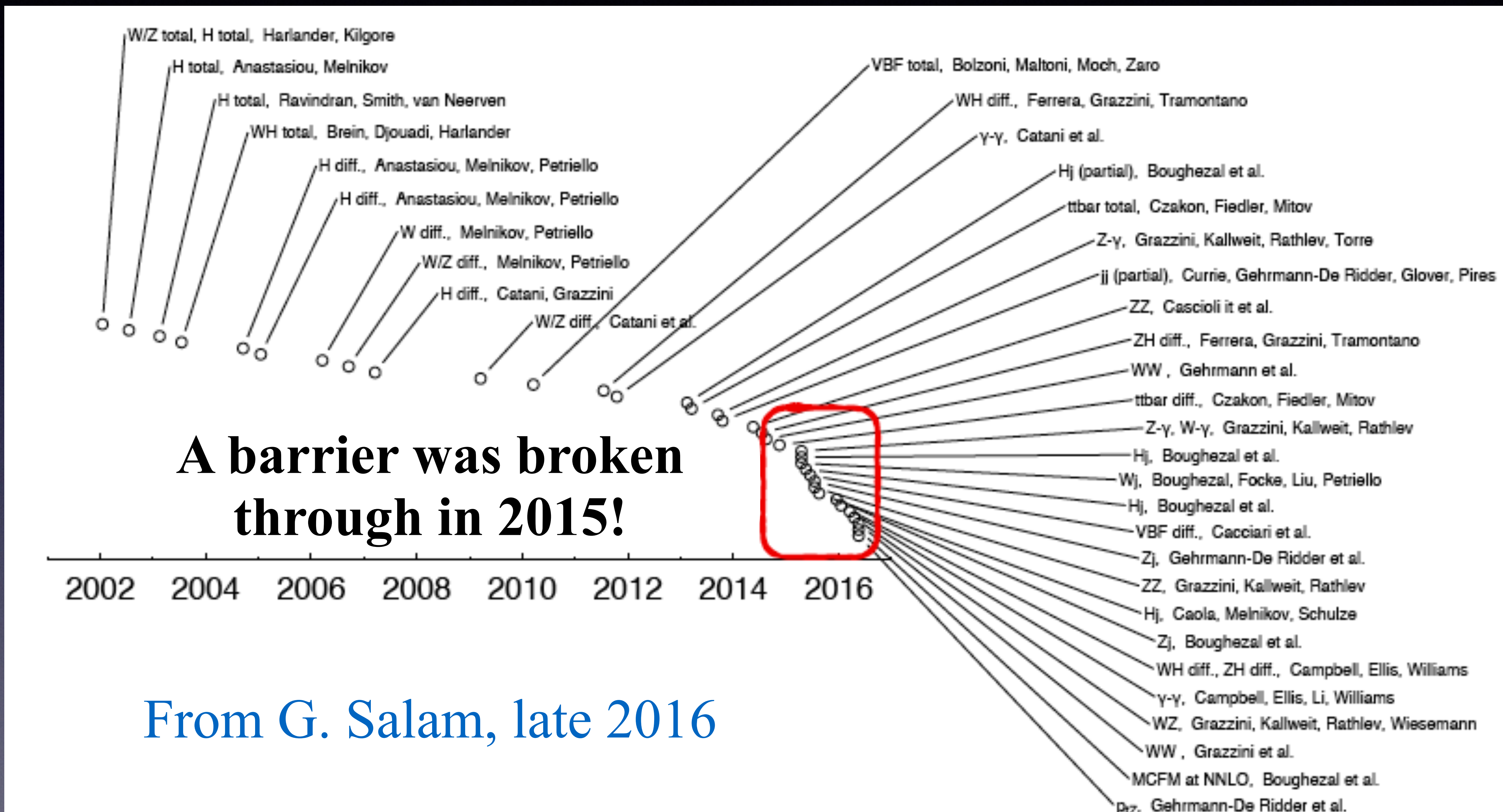

A barrier was broken through in 2015!

From G. Salam, late 2016

Breaking through to NNLO

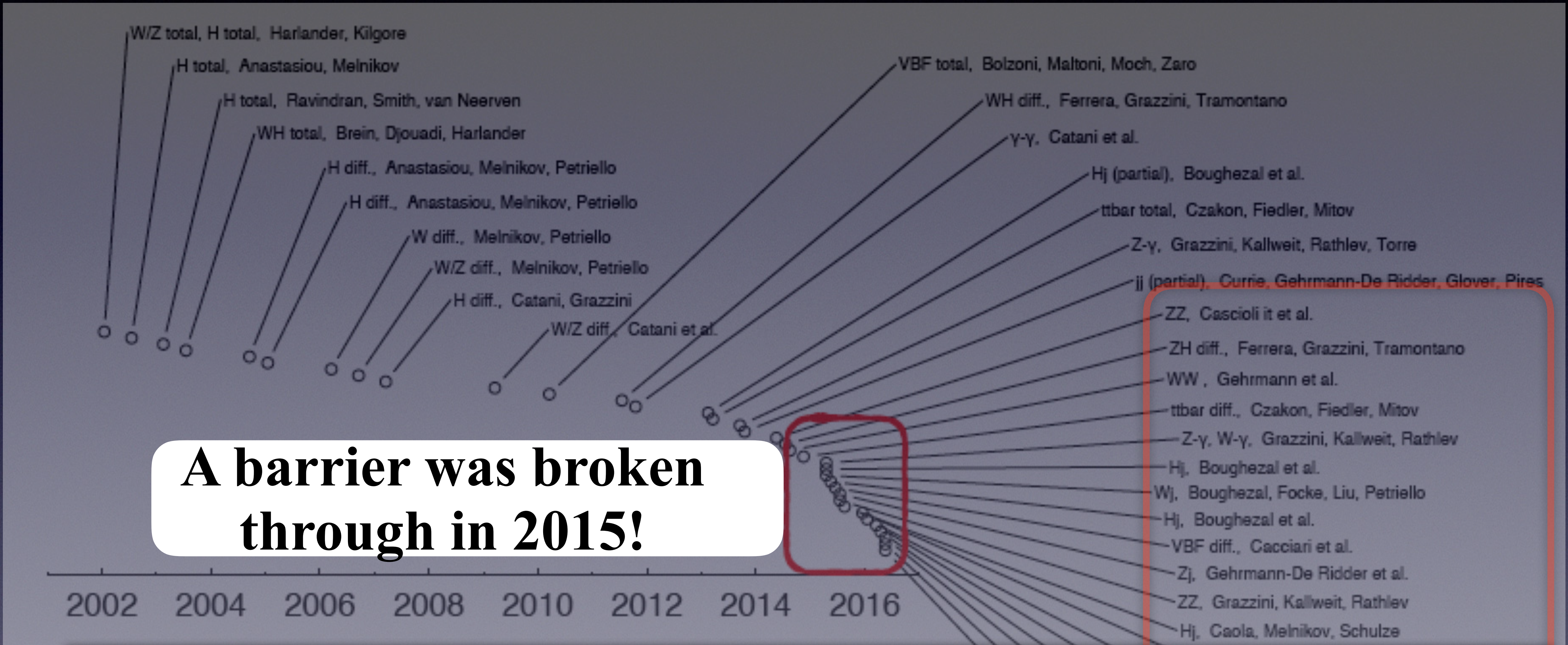

A barrier was broken through in 2015!

This explosion of new NNLO results was made possible thanks to several ideas!

Cancellation of IR divergences @ NNLO

- **Effective field theory methods:**
  - qT subtraction Catani, Grazzini; for processes without jets
  - N-jettiness subtraction RB, Focke, Liu, Petriello; Gaunt, Stahlhofen, Tackmann, Walsh; valid for all processes including jet production

- **Subtraction methods:**
  - Sector decomposition Anastasiou, Melnikov, Petriello; Binoth, Heinrich
  - Antenna subtraction Kosower; Gehrmann, Gehrmann De Ridder, Glover
  - Sector Improved Residue Subtraction Czakon; RB, Melnikov, Petriello; Czakon, Heymes; Caola, Melnikov, Rontsch
  - Colorful subtraction Del Duca, Duhr, Kardos, Somogyi, Trocsanyi
  - Projection to Born Cacciari, Dreyer, Karlberg, Salam, Zanderighi

Traditional subtraction approaches

$$
\begin{aligned}
\mathrm{d}\sigma_{NNLO} = &\int_{\mathrm{d}\Phi_{m+2}} \left(\mathrm{d}\sigma^{R}_{NNLO} - \mathrm{d}\sigma^{S}_{NNLO}\right) \\
&+ \int_{\mathrm{d}\Phi_{m+1}} \left(\mathrm{d}\sigma^{V,1}_{NNLO} - \mathrm{d}\sigma^{VS,1}_{NNLO}\right) \\
&+ \int_{\mathrm{d}\Phi_{m+2}} \mathrm{d}\sigma^{S}_{NNLO} + \int_{\mathrm{d}\Phi_{m+1}} \mathrm{d}\sigma^{VS,1}_{NNLO} \\
&+ \int_{\mathrm{d}\Phi_{m}} \mathrm{d}\sigma^{V,2}_{NNLO} \,,
\end{aligned}
$$

- Introduce subtractions that reproduce the singular behavior of the full differential cross section
- The subtractions should be simple enough to integrate and obtain an explicit form of the divergences
- The difference between the full result and the subtractions is integrated numerically

Another approach

- To see the possibility of another approach, consider Higgs production at **NLO**, or **O(α_S)**, as an example. A real emission correction:

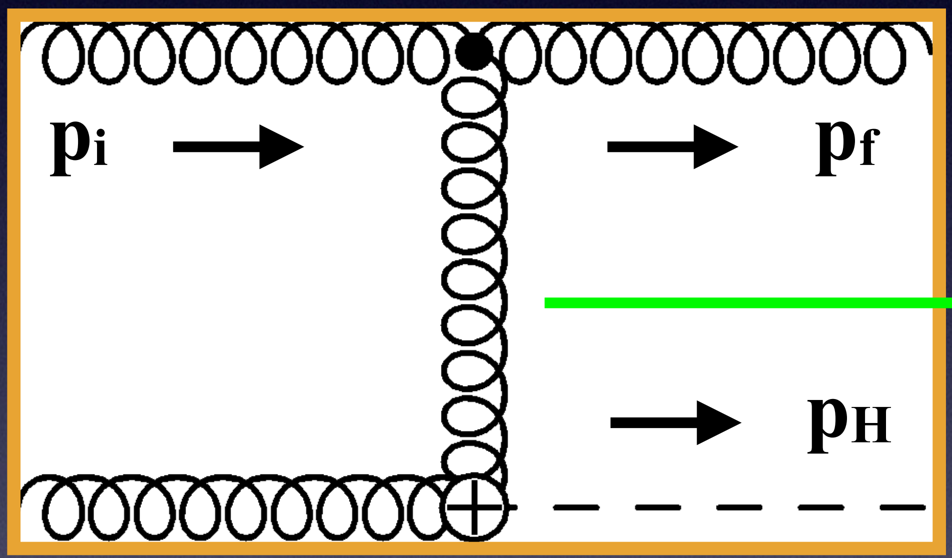

η=rapidity of jet

$$\boxed{\frac{1}{2p_i \cdot p_f} = \frac{1}{2E_i p_{TH} e^{\eta}}}$$

p_{TH}=transverse momentum of Higgs

This propagator can't diverge for finite transverse momentum (note that η must be finite for non-vanishing p_{TH})

O(α_S) becomes a Born-level calculation with no singularities at finite p_{TH}

Another approach

- This observation motivates the following partition of phase space for the differential cross section:

$$\sigma = \int dp_{TH} \frac{d\sigma}{dp_{TH}} \theta(p_{TH}^{cut} - p_{TH}) + \int dp_{TH} \frac{d\sigma}{dp_{TH}} \theta(p_{TH} - p_{TH}^{cut})$$

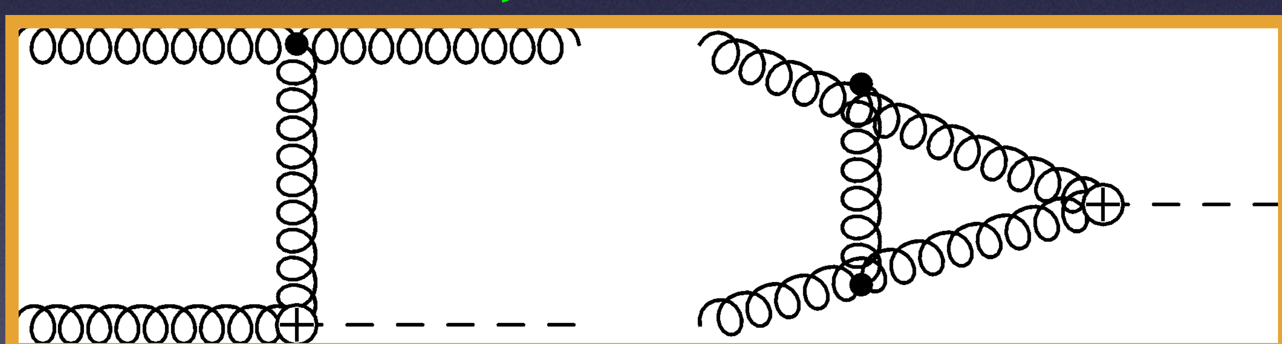

Singular regions of real emissions and virtual corrections go here

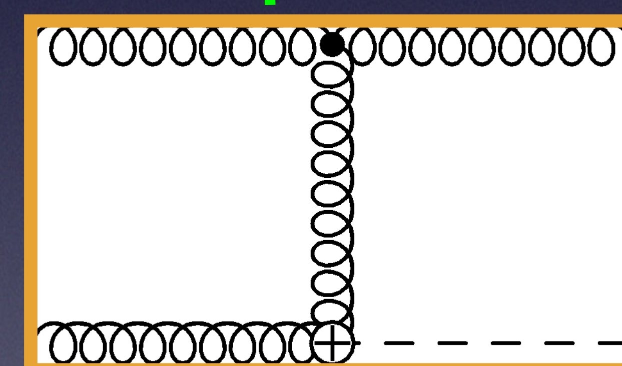

Finite regions of real emissions go here

This is a simple, finite tree-level calculation

Another approach

- This observation motivates the following partition of phase space for the differential cross section:

$$\sigma = \int dp_{TH} \frac{d\sigma}{dp_{TH}} \theta(p_{TH}^{cut} - p_{TH}) + \int dp_{TH} \frac{d\sigma}{dp_{TH}} \theta(p_{TH} - p_{TH}^{cut})$$

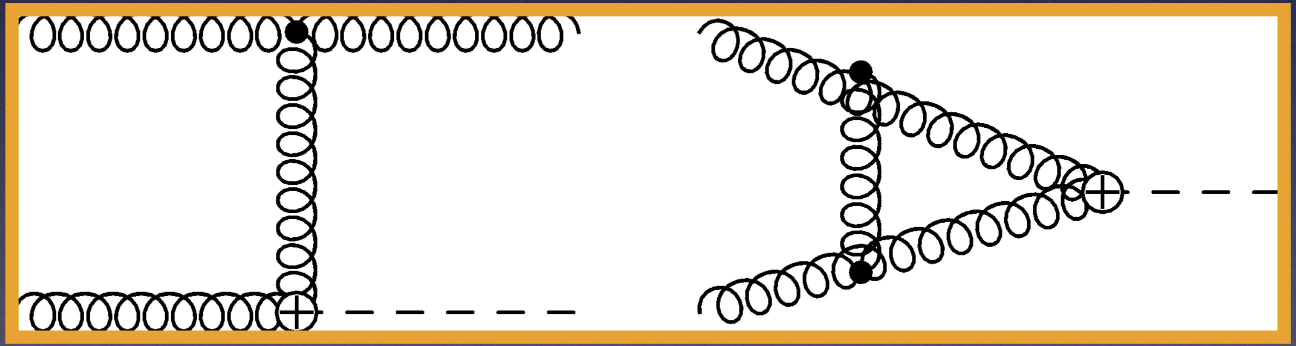

Singular regions of real emissions and

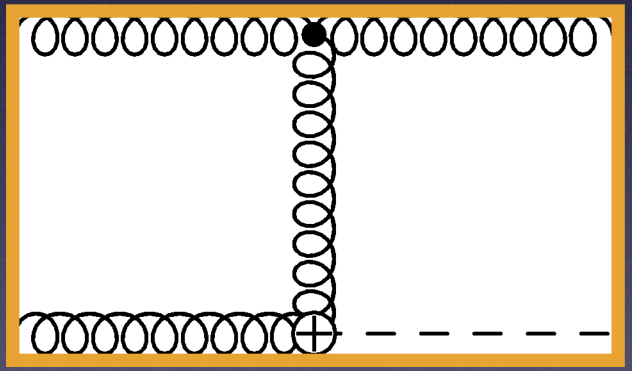

Finite regions of real emissions go here

This split is useful because there is a simpler way to derive the cross section below p_{Tcut}

This is a simple, finite tree-level calculation

Effective field theory for low p_{TH}

- ***Effective field theory*** can simplify the calculation when $p_{TH} \ll m_H$. It provides a systematic way of expanding the full differential cross section for small p_{TH}/m_H.

x_a, x_b=Bjorken-x for each beam

$$\boxed{\frac{d\sigma}{dp_{TH}}(p_{TH} \ll m_H) \sim S(m_H, p_{TH}) \otimes C_a(p_{TH}, x_a) \otimes C_b(p_{TH}, x_b)}$$

Universal function describing soft emissions

Functions which describe virtual corrections and collinear emissions

Collins, Soper, Sterman (1985)

This formula holds at NNLO since S, C_i are known to $O(\alpha_S^2)$

It is a much simpler problem to calculate S and C_i than it is to cancel real and virtual singularities at NNLO for arbitrary observables!

q_T-subtraction

- ***Effective field theory*** can simplify the calculation when $p_{TH} \ll m_H$. It provides a systematic way of expanding the full differential cross section for small p_{TH}/m_H.

x_a, x_b=Bjorken-x for each beam

$$\boxed{\frac{d\sigma}{dp_{TH}}(p_{TH} \ll m_H) \sim S(m_H, p_{TH}) \otimes C_a(p_{TH}, x_a) \otimes C_b(p_{TH}, x_b)}$$

Universal function describing soft emissions

Functions which describe virtual corrections and collinear emissions

Collins, Soper, Sterman (1985)

This formula holds at NNLO since S, C_i are known to $O(\alpha_S^2)$

For $p_{Tcut}/m_H \to 0$ this becomes an ***exact*** expression for the NNLO result. This is the idea behind q_T-subtraction. Catani, Grazzini (2007)

Jets at the LHC?

- A limitation of this approach is that it can only describe partonic processes with no final-state partons.

Consider Higgs+jet at NLO, or Higgs at finite p_{TH}, as an example

$$\frac{1}{2p_1 \cdot p_2} = \frac{1}{2p_{T1}|\vec{p}_{TH} - \vec{p}_{T1}|} \times \frac{1}{\cosh(\Delta\eta) - \cos(\Delta\phi)}$$

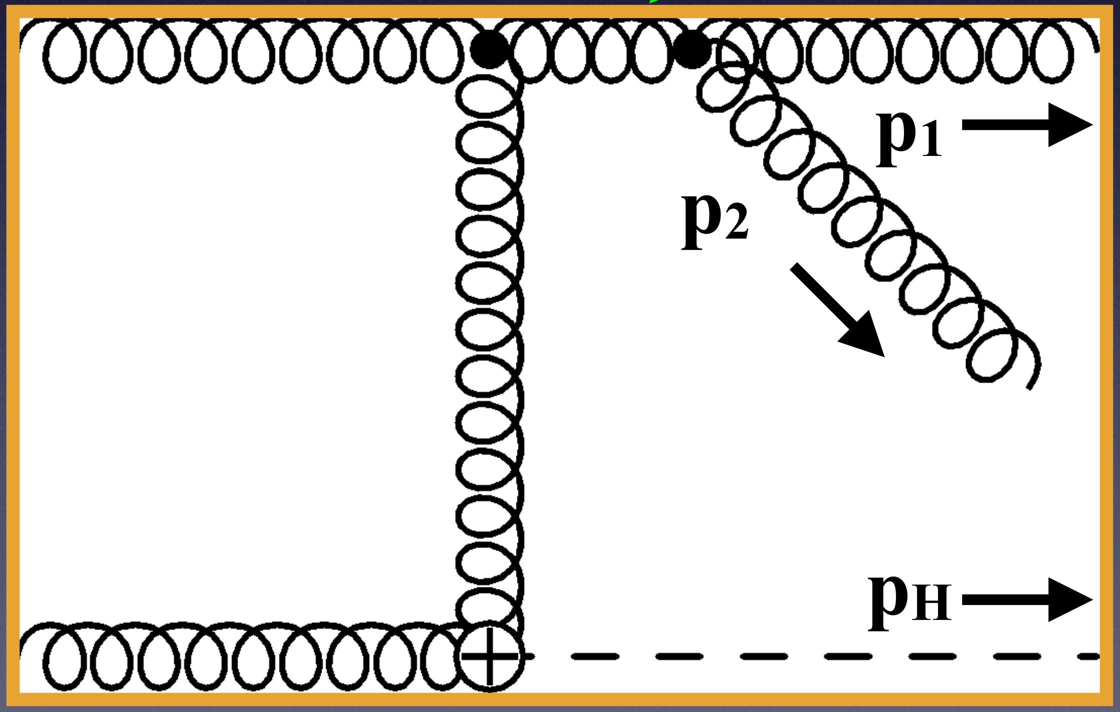

This vanishes independently of p_{TH} for either p_{T1} or p_{T2} soft, or $p_1||p_2$

p_{TH} no longer resolves singularities in the presence of final-state partons

N-jettiness

- There is a resolution parameter suitable for final-state partons!

N=number of jets

$$\boxed{\tau_N = \sum_k \min\{n_i \cdot q_k\}}$$

N-jettiness, an event shape variable (similar to thrust); first introduced in Stewart, Tackmann, Waalewijn (2009)

light-like directions of initial beams and final-state jets

momenta of final-state partons

Intuition:

$\tau_N \sim 0$: all radiation is either soft, or collinear to a beam/jet

$\tau_N > 0$: at least one additional jet beyond Born level is resolved

N-jettiness

- Go back and reconsider our Higgs+jet example using this variable, in the potentially singular kinematic limits $p_1 || p_2$ and $p_{1,2}$ soft:

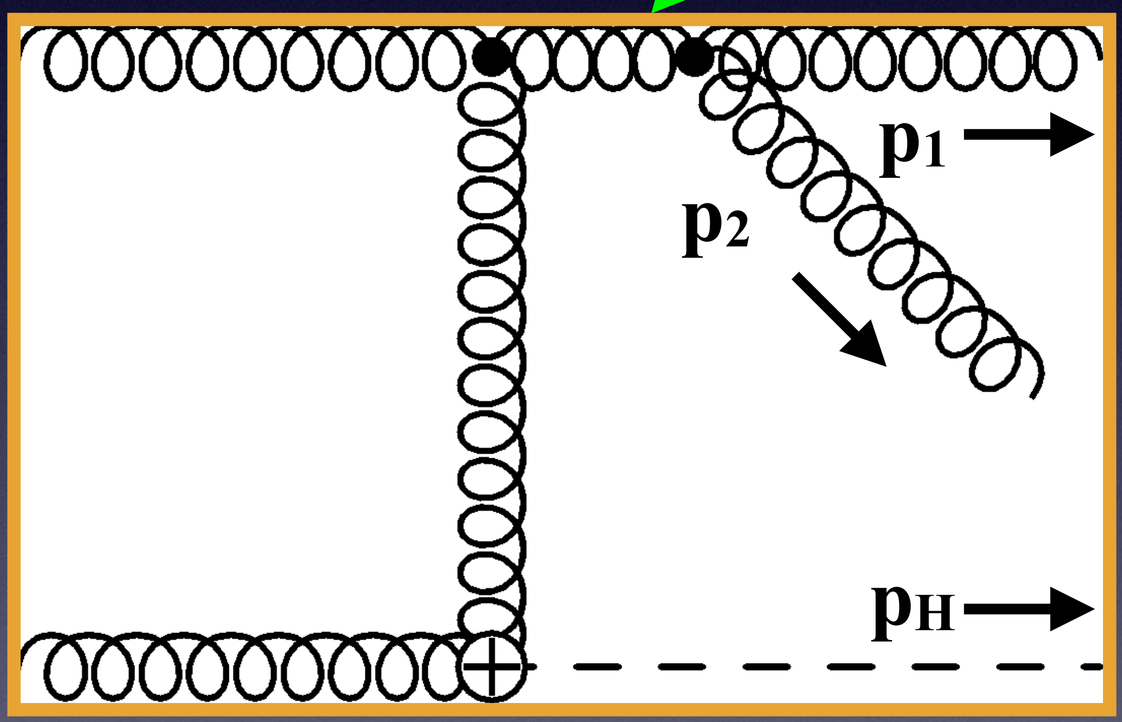

$$\boxed{\frac{1}{2p_1 \cdot p_2} \approx \frac{1}{2E_J \tau_1}}$$

final-state jet energy

1-jettiness, since our Born-level process has a single jet

All final-state singularities are regulated by τ_1!

N-jettiness subtraction

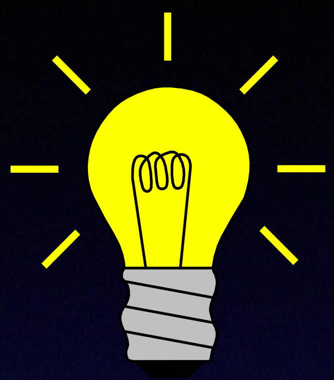

We can obtain NNLO predictions for arbitrary jet production processes using N-jettiness as a resolution parameter!

RB, Focke, Liu, Petriello (2015); Gaunt, Stahlhofen, Tackmann, Walsh (2015)

$$\boxed{\sigma = \int d\tau_N \frac{d\sigma}{d\tau_N}\theta(\tau^{cut} - \tau_N) + \int d\tau_N \frac{d\sigma}{d\tau_N}\theta(\tau_N - \tau^{cut})}$$

a simpler effective theory description is available for the region

have one more resolved jet than at Born level; **only need NLO in this region!**

N-jettiness subtraction

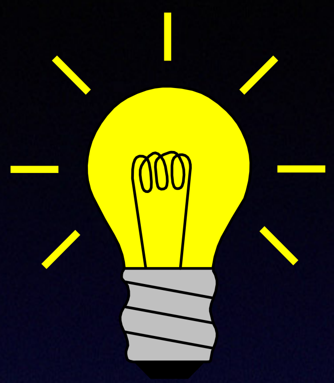

We can obtain NNLO predictions for arbitrary jet production processes using N-jettiness as a resolution parameter!

Stewart, Tackmann, Waalewijn (2009)

$$\boxed{\frac{d\sigma}{d\tau_N}(\tau_N \ll Q) \sim H \otimes B_a \otimes B_b \otimes S \otimes \left[\prod_{n=1}^{N} J_n\right]}$$

hard scales in the process (e.g., transverse momenta of jets)

describes hard radiation

describes radiation collinear to initial-state beams; ***universal***

describes soft radiation; ***universal;*** depends on number of jets

describes radiation collinear to final-state jets; ***universal***

N-jettiness subtraction

- Only one more issue to address: what is known regarding the functions **H**, **B**, **S**, **J**? Do we known them to the requisite NNLO?
  - ***H*@NNLO:** for W/H/Z+j, Gehrmann, Tancredi (2011); Gehrmann, Jaquier, Glover, Koukoutsakis (2011) (see also Becher, Bell, Lorentzen, Marti (2013))
  - ***B*@NNLO:** Gaunt, Stahlhofen, Tackmann (2014), confirmed in RB, Petriello, Schubert, Xing (2017)
  - ***S*@NNLO:** RB, Liu, Petriello (2015)
  - ***J*@NNLO:** Becher, Neubert (2006); Becher, Bell (2011)

Within the past two years all ingredients have become available to apply this idea to jet production at the LHC!

Gauge boson plus jet production

- First example: gauge boson plus jet production. This is an important background to dark matter searches at the LHC.

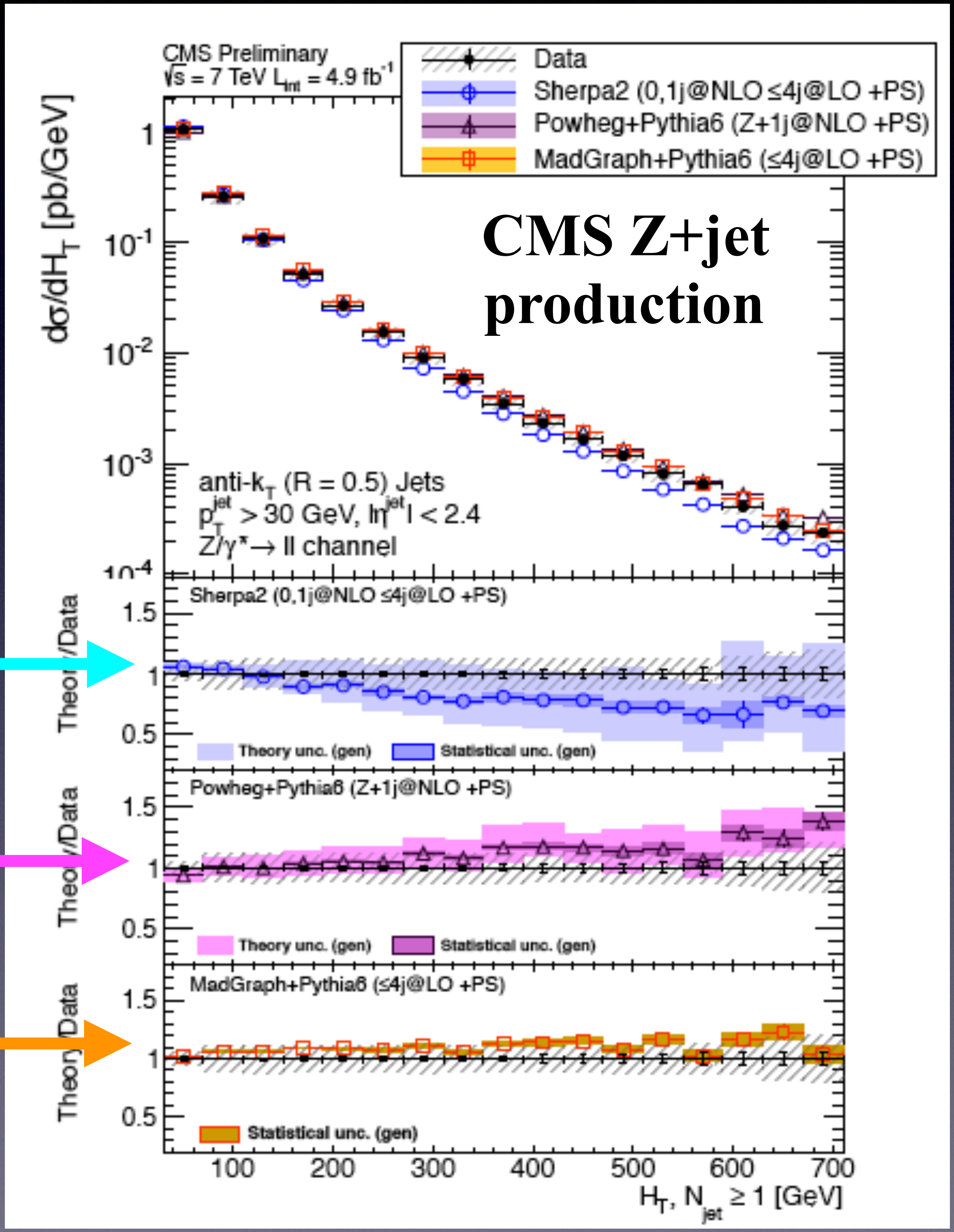

NLO+parton shower; too soft at high H_T

another NLO+parton shower; too hard at high H_T

LO+parton shower; better shape, but normalization difference

H_T=scalar sum of jet transverse momenta

Gauge boson plus jet production

- First example: gauge boson plus jet production. This is an important background to dark matter searches at the LHC.

NLO+parton shower:

Discrepancies in the theoretical modeling of this observable; How does NNLO do?

LO+parton shower; better shape,
but normalization difference

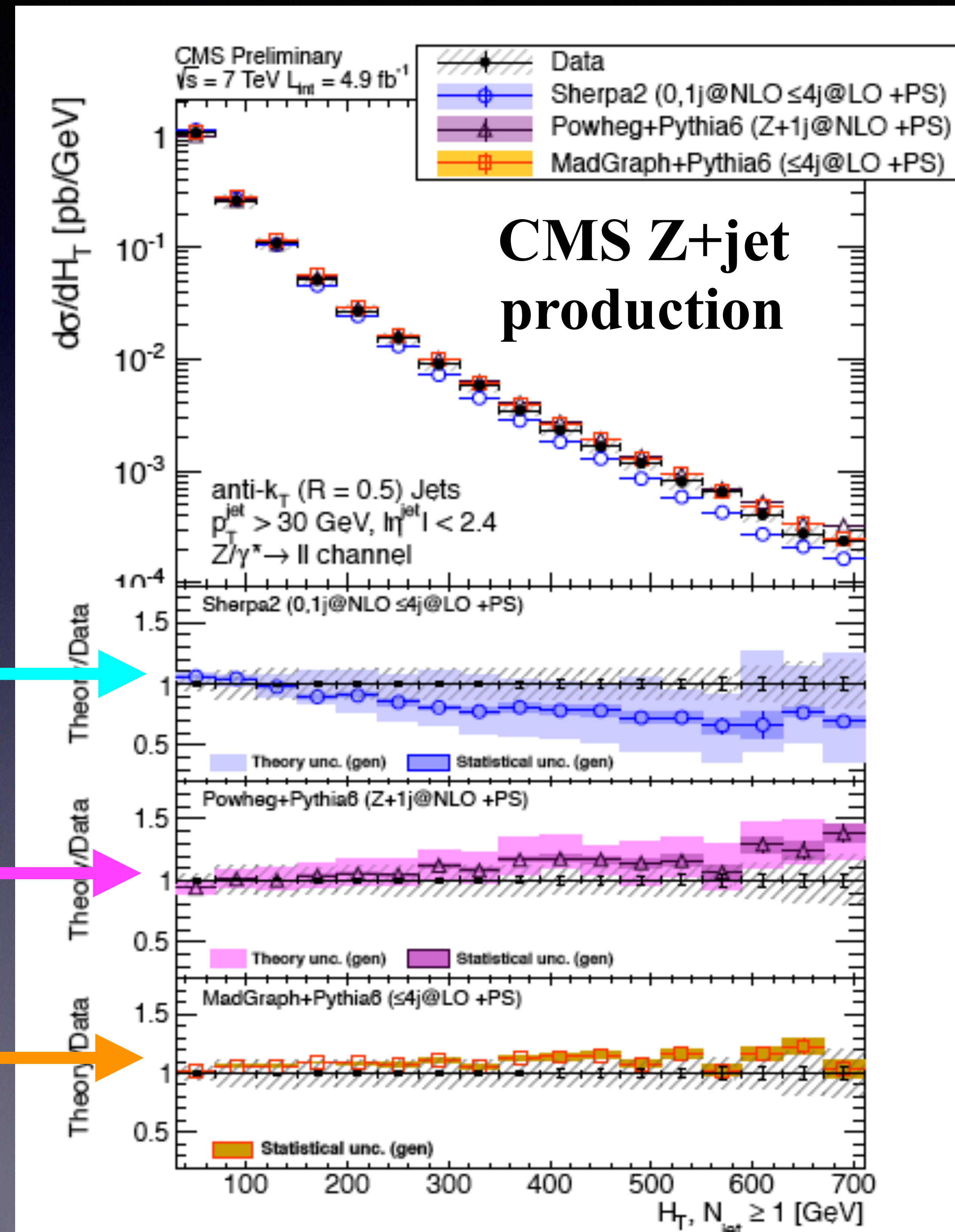

H_T=scalar sum of jet transverse momenta

Comparison to the data

- We have reconsidered the comparison to 7 TeV data of ATLAS and CMS; **shape of corrections depends on the observable!**

RB, Liu, Petriello, (2016), based on N-jettiness subtraction

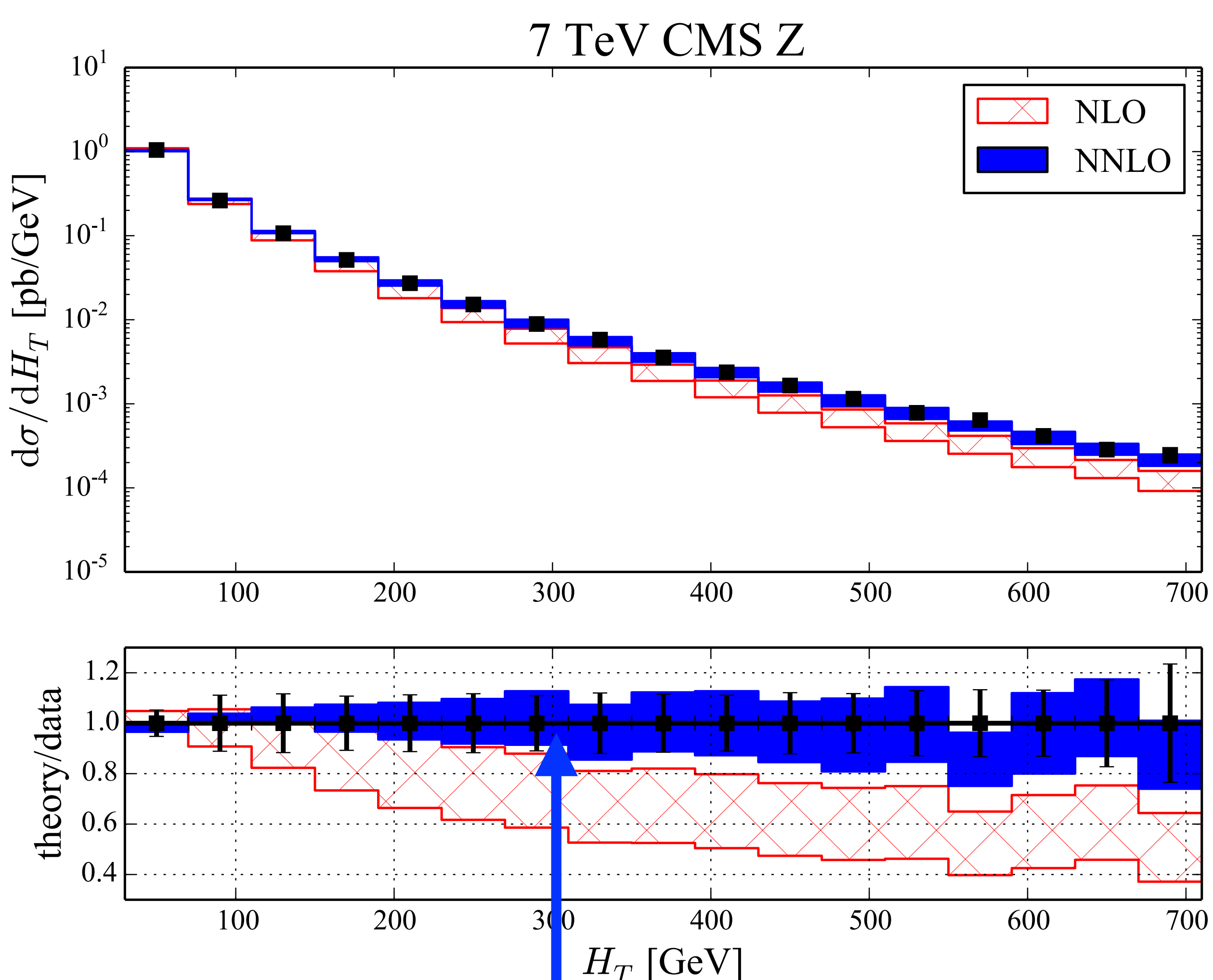

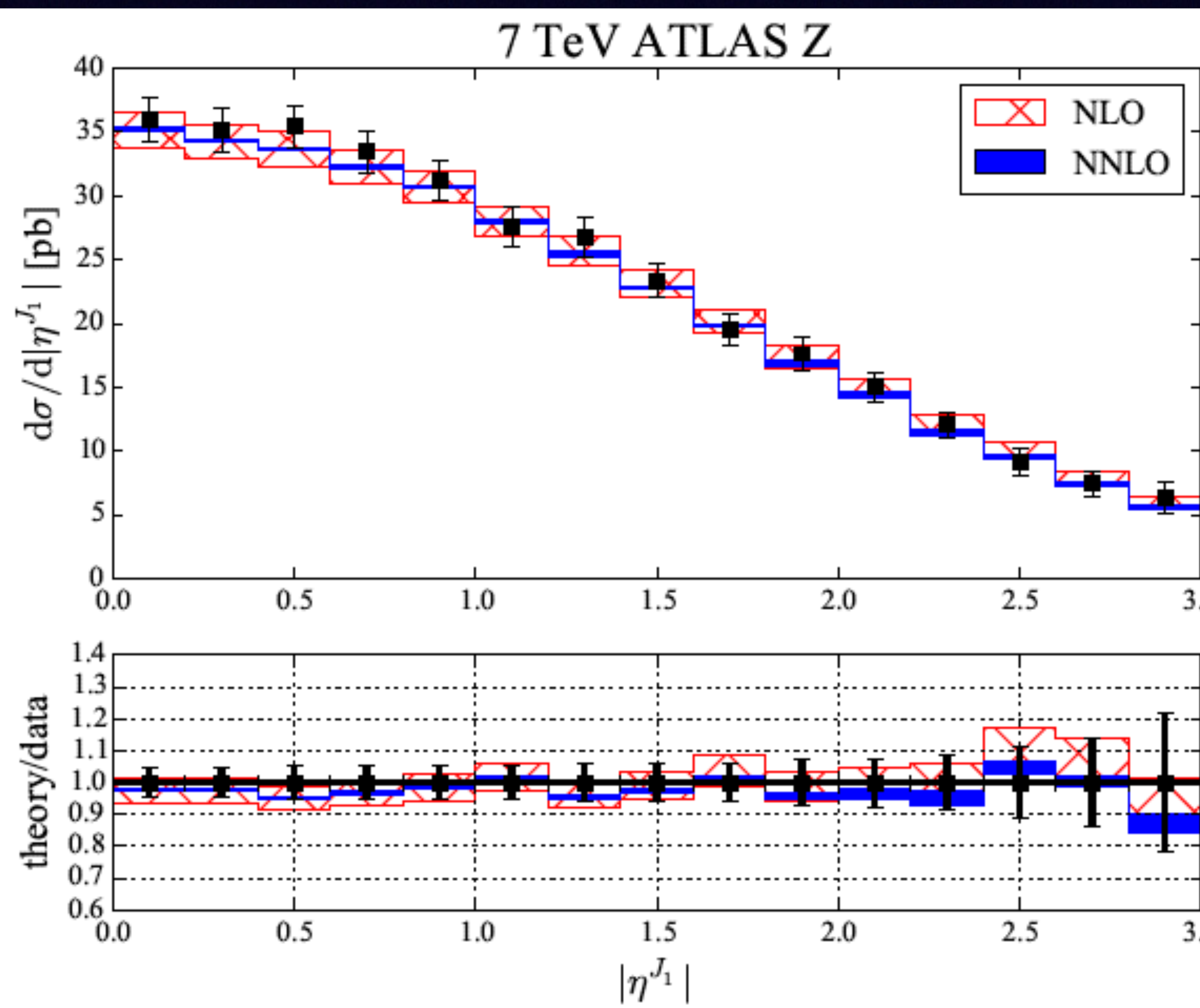

Large 2-jet contribution first opens at NLO; receives a large correction at NNLO

Comparison to the data

- We have reconsidered the comparison to 7 TeV data of ATLAS and CMS; **shape of corrections depends on the observable!**

RB, Liu, Petriello, (2016), based on N-jettiness subtraction

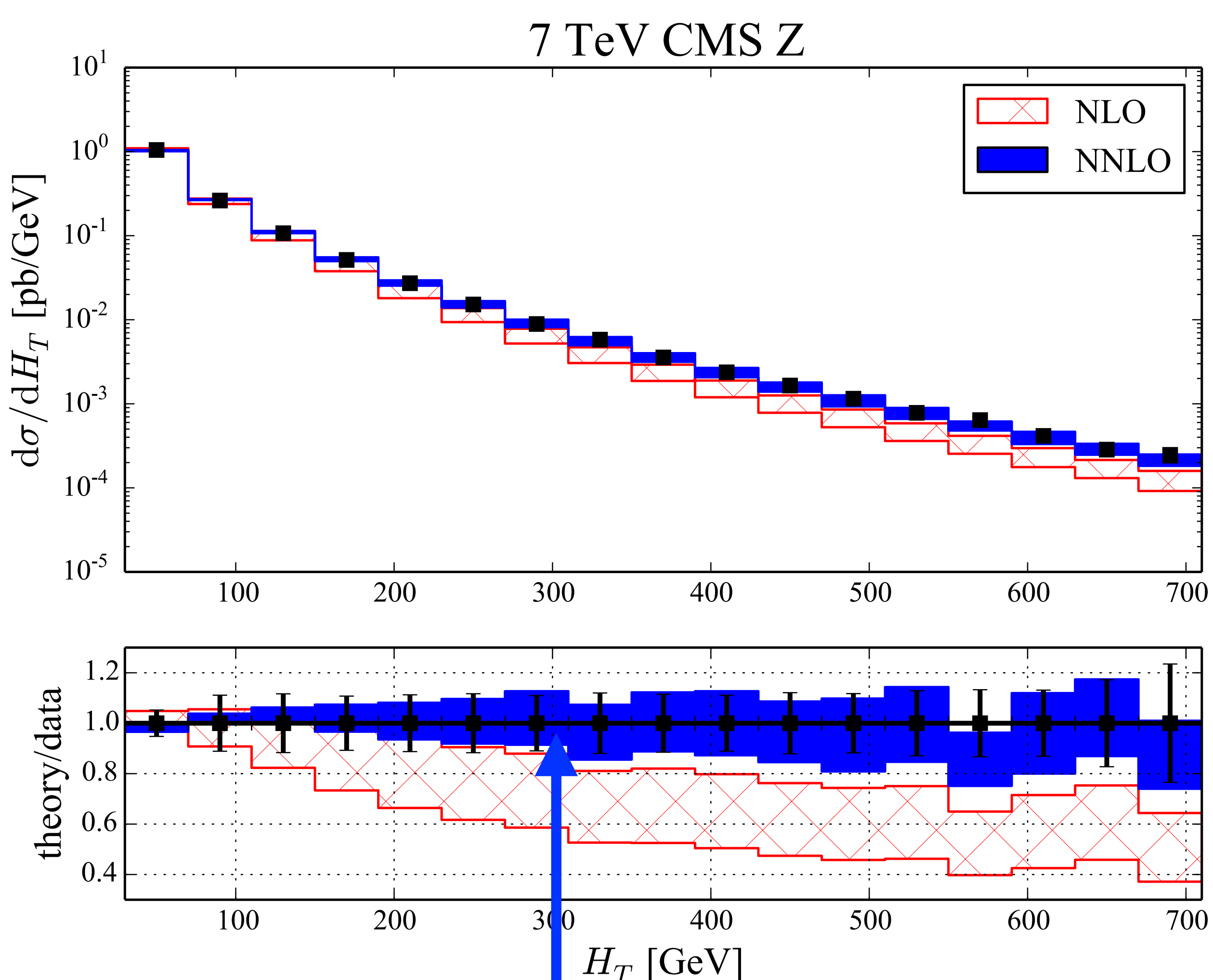

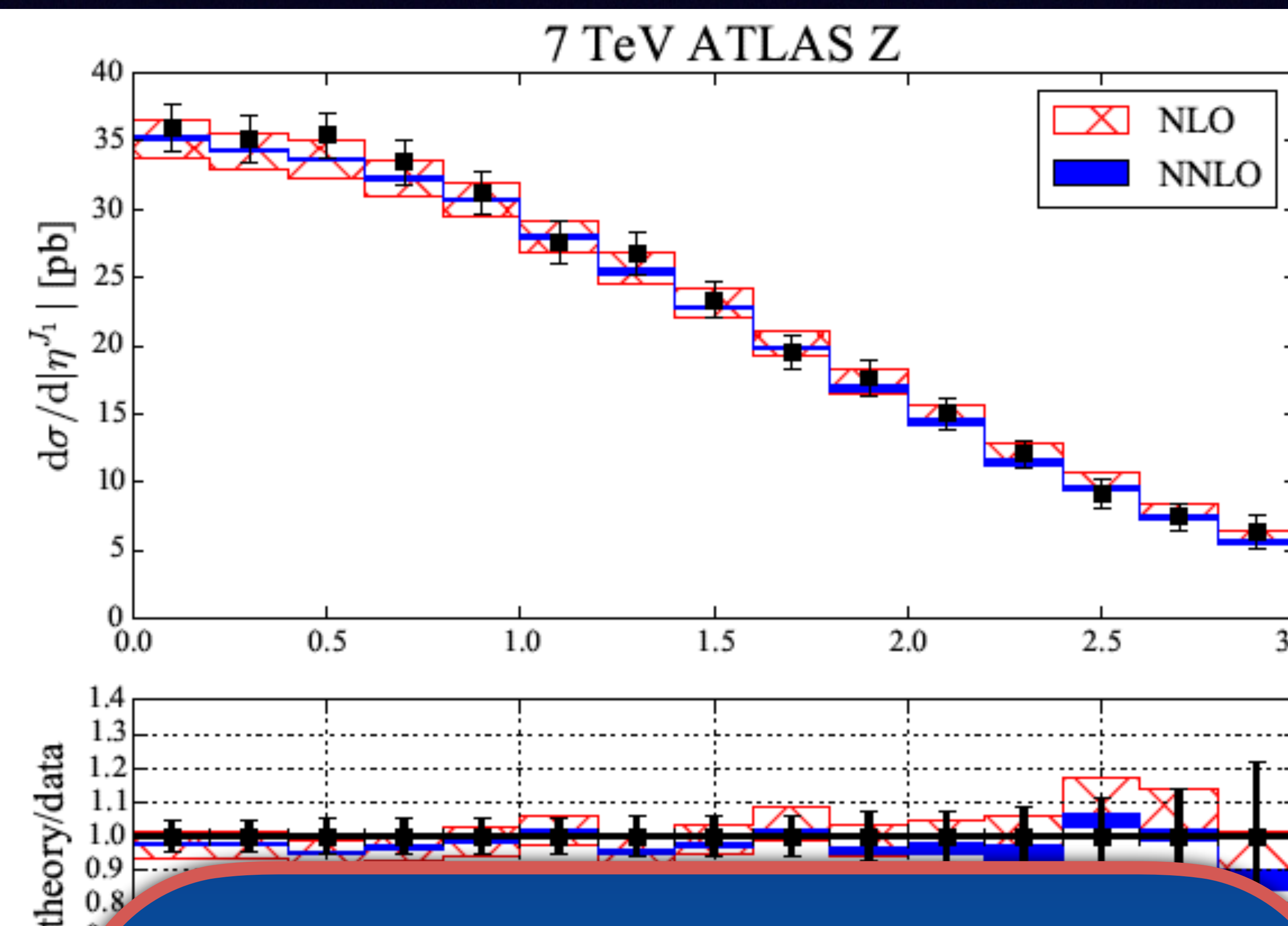

Large 2-jet contribution first opens at NLO; receives a large correction at NNLO

NNLO leads to excellent agreement between theory and data

Comparison to the data

Continued excellent agreement with data at 13 TeV!

NNLO predictions obtained with N-jettiness subtraction

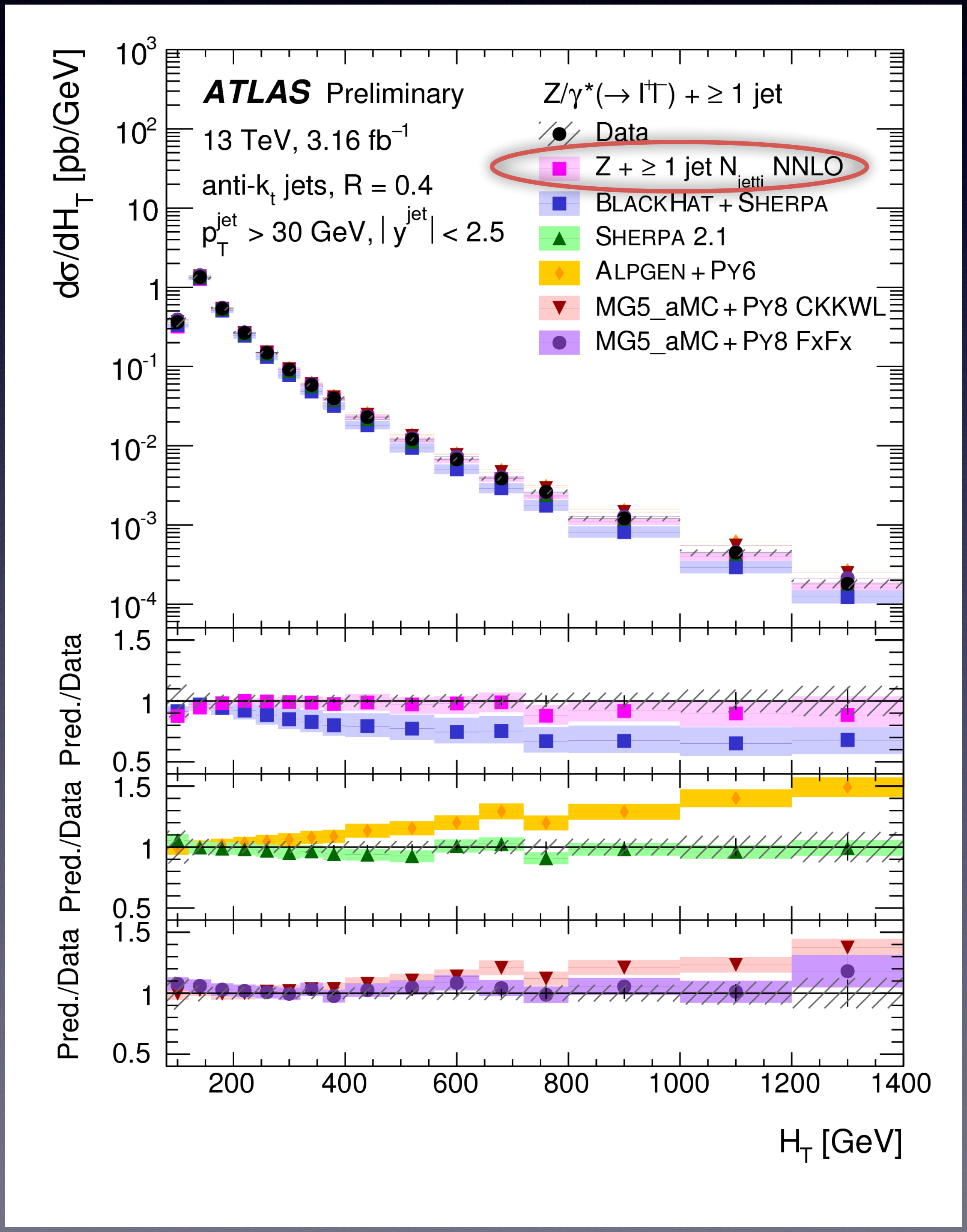

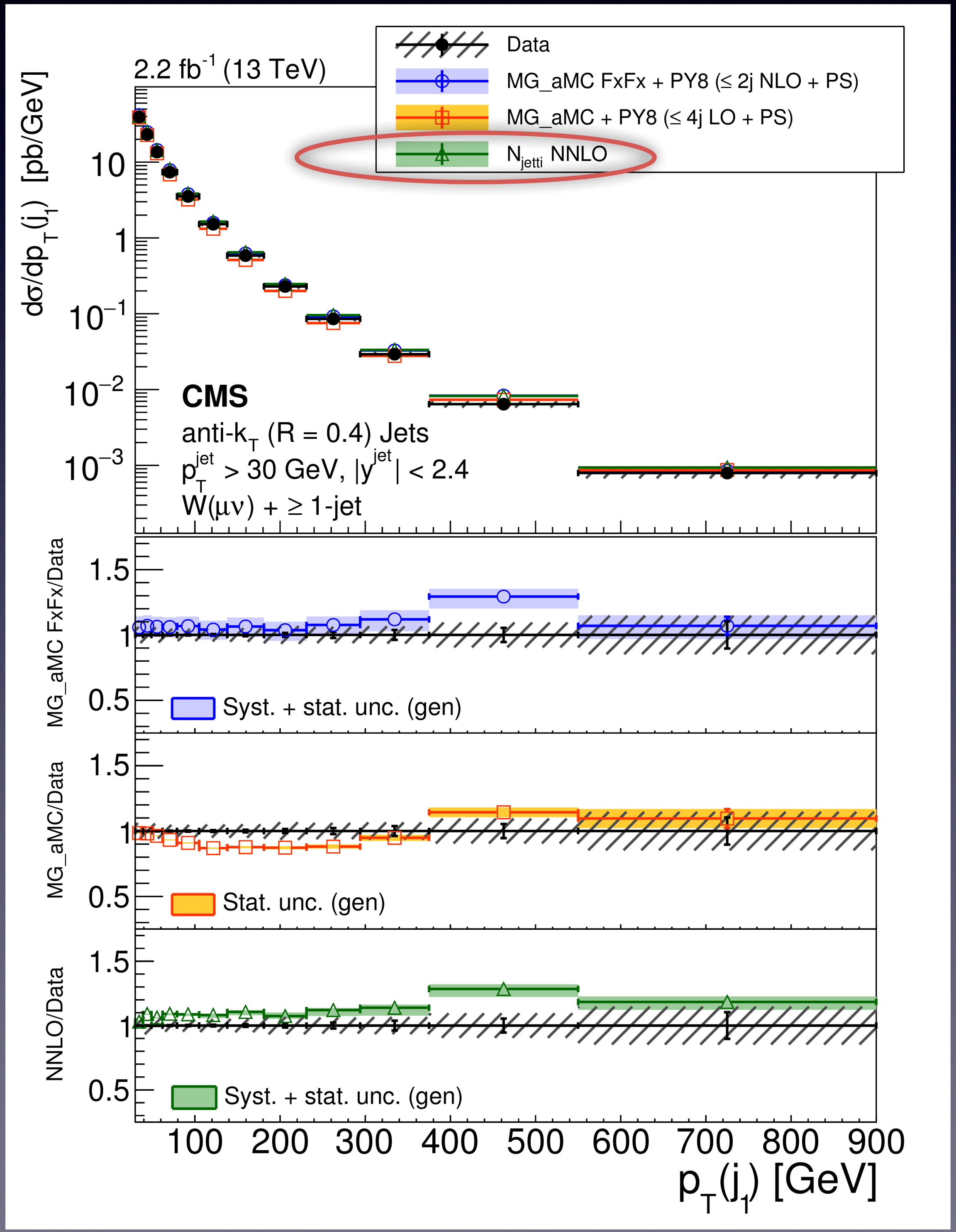

Comparison to the data

Continued excellent agreement with data at 13 TeV!

NNLO predictions obtained with N-jettiness subtraction

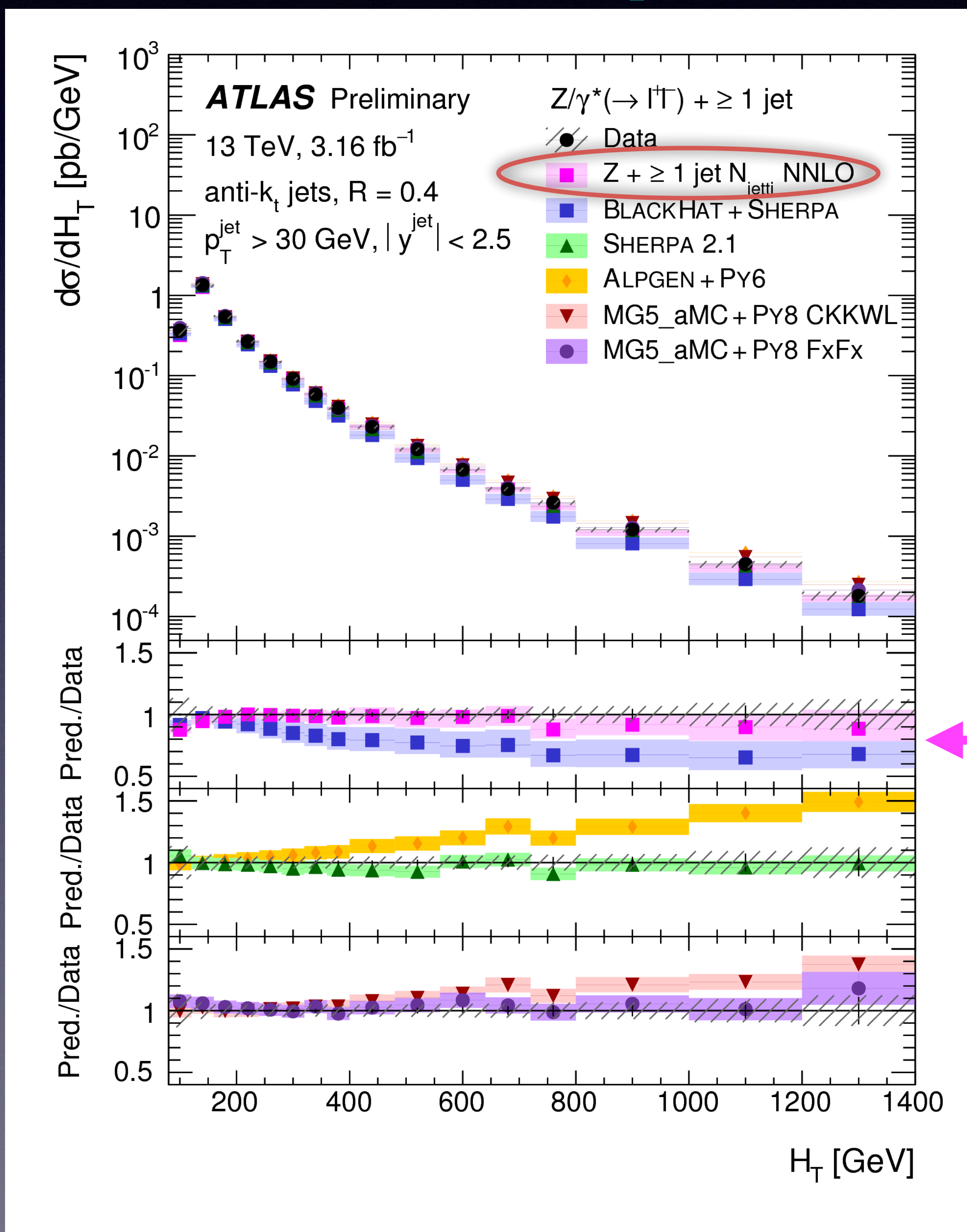

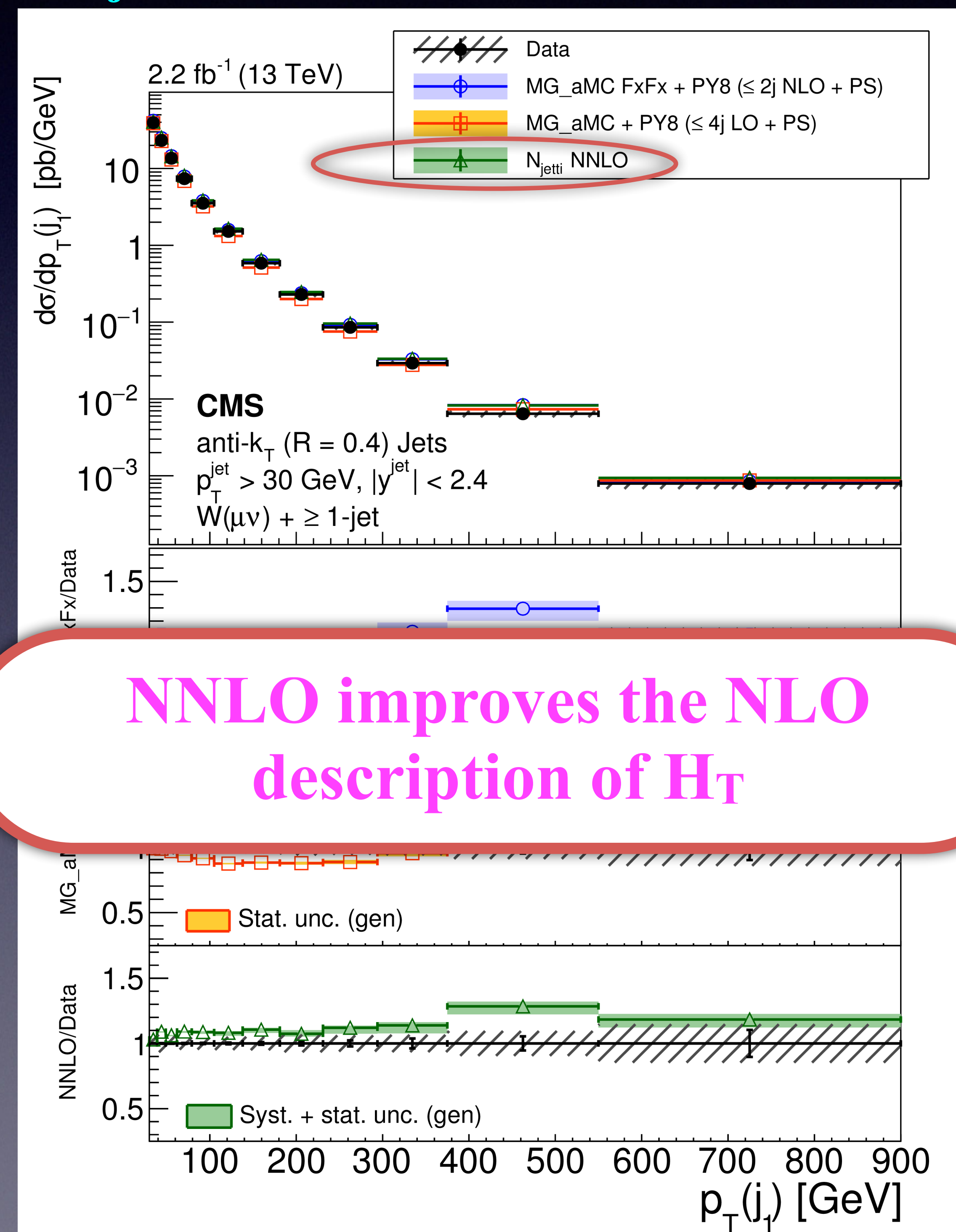

NNLO improves the NLO description of H_T

The Z-boson transverse momentum

- The Z-boson transverse momentum spectrum measurement has reached a remarkable precision at the LHC, with errors below 1% over a large range

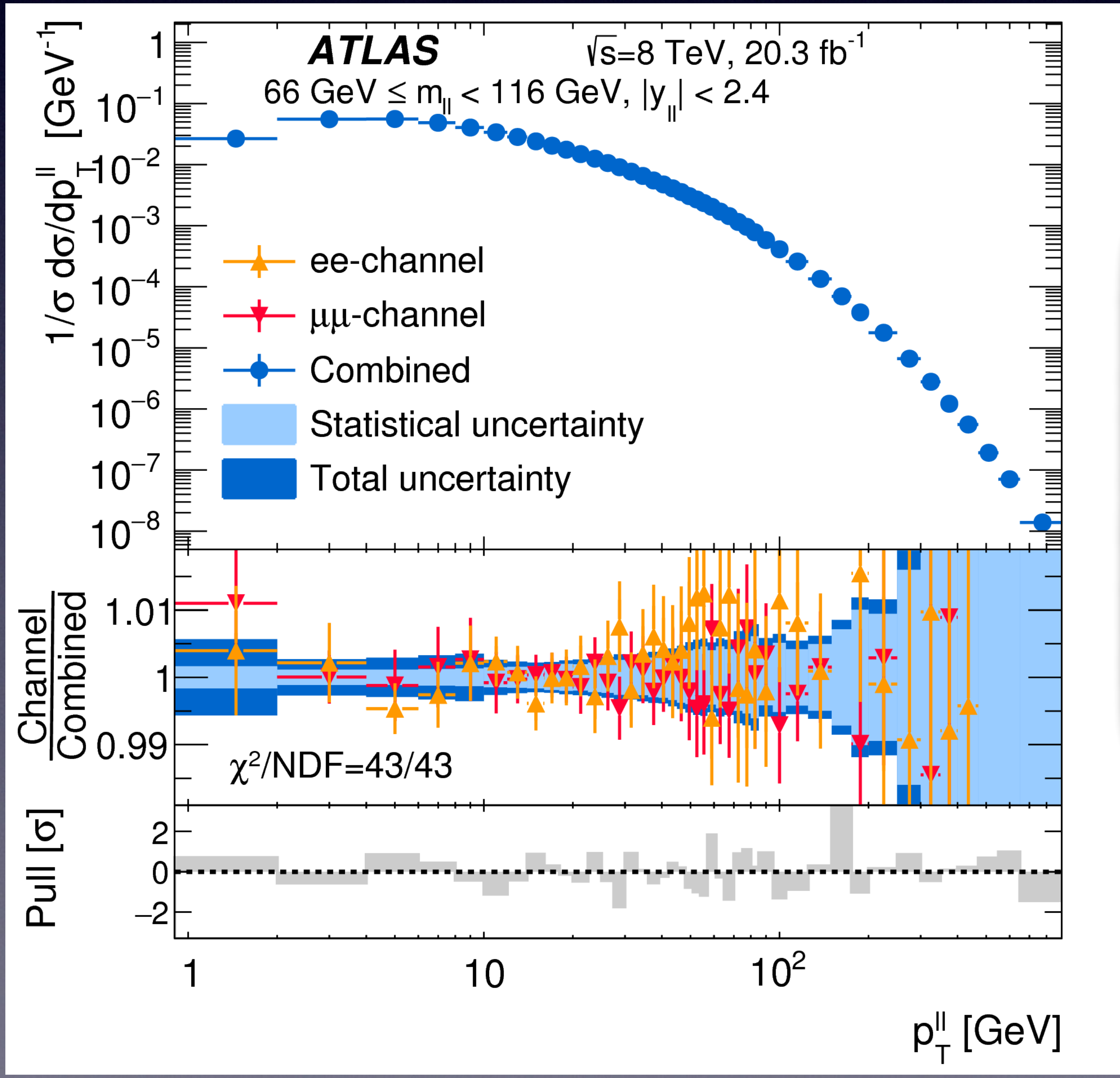

The leading-order cross section for this process depends on the gluon PDF; we can learn about the gluon distribution entering Higgs production from this data!

Comparison with NNLO theory

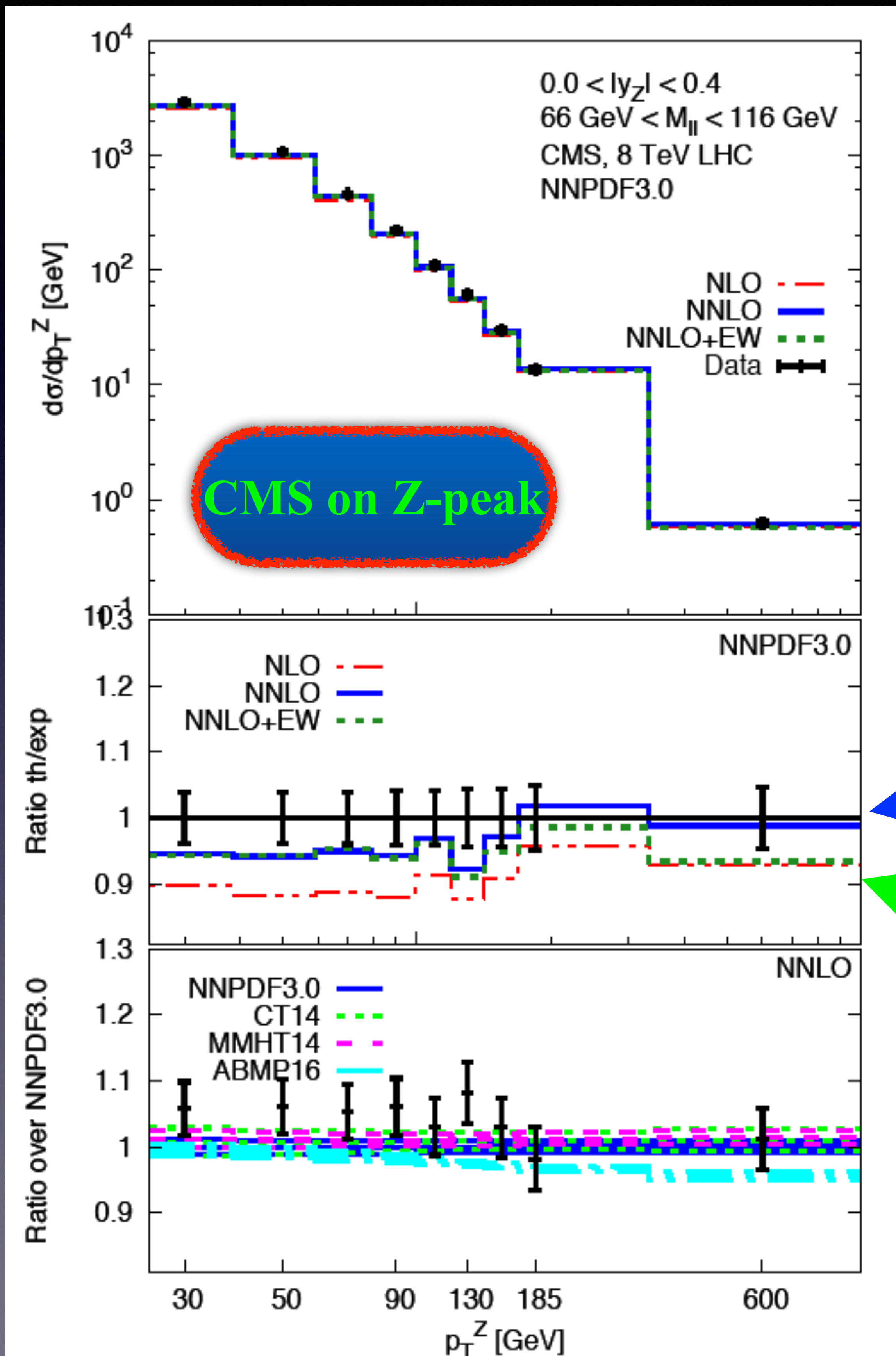

- We have performed an NNLO QCD calculation of p_{TZ} and extensively compared with ATLAS and CMS data.
- We have combined NNLO QCD and NLO electroweak corrections (Kuhn, Kulesza, Pozzorini, Schulze 2005; Denner, Dittmaier, Kasprzik, Muck 2011; Hollik, Kniehl, Scherbakova, Veretin 2015)

NNLO QCD leads to an improved description

NLO EW important at high p_T

No current PDF set describes this well; use this data to improve the PDF fit!

RB, Guffanti, Petriello, Ubiali JHEP 1707 (2017)

Impact on PDFs from Z-pT

- Improvements with respect to a HERA-only baseline fit:

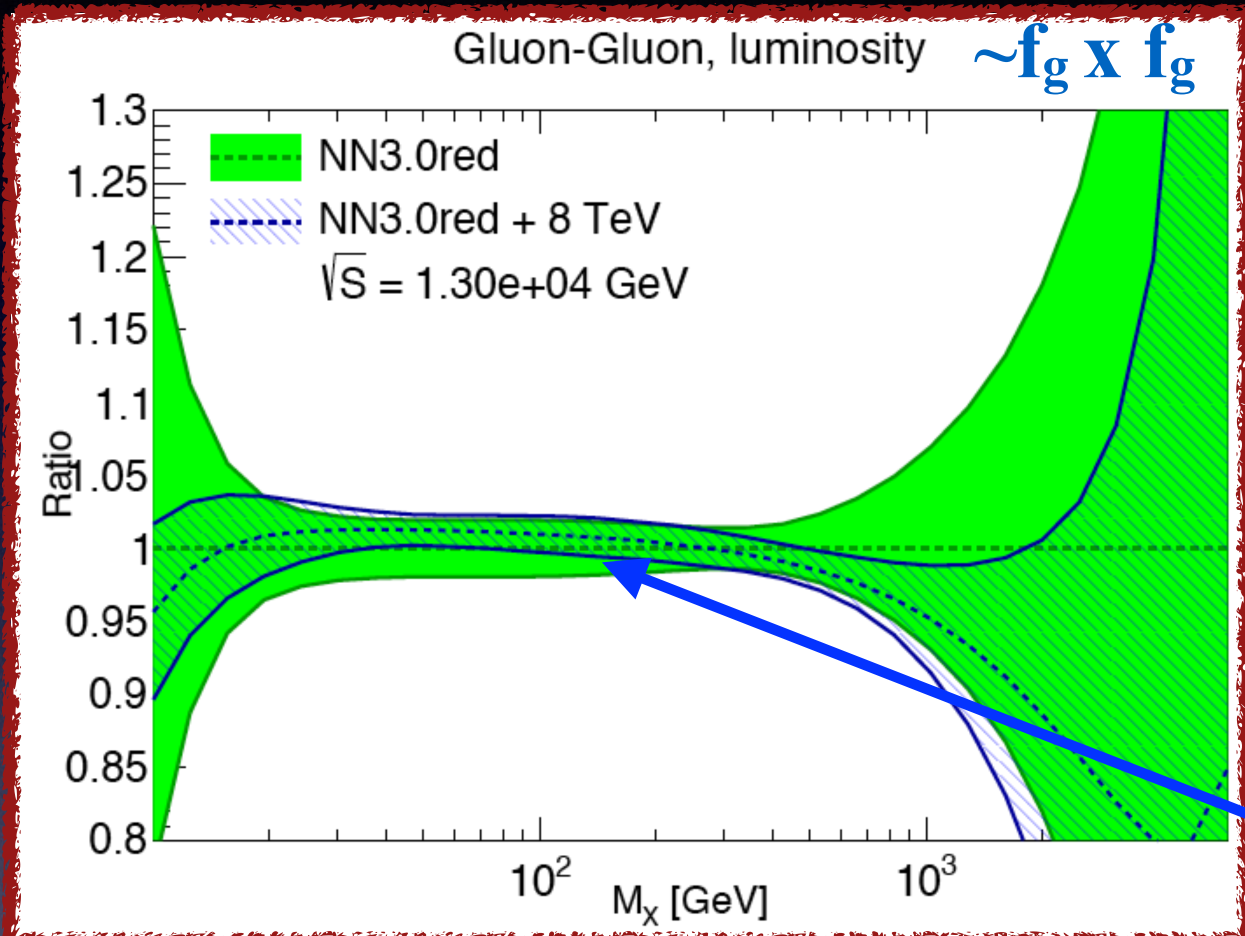

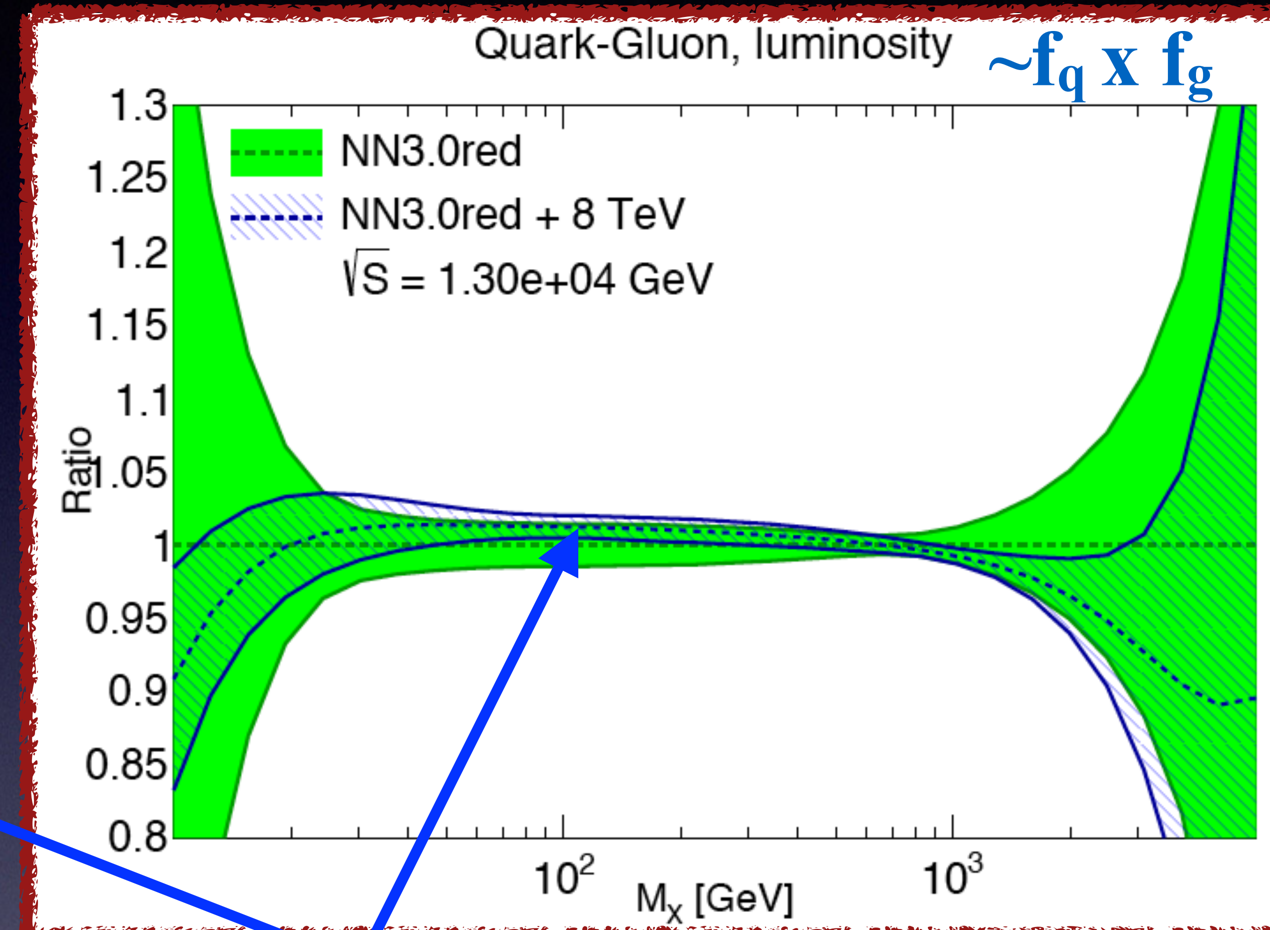

Gluon-gluon and quark-gluon luminosity errors reduced right near $M_X \sim m_H = 125$ GeV!

RB, Guffanti, Petriello, Ubiali (2017)

	Before p_T^Z data	After p_T^Z data
$\sigma_{gg\to H}$ [pb]	48.22 ± 0.89 (1.8%)	48.61 ± 0.61 (1.3%)
σ_{VBF} [pb]	3.92 ± 0.06 (1.5%)	3.96 ± 0.04 (1.0%)

PDF error on Higgs cross sections reduced by 30%!

Further impact on PDFs from top-quark

NNPDF collaboration, 2017

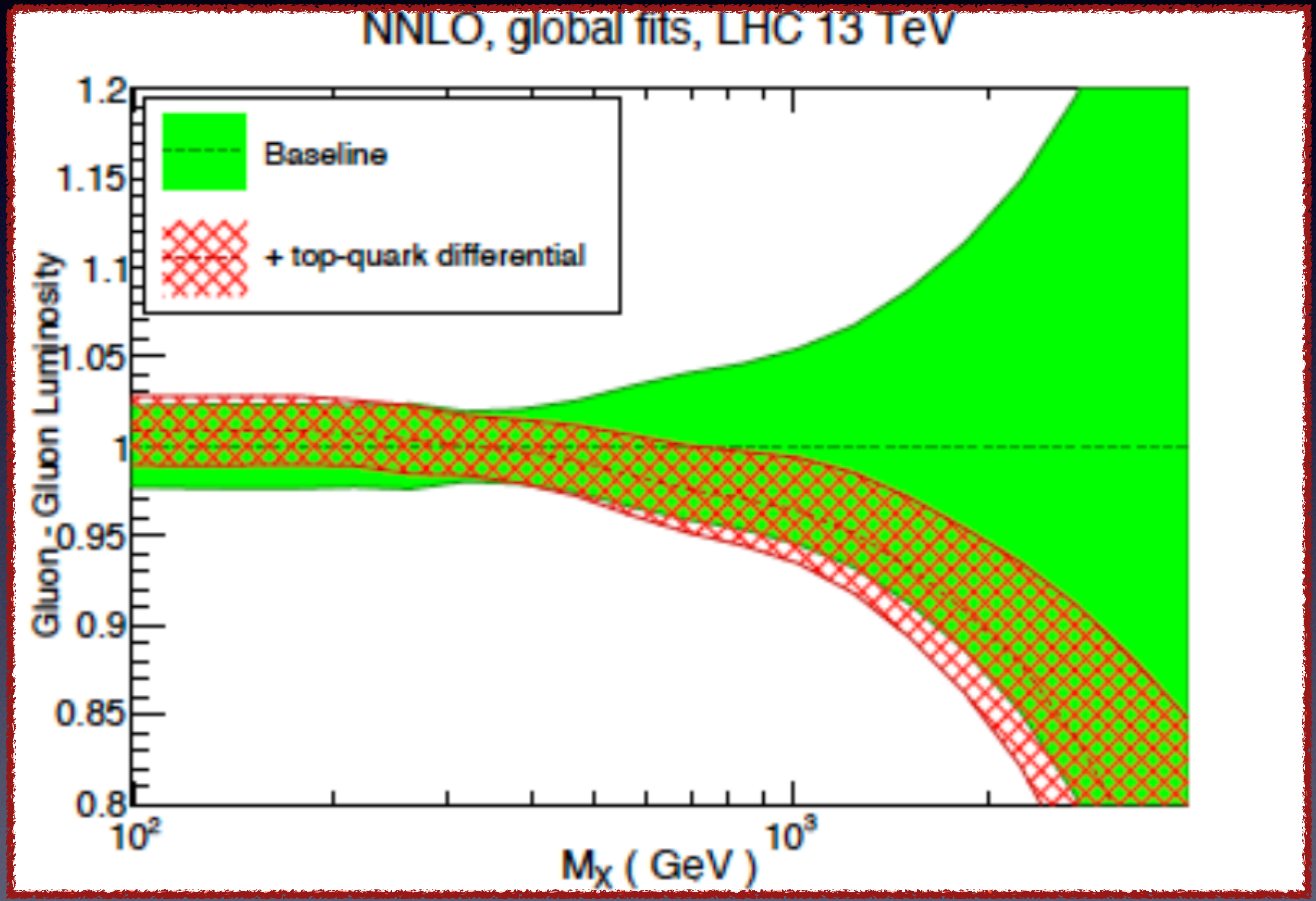

- NNLO differential top results lead to further improvement in the gluon PDF, in particular in the high-x region relevant for new physics searches.

Impact on global fit from new data

In the NNPDF 3.1 global fit, when top-quark, Z-pT and jet data are combined, the PDF errors on the gluon-fusion and VBF production modes are reduced by nearly a factor of 2 with respect to NNPDF 3.0!

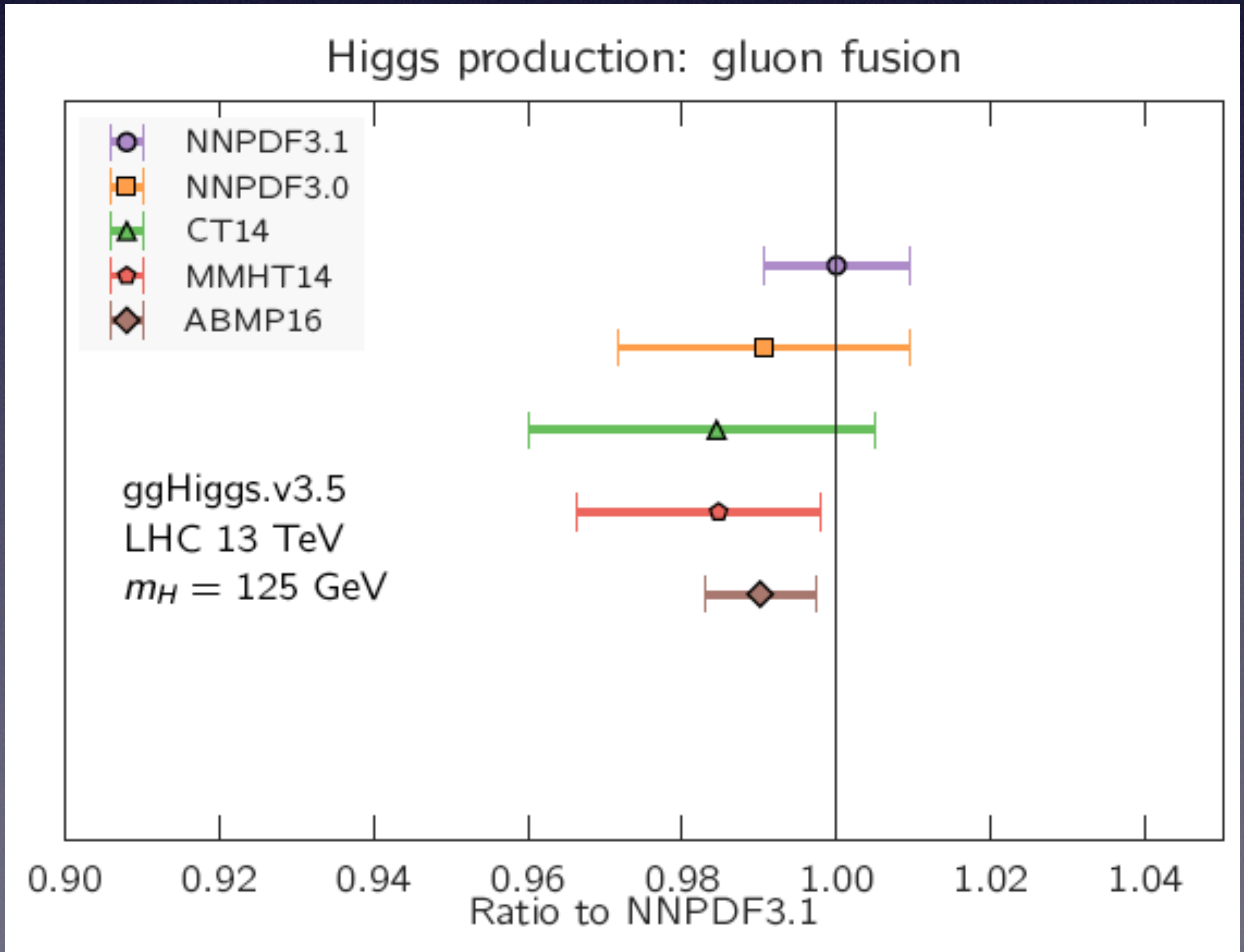

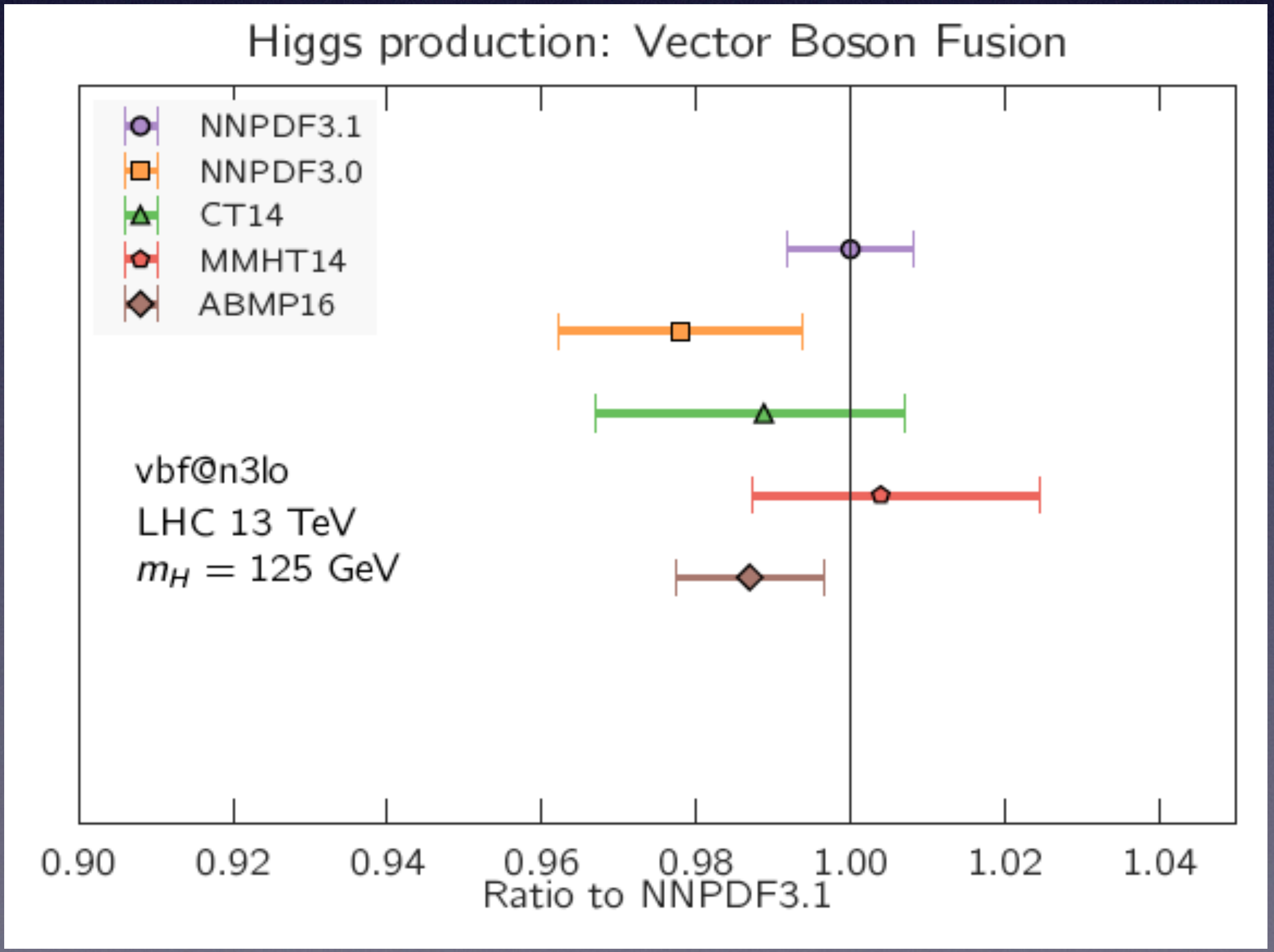

NNPDF 2017

MATRIX

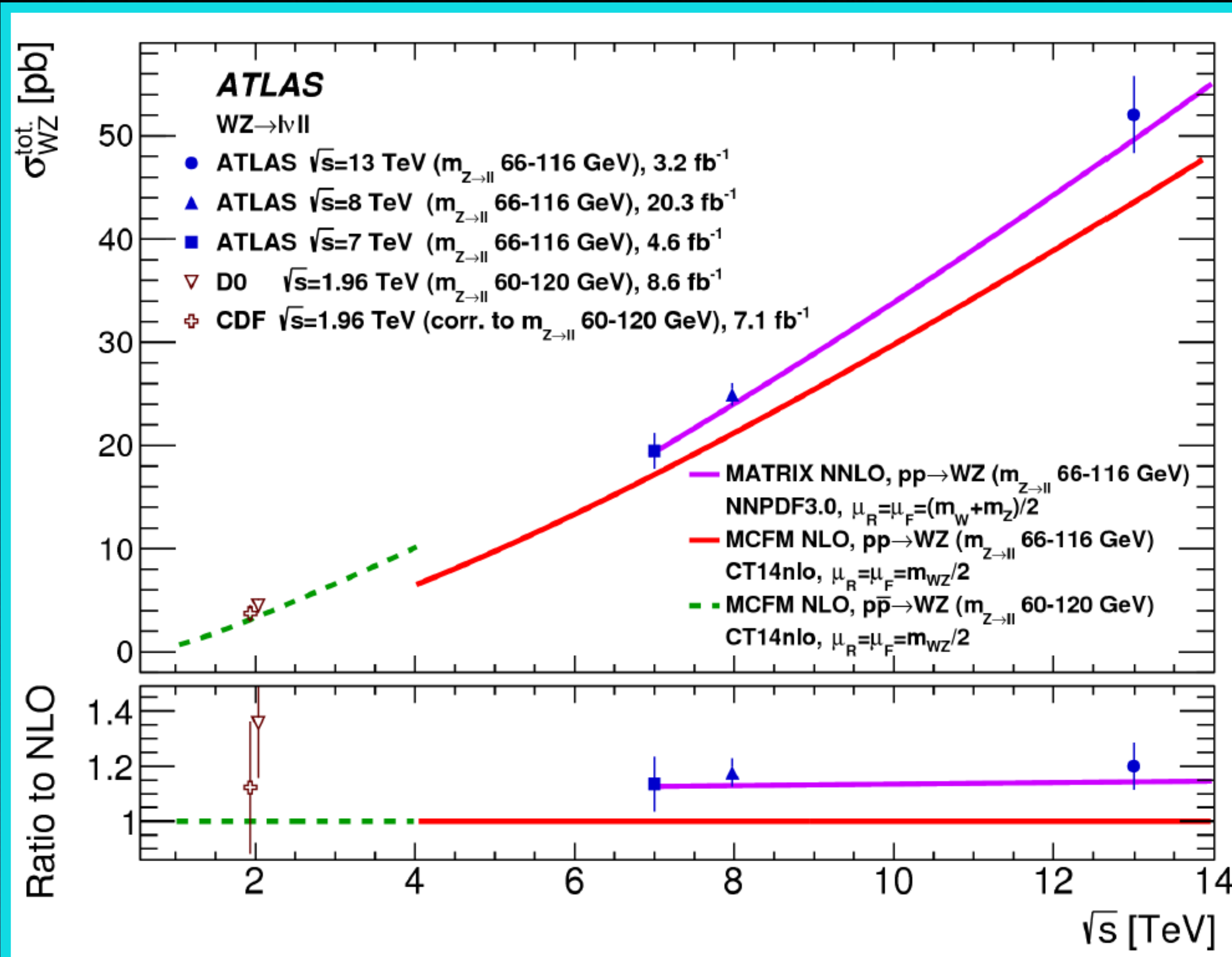

- Another example of the need for NNLO precision to describe LHC data: WZ
- New tool for NNLO 2→2 zero-jet processes: **MATRIX**. Uses qT-subtraction to handle IR singularities.

Kallweit, Rathlev, Wiesemann, Grazzini (2017)

$pp \to Z/\gamma^* \ (\to l^+l^-)$	$pp \to Z\gamma \to l^+l^- \ (\nu\nu)\gamma$
$pp \to W(\to l\nu)$	$pp \to ZZ(\to 4l)$
$pp \to H$	$pp \to WW \to (l\nu l'\nu')$
$pp \to \gamma\gamma$	$pp \to ZZ/WW \to ll\nu\nu$
$pp \to W\gamma \to l\nu\gamma$	$pp \to WZ \to l\nu ll$

Di-jet production at NNLO

- Several important applications of di-jet production at the LHC, including searches for new physics, measurements of α_s, and determination of the high-x gluon

NNLO known in the leading-color approximation, using antenna subtraction:

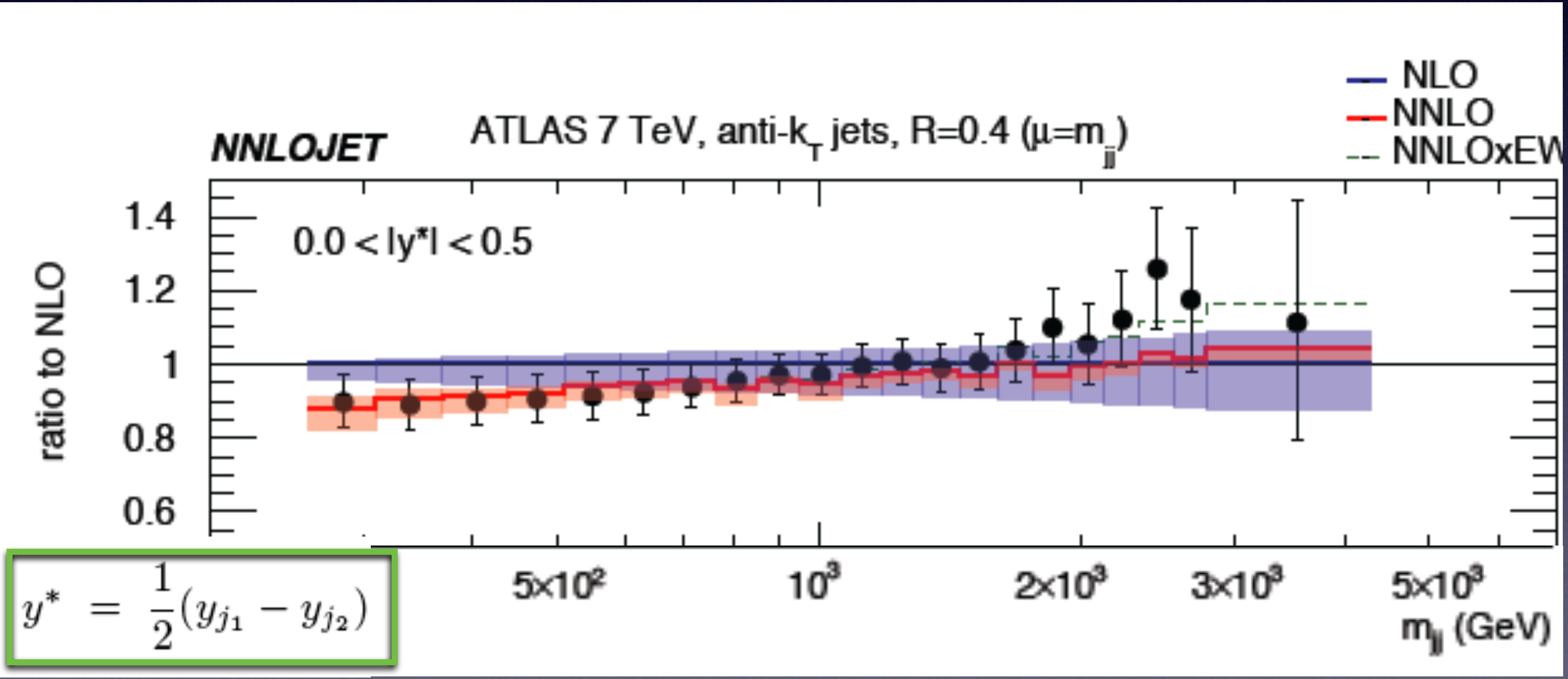

$$y^* = \frac{1}{2}(y_{j_1} - y_{j_2})$$

Currie, Gehrmann-de Ridder, Gehrmann, Glover, Huss, Pires (2017)

Notably improved data/theory agreement in the central y* region

Higgs + 1jet @ NNLO in QCD

- 3 results with 3 different methods are available, allowing cross checks and validation. Calculations done in the infinite top mass approximation.

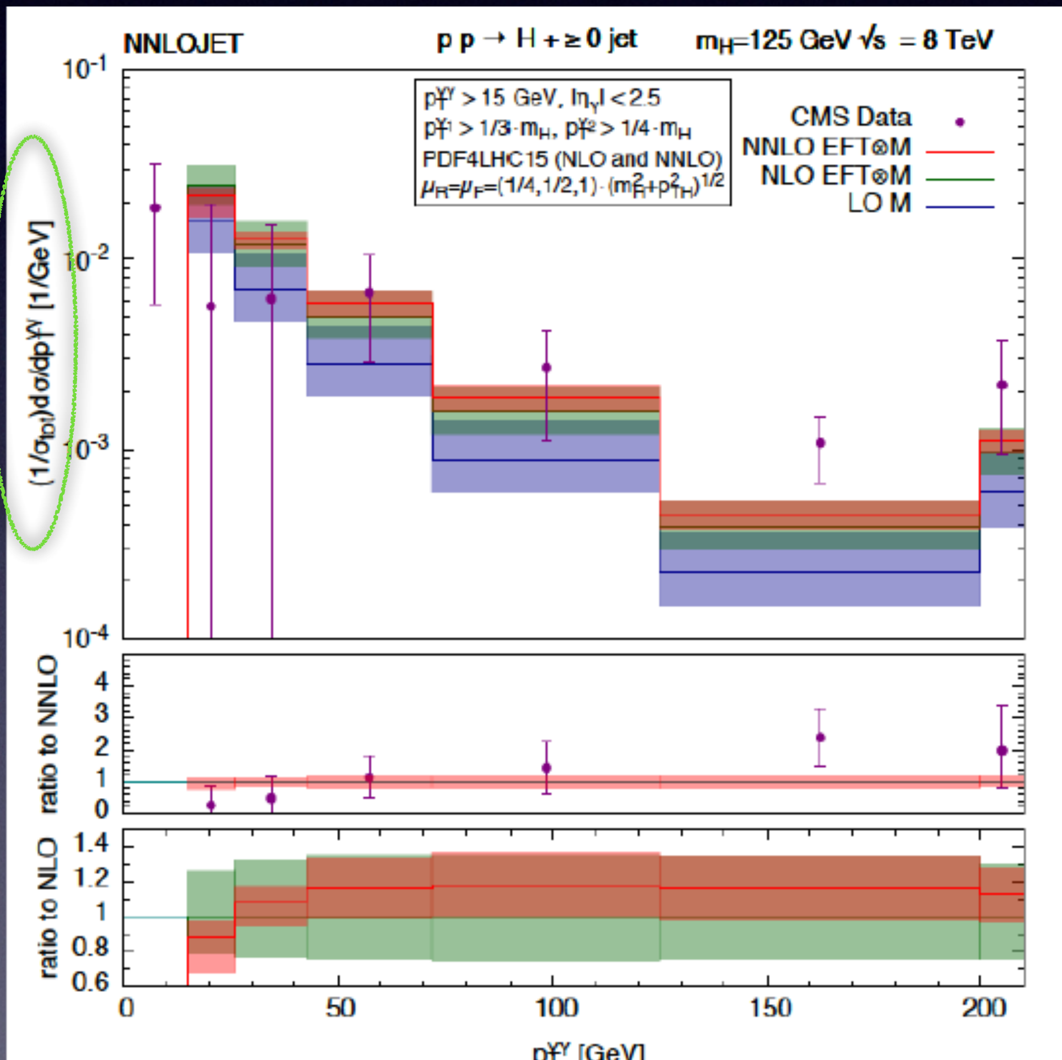

RB, Melnikov, Petriello, Schulze 1504.07922
RB, Focke, Giele, Liu, Petriello 1505.03893
Caola, Melnikov, Schulze 1508.02684
Chen, Gehrmann, Glover, Jaquier 1607.08817

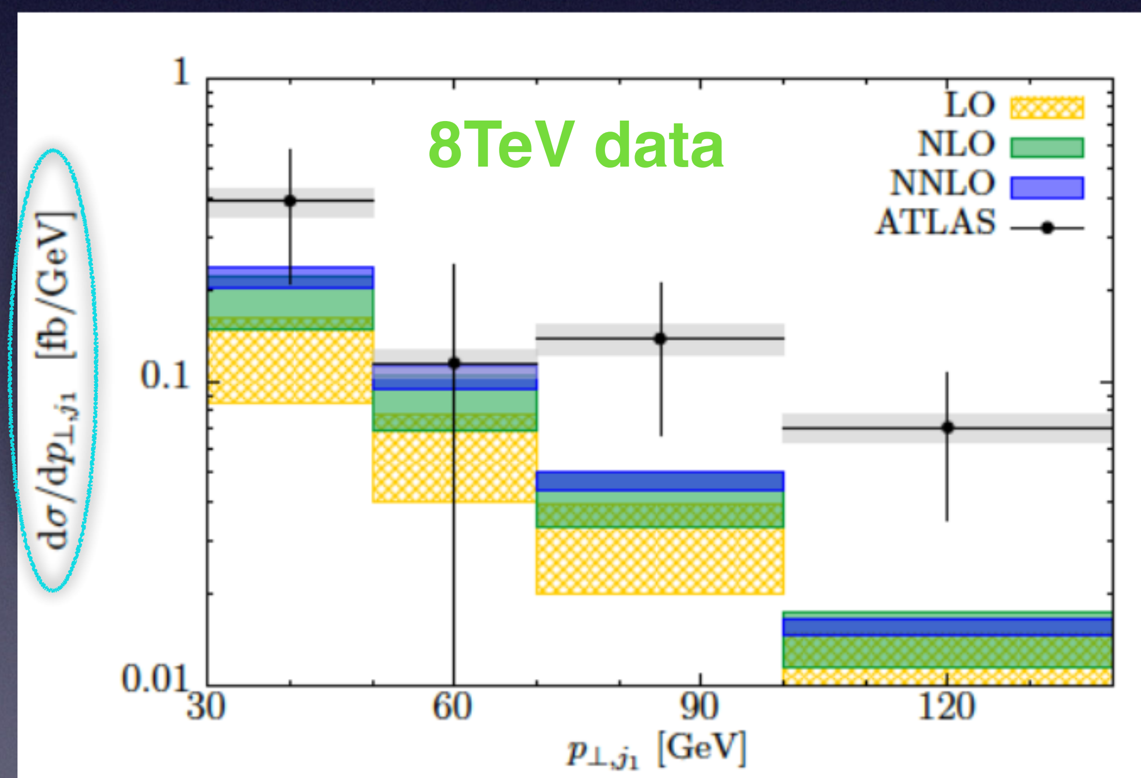

- Normalized distributions agree better with 8 TeV data than unnormalized ones, although data has large experimental error.

Higgs + 1jet @ NNLO in QCD

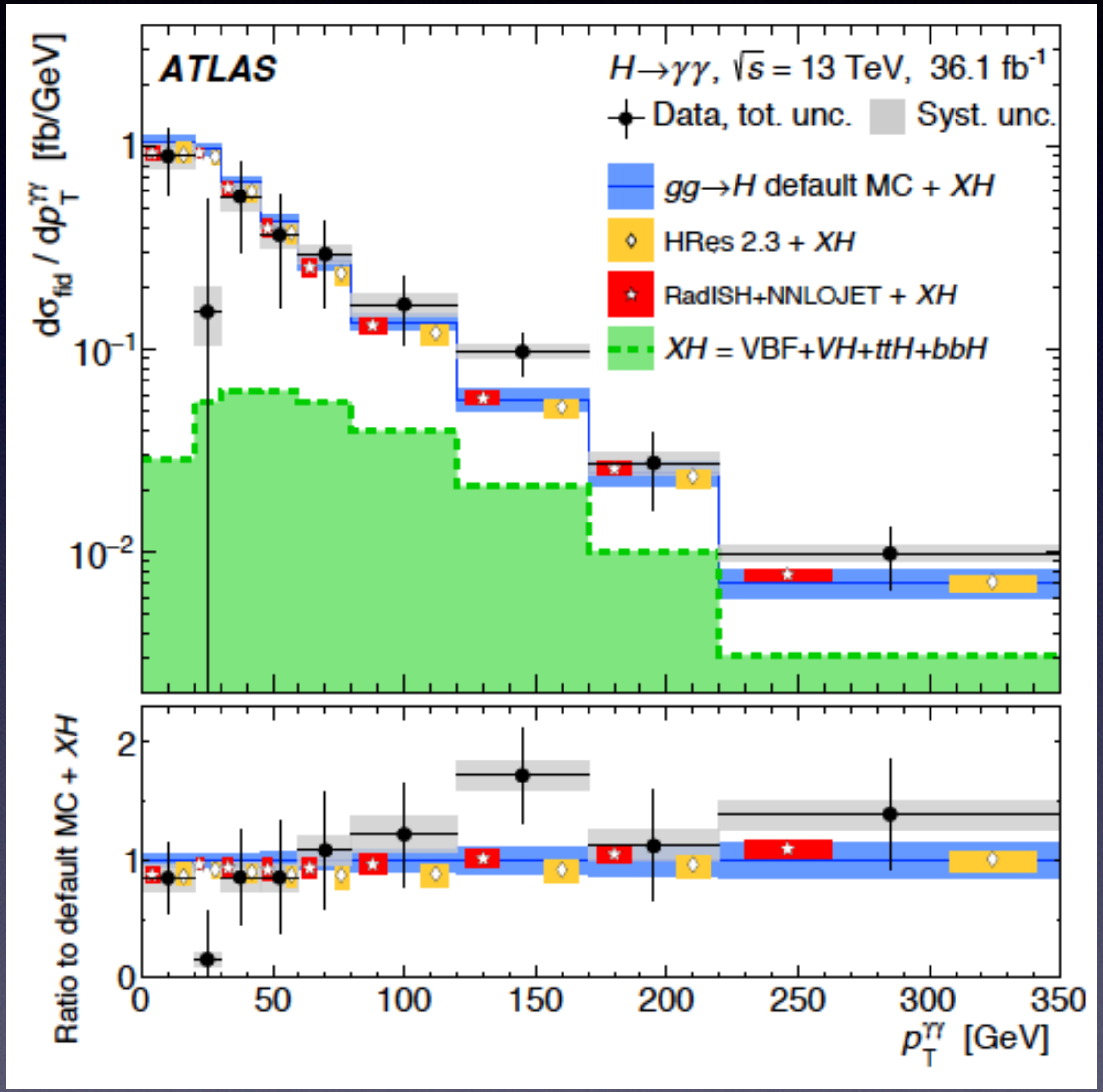

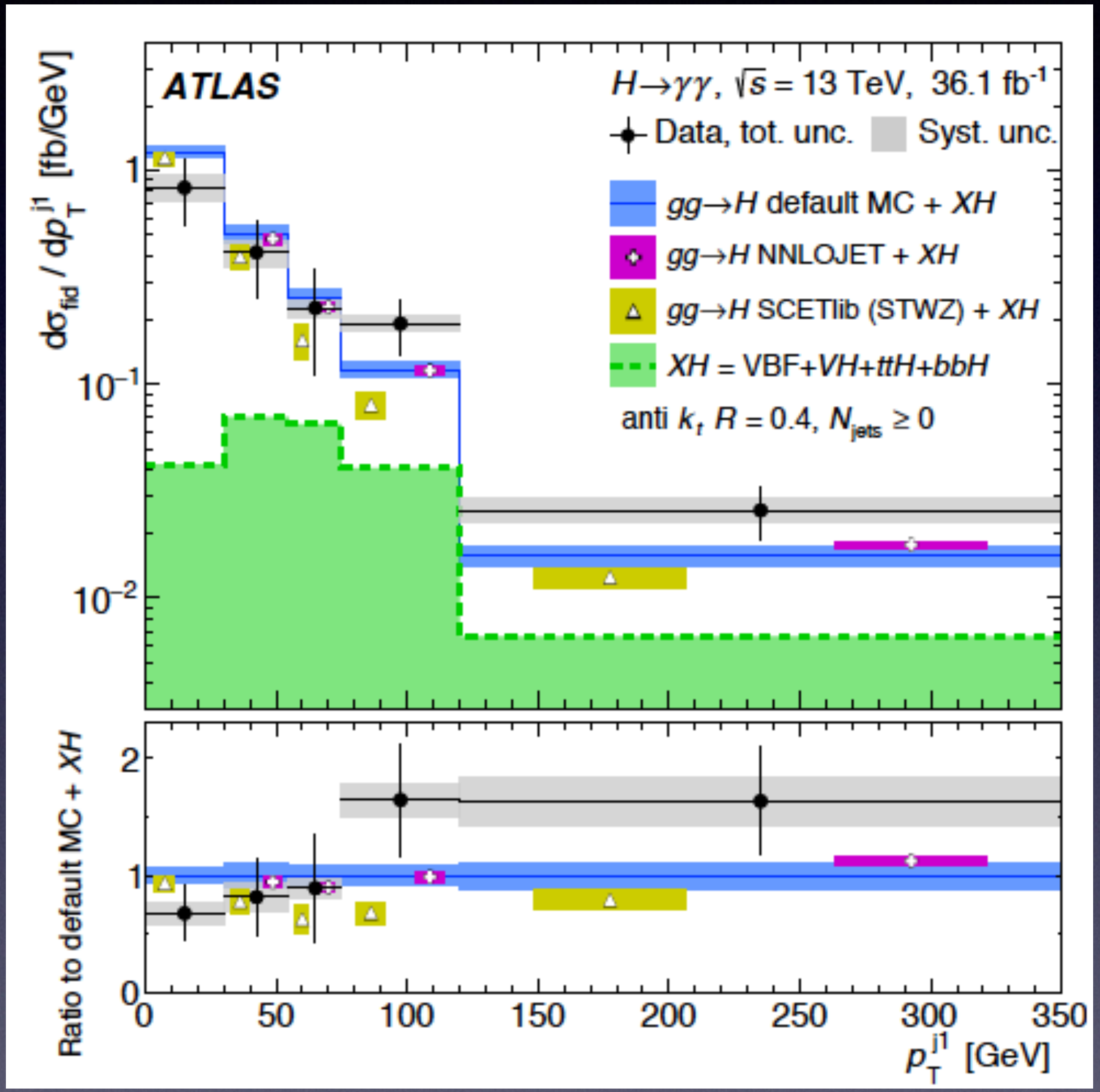

- Slightly better agreement with the 13 TeV data.

Higgs p_T with full m_t dependence

- The Higgs p_T is important to look for BSM effects in the Higgs sector, and to break degeneracies between EFT couplings that appear if only the total cross section is measured.

$$\boxed{\Delta\mathcal{L} = -c_t \frac{m_t}{v} + \kappa_g \frac{\alpha_s}{12\pi}\frac{h}{v} G^a_{\mu\nu} G^{a,\mu\nu} \quad \Rightarrow \quad \frac{\sigma(c_t, \kappa_g)}{\sigma_{\rm SM}} = (c_t + \kappa_g)^2}$$

SM: $c_t = 1$, $k_g = 0$

NLO for finite m_t now known, important input to future Higgs analyses!

Jones, Kerner, Luisoni (2018)

- Numerical evaluation of the 2-loop virtual master integrals with SECDEC (Borowka et al (2015))
- Compare with previous result **$\mathrm{FT}_{\mathrm{approx}}$**, which used EFT for virtual corrections reweighed by exact Born-level amplitudes, and full m_t dependence everywhere else

Higgs p_T with full m_t dependence

- The Higgs p_T is important to look for BSM effects in the Higgs sector, and to break degeneracies between EFT couplings that appear if only the total cross section is measured.

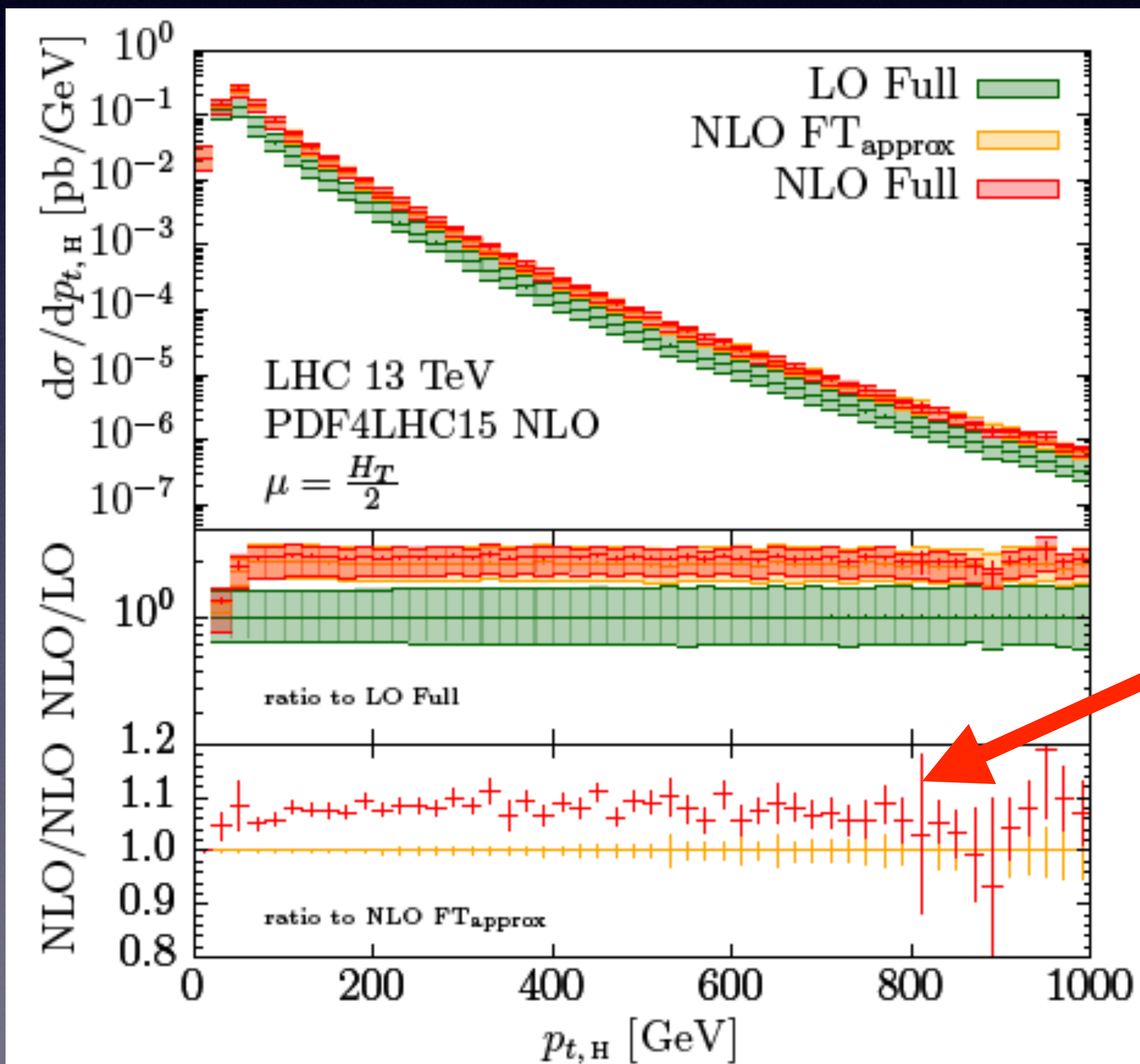

FT$_{approx}$ gets shape of p_T spectrum correct, but full NLO gives an additional 6-8% enhancement!

Jones, Kerner, Luisoni (2018)

Higgs production at N3LO

- Perturbative expansion of the cross section stabilized after the inclusion of the N3LO contribution (N3LO band contained in the NNLO one).
- Dashed lines provide fixed order results improved with resumation. The resummation does not have an impact on the central value for the scale choice mu=mH/2
- Calculation done in the infinite top mass limit.

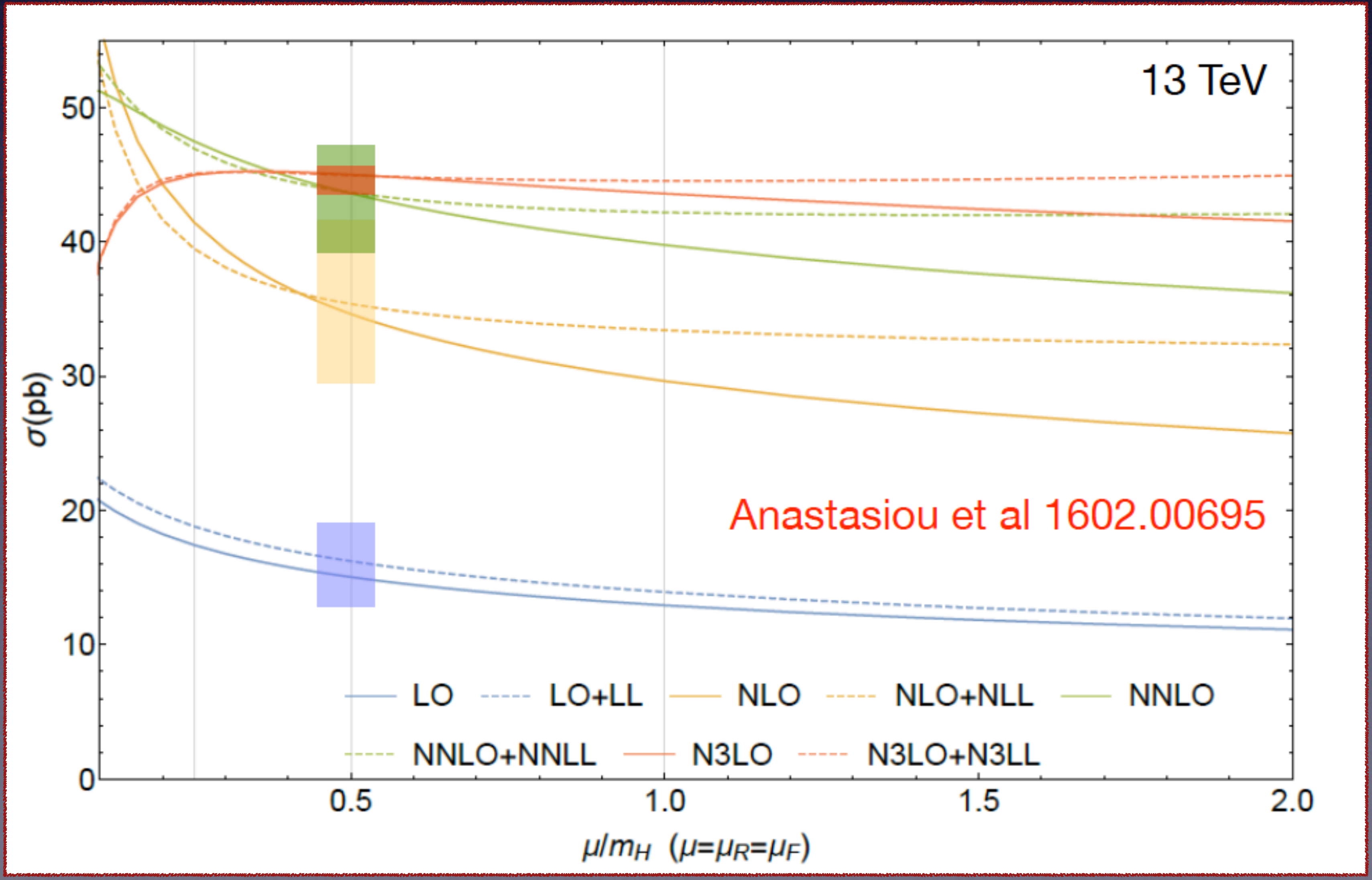

Higgs production at N3LO

- Perturbative expansion of the cross section stabilized after the inclusion of the N3LO contribution (N3LO band contained in the NNLO one).
- Dashed lines provide fixed order results improved with resumation. The resummation does not have an impact on the central value for the scale choice mu=mH/2
- Calculation done in the infinite top mass limit.

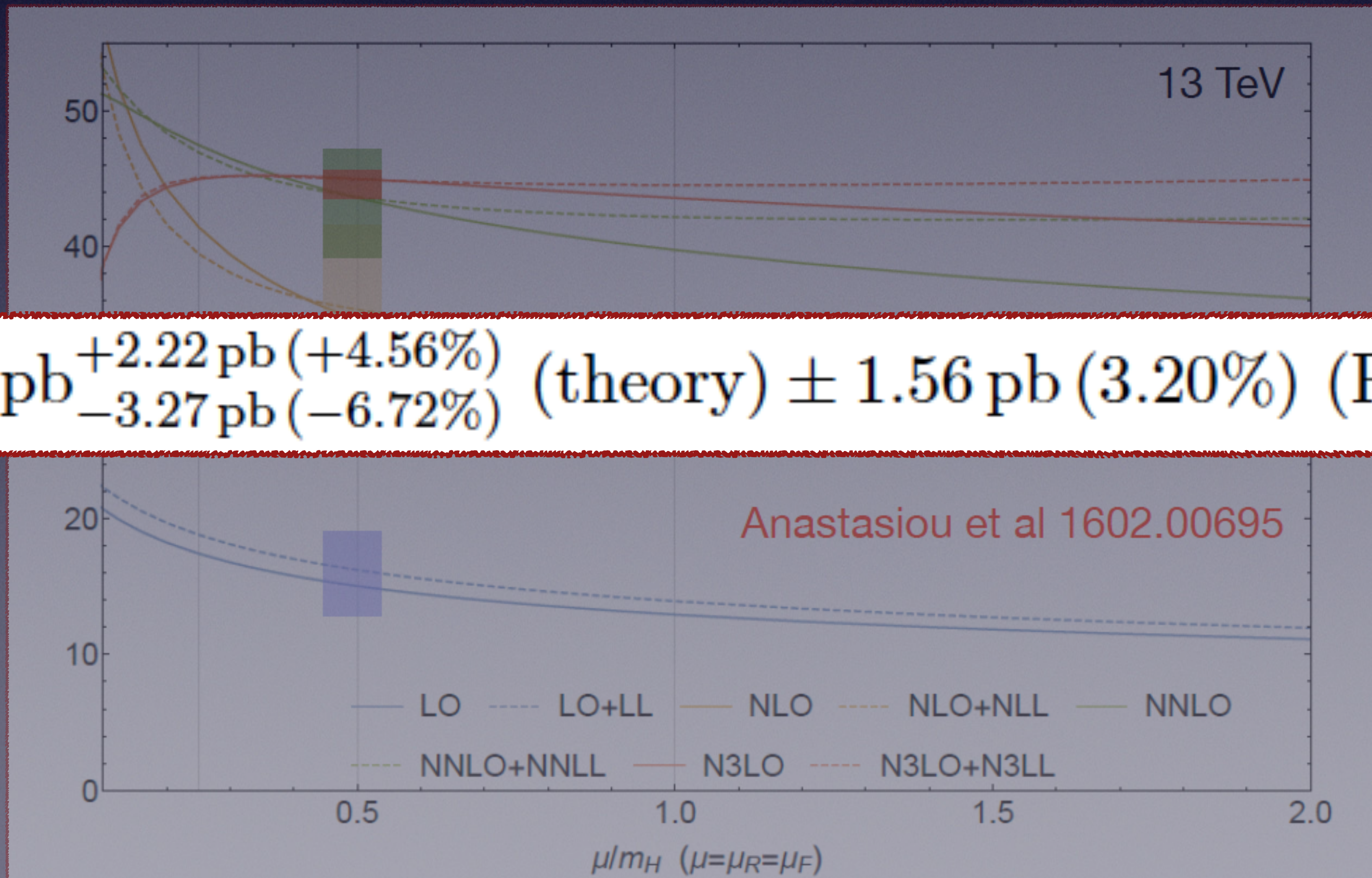

$$\sigma = 48.58\,\mathrm{pb}^{+2.22\,\mathrm{pb}\,(+4.56\%)}_{-3.27\,\mathrm{pb}\,(-6.72\%)}\ (\mathrm{theory}) \pm 1.56\,\mathrm{pb}\,(3.20\%)\ (\mathrm{PDF}+\alpha_s)\,.$$

Future Directions at NNLO and Beyond

- **Current topic**: 2-loop amplitudes for 2→3 processes. Currently an active subject of study, with initial results for 3-jet amplitudes appearing (Gehrmann, Henn, Lo Presti (2016); Badger, Bronnum-Hansen, Hartanto, Peraro (2017); Abreu, Febres Cordero, Ita, Page, Zeng (2017); …)

- **Current topic**: multi-scale 2-loop amplitudes with massive internal particles, relevant for Higgs, top, vector boson production. New mathematical structures beyond multiple polylogarithms appear (Remiddi, Tancredo (2016); Bonciani et al (2016); Weinzierl et al (2016-2017); Ablinger et al (2017); Broedel, Duhr, Dulat, Tancredi (2017); Caola, Lindert, Melnikov, Monni, Tancredi, Wever (2018),…)

- **New results at 3 loops**: completely analytic calculation of 3-loop inclusive gluon-fusion Higgs production in terms of elliptic integrals (Mistlberger (2018)); first results for N^3LO splitting functions (Moch, Ruijl, Ueda, Vermaseren, Vogt (2017-2018))

Summary

- Precision QCD calculations are becoming ever more important as the LHC program progresses.
- In this lectures, we have studied the framework in which predictions are calculated. Two major components need an accurate understanding: PDFs and partonic cross sections.
- Various new ideas and tools have been developed to best describe LHC data.
- More exciting developments are ahead of us, stay tuned!